UNIVERSITY OF Southampton

Faculty of Engineering

and the Environment

Astronautics

Evacuation Simulation Modelling in the event of a Near Earth Object impact

PhD Thesis

Charlotte Camilla Flindt Nørlund

September 2013

University of Southampton

Faculty of Engineering and the Environment

Evacuation Simulation Modelling in the event of a Near Earth Object impact

by

Charlotte Camilla Flindt Nørlund

Thesis submitted for a degree of Doctor of Philosophy

September 2013

Abstract

Near-Earth Objects (NEOs), a group of small interplanetary objects whose orbits around the Sun approach the Earth's orbit to within 45 million km (~0.3 Astronomical Units), have the possibility to impact with the Earth. Such a hazard could potentially cause major damage and result in many casualties depending on impact location and impactor composition and energy. Unique to this type of natural hazard is the possibility of advance warning and the ability to reduce or remove the NEO threat through mitigation such as deflection and evacuation.

This work investigates the human vulnerability in the form of human injuries and fatalities expected from an NEO impact on Earth along with the ability to evacuate. New models have been developed to predict the potential human loss from six individual land impact hazards, using historical data about earthquakes and large explosions, models regarding roof collapse and casualties due to ignition exposure and the uncertainty in the data available.

Models have also been developed that mimic human travel behaviour during an evacuation. These models were based on survey data regarding human behaviour during evacuations from hurricanes in the US along with models that estimate local road network capacity and flow-time.

The development of a decision support toolbox, the Near Earth Object Mitigation Support System (NEOMiSS) supports this research. NEOMiSS is a collection of tools that individually and in collaboration provide useful information to decision-makers regarding human vulnerability (i.e. the number of human injuries and fatalities), ability to evacuate, physical impact effects and uncertainties in models, input data and risk corridor knowledge. This enables decision-makers to gain a better knowledge about the potential consequences of their decisions.

A number of case studies were investigated using NEOMiSS. These illustrate how the impact location and impactor energy can result in very different outcomes with regards to human vulnerability. They also illustrate how local road networks and the location of local settlements along with the evacuation strategy affect the ability to perform a successful evacuation. The success of such an evacuation will influence the human vulnerability by reducing the number of expected casualties.

For Thomas, Oliver and Philip

My biggest supporters

List of Contents

List of Figures

List of Tables

Declaration

I, Charlotte Camilla Flindt Nørlund declare that the thesis entitled “Evacuation Simulation Modelling in the event of a Near Earth Object Impact” and the work presented in the thesis are both my own, and have been generated by me as the result of my own original research.

I confirm that:

• this work was done wholly or mainly while in candidature for a research degree at this University;

• where any part of this thesis has previously been submitted for a degree or any other qualification at this University or any other institution, this has been clearly stated;

• where I have consulted the published work of others, this is always clearly attributed;

• where I have quoted from the work of others, the source is always given. With the exception of such quotations, this thesis is entirely my own work;

• I have acknowledged all main sources of help;

• where the thesis is based on work done by myself jointly with others, I have made clear exactly what was done by others and what I have contributed myself;

• none of this work has been published before submission.

Signed:

Date:

Acknowledgements

I would like to send a big thank you to my supervisors Hugh Lewis and Peter Atkinson for their support and patience. My Husband Thomas also deserves a big thank you for his patience. Thank you to Ian Hoult, Head of Emergency Planning & Business Continuity, Hampshire County Council, for taking time to meet with me and my supervisors and tell us about how Hampshire County Council plan for and deal with emergencies. Jessica Guo likewise deserves a big thank you for being my host supervisor while I spend 3 month at University of Madison Wisconsin. A big than you to Gareth Collins and Adrian Tatnall for their grilling during the viva and their comments. Last but not least a thank you to Rebecca, Jaye, Jenny, Warin and Martin for being such good university friends and office colleagues.

List of Acronyms

Acronym	Name
ATC	Automatic traffic counts
AU	Astronomical Unit
CEMDAP	Comprehensive Econometric Micro-Simulator for Daily Activity Travel Patterns
CEMEVAC	Comprehensive Econometric Micro-Simulator for EVACuations
CODATA	Committee on Data for Science and Technology
CLC	Classified Link Counts
CRED	Centre for Research on the Epidemiology of Disasters
ECA	Earth-Crossing Asteroids
EM-DAT	Emergency Events Database
FEMA	Federal Emergency Management Agency
IEO	Inner Earth Object
JPL	Jet Propulsion Laboratory
LoV	Line of Variance
LPC	Long Period Comets
MOID	Minimum Orbit Intersection Distance
NEA	Near Earth Asteroid
NEC	Near Earth Comet
NEO	Near Earth Object
NEODyS	Near Earth Object Dynamic Site
NEOMiSS	Near Earth Object Mitigation Support System
NHC	National Hurricane Center
NOAA	National Oceanic and Atmospheric Administration
OSM	Open Street Map
PAGER	Prompt Assessment of Global Earthquakes
PHA	Potentially Hazardous Asteroid

PHC	Potentially Hazardous Comet
PHO	Potentially Hazardous Object
PoR	Path of Risk
RC	Risk Corridor
SEDAC	Socio Economic Data and Applications Center
SPC	Short Period Comets
TRANSIMS	TRansportation ANalysis SIMulation System
UN	United Nations
UNDP	United Nations Development Programme
USGS	United States Geological Survey
VA	Virtual Asteroids
VI	Virtual Impactor
WHO	World Health Organization

Nomenclature

a	Semi major axis
A_{total}	Total number of people living in the affected area
B	Recommended braking distance
c	Number of cars
c_a	Average car length
C	Road network capacity
C_{max}	Maximum road network capacity
C_{total}	Total number of casualties
d	Object diameter
h	Hurricane intensity
H	Absolute magnitude
ing	Ignition exposure
l	number of road lanes
l_a	Average road length
L	Road length
mag	Seismic magnitude
M	Moment magnitude scale
O	Overpressure
p	Proportion of population that will evacuate
P	Orbital period
P_C	Proportion of casualties with respect to the number of people living in the affected area
P_F	Proportion of fatalities with respect to the number of people living in the affected area
P_I	Proportion of injured with respect to the number of people living in the affected area
q	Orbit perihelion

Q	Orbit aphelion
r	Average road length
s	Vehicle speed
S	Speed limit
t_f	flow-time
v_g	average weighted velocity
vul	Human vulnerability [%]

Chapter 1
Introduction

Near Earth Objects (NEOs) are a group of small interplanetary objects. Some are left over building blocks from when the planets were created. Others are fragments from collisions between planets and smaller objects. The orbits of NEOs have been changed by the gravitational attraction of nearby planets and thereby entered the Earth's neighbourhood. If an asteroid, comet or meteorite has an orbit around the Sun where it approaches the Earth Orbit within 194 million km (~1.3 Astronomical Units) it is categorised as a NEO.

This chapter provides an introduction to NEOs and the hazard they pose along with the research problems that have been identified and the main objectives of this work. The main contributions to NEO research will be discussed followed by an overview of the thesis structure.

1.1 Introduction to NEOs

Some of the earliest definitions of comets were made by the Greeks. Anaxagoras and Democritus defined comets as “planets or the conjunction of two planets”, whereas Aristotle’s explained them to be caused by two types of exhalation that rise to the top stratum where they bursts into flame creating tails that were carried around with the star’s daily revolution (Dicks 1970) or a “meteorological phenomena, confined to the Earth’s upper atmosphere” (Taton et al. 1989). In 1577 it was found that comets were not sub-lunary objects (situated beneath the moon) or phenomena but supra-lunary objects

(situated beyond the moon). This was based on work performed by the astronomer Michael Mästlin from Tübingen in Germany and the Danish astronomer Tycho Brahe. In the 1680s Newton and Halley were the first to calculate the orbits of several comets and they found that some comets passed Earth relatively frequently. These have orbital periods of less than 200 years and are called short period comets (Taton et al. 1989). Simon Laplace, a seventeenth century natural philosopher and mathematician, was the first to suggest that comets were made of ice. His suggestion was ignored by the scientific society and it was only in the 1940s that the idea about comets being dirty snowballs first became widely accepted (Whipple et al. 1986). Jan Hendrik Oort and Kuiper both contributed to the description of the origin of comets. Jan Hendrik Oort was the first to write about the possibility of a vast and distant cloud of comets. The Oort cloud is believed to be one of these comet reservoirs together with the Kuiper belt (Van De Hulst 1994, Chaisson et al. 2002). Two groups of comets were identified. The first group, called short-period comets, primarily originates from the Edgeworth - Kuiper Belt beyond the Neptune orbit and the second group, long-period comets, originates from the Oort cloud (Chapman 2004, Chaisson et al 2002).

The first asteroid observation was in January 1801 by Giuseppe Piazzi. This asteroid is named Ceres and is the largest known asteroid with a diameter of 940 km and a mass of 1/10.000 of Earth's mass. It was 1802 that Herschel decided to put Ceres into its own class of celestial bodies called asteroids (Armitage 1962).

The idea that these celestial bodies potentially could impact with the Earth causing major damage was first suggested by Simon Laplace around 1802-1803 (McCall et al. 2006). Daniel Barringer (1860-1929) was the first to suggest that certain geological structures on Earth were the result of an impact by NEOs (Seddon 1970), but at that time it was widely believed that some great volcanic eruptions had created these structures. It was in the 1970s that Carlyle S. Beals and colleagues at the Dominion Observatory in Canada, and Wolf von Engelhardt of the University of Tübingen, Germany arrived at similar conclusions (Springer 2008, Impact Craters 2008) and, together with new knowledge from the Apollo moon landings, people started realizing the violent history of the Earth and the hazards that such an impact could pose to everyone living here (NASA 1992).

Craters from some NEO impacts still scar the planet and can be found across the globe. Today, around 180 impact craters have been identified on the Earth, some dating back to almost 2 billion years ago (Impact Craters 2008). One of the most documented craters is the Chicxulub-impact where a 10 km diameter asteroid struck the Gulf of Mexico around 65 million years ago. It is believed that this impact contributed to the extinction of the dinosaurs (Keller et al. 2007) together with other impacts, such as one near the west coast of India (Chatterjee et al. 2002). Due to a large population of small NEOs, impacts of sub-kilometre sized NEOs occurred more frequently (Chapman 2008) and with slightly less damaging consequences. In addition, even if a NEO does not reach the Earth's surface it can still cause widespread damage. For example, in 1908 a 40 m diameter asteroid exploded in the lower atmosphere over the forest in Tunguska, Siberia, flattening some 2000 km^2 of coniferous forest (Napier et al. 2009). Events of this magnitude occur every 500-1000 years (Rincon 2010).

The oldest written record of a NEO impact is The Planisphere tablet, a small disk from the seventh Century BC (Bond et al. 2008). This disk is believed to be a copy of a much older Sumerian tablet from a period between 4000 BC and 2000 BC. The information on this tablet is believed to be a set of astronomical observations describing a NEO impact. Bond et al. (2008) traced back these observations using night sky modelling programs and suggested that the NEO described on the disk was spotted on the 29th June 3123 BC shortly before dawn and that the NEO impacted the Austrian mountain of Köfels. In recent history, the Carancas impact event of September 2007 involved a 2.5 m-diameter meteorite, which created a 15 m-diameter crater in Peru (Tancredi et al. 2009), and the Sudan desert event in October 2008 involving asteroid 2008 TC3. This asteroid had been tracked by astronomers and an atmospheric explosion had been predicted over the Sudan desert. After the incident, researchers collected small fragments of the asteroid in the desert (Courtland 2009). In February 2013 a 17-20m in diameter object entered the Earth atmosphere and exploded at ~23 km altitude just south-west of the Russian city of Chelyabinsk causing windows to shatter and injuring hundreds of people. This event was followed by hundreds of eyewitnesses and captured on camera (the Guardian 2013) (NASA 2013). These events show that the threat of an NEO impact is genuine, although the likelihood of a large NEO impact is low. Chapman (2008) has created a graph that

illustrates the asteroid size distribution together with the impact energy and the impact probability on Earth, see Figure 1.1. This graph shows that the NEO size distribution follows power law, where the number of NEAs increases with decreasing size.

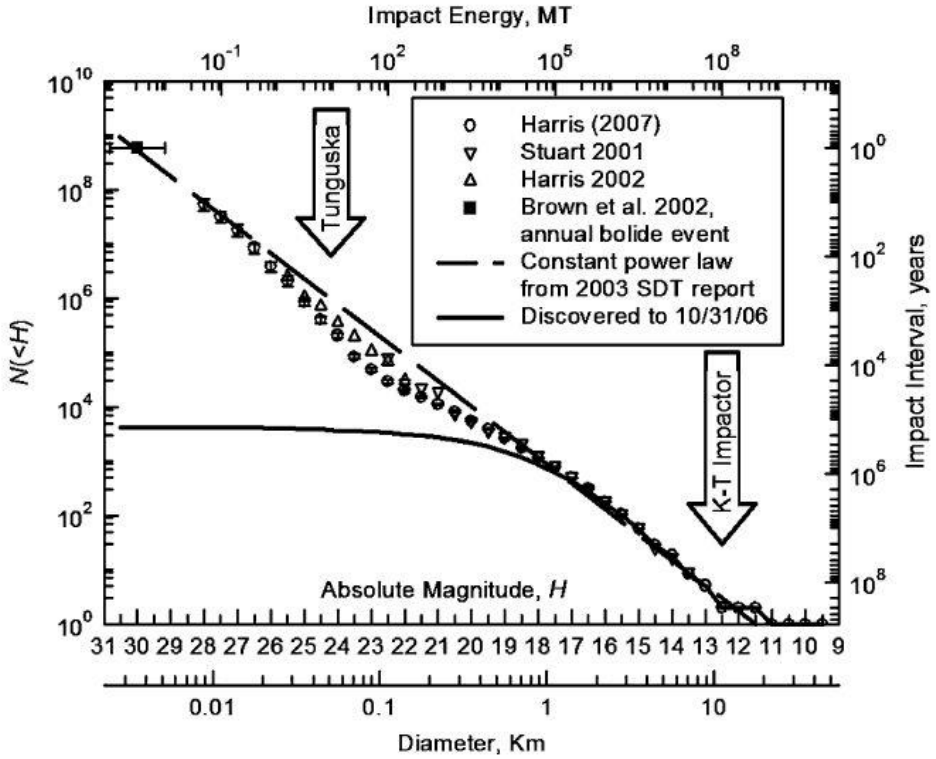

Figure 1.1: Various estimates of NEO size vs. impact frequency. Equivalent astronomical magnitude and impact energy in megatons.

1.2 NEO research problems

With the realisation of the potential threat from NEOs the space community has started search campaigns for NEOs, gaining more knowledge about their composition, the Earth impact probability, the physical effects such impacts could cause on the Earth and the mitigate of the hazard. With the increased knowledge about NEOs the probability of finding NEOs that are threatening the Earth increases. Knowing which NEOs are on a collision course with the Earth provides decision-makers with the possibility of mitigating the threat. The decision-making process is complex and legal, social and national/regional issues must be taken into consideration (Schweickart 2008).

A need for tools that can provide useful information to decision-makers along with informing the public in an educational way was identified at the University of Southampton and initial tools were developed in the form of NEOimpactor (Bailey et al. 2007) and NEOSim (Morley 2009). These two projects provided physical impact models for land and water impact along with atmospheric explosion. NEOimpactor additionally compared the costs and casualties for each country. The need for detailed decision support tools was furthermore identified by the US Air Force. The 2008 US Air Force "Natural Impact Hazard (Asteroid Strike) Interagency Deliberate Planning Exercise After Action Report" suggested that the information available to decision-makers regarding the threat and the potential consequences of decisions taken was insufficient (Garretson 2008). As such, the work described in this thesis addresses the need for this information.

This PhD project extends the functionality offered by the NEOSim and NEOimpactor tools, developed at the University of Southampton. It provides an improved human casualty estimator (i.e. fatalities and injuries) using improved vulnerability models of multiple NEO impact hazards along with uncertainty estimates. In addition, it also offers an evacuation simulator for prediction of the ability to evacuate a threatened area, which is used for modifying the human vulnerability. These tools enable the Near Earth Object Mitigation Support System (NEOMiSS) to deliver reliable predictions of the human casualties arising from impact hazards along a NEO risk corridor. As such, decisions affecting NEO deflection campaigns (which modify the risk corridor) can be taken in the context of the human consequences. In addition, NEOMiSS provides a mechanism for managing the uncertainties in the data and model fitting, thereby enabling the confidence in risk assessments to be quantified.

NEOMiSS has the potential in the future to be applied to all natural hazards where there is some advance warning time such as tsunamis, hurricanes and volcanic eruptions.

1.3 Objectives

When an extreme event, natural- or man-made, occurs in a populated area, bringing the population living there into life-threatening danger, protective measures, which can help bring the population to safety, are needed. This can be done by providing

shelters or by evacuating people living in the affected area. A potential NEO impact could be one of these hazardous events that would require such protective measures to be implemented. Evacuating a large area can be very complicated. This could be due to the topography, road layout, due to densely populated cities, the local governance and the local culture.

Before initiating an evacuation it is important to gather information about the threat, its physical effects and the likely impact on the local population. The next step is to perform a more in-depth analysis of the ability to evacuate. How well an evacuation goes depends very much on the preceding work and planning done by the local government and emergency services along with how well the local population has been prepared. Using evacuation simulation modelling can help emergency services to plan and prepare.

The main objective of this project was to investigate the critical issue of timing, uncertainty and decision-making when estimating local human vulnerability and ability to evacuate, along with the reduction in human vulnerability to a successful evacuation. This will be achieved through the development of human vulnerability models due to the different types of natural hazards that can be expected from a NEO land impact. Ocean impacts will not be considered in this thesis due to major concerns about the many different ocean impact models that exist and the large difference in their outcomes. The outcomes from these models will inform about the potential human losses that can be expected. This will be followed by the development of an evacuation simulator that uses behaviour based models. The outcomes from such a simulator will provide information regarding the temporal issues related to evacuations of different areas along with information regarding an area's ability to evacuate.

1.4 Contributions

Through the use of models that describe the potential human vulnerability to the different types of physical hazards coming from a NEO impact on the Earth it has been possible to gain more in-depth knowledge into how such an impact will affect the potential impact locations along its risk corridor. Uncertainties in the models and the

available data have been included into these models and the areas of knowledge where more information is needed was identified.

An advanced, coarse-scale evacuation simulator was used to illustrate how mitigation measures such as evacuation can be used to reduce the vulnerability. A number of different case studies were run using the human vulnerability simulator and the evacuation simulator. These studies investigated how different evacuation strategies affected the evacuation outcome, how the impact location and its surrounding geography affected the evacuation outcome and how the impact energy affected the evacuation outcome. Finally they also investigated how the human vulnerability was reduced through performing an evacuation. The outcome from different case studies shows how factors such as time, local road network infrastructure, geography and impact energy affects an area's ability to evacuate. The evacuation simulations can also be used in the decision making process when a deflection mission is being planned.

1.5 Thesis structure

The overall structure of this thesis is as follows:

Chapter 2 provides an overall NEO threat analysis along with an investigation into evacuation. It will describe the different types of NEOs that exist and provide basic knowledge regarding NEOs, overall definitions, the probability of an impact, different types of impacts, the potential consequences from such an impact, other impact assessment tools and the information they can provide, different ways of performing mitigation and finally an overview into evacuation surveys, strategies and evacuation simulation.

Chapter 3 provides an analysis of available global datasets and available road network data.

Chapter 4 concentrates on the human vulnerability and how models have been developed that can provide useful measures of human vulnerability. It will also describe the testing of these models, a number of case studies and their corresponding results.

This is followed by an investigation into how road network data can be converted into global gridded data which should be used in a coarse-scale evacuation simulator.

Chapter 5 also presents a number of behaviour-based evacuation travel models developed in order to describe household's decision-making and evacuation travel patterns. The last sections of Chapter 5 describe the coarse-scale flow-based evacuation simulation software developed along with other models and general assumptions used in this simulator. There will also be testing of the models used as well as multiple case studies and their results. The final case studies will be investigations into how evacuations can reduce the expected number of human casualties.

Chapter 6 provides the overall discussion of the developed models, tools and simulators. The outcomes generated from using them. Finally there will be a discussion into how to improve these models and into areas of possible future work.

The conclusion regarding the results and outcomes from this thesis are covered in Chapter 7.

A number of appendices will provide additional information regarding e.g. global datasets, the investigation into how time of day can affect the models and about CEMEvac, an agent based micro-simulator for simulating evacuation.

Chapter 2
NEO Threat Analysis

The threat of NEO impacts is global and the outcome, potentially, is many times more devastating than any of the more regularly occurring natural disasters. Due to the unique ability of observing an approaching NEO prior to impact using telescopes, such a disaster can be fully or partly avoided using different mitigation techniques such as deflection, fragmentation or evacuation. Before such techniques can be applied information regarding the following topics are needed:

- risk
- exposure
- vulnerability
- response

Risk is defined by the UNDP as

"The probability of harmful consequences, or expected loss of lives, people injured, property, livelihood, economic activity disrupted (or environmental damage) resulting from interactions between natural or human induced hazards and vulnerable conditions." (UNDP 2004)

In the context of an NEO impact the risk is initially defined as the probability of potential loss within a large area in which the NEO will travel called a risk corridor.

According to the Oxford dictionary Exposure is:

"The state of having no protection from something harmful" (Oxford 2010)

Exposure can be exposure to the physical effects from a NEO impact on the Earth, on humans, the environment or the infrastructure. Human exposure depends, amongst other things, on the physical effects from the NEO impact along with the possibility of shelter.

Vulnerability can for example be human, social, economic and environmental. Vulnerability is defined as:

Vulnerability is an objective measure of the effects and damage on people, infrastructure, building, economy and the environment due to a specific hazard at a given time.

This definition is inspired by the definition from Blaikie et al. (1994)

"Vulnerability is a measure of the extent to which a community, structure, service or geographical area is likely to be damaged or disrupted, on account of its nature or location, by the impact of a particular disaster hazard."

Response describes what can be done in reply to the hazard. Response is both about what can be done prior to the arrival of a hazard and after the hazard occurs.

This chapter looks at NEOs along with the impact probability and the uncertainty attached to it, the physical effect from an impact on the Earth, the wider effects from an impact on the Earth such as social, economic and psychological. Finally ways of mitigating are discussed.

Section 2.1 investigates the NEO population, how the different types of NEOs are defined, how much is currently known about NEOs and the NEO population, how possible impacts are predicted, the impact probability and the uncertainty in these predictions.

In part 2.2 possible NEO impacts on the Earth are discussed along with possible consequences that can be expected after an impact. There will also be a brief description of the impact analysis tools that already exist.

The third section 2.3, investigates how the threat from NEOs can be approached through different mitigation techniques.

Section 2.4 provides a summary of Chapter 2.

2.1 NEOs

The following section considers in detail the different types of NEOs, their composition and their origin.

2.1.1 NEO types and definitions

NEOs can be divided into three subcategories: asteroids, comets and meteoroids.

Asteroids

Most asteroids originate from the main asteroid reservoir located between the orbits of Mars and Jupiter (Chaisson et al. 2002), but some are also located 60^{o} ahead and 60^{o} behind Jupiter (Chapman 2004) in orbit around Jupiter's two stable Lagrangian points (Chaisson et al. 2002). Asteroids can be divided into three main categories, C-type, S-type and M-type based on their composition. Table 2.1 provides an overview of the type, composition, density, main features and the expected percentage of the different types of asteroids, and shows that most asteroids are C-type asteroids, which also are the darkest type and, therefore, more difficult to observe with a normal telescope (Chaisson et al. 2002, Carry 2012, Margot et al. 2003).

Table 2.1: Asteroid types (Chaisson et al. 2002, Carry 2012, Margot et al. 2003).

Asteroid type	Composition	Density [g cm^{-3}]	Main feature	Percentage of asteroids being this type
C-type Carbonaceous	Large amounts of carbon	1.57 ± 1.38	The darkest type	75%
S-type Silicaceous	Rocky/silicate material	2.66 ± 1.29	More reflective/bright	15%
M-type Metallic	Iron and nickel fractions	2.37 ± 0.4 (asteroid 22 Kalliope)	Moderately bright	10%

Comets

Comets can be divided into two groups. The first group, called short period comets, are those originating from the Edgeworth - Kuiper Belt beyond the Neptune orbit. The second group, long period comets, originates from the Oort cloud (Atkinson 2000, Chaisson et al. 2002, Morbidelli et al. 2002). Table 2.2 describes key differences between the two types of comets.

Table 2.2: Comet types.

Comet type	Origin	Orbital period	Orbit type	Distance from the Sun
Short period comets	Edgeworth - Kuiper Belt	< 200 years	Roughly circular	Between 30 and 100 AU
Long period comets	Oort cloud	>= 200 years	Highly elliptical	As far as 50,000 AU

Comets contain a mixture of gas, iron and dust. Due to the temperature, the gas is like packed ice with an average density of around 100 kg/m^3. Their masses range from around 10^{12} to 10^{16} kg (Chaisson et al. 2002).

Meteoroids

Meteoroids are small fragments from asteroids and comets and a few are believed to be fragments from large impacts on planets. Meteoroids from comets are created when comets approach the Sun. A few astronomical units (AU) from the Sun, the comet starts to release large amounts of material (Chaisson et al. 2002). These comet fragments create clusters of meteoroids like the Taurids Meteor Stream (Napier 1997) and the Perseid shower (Chaisson et al. 2002).

From asteroid, comet and meteoroid to NEO

An asteroid, comet or meteoroid is classified as a NEO when its closest approach to the Sun (perihelion) is less than 1.3 AU (1AU = 149 597 871 km), which is the average of the Earth distance to the Sun and Mars' distance to the Sun. NEOs can be divided into several groups based on certain definitions. Table 2.3 shows the various types of NEOs, their definitions and a short description. *Q* is the orbit aphelion, *q* is the perihelion, *a* is the semi-major axis, *d* is the object diameter, *H* is the absolute magnitude and *P* is the orbital period. The perihelion for a NEO orbiting the Sun is the point of the

orbit which is nearest the Sun. The aphelion is the point where the NEO is furthest away from the Sun.

Table 2.3: Types of NEOs and their definitions.

Type	Definition	Description
NEO	$q < 1.3$ AU and $Q > 0.983$ AU	Interplanetary Object with a closest approach to the Sun (perihelion) of less than 1.3 AU and an aphelion > 0.983, which is the same as the perihelion for the Earth
NEA (Near Earth Asteroid)	$q < 1.3$ AU and $Q > 0.983$ AU	Asteroid with a closest approach to the Sun of less than 1.3 AU and an aphelion > 0.983
NEC (Near Earth Comet)	$q < 1.3$ AU and $Q > 0.983$ AU and $P < 200$ years	Comet with a closest approach to the Sun of less than 1.3 AU and an aphelion > 0.983
PHO (Potentially Hazardous Object)	$d \geq 50$m and $q \leq 0.05$AU (Earth Minimum Orbit Intersection Distance (MOID))	Object with a diameter of more than 50 m and with a perihelion of less than 0.05 AU
PHA (Potentially Hazardous Asteroid)	$q \leq 0.05$AU and H<=22	Asteroid with a diameter of more than 50 m and with a perihelion of less than 0.05 AU
PHC (Potentially Hazardous Comet)	$q \leq 0.05$AU	Comets with a diameter of more than 50 m and with a perihelion of less than 0.05 AU
Apollos	$a \geq 1.0$ AU and $q \leq 1.0167$ AU	Earth-crossing NEA with a semi major-axis larger than Earth's
Atens	$a < 1.0$ AU and $Q \geq 0.983$ AU	Earth-crossing NEA with a semi major-axis smaller than Earth's
Amors	$a \geq 1.0$ AU and 1.0167 AU $< q \leq 1.3$ AU	Earth-approaching NEA with orbit perihelion larger than the Earth perihelion but smaller than the defined NEO perihelion
IEO (Inner Earth Object) / Atiras / Apoheles	$Q < 0.983$ AU	Interplanetary object with an orbit aphelion smaller than Earth's perihelion

2.1.2 NEO population

Due to a great effort from the astronomical community, large databases containing detailed observatory knowledge regarding NEOs have been created and are regularly being updated with new NEO discoveries. The Italian-based Near Earth Object Dynamic Site (NEODyS) database and NASA's Small-Body Database are the two main sources and most data are accessible by the public. A large number of surveys have been performed in an attempt to find most of the larger asteroids (≥250 m in diameter) and asteroids in orbits such as IEOs.

Current surveys, such as the NASA survey program of Near-Earth Objects (NEO), are now aiming to detect, track, catalogue and characterize 90 percent of PHOs with a diameter greater than 140 m and whose orbit pass within 0.05 AU of the Earth's orbit by 2020 (NASA 2007).

In January 2009 and again in September 2011 the NEODyS Database was used to collect the number of known asteroids based on their diameter and absolute magnitude. The results can be found in figure 2.1. This figure shows the number of NEOs as a function of diameter (*d*) and absolute magnitude (*H*). The graph reveals that the database has grown. The most noticeable growth is sub kilometre NEOs with diameters of around 25 m. Here an increase of almost 98% was observed in the number of known NEOs with a diameter between 11 and 37 m. It is important to note that comets represent only about 1% of the hazard from NEOs (Chapman 2008).

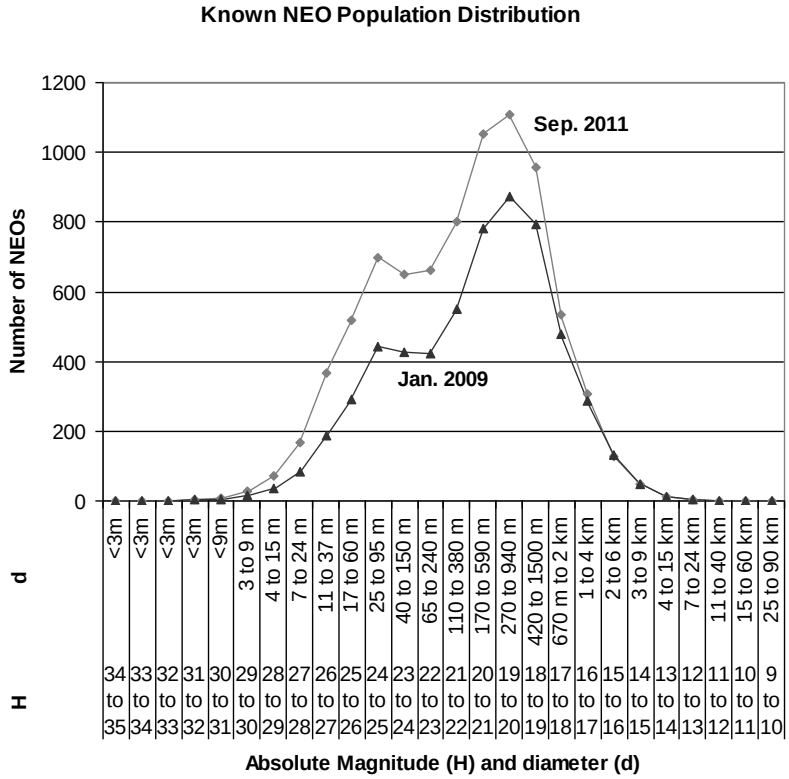

Figure 2.1: Number of known NEOs in the NEODyS database in January 2009 and September 2011 based on diameter (d) and absolute magnitude (H).

A power law has been fitted to the cumulative number of NEOs with an absolute magnitude between 9 and 18, this was done based on the assumption that within this size distribution of NEOs almost 90% of NEOs have been observed. Figure 2.2 shows this cumulative model along with the data gathered from the NEODyS database. This model can be used to estimate the number of NEOs that still need to be observed. Ideally all

NEOs up to an absolute magnitude of 28 should be discovered in order to predict atmospheric explosions and impacts from NEOs such as the Chelyabinsk meteor. Figure 2.2 shows that ~230,000 NEOs still need to be observed in order to reach such a target.

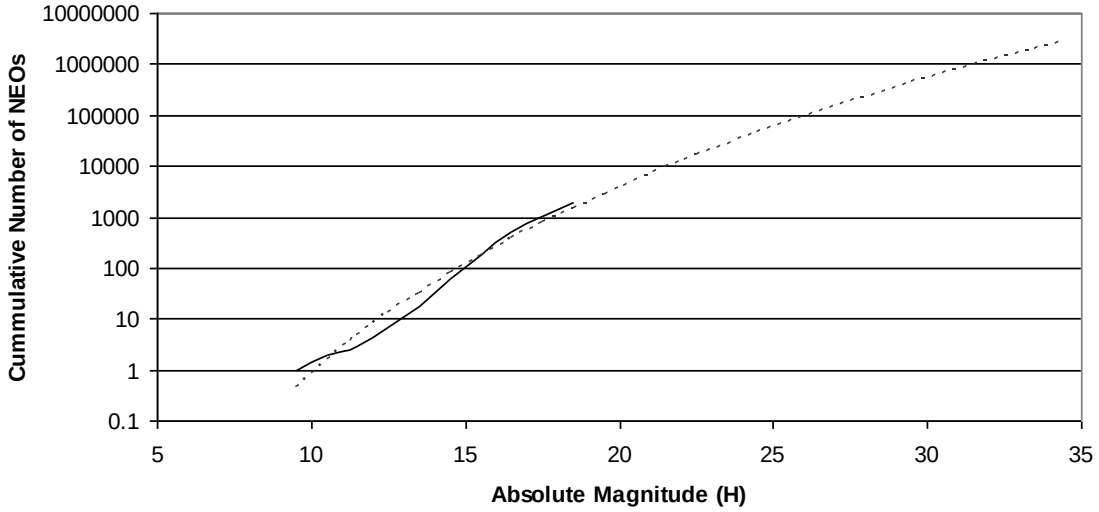

Figure 2.2: Cumulative number of NEOs (cumulative NEODyS data is the solid line and the cumulative model is the dashed line).

The large effort in observing NEOs has provided an increased knowledge of the NEO population and the risk of a NEO impact on Earth. However, there is still a need to catalogue the NEO population with a diameter > 50 m. These Tunguska-sized NEOs are the most likely Earth-impactors and would cause major, local damage. Observation campaigns could provide these data, whilst knowledge regarding NEO composition, shape, size and spin-rate could be achieved from rendezvous missions and flybys of particular NEOs.

2.1.3 NEO impact predictions

NEO impact predictions have large uncertainties attached to them. These uncertainties are, in part, due to the relatively low number of observations and the increasing uncertainties of extrapolating their orbits. Collisions and the gravitational forces from the planets and other larger objects such as the moon will also influence their

orbits. As more observations become available over time the uncertainties regarding the orbits are reduced.

Since the early 1980s several missions have been dedicated to the search for NEOs to gain more knowledge about their orbits, structure, composition and physical properties. Observational data about discovered NEOs are being collected in the NEODyS database and the Jet Propulsion Laboratory (JPL) Small-Body Database Search Engine.

To provide long-term prognoses of NEOs orbits Milani developed a novel approach to predict the future orbit of a NEO using Virtual Asteroids (VAs) (Milani et al. 2000) (NASA 2005). In order to account for the uncertainty in the orbit over time, a cloud of VAs are created. Each VA is a possible orbital outcome based on the currently known trajectory. The cloud of VAs is then propagated forwards in time. The many possible VAs will, when their orbits are propagated forward in time, create an area of possible future positions of the object. This area will have the shape of an elongated tube and is called a Line of Variance (LoV). With an increased number of observations the accuracy in the orbital prediction can be improved and the LoV will reduce in size. If a part of the LoV intersects the Earth, this part is called the risk corridor. The risk corridor shows the area where an impact could happen.

A NEO can have many close encounters with the Earth due to its frequently close passes, also called resonant returns. These encounters can be of great importance since the gravitational forces that the NEO will experience during such a close encounter either can cause an increase in NEO heliocentric velocity or a decrease in NEO heliocentric velocity and thereby a change in orbit. If a NEO passes behind the Earth, the Earth's gravitational forces will increase the sun-relative speed and thereby increate the orbit and the orbital period. If the NEO during its close encounter passes in front of the Earth the Earth's gravitational forces will decrease the sun-relative speed of the NEO and thereby shorten the orbit and the orbital period. Figure 2.3 illustrates the change in NEO speed due to the gravitational forces during a close encounter with the Earth. These changes in velocity can cause future close encounters to become an impact due to the changes to the NEO orbit. The region in space, where the gravitational forces change the relative speed of the NEO, and thereby its orbit in such a way that the probability of a future impact

increases is called a gravitational keyhole (Schweickart et al. 2007b, Valsecchi et al. 2003).

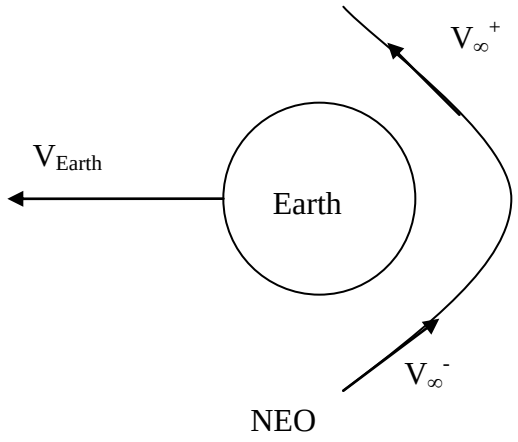

Figure 2.3: NEO close gravitational encounter with the Earth.

Gravitational keyholes and inverse keyholes (Jabbas)

During a close approach by a NEO with the Earth the gravitational forces from the Earth can change the speed of the NEO. In the previous section gravitational keyholes were explained as being regions where the gravitational forces from the Earth (and Moon) affect the speed of the NEO in such a way that the probability of a future NEO impact increases. A second type of uncertainty region has been identified. These regions are called inverse keyholes or Jabbas. Gravitational keyholes and jabbas will affect a NEO deflection mission in two different ways:

- A NEO that has undergone deflection, prior to passing through a gravitational keyhole, will see an amplification of the deflection it had undergone (Schweickart 2008b, Chodas 2011).
- Inverse keyholes or jabbas are regions located, 15-60 lunar distances from the Earth. A NEO that has undergone deflection, prior to passing through a jabba region, will have its deflection reduced (Chodas 2011).

How precise can a NEOs orbit be predicted

The precision with which a NEOs orbit can be predicted will depend on factors such as the number of observations, the time spanned by those observations, the quality of the observations (e.g. radar versus optical and ground-based versus space-based telescopes). The time spanned between observations generally has the greatest effect on the orbital uncertainty. When new observations become available the new orbital predictions can change greatly from previous predictions. Two examples of NEOs that recently have made close approaches and where the orbital uncertainties vary greatly are presented below in order to illustrate how greatly such orbital estimations can vary.

The first NEO is asteroid 2014 DO7. This 48 to 110 metre diameter asteroid had a close approach on the 6th March 2014 and its next close approach is predicted to be on the 2nd March 2130. It orbital parameters and their uncertainties given on the JPL Small-Body Database are listed in table 2.4 along with its orbital values.

The time uncertainty for the two close approaches is:

0.16 minutes for the 2014 close approach

4118 minutes for the 2130 close approach

The second NEO is asteroid 2005 EY95. This 230 to 520 metre diameter asteroid has been known for a long time and the list of close approaches provided on the JPL Small-Body Database show close approaches as early as 1904. Its orbital parameters and their uncertainties given on the JPL Small-Body Database are presented in table 2.5. The time uncertainty for the two close approaches is:

0.06 minutes for the 9th March 2014 close approach

0.09 minutes for the 7th July 2019 close approach

0.32 minutes for the 4th July 2020 close approach

0.79 minutes for the 20th September 2020 close approach

The time uncertainty grows with the growing time duration to the close approach.

The uncertainties for the orbital parameters for asteroid 2005 EY95 are much lower than for asteroid 2014 DO7. Knowing that asteroid 2005 EY95 has made several close approaches since its discovery by Catalina Sky Survey on the 5th March 2005 could also mean that more observation data are available, making the orbit predictions more precise.

Table 2.4: Asteroid 2014 DO7 orbit values and uncertainties from the JPL Small-Body Database.

Element	Value	Uncertainty (1-sigma)	Units
e	0.40091589730711	0.00047519	
a	1.685556954091082	0.0013707	AU
q	1.009790375379417	2.019e-05	AU
i	13.5660398970744	0.011843	deg
node	154.3971983318311	0.0019275	deg
peri	35.14924846082375	0.00074778	deg
M	24.67750277285746	0.028906	deg
tp	2456745.708614435076 (2014-Mar-29.20861444)	0.0026545	JED
period	799.306922784256 2.19	0.97498 0.002669	d yr
n	0.45039019397705	0.00054938	deg/d
Q	2.361323532802747	0.0019202	AU

Table 2.5: Asteroid 2005 EY95 orbit values and uncertainties from the JPL Small-Body Database.

Element	Value	Uncertainty (1-sigma)	Units
e	0.5383344308710299	8.1216e-08	
a	1.083432161809646	1.1162e-08	AU
q	0.5001833255944804	8.67e-08	AU
i	3.169896403737441	6.9247e-06	deg
node	72.92723522214183	0.00017726	deg
peri	342.0600855016141	0.00017773	deg
M	116.8694489554668	5.5996e-05	deg
tp	2456666.779033247838 (2014-Jan-09.27903325)	6.2272e-05	JED
period	411.9087448518899 1.13	6.3654e-06 1.743e-08	d yr
n	0.8739799882846508	1.3506e-08	deg/d
Q	1.666680998024811	1.7171e-08	AU

2.2 NEO impact

The magnitude of a NEO impact hazard depends on the energy of the NEO along with its composition, impact angle and impact location. The typical Earth-relative speed for NEAs is between 15 and 30 km s^{-1}. For NECs the Earth-relative speed is much higher, at around 75 km s^{-1} (Atkinson 2000). The Earth's atmosphere provides good protection against NEOs with a diameter of less than ~30 m, but NEOs larger than ~30 m in diameter could reach the Earth's surface along with small m-type NEOs that are much stronger due to their metallic composition, as was the case in the Carancas impact event. The 15-m in diameter crater in Peru was created by a 2.5 m-diameter meteorite (Tancredi

et al. 2009). Table 2.6 shows the impact consequences due to differently sized NEOs (NASA 2000c). The affected area increases with respect to e.g. the NEO diameter, NEO composition and NEO impact energy.

Table 2.6: Impact consequences.

NEO diameter [metre]	Impact consequences
0-20	Very local
20-100	Local
100-1000	Regional
1000-	Global

An impact event can be divided into three stages (Toon et al. 1997):

1. Interaction between the object and atmosphere
2. Interaction between the object and surface
3. Interaction between the debris cloud and the atmosphere

When an object starts entering the atmosphere, the increase in pressure causes it to heat up and a bow shock is formed in front of it. The surrounding air is also heated and turns into a hot plasma. Large stresses, due to the increased pressure in front of the object and the decrease in pressure behind the object, are applied on the object during it's descent through the atmosphere. This difference in pressure can be equated to a force. If this force is greater than the forces holding the object together the object will break up into several smaller fragments. In the event where the NEO cannot withstand the forces and temperature applied to it during its descent through the atmosphere the NEO will explode in the atmosphere and create a blast wave and thermal radiation. Boslough et al. (2008) identified two types of airbursts. The first is a Tunguska-type airburst, where the explosion of the NEO will happen at an altitude high enough (this altitude will depend on the properties of the NEO along with its impact angle) so that the effects from this explosion experienced on the Earth surface primarily will be a blast wave and a small fraction of thermal radiation. The second type is a Libyan Desert-type airburst where the atmospheric explosion occurs at an altitude where the effects experienced on the Earth

surface from the explosion both will be a blast wave and a large proportion of the thermal radiation.

If the object survives its descent through the atmosphere it can either hit the ocean or land. The following two sections will describe the effects that could be experienced from a NEO ocean impact and a NEO land impact respectively.

2.2.1 Ocean impact

With 71% of the Earth being covered by oceans an ocean impact is the most likely type of NEO impact (NOAA 2009). An impact in the ocean would result in tsunami-like waves and, and if hitting the seafloor, earthquakes and underwater land slides (Atkinson 2000). The NEO energy is primarily converted into thermal energy, kinetic energy of ejecta and kinetic energy is transferred to the water. Large amounts of water and material are injected into the atmosphere. Multiple scenarios of how this injection of water into the atmosphere will influence the climate both short and long-term should be considered (Pierazzo et al. 2010). In one scenario a water-steam cloud would rise to around 100 km where the water-steam converts into ice crystals. These would then descend, evaporate and result in a drop in temperature. Another scenario is where water is injected into the upper atmosphere. This would result in an increase in temperature on Earth due to a greenhouse effect. The injected water is also a good infra-red radiator and as such it will cause a further drop in temperature. These are competing effects and it is uncertain how they would affect the climate both short and long term (Toon et al. 1997).

Several ocean impact models have been developed. Three of these models will be described in this section.

The model of Ward et al. (2000) uses probabilistic hazard assessment by coupling the probability of asteroid impacts with idealizations of oceanic cavity formation and linear theories of tsunami propagation and shoaling. In Ward's model the depth and diameter of parabolic impact cavities with respect to asteroid density, radius, and impact velocity are first calculated. Then, linear tsunami theory is used to illustrate how these cavities evolve into sea surface waveforms. This is done by propagating these waveforms in distance and time. Finally, maximum wave amplitudes at many distances for a variety

of impactor sizes are measured and a simplified attenuation relation is derived. It is important to note that Ward's model assumes uniform depth oceans.

Hills et al. (2001) simulate an ocean impact using shallow water approximation. Their models are among others using a shallow-water SWAN code, developed by Dr. Charles L. Mader which solves the long wave, shallow water, nonlinear equations of fluid flow.

Ward et al. (2000) compared the result from their own model with results generated by Hills et al. (1994) and Crawford et al. (1998). Table 2.7 show these results. The estimated wave amplitude expected 1000 km from a deep ocean impact location varies between imperceptible and 15 m according to table 2.7.

Table 2.7: Estimated deepwater wave height (above sea level) from a NEO impact.

NEO diameter (m)	Distance from Impact (km)	Wave amplitude (m)	Model by
250	1000	15	Hills et al. 1994
250	1000	~0	Crawford et al. 1998
250	60	10	Crawford et al. 1998
250	1000	7	Ward et al. 1999

The third model developed by Gisler et al. (2009) is a detailed wave model. The results from this model shows that the waves generated, in the event of a mid ocean impact, will break up in mid-ocean due to turbulence within the waves. Gisler et al. argue that the waves that are produced due to a NEO ocean impact are of shorter length and lower speed. Their shape is chaotic and the wave amplitude will decay more rapidly. They will therefore not propagate over long distances. These results show that the hazard coming from the waves generated by impacting NEOs to the coastal regions might not be as large as suggested by Ward and Hills, depending on the size of the impactor and the impact location. Deep water impacts by asteroids with a diameter less than 500 m do not pose a significant risk, according to Gisler, regarding the development of tsunami-like waves that could travel long distances.

A NEO impact in more shallow water would create an underwater crater when the water depth is less than 5-7 times the asteroid's diameter, and tsunami-like waves that will reach nearby shores (Gisler et al. 2010).

The atmospheric effects from a water impact are the most dangerous to humans according to Gisler, with hurricane force winds that can extend tens of kilometres from the impact location (Gisler et al. 2010). There will be a ground shock, hot winds (60 to 65 degrees Celsius) and overpressure "pulses" of 20-40% overpressure that could cause severe local damage (Gisler 2011).

2.2.2 Land impact

A NEO land impact will cause the following physical effects: When reaching the Earth's surface, the energy contained in a NEO is released in an explosion releasing heat and creating a blast wave. The plasma and hot pulverized material is ejected at orbital or near-orbital speeds and a large crater is created. The crater size and type depends on the size, composition and energy of the impactor and the local geology in the impact region. Distinctive signs in an impact crater are the presence of rock that has undergone huge temperatures and blast wave-induced shatter cones, melted rocks, and crystal deformations. Land craters can be divided into two types of craters.

1. Simple craters
2. Complex craters.

A simple crater is a straightforward bowl in the ground and is generally less than four kilometres across on Earth. A perfect example of a simple crater is the Barringer crater in Arizona. Complex craters are generally larger. They have uplifted centres that are surrounded by a trough and the rims are broken. The uplifted centre is created by the "rebound" of the earth after the impact. The transition at which a crater goes from a simple to a complex crater is around 3.2 km on the Earth (Collins et al. 2005).

The ejecta created from the impact are blown back into the atmosphere and will over time re-enter. The ejecta can travel several times around the planet before re-entering as secondary meteors in the event of a very large impact. Chemical reactions and the heat can ignite fires that will generate soot and poison the air. Acid rain and damage

to the ozone layer are also effects that can be expected. The depletion of the ozone layer would result in more ultra-violet radiation from the Sun reaching the surface. Electromagnetic disturbances in the upper atmosphere can affect radio communication and result in power line failures. Earthquakes and volcanic activity are also possible events (Atkinson 2000). The large amounts of matter that is injected into the atmosphere could create long-term environmental problems such as cooling down of the planet for a considerable time, such as month, years and even decades, as mentioned earlier (Toon et al. 1997). This would create secondary hazards such as a reduction in global food production and result in famine in the most vulnerable places on Earth. Another secondary hazard that has been investigated by Schuiling is the release of toxic and flammable gasses from the bottom of lakes and oceans such as the Black Sea in the event of a NEO water impact. These gasses might kill more people than the actual tsunami wave (Schuiling 2007).

The land impact model from Collins et al. (2005) looks at the different impact stages and the effects from the different hazards such as impact energy, crater size, thermal radiation, seismic effects, ejecta and air blast and was used as a basis for NEOimpactor and NEOSim. The energy is calculated using the relativistic energy equation.

The crater formation depends on the NEO size, composition and energy along with local geology. Collins et al (2005) uses following equation to calculate the transient crater:

$$D_{tc} = 1.161 \left(\frac{p_i}{p_t} \right)^{1/3} L^{0.78} v_i^{0.44} g_E^{-0.22} \sin^{1/3} \theta \ , \qquad (2.1)$$

where p_i is the density of the impactor (kg m^{-3}), p_t is the density of the target (kg m^{-3}), L is the diameter of the impactor after atmospheric entry (m), V_i is the impact velocity at the surface (m s^{-1}), g_E is the Earth surface gravity and θ is impact angle measured to the horizontal. This is followed by an equation to calculate rim to rim diameter of a simple crater:

$$D_{fr} \approx 1.25 \, D_{tc} \qquad (2.2)$$

The depth of the transient crater is given by:

$$d_{tc} = D_{tc} / (2\sqrt{2}) \quad (2.3)$$

And the final crater depth from rim to crater floor is:

$$d_{fr} = d_{tc} + h_{fr} - t_{br}, \quad (2.4)$$

where h_{fr} is the rim height and t_{br} is the thickness of the breccia lens.

For the complex crater with a diameter larger than 3.2 km the rim-to-rim diameter is:

$$D_{fr} = 1.17 \frac{D_{tc}^{1.13}}{D_c^{0.13}}, \quad (2.5)$$

where D_c is the diameter (km) at which a crater changes from being simple to become complex. The average depth for the complex crater (from rim to crater floor) is given by:

$$d_{fr} = 0.4 D_{fr}^{0.3} \quad (2.6)$$

The fireball radius in m depends on the impact energy in joules and is defined as:

$$R_f = 0.027 E^{1/3}, \quad (2.7)$$

where E is the impact energy.

The thermal exposure Φ is defined as the amount of heating per unit area at a specified location and can be derived as:

$$\phi = \frac{\eta E}{2\pi r^2}, \quad (2.8)$$

where η is a small fraction of the impact emergy E, so ηE is the total amount of thermal energy radiated. As the heat reduces over time the duration of irradiation is:

$$\tau_t = \frac{\eta E}{2\pi r_{f*}^2 \sigma T_*^4}, \quad (2.9)$$

where σT_*^4 is the radiant energy flux, where σ is set to be 5.67 × 10-8 W m^{-2} K^{-4} and T_* = 3000 K. Whether a given material catches fire will depend on both the thermal exposure and the duration of irradiation and can be calculated as follows:

$$\phi_{ignition} \approx T_{ignition} \rho c_p \sqrt{\kappa \tau_t}, \quad (2.8)$$

where $\Phi_{ignition}$ is the thermal exposure required to ignite a material, $T_{ignition}$ is the ignition temperature, ρ_{is} the density, c_p is the heat capacity. κ is the thermal diffusivety of the material that is heated, which is the thermal conductivity divided by density and specific heat capacity at a constant pressure. It is a measure of a materials ability to conduct thermal energy relative to its ability to store thermal energy. τ_t is the irradiation time.

In order to estimate the seismic effect following assumption has been used by Collins et al. (2005): *'the "seismic efficiency" (the fraction of the kinetic energy of the impact that ends up as seismic wave energy) is one part in ten thousand (1 × 10−4)'*. The Gutenberg-Richter magnitude energy relation is then used to calculate the seismic magnitude M. The seismic effects models depend on the distance from the impact location, r_{km} (in km). Three models are used:

$$M_{eff} = M - 0.0238\ r_{km} \quad \text{for } r_{km} < 60 \text{ km} \tag{2.9}$$

$$M_{eff} = M - 0.0048\ r_{km} - 1.1644 \quad \text{for } 60 \leq r_{km} < 700 \text{ km} \tag{2.10}$$

$$M_{eff} = M - 1.66 \log_{10} \Delta - 6.399 \quad \text{for } r_{km} \geq 700 \text{ km} \tag{2.11}$$

Where M_{eff} is the effective seismic magnitude and M is the seismic magnitude at the impact location.

The maximum ejecta thickness depends on the transient crater rim height h_{tr}, the depth of the transient crater and the distance from the impact location and is given by:

$$t_e = \frac{h_{tr}}{8}\left(\frac{d_{tr}}{r}\right)^3 \tag{2.12}$$

Finally the air blast the peak wind velocity is given by:

$$u = \frac{5p}{7P_0}\frac{c_0}{(1 + 6p/7P_0)^{0.5}}, \tag{2.13}$$

where p is the overpressure, P_0 is the ambient pressure and c_0 is the ambient sound speed in air. For more detailed information regarding the equations and how they have been derived please read Collins et al. 2005.

2.2.3 Social and economic impact

Natural hazards, not only cause physical destruction and damage, but also affect the economy and can cause psychological and social problems. In Cardona (1997) the threat of a volcano erupting close to populated areas resulted in social and economic problems. This was in fact due to how the local authorities handled the situation. Scientists had difficulties in forecasting the behaviour of the volcano, political authorities were reluctant to accept the risk and there was an inadequate management of the warning

that was issued. This resulted in large parts of the population being inadequately prepared. Problems such as anxiety among the population, recession and unemployment were some of the outcomes. This example illustrates the importance of clear communication between the authorities, scientists and the public, and the need for educating the public about the threat. How people would react to natural hazards and the social impact varies and depends on age, gender, education, ethnic minorities, income, religion (AIAA 2007, Drabek 1999), acceptance of risk (Starr 1969) and whether it is a small town or a megacity that is under threat (Cross 2001). All these dependencies can be merged into a single measure "Social Capital" which is the "Stocks of social trust, norms and networks that people derive from membership in different types of social collectives" (UNDP 2004).

Secondary and tertiary hazards were not described in the previous sections, but should be taken into account. The many primary hazards due to a land impact, ocean impact or atmospheric explosion would, in an inhabited area, cause many secondary hazards such as falling power lines, broken water pipes and gas pipes which could cause local fires and explosions. With the local health services being affected along with the sanitation, there is a high risk for diseases such as cholera, as was experienced in Haiti after the 2010 earthquake (BBC 2010).

The economic impacts from damaged infrastructure, workplaces and from relocation of people must also be considered. This could create a social distortion, and in the worst case, a recession as was observed by Cardona (1997) and for New Orleans after hurricane Katrina (Cashell et al. 2005).

2.2.4 Post disaster habitation and shelter

When a natural hazard strikes evacuating people from the worst affected areas is crucial. This should ideally happen prior to the hazard, though this is not always possible. Prior to an evacuation it is useful to have some estimates regarding how many are expected to be evacuating. This can be done by using local population data or global population density maps along with knowledge regarding the expected physical effects from the approaching hazard and the extent of the area that is likely to be affected.

Knowledge regarding the expected physical effects from the approaching hazard on infrastructure and housing e.g. damage to roof, windows, walls and partly or complete collapse, can be used for estimating the amount of different types of shelters needed for the evacuated population. The physical effects on homes and infrastructure will have great importance on how long evacuees have to stay away from home. Evacuees can be divided into four groups and these are often colour-coded (black, red, amber and green) also called BRAG by e.g. insurance companies (Jorgensen 2011). People in the black group are those that have to be permanently resettled. Their homes have been completely destroyed or are in danger of collapsing and it is not advisable for them to move back and rebuild. After the magnitude 6.3 earthquake in February 2011 near Christchurch, New Zealand many properties where found to be unsafe to return to and the state started buying these homes. People could then use the money to buy another home or rebuild their home elsewhere (Hartevelt 2011). The red group are people where their homes are completely destroyed or badly damaged and where a rebuild is necessary. These people will need long-term accommodation until their homes have been replaced. In the amber group, people's homes have been damaged and repairs might take up to a few months. This group of people need shorter-term shelter. In the green group, people's homes have escaped undamaged or with minor damage. These people can return very shortly after the hazardous event has passed and their neighbourhood has been declared safe.

The psychological effects from living in sheltered accommodation increases with the duration of the stay: long stays introduce more noticeable psychological effects on evacuees. Not being able to return to their homes and not knowing when they will have a permanent home is very stressful (Galea et al. 2007). Being dependent on charity and not being able to get back to work or school along with the traumatic experience of evacuating, causes a perception of control loss which can cause mental health problems such as depression, sleep disorders and anxiety (Harrison 2007). It is, therefore, extremely important to try and make the stay as short as possible and keep the evacuees active by asking them to help run the camp and work on the reconstruction and repairs.

The type of shelters used will depend on the duration people are expected to stay in the camps along with the geographic location and the local climate. Short-term accommodation can be schools, church or sports halls and other buildings where people

can stay for a short duration. Tent camps can also be used for the short-term depending on location and time of year. Camps where people are expected to stay for the long-term should have shelters that can cope with changing weather conditions and the long-term usage. There are several examples from the past where either the wrong types of shelters were provided or an unhealthy camp location was chosen. For example, after the Pakistan earthquake in 2006, people were provided with tents that were not suitable for the cold winter in the mountains (Rivers 2006) and a UN evacuation camp in Kosovo was located on a site heavily polluted by lead, causing serious health problems among all evacuees (Thorpe 2009).

2.2.5 Interconnectedness of the NEO threat

In the previous sections a number of primary, secondary and tertiary hazards that could be the potential outcome of a NEO impact have been mentioned. This domino effect could affect human lives as well as the economy as has been observed in the following major hazards such as the 2005 Hurricane Katrina, the 2010 Haiti earthquake and the 2011 Japan earthquake that resulted in a major tsunami wave hitting the coast of Japan.

Figure 2.4 show the close interconnectedness between the NEO hazard and its primary, secondary and tertiary hazards. This figure provides an overview of links between hazards and illustrates how different hazards can result in many other hazards locally, nationally and globally.

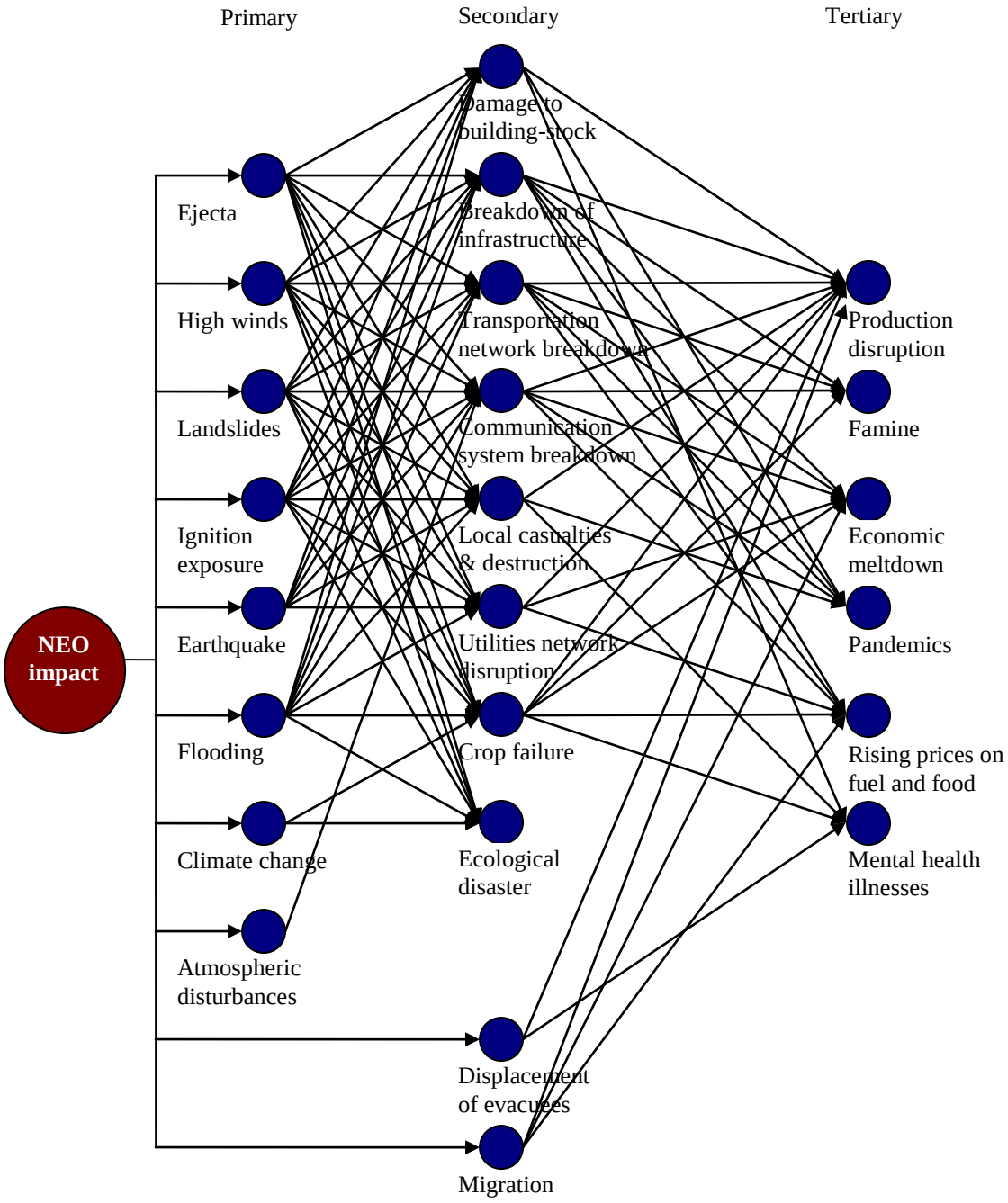

Figure 2.4: Primary, secondary and tertiary hazards caused by a NEO impact.

2.2.6 NEOimpactor, NEOSim and Impact Earth

At the University of Southampton a software package entitled, NEOimpactor, was developed, which addresses not only the physical effects from a NEO impact but also the social and economic consequences of a NEO impact event (Bailey et al. 2007). The social

consequences are addressed by calculating the expected number of casualties due to the different physical hazards e.g. crater, ejecta, blast wave, ignition exposure, earthquake for land impacts. The economic consequences are based on damage assessment in the form of loss of wealth. The physics used to estimate the physical hazard due to a NEO impact are, in this tool, based on the land impact model developed by Collins et al. (2005) and the ocean model from Ward et al. (2000). The results from the NEOimpactor predict the human and economic losses in individual countries to a NEO impact. Countries were then ranked based on human and economic loss. This provides a type of global Disaster Risk Index (DRI) (UNDP 2004) for NEO impacts.

NEOSim is a similar type of software, developed by Andrew Morley. This tool uses the physical impact models, primarily from Collins et al. (2005). The human loss models used were primarily based on textual descriptions from Collins et al. (2005) regarding how people, infrastructure and buildings would be affected by the individual hazards. These descriptions were converted into a percentage of human loss due to the hazard magnitude but they do not take into account any uncertainties.

The third impact simulator Impact Earth was developed by Collins et al. and can only provide information regarding the physical effects and some textual description of expected hazards and their impact on people, buildings and infrastructure at a specific distance from the impact location. It benefits from an easy to use online user interface.

The physical impact simulators in NEOSim, NEOimpactor and Impact Earth do not take into account geological features and building strength. Such factors could potentially modify the local physical impact and the level of damage caused by the individual hazards. Hills or mountains could shelter communities from the worst effects of the blast wave or the ignition exposure, and valleys could act as funnels increasing the damage from these sub-hazards, as observed in nuclear tests (Glasstone et al. 1977).

Geology also plays an important role when simulating earthquakes. Local geological features and composition can change the speed of earthquake waves. It is important to note that earthquakes are subterranean events and the depth at which the earthquake originates will influence the effects experienced on the Earth's surface. In contrast, a NEO impact creates seismic waves on the Earth's surface. A NEO impact should be regarded as a shallow or crustal earthquake and it is important to note that the

seismic waves which are created at the Earth's surface in the event of a shallow earthquake cause most destruction (Cascadia 2009).

2.3 NEO risk analysis and mitigation

Classic risk analysis usually consists of four parts (Coburn et al. 1994):

1. Identify the hazard.
2. Investigate the probability of that hazard occurring.
3. Identify and calculate the vulnerability that relates to that hazard.
4. Identify possible action to take to reduce the vulnerability.

In this case, the hazard is a NEO impact. The probability of the hazard occurring is reflected in the risk corridor, which is the subsection of the LoV that intersects the Earth, the number of possible resonant returns and the NEO size, composition and energy distribution. The risk corridor provides the probability of a NEO impact occurring during a specific orbit, while the resonant returns provides the probability of the NEO impact occurring on a number of occasions. Finally the NEO size, composition and energy distribution provides the means to estimate the extent of damage that a specific NEO potentially could cause should it impact with the Earth. The NEO size distribution follows a power law, where the number of NEAs increases with decreasing size (Chapman 2004). With an expected Earth impact frequency of Tunguska sized NEOs being once every 2000 years (Harris 2009) and the expected impact frequency of a 1 km diameter NEO being once every 600.000 years the probability of a smaller Tunguska sized NEO impacting is 300 times higher than the probability of a kilometre-sized NEO impacting.

The extent of the physical effects depends on the NEO energy and the impact location e.g. shallow water ocean impact, deep water ocean impact, low altitude airburst, high altitude airburst, land impact and the geological features in the affected region, see section 2.2 to 2.2.3 for details regarding different physical impacts effects. The vulnerability is closely related to the physical effects expected from a NEO impact e.g. a

land impact in close proximity to populated areas is likely to cause a higher casualty number due to damaged or collapsing buildings, damaged infrastructure, falling trees and fires compared to an impact in a remote region. The possible actions to take will depend on the notice time and the NEO energy, size, composition and the impact location.

There are four ways to approach an actual NEO impact threat depending on the particular scenario (Chapman et al. 2006):

1. Continue remotely to observe the object.
2. Launch a spacecraft transponder mission in order to improve the knowledge about the NEO.
3. Launch a spacecraft mission to either deflect or fragment the approaching NEO.
4. Prepare for impact by mitigating the consequences of an impact. Different mitigation methods are described in section 2.3.2 to 2.3.5.

The approach used will depend on the scenario. In e.g. scenario 1, just continuing to remotely observe a NEO is enough since this often improves the knowledge regarding the orbit and an impact can be ruled out. In the event where the probability of an impact is high the other approaches should be considered. If there is sufficient lead time to send a transponder mission followed by a deflection mission this could be considered. The transponder mission could provide crucial details regarding the specific NEO, which is of importance when choosing a mitigation strategy and to ensure a successful outcome of the mitigation mission.

Various types of people involved in decision-making and performing the tasks has been identified. Table 2.8 provides a list of these groups of people and their roles (Schweickart 2008) (Lindell et al. 2005).

With the current aim from NASA to detect 90 percent of PHOs with a diameter greater than 140 m and whose orbit pass within 0.05 AU of the Earth’s orbit by 2020 (NASA 2007) and with NEOs as small as 2.5 m-diameter causing damage on the Earth (see the Carancas impact event in section 1.1 or Tancredi et al. (2009)), there is still a need to find more NEOs with a diameter smaller than 140 m. In section 2.1.2 a

cumulative model was derived that shows the expected number of NEOs above a specific absolute magnitude. The outcome from this model showed that for NEOs with an absolute magnitude smaller than 28 around 230,000 NEOs still need to be observed. In the likely event where a NEO impacts the Earth without prior having been observed the use of any deflection, fragmentation or pre evacuation strategies will not be possible. The only thing to do is to develop a society that is less vulnerable to disasters (Coburn et al. 1994) and become better at coping with the aftermath. "A strong economy is the best defence against disaster" according to (Coburn et al. 1994), but actions such as engineering and construction, physical planning along with institutional and social measures are also important (Coburn et al. 1994b).

Table 2.8: Decision makers.

Group	Role
Space and science community	Observe known NEOs Find new NEOs Increase the knowledge about NEOs Do research in deflection strategies Improve the detection technologies Guide the UN, governments, hazard mitigation communities and rescue services Educate the public
UN	Take responsibility for the key decisions (for example deflection missions). Inform, work together with and support national and local governments in affected areas.
Governments (cross national, national and local)	Prepare for evacuation Do emergency planning Prepare local governments and rescue services Provide funding and work together with local rescue services on planning the evacuation Make sure that the public is informed and educated about the hazard and what is being done to reduce the vulnerability.
Rescue services	Plan for the evacuation. The rescue services know the area and the people. Prepare and support the public. Do the practical evacuation work. Do rescue and recovery work after the impact.
The public	Follow the advise from governments and rescue services Prepare for impact and evacuation. Improve resilience.

The following sections describe the different strategies identified by Chapman et al. (2006).

2.3.1 Observation missions

The different observation missions can be divided into two main types, observation missions and rendezvous missions:

Observatory missions:

- Ground based missions (G)
- Space based mission (S)

Rendezvous missions and flybys, where the rendezvous can be:

- In-situ observation missions
- Impact missions
- Landing and return missions

A number of ground based observatory missions have been run in the past such as the Catalina Sky Survey (Stiles 2009), SpaceGuard (Chapman 2008), SpaceGuard Two (Chapman 2008), SpaceWatch (McMillan 2009), LINEAR (Evans et al. 2003), NEAT (Evans et al. 2003), LONEOS (Bowell et al. 2011), Pan-STARRS (Jedicke et al. 2009), ADAS (Thomas 2006), JSGA (Thomas 2006) and CINEOS (Bernardi et al. 2002). These surveys benefit from existing observatories on the Earth. The earth atmosphere does though limit the detail with which NEOs can be observed, the regions that can be investigated and the minimum NEO size that can be observed. Improvement to this can be achieved through space based observatory missions. The duration of such missions are usually much shorter than for Earth based observatory missions, they are more expensive but benefit from not being affected by the Earth's atmosphere. Some of the past missions are NEOSSAT (Hildebrand et al. 2008), NERO (Cellino et al. 2006), Euneos (Martinot et al. 2006), EarthGuard 1 (Leipold et al. 2002), GAIA (Delbo et al. 2008), Herschel (Harwit 2004) and WISE (Conners et al. 2011). Of rendezvous missions and flybys, several can be mentioned: Simone (Wells et al. 2006), Ishtar (D'Arriago et al. 2002), Rosetta (Thomas 2006), Giotto (Reinhard 1986), NEAR (Yeomans et al. 2000), Deep Impact (Thomas 2006), Deep Space 1 (Thomas 2006), STARDUST (Thomas 2006), Dawn (Thomas 2006) and Hayabusa (Thomas 2006). These missions provide more detailed information about individual NEOs and more of such missions are planned for the future such as Marco Polo (Dotto et al. 2008).

2.3.2 Mitigation: active or passive?

Mitigation can be divided into two groups: passive and active (Coburn et al. 1994) (Gillick 2005), where **passive mitigation deters and disrupts potential threats** e.g. by using engineering and construction to improve the local building stock and construction of safety shelters, economic help, institutional and social measures and evacuation planning and execution and **active mitigation uses systems to actively react against the threat** e.g. NEO deflection and NEO fragmentation missions.

The space community has developed several different deflection and fragmentation strategies. A list of different deflection and fragmentation strategies can be found in Appendix A. The following sections will describe deflection and fragmentation along with passive mitigation strategies.

2.3.3 Fragmentation

The first time a planetary defence system against NEOs was proposed was in 1967, when students at Massachusetts Institute of Technology (MIT) presented "PROJECT ICARUS" (Kleiman 1979), which focused on the potential impact of asteroid 1566 Icarus with the Earth. Project Icarus suggested the use of six 100-megaton hydrogen bombs to fragment the asteroid into harmless debris.

In some cases, fragmenting a NEO might be the only active mitigation solution possible, if for example, the object is large and the lead time is relatively short. However, it also has some drawbacks. One issue is that fragmentation could create several smaller NEOs. These fragments could potentially be an additional threat to the Earth and cause impacts at several locations on the Earth along with being an additional threat to Earth orbiting satellites. The use of nuclear bombs in outer space was also banned by the UN in 1967 in the "Treaty on Principles Governing the Activities of States in the Exploration and Use of Outer Space". Fragmentation is no longer perceived as a viable strategy among many researchers in planetary defence due to the risk of producing multiple impacts. New approaches on how to fragment a NEO are though still being considered by some within the planetary defence community (Dearborn et al. 2007, Kaplinger et al.

2011, Weaver et al. 2011). Dearborn has been investigating how nuclear explosives could be used to change the orbit of an asteroid while Kaplinger and Weaver both work on simulating a sub-surface nuclear explosion on NEOs.

2.3.4 Deflection

Deflection is achieved by changing the NEO orbit so that the NEO will miss the Earth. There are two main types of deflection:

1. Near-instantaneous techniques
2. Slow constant effects (Rogers 2007)

Many different types of deflection have been suggested. A list of different proposed methods for deflection and fragmentation can be found in Appendix A. Only a few of the many suggestions are currently realizable with existing technology. Two of the most promising deflection methods are the Kinetic Impactor (McInnes 2004) and the Gravity Tractor (Schweickart et al. 2007). Both methods are possible with existing technology, but they both need a long lead time and they are only effective against NEOs of a small size and energy. For example: NEOs with a diameter below 150-200 m for the Gravity tractor (Schweickart et al. 2007).

The main principle of the Gravity Tractor is to fly a large spacecraft in close proximity to the NEO. The gravity from the spacecraft will change the speed and direction of the NEO. This deflection strategy should be applied over a long period of time and is a slow deflection technique (Schweickart et al. 2007).

The Kinetic Impactor is a near instantaneous deflection technique. A spacecraft is used as an impactor. The spacecraft is first accelerating in order to gain speed and impact energy. It is then steered into a collision course with a NEO. When the spacecraft impacts with the NEO a crater is created and kinetic energy stored in the spacecraft is used to provide additional thrust to the NEO. The impact causes large amounts of material from the NEO and the spacecraft to be ejected out into space providing additional impulse to the NEO. This additional impulse can be very significant depending on the density of the NEO (Dachwald et al. 2006). Loosely coupled NEOs are likely to eject more material than more dense NEOs.

A combination of different deflection strategies are also being suggested by many (Hyland et al. 2011) along with the use of gravity tractors as kinetic impactors at the end of their lifetime. This was an idea that was mentioned at the IAA Planetary Defence Conference 2011.

During the deflection the nominal impact location will move along the risk corridor, which results in a change in the nominal impact time. The threat of a NEO impact will overall be reduced and ideally completely removed during a deflection mission.

2.3.5 Evacuation strategies

Having the ability to remove the threat entirely is unique to this type of natural hazard, but in the event where a spacecraft mitigation mission is impossible or it fails then it is important to consider how to reduce vulnerability and to plan for evacuation and other means to protect people in the worst affected areas.

Two types of evacuation strategies have been identified: managed and guided evacuations along with a mix of these two strategies.

In the UK evacuation plans are designed to follow managed evacuation strategies. For example, people are relocated to rest centres using public transportation. There is a focus on people with disabilities and the elderly. They will be picked up in special disability buses or ambulances and driven to designated shelters (Hoult 2009). In contrast, countries such as the United States tend to adopt a more self-managed evacuation policy, whereby local authorities inform the population about the threat and provide them with guidance about relocation, evacuation routes and how to prepare for the hazard.

Marusek (2007) found that the individuals involved in the evacuation must be given the freedom to make their own choices; but people must then also bear the responsibilities for their actions.

2.3.6 Evacuation simulation

Passive mitigation in the form of evacuation is one possible mitigation method and should be applied in areas predicted to be worst affected from the approaching hazard in the event where active mitigation methods cannot be applied. Such an evacuation could potentially be on a scale never experienced in the past, given the potential damage a NEO with a diameter of more than 50 m could cause. Such an evacuation requires detailed planning and a good knowledge regarding how many to evacuate and how many will need long-term and short-term sheltering in order to be successful. Evacuation simulations of such evacuation can provide such knowledge.

Evacuation simulations can be divided into three simulation categories: micro-, meso- and macro-simulations. Micro-simulations track the movement of individual entities, for example, a person or a car. These simulations are usually computationally demanding due to the detail in this type of simulation, but the detail enables the model to have real-life factors. Individuals and their individual behaviour can be simulated illustrating the diversity in human behaviour. Macro-simulations look at the flow of people, for example, using analogies from fluid flows. The meso-simulation model tracks the movement of groups, for example cars or small groups of people. Meso-simulations are a compromise between micro and macro by making the simulation coarser through the use of for example groups of people and by simulating the joined behaviour within a group. The reduction in detail results in a reduction in computational demands compared with micro-simulations (Bryant 2005). Various types of evacuation simulators have been developed for evacuating buildings (Shen 2005, Murakami et al. 2002), airplanes (Hobeika et al. 1998), ships (Boulougouris et al. 2002) and difficult geographical areas (Chen et al. 2006). These models use various techniques to model the evacuation, such as network theory (Kuligowski 2005), agents (Adams et al. 2008), stochastic methods (Hobeika et al. 1998), cellular automata (Kirchner 2003), behavioural force models, queuing models, route choice behavioural models and transition matrix models (Helbing et al. 2002). In evacuation simulation modelling it is important to create a representation of the real world that is realistic. Many existing simulation modellers try to find optimal evacuation solutions, but given that people are involved in such evacuations their actions

might not follow an ideal solution. Being able to simulate behaviour is essential to capture a more realistic picture of an evacuation. Unfortunately, *"Human behavior is the most complex and difficult aspect of the evacuation to simulate"* (Gwynne et al 1999). When that is achieved it is possible to add constraints and planning measures to the simulations that could be used to optimize an evacuation, such as contra flow. When investigating more long-term local resilience the creation of new roads and train lines could be taken into consideration to improve local infrastructure, and ability to evacuate more efficient.

The interaction of people with their surroundings can be divided into three categories (Johnson 2005):

1. Psychological interaction, where the response is based on available information such as experience
2. Sociological interaction which is about how people are interacting with other people
3. Physiological interaction, this is about people's response to, for example, gasses or other form of physical irritation.

Perception and acceptance of risk

How the public perceives the risk from NEOs is influenced by direct experience, e.g. previous experience of the risk due to a hazard, indirect exposure from, for example, books, movies, television programmes, newspapers (Liechtenstein 1978), education and the internet. How much risk can be accepted depends on the type of hazard and the probability of it occurring (Fischhoff et al. 1978). The public are willing to accept much higher risks from voluntary activities e.g. sky diving, skiing, and driving, than from involuntary e.g. passive smoking, chemical weapons, and terrorism. A number of determinants have been found regarding how people behave in extreme situations (Drabek 1999). Some of these are described in table 2.9.

Table 2.9: Behavioural determinants.

Determinant	Description
Experience	Prior experience may make people more alert and not as much in denial
Age	Younger people generally respond more quickly Older people often believe they have "seen it all"
Gender	Females react more quickly Men sometimes ridicule those who propose fleeing.
Level of education	Higher educated people are more likely to react and they also react faster
Ethnic minorities	These groups do not always trust the officials and their warnings
Wealth	People living in poverty often delay responses and often perceive officials with lower credibility

Government response to a disaster

Officials and local governments must react swiftly when a disaster strikes or is found to be imminent. Knowing the probability of the hazard occurring, the location and timing of the threat and the corresponding vulnerability is important when preparing a response.

When a hazard is imminent the public should be notified. The context of this message and how the message is presented by officials is important and will depend on cultural difference. The information provided should be of the highest possible accuracy, consistency and quality and the threat warning should include (Joost et al. 2008s):

- Communications through multiple media
- A timely notification
- Specific information on the type of disaster, location, time the hazard will arrive and guidance on actions to take.

The areas at risk must be clearly specified, the evacuation plan should be detailed and local emergency services must be familiar with how to work together in such situations (Cardona 1996).

In hurricane evacuations in America three types of notice are used:

1) Hurricane watch
2) Voluntary warning
3) Mandatory warning

The hurricane watch is used to inform the population that a hurricane is approaching, but there is some uncertainty regarding its landfall location and its magnitude at landfall. When a watch has been issued people should continue to follow the situation through the official information channels. The voluntary evacuation warning means that people are **advised** to evacuate whereas the mandatory means that people **must** evacuate from an area where such a warning has been issued.

2.3.7 Evacuation surveys

Evacuation surveys which describe people's travel behaviour during an evacuation are a good way to gather knowledge regarding people's behaviour during an evacuation. The main issues with surveys are that they are very time consuming, expensive and rely on people's memory, which might decay over time (Bourque et al. 1997).

The following information would be useful in order to create evacuation behaviour models:

- The proportion of the population evacuated
- The time people started to evacuate
- What people were doing up to an evacuation
- Where the evacuees evacuated to
- Type of shelter that was used
- Number of vehicles used during the evacuation
- How long did it take them to evacuate
- Reasoning behind deciding to evacuate
- Demographic predictors

This type of information can be gathered from surveys in communities that have been evacuated or are likely to be evacuated at some point in the future. Three types of survey exist (Baker et al. 2006):

- Single (question households regarding their decisions and behaviour during a single evacuation event)
- General (question households regarding several evacuation events and their decision and behaviour during these)
- Intended (question households regarding a possible "what if" scenario and what they believe they would do)

2.3.8 Natural hazard evacuation surveys

Due to the rare nature of large NEO impacts on the Earth, no evacuations have ever been performed due to this hazard. This makes it impossible to perform any surveys regarding evacuations due to an approaching NEO, except "intended" surveys.

An approaching NEO could, if observed, provide information regarding risk corridor and time of impact. Such information would make it possible to issue an evacuation, given enough warning time. A natural hazard with similar predictive characteristics is a hurricane. Hurricanes occur several times each year and households living in areas likely to experience these hurricanes can be evacuated. These areas are a rich source of evacuation behaviour that can be gathered using surveys. Tsunamis and flooding are also hazards where an event can be predicted, but the potential warning time is typically shorter than for hurricanes and some NEO impacts, so people's evacuation behaviour during such events are less transferable compared to people's behaviour during hurricane evacuations.

2.3.9 Hurricane evacuation surveys

Surveys regarding household's behaviour during evacuations, for approaching hurricanes, date back to the 1960s, when Earl J. Baker and colleagues started collecting

such information (Baker 1991). The early surveys looked primarily at key issues such as the proportion of people evacuating, notice type heard, number of vehicles used, evacuation destinations and shelter type (Baker 1991, Baker 1995a, Baker 1995b). Only a few predictors (e.g. age, wealth and gender) were identified in these early reports. It was found that shelter type depended on income and race and that mobile home owners were more likely to evacuate due to the fragility of their homes.

Later surveys looked at more demographic indicators (Baker 1997, Baker 2006, Post et al. 1993, Post et al. 2003, Dash et al. 2007, Bateman et al. 2002, Whitehead et al. 2002). Main demographic predictors for whether to evacuate were found to be:

- housing type (mobile home owners are more likely to evacuate)
- gender (women are more likely to evacuate than men)
- pets (households with pets are less likely to evacuate)
- children (households with children are more likely to evacuate)
- income (high income households are more likely to evacuate)
- race (black and Hispanic are less likely to evacuate, this might also relate to income and from which source an evacuation notice is received (e.g. officials talking on public television or through friends and neighbours). Perry et al. (1988) discovered that Mexican-Americans rely more on family and friends when becoming aware of a warning and both groups have, on average, a lower income than whites in America)

Other factors were found to be:

- hearing the public notice (more evacuate when they believe they hear a mandatory evacuation warning)
- regional differences

The mobilisation, or evacuation preparation, time is a critical issue to investigate, as, during this period, people travel home and prepare for the actual evacuation. This preparation could result in extra trips being performed, which would increase road traffic. Only a few surveys look at this critical period (Goldblatt et al. 2005, Kang et al. 2007).

2.4 Urbanisation

The world is currently experiencing a rapid change in where people live. People are moving to urban areas. In 2011 3.6 billion people, out of a total 7 billion people, were living in urban areas and this is predicted to grow to 6.3 billion out of 9.5 billion people in 2050, a growth from 51% to 66% (United Nations 2011, UN News Centre 2008). This rapid urbanisation makes these areas more vulnerable to disasters. The United Nations has projected that, by 2015, 33 cities will have a population of more than eight million people. Of these, 21 cities are located in vulnerable coastal zones. Approximately 40% of the Earth's population live less than 100 km from the coast and around 100 million people live less than 1 m above sea level. Around one billion people are living in slums, lacking basic infrastructure, housing and employment. (UN-Habitat 2007).

Mann (1965) identifies eight characteristics used for comparing urban and rural areas: Occupation, environment, size of community, density of population, heterogeneity and homogeneity of population, social differentiation and stratification, mobility and system of interaction. Table 2.10 briefly explains the difference between urban and rural areas using these characteristics.

Distinguishing between rural and urban areas should be taken into consideration when simulating evacuations since it can be expected that traffic flow will differ in those two types of areas (Department for Transport 2005). Urban road networks are often designed to handle high volumes of traffic, while the rural road networks often are designed to handle small traffic volumes between smaller settlements (Hallenbeck et al. 1997). The speed limits are often lower in urban areas compared to rural areas (Butcher 2013). How well the traffic will flow will depend on factors such as the number of vehicles, quality of road network and topography. Centres of cities and towns that date back to medieval time have developed into an organic layout (Lahart et al. 2013). These towns with their narrow lanes and dense population were originally not created for motor vehicles (British Library 2013) often making it difficult for vehicles to drive around in.

Urban communities generally have a higher road density (road network per square km), which is needed due to the higher population density. The structure of urban areas is

also much more complex than in rural areas (Roughan & O'Donovan – AECOM Alliance et al. 2011). This can potentially have large effects on the outcome of an evacuation.

Table 2.10: Rural and urban characteristics.

Characteristics	Rural	Urban
Occupation	Generally cultivators and their families. Only few non-agricultural workers (note: this was in 1965).	People working in manufacturing, trade, commerce, governing and other non-agricultural occupations.
Environment	Predominance of nature.	Predominance of man-made environment. Poor air quality. Tarmac, concrete and iron.
Size of community	Open farms or small communities.	Large urban community.
Density of population	Low density.	High density.
Heterogeneity and homogeneity of population	More homogeneous in racial and psycho-social traits.	More heterogeneous community. (More subcultures and sub communities)
Social differentiation and stratification	Not as social differential as urban settings.	More differential than rural areas.
Mobility	Large migration from rural to urban in many countries. Large daily mobility from village to city due to the higher number of jobs.	Less migration from urban to rural except in the event of a catastrophe. Large mobility within a city.
System of Interaction	More likely to know fewer people than in an urban community, but more likely to know them better.	More likely to know more people, but many are only superficially known.

2.5 Summary and conclusions

Detailed knowledge regarding NEOs is still limited and ongoing surveys are trying to gather a more complete knowledge of the NEO population and potential hazardous objects within this population. Active mitigation techniques such as deflection and fragmentation are favoured by the space community, but before such measures are used the potential risks and consequences that such a strategy poses should be investigated. This can be achieved by investigating the risk, potential loss and preparedness in the local areas at risk during potential deflection missions. These

forecasts and assessments can also be used when investigating the use of passive mitigation strategies such as evacuation and civil protection.

The potential complexity of a NEO impact due to the many primary, secondary and tertiary hazards, that could arise, makes the issue extremely complicated and could require support from the world community and international organisations such as the United Nations.

Chapter 3

Data

For the development of models that can predict the human vulnerability to an approaching NEO, along with an areas ability to evacuate, a number of datasets was required. As the NEO risk is global in nature, it is important to provide assessments that are global. For the development of vulnerability models, historical data regarding e.g. vulnerability to a number of hazards was used. Finally for the modelling and simulation of evacuations global road network data was required.

3.1 Global data

A large variety of global data sets have been investigated and a list can be found in Appendix B along with information such as the different types of data, data quality, availability and usage. The data used for modelling and simulating in this project come from two sources of global data: global gridded datasets and statistical data per country. The statistical data provide a diverse range of information for each country, including socio-economic, demographic, environmental and commercial data. In contrast, global gridded datasets provide detail on a fine spatial resolution (typically from one degree down to 30 seconds grid cells), illustrating the diversity across countries and continents in, for example, population density, land usage, climate, elevation and wealth. However, the gridded data available today do not yet provide the range of data that can be found in the statistical data.

For the human vulnerability models, global gridded data from the SocioEconomic Data and Applications Center (SEDAC) were used to describe population and land usage, whilst the building strength in each country were collected from the United States Geological Survey (USGS) Prompt Assessment of Global Earthquake's Response (PAGER) project (Porter et al. 2008).

The coarse-scale evacuation simulator uses global gridded data from SEDAC regarding population and land usage. In addition, data from the Worldmapper regarding the number of cars and mopeds and motorcycles per person in each country were used. The Worldmapper is a collection of maps based on data collected from, amongst others, The World Bank, United Nations and the Central Intelligence Agency. Gridded data regarding road network capacity and flow-time were generated using road network data from Open Street Map (OSM) with official average speed limits for cars in each country investigated. Road network capacity and flow-time models that distinguish between urban and rural areas were derived from OSM data and applied to grid cells where the population was non-zero and where OSM data were not available. Chapter 6 will provide a more detailed description about how road network capacity and flow-time were calculated and how models describing the road network capacity and flow-time for urban and rural areas were derived and used to improve the generated gridded maps.

3.2 Historical data

There are several sources where it is possible to find historical data regarding human casualties and economic loss due to different hazards.

The "Significant Earthquakes of the World" database from the USGS earthquake hazards program provides detailed data regarding historical earthquakes and the loss due to each of them. EM-DAT provides similar information for a range of different hazards but only for medium and large hazards. A third example of a database that provides data regarding historical earthquakes is from the Significant Earthquake Database located at the National Geophysical Data Center at the National Oceanic and Atmospheric Administration (NOAA); see Appendix B for more detail regarding the data available. The EM-DAT database unfortunately does not provide as detailed information regarding

each disaster events as would be needed. Data regarding the precise location along with the magnitude of the hazard would be useful when creating models that can estimate the loss due to a specific hazard type of a specific magnitude in areas with different building strength. Such data have to be found elsewhere, for example in reports regarding particular events.

3.2.1 Assumptions

In previous NEO hazard vulnerability models many assumptions have been made. In NEOimpactor textual description regarding the physical effects of different hazards at different magnitudes were converted into a percentage loss based on common sense. Several models regarding vulnerability to earthquakes are based on the assumption that the time of day when an earthquake hits an area will influence the local loss. People might be worse off if the earthquake strikes in the early morning hours according to Lomnitz (1970) and Porter et al. (2007) from the 1970s. Both of these investigations were based on small sets of historical earthquake events. Lomnitz used a set of 22 historical earthquakes in Chile stretching from 1570 to 1960, and Scawthorn used a set of historical earthquakes from the 20^{th} century that spanned across the Earth. Scawthorn fitted a trend line to his historical data and found an average ±62% fluctuation in fatality rate. There are large fluctuations in the historical data used and the fit of this trend line is questionable.

Two large sets of historical data regarding historical earthquakes were collected in this project from the "Significant Earthquakes of the World" database provided by USGS and the Emergency Events Database (EM-DAT) from the World Health Organization (WHO) Collaborating Centre for Research on the Epidemiology of Disasters (CRED) and statistical analysis was performed on these in order to investigate this claim (see Chapter 5 for a more thorough description of this work).

3.3 Road network data

Multiple sets of detailed, global road network and infrastructure data were identified in Appendix B. The VMAP0 dataset not only covers road networks globally, but also rail networks, utility networks and major airports. Having been released in the early twenty first century, means that it starts to be outdated. It has also been criticized for being incomplete by the Committee on Data for Science and Technology (CODATA). This Committee started a project in 2007 to create a better global roads dataset named the Global Roads Open Access Data Set (gROADS) which should be available in the near future. The last global dataset described in Appendix B is the Open Street Map dataset (OSM). The OSM road network dataset is a large free set of data describing the road network infrastructure globally. It also provides information regarding train lines, bus stops and ferry routes along with the location of airports, emergency services, and schools. OSM has been created by a large number of volunteers and is still growing. In most of Europe and North America the data available are very detailed, but unfortunately for continents such as Africa and South America the data are incomplete. Figure 3.1 illustrates the problem. This figure shows an OSM map of the town of La Fortuna in Costa Rica along with Google Earth satellite imagery for the same town. The red circles show how a large residential area exists, but this information has not yet been provided in OSM.

OSM is probably the most complete global infrastructure dataset available at the moment, but there is a need for creating models that can provide estimates for road capacity and flow-time in areas where data are lacking. For a coarse-scale evacuation simulator it is also necessary to convert this detailed data into a gridded description of the local road network capacity and flow-time in order to reduce the computational time needed to simulate major evacuation scenarios. A fine scale evacuation simulator could use the fine scale OSM data as they are. Such a simulator could run detailed evacuation scenarios that could be used for calibration of the coarse-scale evacuation simulator.

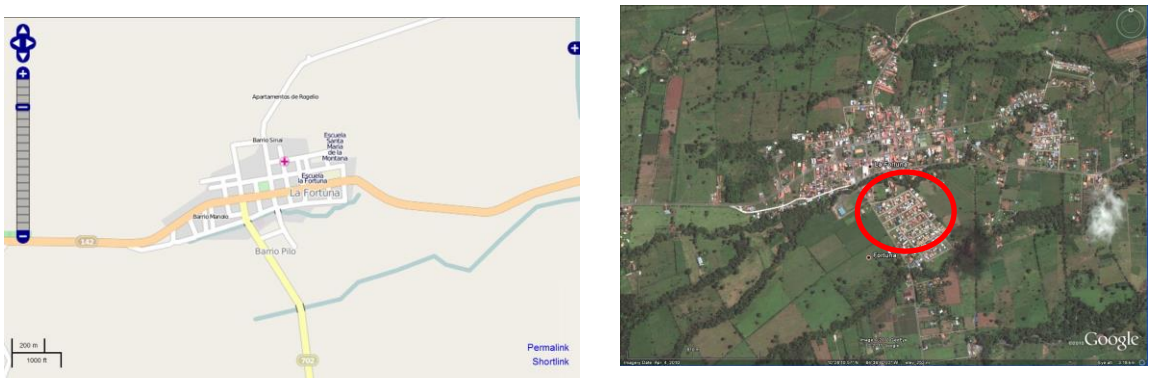

(a) (b)

Figure 3.1: (a) Open Street Map data for the town of La Fortuna in Costa Rica from April 2011. (b) Google Earth satellite imagery of La Fortuna.

3.4 Summary

As the NEO risk is global in nature, it is important to provide assessments that are global. This requires access to global data that can be used for the modelling and simulation of the human vulnerability to a NEO impact and the evacuation of potentially affected areas.

Global data was found to be essential due to the global threat a NEO pose to the Earth and its inhabitants. Several global datasets were identified and a more complete list of global datasets can be found in Appendix B. Many of the identified datasets were found suitable for the modelling and simulation required.

The human vulnerability models are in part based on historical data regarding individual hazards, when possible, along with knowledge regarding the local building stock. This will enable more reliable models to be created. A more detailed description of this analysis can be found in Chapter 5.

Finally road network data are needed for the simulation of evacuation. It was found that the existing road network data is incomplete in some areas. It is therefore necessary to compensate for this through the modelling of road networks in areas where road network data does not exist.

Chapter 4
Global Vulnerability Analysis

This chapter provides the results from a global investigation of vulnerability based on national building stock and population size, see section 4.1. This is followed by a more in depth vulnerability investigation in section 4.2. Vulnerability is in this work defined as the number of casualties (i.e. people injured and fatalities) divided by the number of people living in a specified region affected by the impact.

4.1 Global vulnerability analysis

For the investigation global data regarding population size for each country was used along with the average building strength in each country. This data was then used to derive a measure of human vulnerability for each country.

The PAGER database provides national data on building stock and a measure of the average building stock strength for each nation. PAGER provides a vulnerability code for each country describing the general strength of urban and rural buildings. This value is in the range from 1 to 5 (Jaiswal et al. 2010), where larger numbers implies that the vulnerability is likely to be higher due to a weaker building strength.

- 1 represents countries with a predominantly strong building stock and only few buildings that were built prior to any building codes.
- 3 represents countries with a large building stock of poorly engineered buildings.
- 5 represents countries where the building stock is predominantly adobe and rubble masonry buildings.
- 2 and 4 represents countries where the local building stock does not fit into category 1, 3 and 5.

It can hereon be assumed, that in countries with a high PAGER number i.e. 4 or 5, that the vulnerability would be higher than in countries with a low PAGER number. PAGER building stock data were used together with national data showing the total population in each country. These population data were collected from the UN habitat database. A vulnerability classification map was created by plotting the build strength against the population size for each country. The building strength times the population size was then illustrated as the size of circles in Figure 4.1, which includes the vulnerability of a selection of nations and the state of California, using population data from 2000 and the PAGER building strength. The state of California was selected because within this US state the local building strength is stronger than in the rest of the country. The graph in figure 4.1 show four squares, where the lower left square shows countries with a low vulnerability and the upper right square includes countries with a high vulnerability. The figure shows how China and India have a high vulnerability to the weak building strength and their large populations. In contrast, countries such as the United Kingdom and The Netherlands have a generally strong building stock and relatively small populations, so the vulnerability in these countries is low compared to China and India. Italy has a building strength of three placing it in the median. California and New Zealand are unique by having the strongest building stock, so these regions both have a low vulnerability to earthquake hazards.

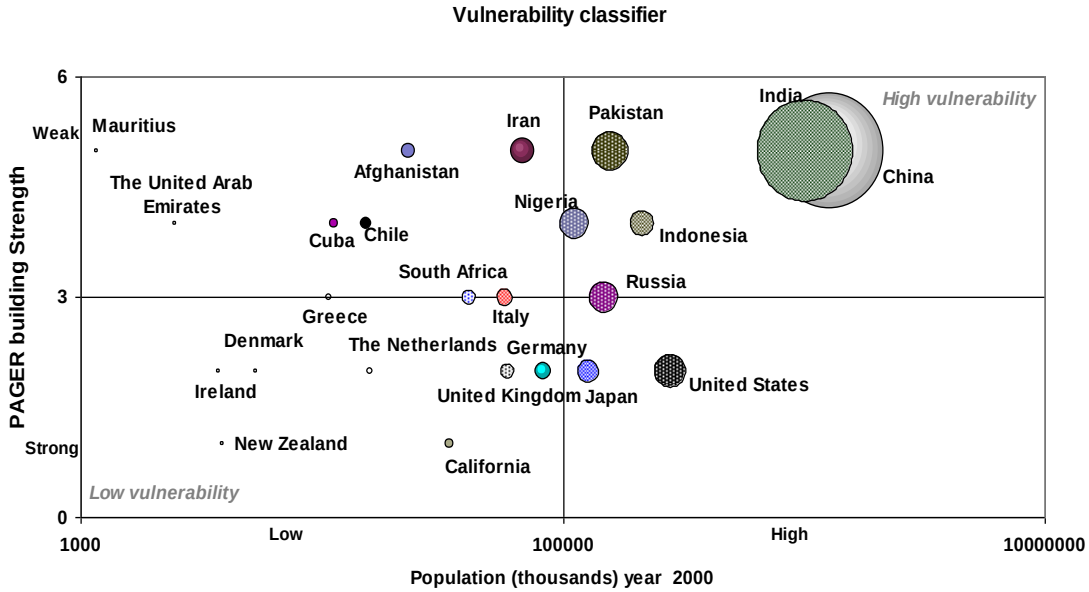

Figure 4.1: Vulnerability classification of a selection of countries.

4.2 Human vulnerability modelling

The following sections describe the models derived in order to estimate human casualties (i.e. fatalities and injured) due to a NEO impact. It will investigate how to estimate the number of human casualties due to the different primary hazards that can be expected from NEO land impact individually as well as in combination. Six primary NEO land impact hazards were identified in section 2.2.2: crater, fireball, air blast, ejecta, ignition exposure and earthquakes. Human vulnerability models were developed, describing the effects from each hazard on the affected population by predicting the number of human casualties.

4.2.1 Earthquake

A model describing the human vulnerability of an affected population to an earthquake was developed using historical data for 641 earthquake events. These events were collected from the NOAA earthquake database. They range from year 1980 to 2013 and are all earthquakes with epicentres on land.

The historical earthquake data was analysed before it was used to derive a model. Table 4.1 shows some key facts regarding the historical data. It shows that the seismic magnitude ranges from 3.4 to 7.2 and that the number of casualties range from 1 to 461823.

Table 4.1: Facts regarding NOAA Earthquake Dataset.

	Max	Min	Average
Seismic magnitude	7.2	3.4	5.66
Deaths	116000	1	1530
Injuries	174171	1	2128
Casualties (Deaths + Injuries)	461823	1	2866

Figure 4.2 show the number of casualties and the seismic magnitude the historical event had. The figure shows that for events with large seismic magnitude more casualties can be expected, but there are also many large seismic magnitude historical events where the numbers of casualties are low. The spread in casualties increases as the seismic magnitude goes up.

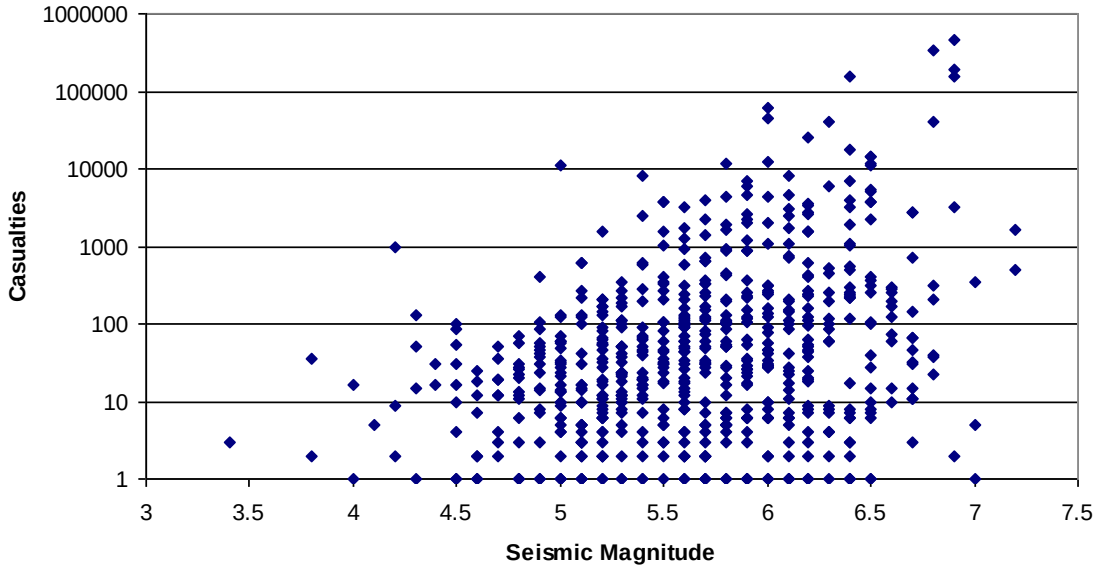

Figure 4.2: NOAA historical earthquake events, casualties and the seismic magnitude.

A test for correlation between seismic magnitude and casualties was performed for the complete dataset. The Pearson correlation coefficient was calculated to be **0.175** showing that there is a weak uphill (positive) linear relationship between seismic magnitude and casualties.

A subset of 107 historical earthquakes was then tested for, whether it is an adequate representative of the NOAA dataset (the 641 earthquake events). First a test for variance was performed using an f-test on the two datasets. The f-test for the NOAA subset and the NOAA main dataset for casualties returned following results shown in table 4.2 when using the f-test in Microsoft Excel:

Table 4.2: F-Test Two-Sample for Variances.

	Variable 1	*Variable 2*
Mean	2865.552	6561.318
Variance	6.6E+08	2.22E+09
Observations	641	107
df	640	106
F	0.297896	
P(F<=f) one-tail	0	
F Critical one-tail	0.792605	

F < Fcritical this means that the null hypothesis can be kept and that the variance for the two casualty sets are equal.

This test was followed by a comparison of the sample mean and the mean of the entire NOAA dataset. The t-test (assuming equal variance) returned following result in table 4.3 when using the t-test in Microsoft Excel:

Table 4.3: t-Test: Two-Sample Assuming Equal Variances.

	Variable 1	*Variable 2*
Mean	2865.552	6561.318
Variance	6.6E+08	2.22E+09
Observations	641	107
Pooled Variance	8.81E+08	
Hypothesized Mean Difference	0	
Df	746	
t Stat	-1.19238	
P(T<=t) one-tail	0.116746	
t Critical one-tail	1.646899	
P(T<=t) two-tail	0.233492	
t Critical two-tail	1.963149	

The result show that t Critical two-tail > t Stat > -t Critical two-tail. This means that the null hypothesis is not rejected and that the observed difference between the sample means (6561 - 2856) is not convincing enough to say that the average number of casualties for the subset and the main datasets differ significantly, showing that the subset is representative of the main NOAA dataset and can be seen as a suitable representative of the main NOAA dataset.

After establishing that the drawn subset is an adequate representative of the NOAA dataset the number of people living in the affected area for each earthquake event in the subset was found. These values are required in order to estimate the probability of becoming a casualty.

To determine the number of people living in an affected area it was necessary first to simulate the relevant earthquake. The physical model for NEO land impacts in NEOSim was used for this purpose. In the model it is possible to simulate the seismic magnitude at the impact location and then calculate the effective seismic magnitude felt away from the impact location for every 1000 m.

The model does not take into account geological features that might change the earthquake magnitude or the speed of seismic waves nor the depth at which the earthquake occurred. This is a simplified approach to modelling an earthquake. It does not require any geological knowledge about the Earth layers in the affected area. The following approach was used to estimate the number of people living in the affected area:

An “affected population area” was defined to be the radius of a threshold effective seismic magnitude, M_threshold, where M_threshold was set to 3.0.

Global gridded data from the year of the individual earthquakes were used where possible. If this was not possible, the population was derived for the given year by interpolation. The growth or reduction in population in each affected grid cell for the two years closest to the impact year and available from SEDAC was used for this using equation 4.1, where Pop_y is the population in the year of the earthquake, Pop_{y+} is the population after the event available through SEDAC and Pop_{y-} is the population available through SEDAC before the event.

$$Pop_y = \frac{Pop_{y^+} - Pop_{y^-}}{y^+ - y^-}(y - y^-) \tag{4.1}$$

Having found the number of people living in the affected area for each historical earthquake, it was then possible to derive the proportion of casualties in the affected areas also called the vulnerability in this thesis.

$$v = \frac{C_{total}}{A_{total}}, \tag{4.2}$$

where v is the vulnerability i.e. the proportion of casualties with respect to the number of people living in the affected area, C_{total} is total number of casualties given by the historical data and A_{total} is the total number of people living in the affected area.

It was assumed and later verified that, in areas with a weak building strength, buildings were more likely to be damaged or even collapse due to an earthquake. This would cause more casualties in areas with a weak building stock than in areas with a stronger building stock. Building damage also depends on the seismic magnitude of the earthquake. The verification of this assumption was done through statistical analysis of earthquake events and the results from this can be found in Appendix F. The PAGER project by USGS has investigated building strength at different level of seismic magnitude for buildings of different construction (Porter et al. 2008). From the USGS PAGER project, data on building strength can be found on a country-by-country basis. Building strength data were combined with the SEDAC National Identifier Grid to obtain a measure of the average building strength in each affected grid cell.

The proportion of casualties was derived for the NOAA earthquake events in the drawn subset.

A test for correlation between seismic magnitude (M), affected population (P) and casualties (C) was then performed on the subset and its corresponding affected population. This was done by first calculating the Pearson correlation coefficient between all 3 combinations of datasets, see table 4.4:

Table 4.4: Correlation matrix for subset.

	Seismic magnitude	Casualties	Affected population
Seismic magnitude	1		
Casualties	0.205121	1	
Affected population	0.327063	0.579442322	1

The multiple correlation coefficients, assuming that casualties are the dependent variable, depending on seismic magnitude and population can be found using the next equation:

$$R_{C,MP} = \sqrt{\frac{r_{MC}^2 + r_{PC}^2 - 2 r_{MC} r_{PC} r_{MP}}{1 - r_{MP}^2}} \tag{4.3}$$

This gives $R_{C,MP} = 0.58$ and $R^2_{C,MP} = 0.34$. The adjusted R^2 is calculated as follows:

$$\text{Adjusted } R^2 = \sqrt{1 - \frac{(1 - R^2)(n - 1)}{n - k - 1}}, \tag{4.4}$$

where k is the number of independent variables, in this case 2 (M and P).

This gives 0.57, showing a moderate uphill (positive) linear relationship between casualties, seismic magnitude and affected population.

The same calculations were performed for the entire dataset with the following results in table 4.5 and with an adjusted R^2 of 0.24, which is a weak uphill positive correlation.

Table 4.5: Correlation matrix for NOAA dataset.

	Seis mag	Casualties	Population
Seis mag	1		
Casualties	0.175482	1	
Population	0.345455	0.263374656	1

$R_{C,MP} = 0.28$ and $R^2_{C,MP} = 0.08$ and Adjusted $R^2 = 0.24$.

Figure 4.3 tries to illustrate this correlation showing the seismic magnitude and the corresponding affected population and casualties (shown as size bubbles) for the entire NOAA dataset. It must be noted that small numbers of casualties cannot be seen on the figure, their bubble sizes are too small to be seen.

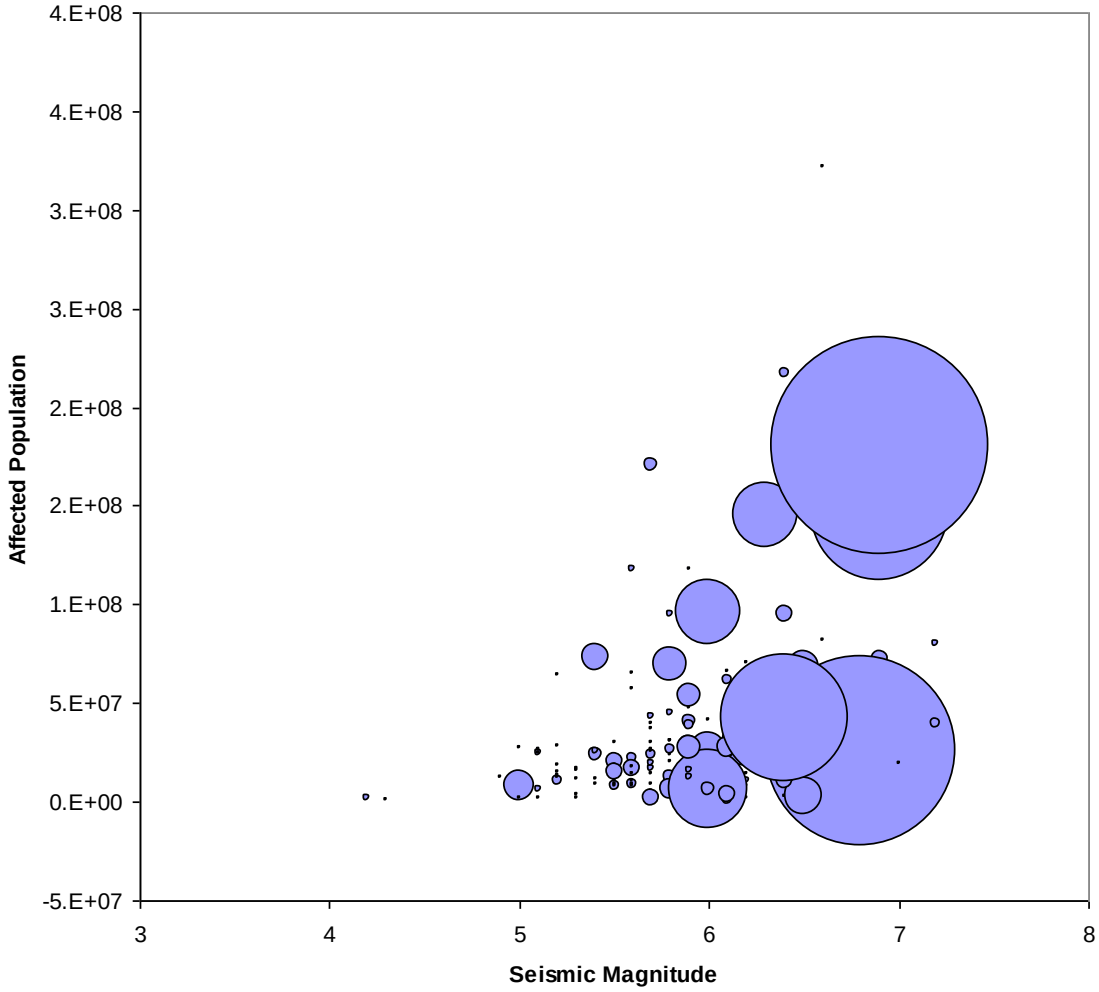

Figure 4.3: Seismic magnitude and corresponding affected population and number of casualties (bubbles).

Similar relationships can be observed between seismic magnitude, PAGER building strength and casualties as illustrated in figure 4.4, with casualties as size bubbles.

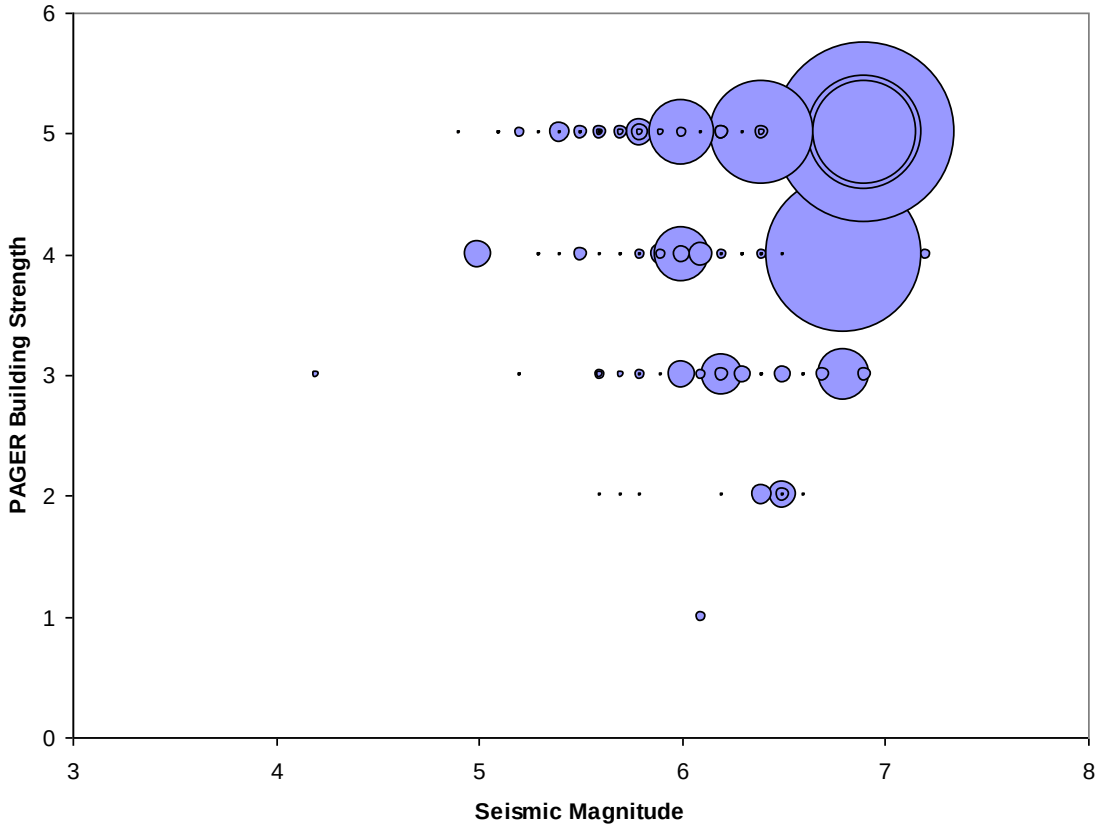

Figure 4.4: Seismic magnitude, PAGER building strength and casualties.

After having derived the affected population for each subset event, the human vulnerability was calculated for each event using equation 4.2. The outcome is shown in figure 4.5 along with the fitted model. This figure shows that overall the human vulnerability grows when the seismic magnitude increases, so overall more casualties are to be expected when the seismic magnitude increases. The Pearson correlation coefficient between seismic magnitude and human vulnerability is 0.18 showing a weak uphill (positive) linear relationship.

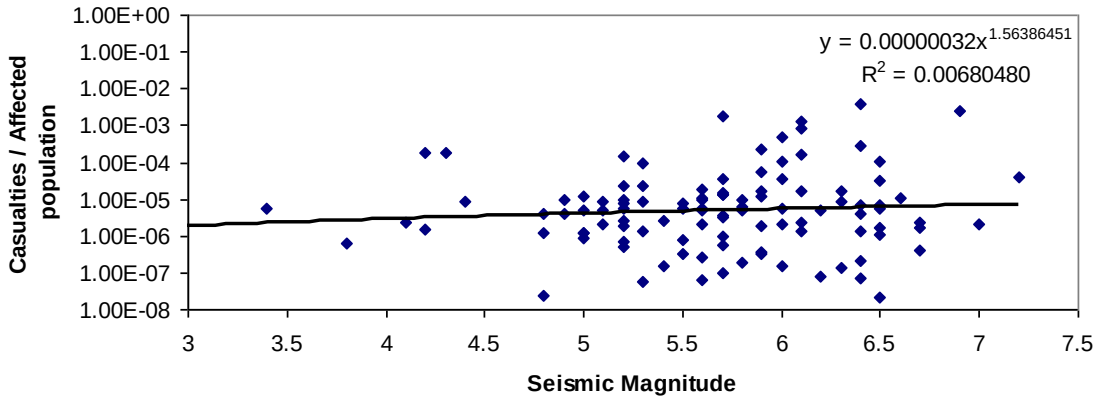

Figure 4.5: Human vulnerability with respect to seismic magnitude for each subset event.

A model was fitted to the generated data presented in figure 4.5 as follows:

$$v = 0.00000032 \times m_s^{1.56386454} \tag{4.5}$$

where m_s is the seismic magnitude and v the human vulnerability.

The model goodness was assessed by using the model on the subset earthquake events and compares the model results with the historical results, see figure 4.6. This figure shows the predicted number of casualties for the NOAA subset against the observed number of casualties. The solid line indicates where the simulated number of human casualties should be in order to be in agreement with the historical number of casualties. The dotted lines illustrate the one and one and a half uncertainty bounds. Figure 4.6 shows that it is not possible for all model results to be within the uncertainty bounds. Several of the historical events where a large number of casualties was observed has not been captured by the model. Many historical events where only very few casualties were observed was likewise not captured by the model.

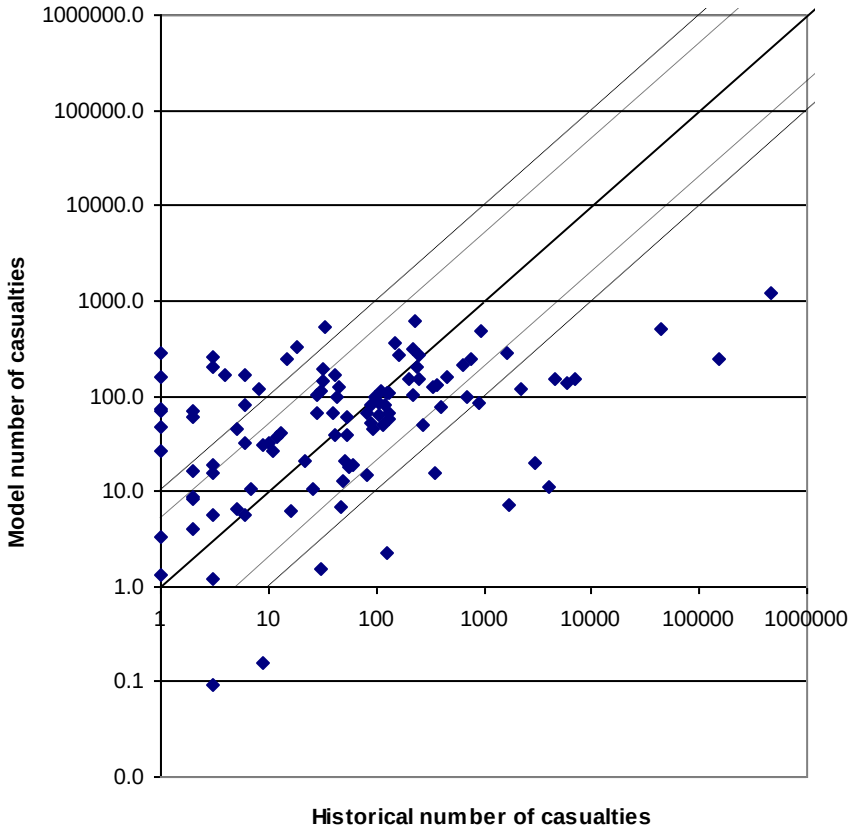

Figure 4.6: Plot of predicted number of casualties for the NOAA subset against the observed number of casualties. The dotted lines illustrate the one and one and a half uncertainty bounds.

A larger test was performed with the remaining NOAA dataset. Figure 4.7 shows the outcome from this test. An assessment of how well the model fit with the historical data was performed. First the R^2 was calculated and found to be 0.045 showing that the model does not fit particularly well.

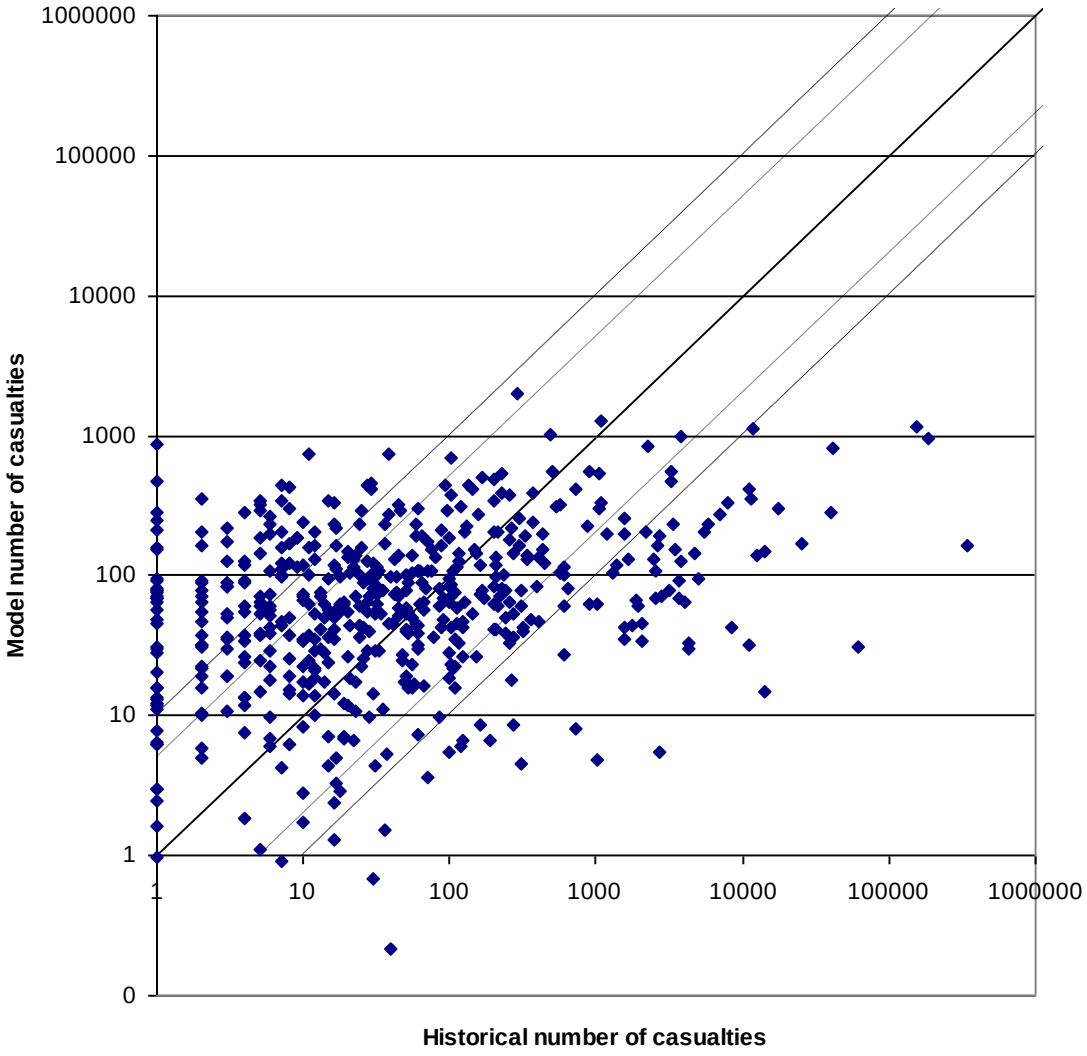

Figure 4.7: Plot of predicted number of casualties for the remaining NOAA dataset against the observed number of casualties. The dotted lines illustrate the one and one and a half uncertainty bounds.

Secondly the difference between the observed number of casualties in each event and the number of casualties found using the model has been investigated. Figure 4.8 show the difference between the model results and the historical data. 4.8 (a) show all the results while 4.8 (b) show a close-up around a difference of +1000 and -1000. The majority of differences lie within the +200 and -200 range and the close-up look show that the differences are very random. If the model fit to the data were correct, the difference would approximate the random errors that make the relationship between the historical values and the model values a statistical relationship.

(a)

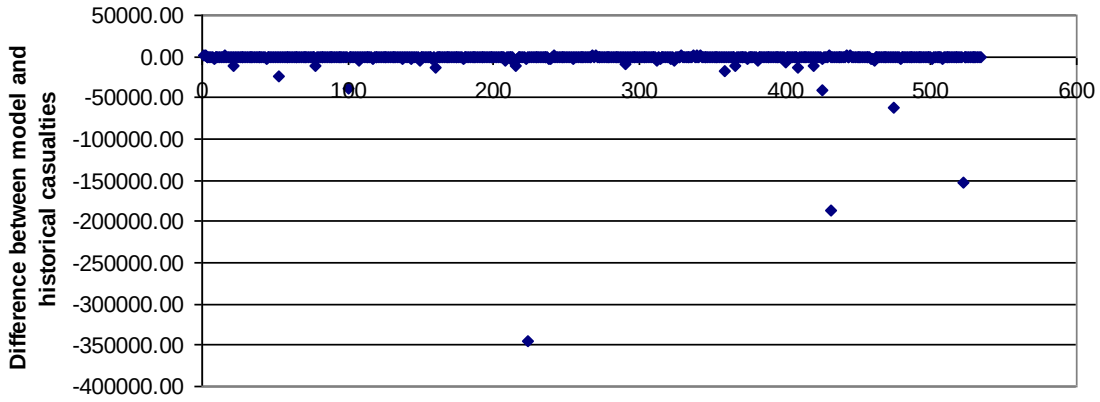

(b)

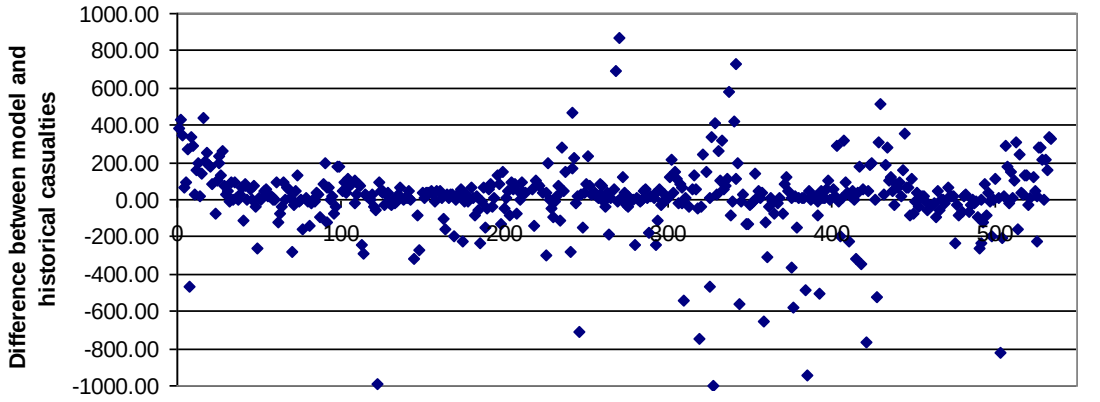

Figure 4.8: Difference between casualties using the model and historical casualties.

4.2.2 Air blast

It was found that, unlike earthquakes, very few historical events with large air blasts or large explosions were registered to a degree where sufficient information, such as year, location, number of casualties and size of explosion, is available to perform a detailed analysis. To create an air blast vulnerability model, eleven historical events were used in a similar way as for the earthquake vulnerability model. Table 4.6 shows a list of these events, the year and the magnitude of the explosion measured in tonnes of TNT along with the number of casualties. The largest events were around 800 Tons TNT.

Due to the limited knowledge about the vulnerability at these events where only the explosion magnitude measured in TNT and the casualty number is available it was not possible to perform an equally detailed analysis of the available data as for the historical earthquakes. It was instead found that for example the radius within which people became casualties in the AZF, Toulouse chemical factory explosion was 5 km (Craig 2012) at this distance the overpressure found using the NEOSim models were around 350 PA. This provides a lower vulnerability threshold where below this overpressure magnitude it will be assumed that nobody will become casualties due to overpressure. From Collins et al. (2005) it is known that around 28 kPA, injuries are universal and fatalities occur. This provides an upper boundary for the model. Above this threshold it can be assumed that everyone becomes a casualty. The model developed is illustrated in figure 4.9.

The developed model was used to estimate the number of casualties for the different explosion events listed in table 4.6. These results were then compared with the actual number of casualties. Figure 4.10 show the estimated number of casualties against the historical number along with the one and one and a half uncertainty bounds. Figure 4.10 show that the majority of the estimated casualty numbers are too large compared with the historical values. A refinement of the developed model was performed based on this information.

Table 4.6: Historical explosion events.

Location	**Citation**	**Event type**	**Year**	**Tonnes TNT**	**Number of casualties**
Enschede, The Netherlands	Enschede1,2,3	Firework factory explosion	2000	4.5	969
Seest, Kolding, Denmark	Seest1,2,3	Firework factory explosion	2004	284	18
AZF, Toulouse, France	AZF1,2,3,4	Chemical factory explosion	2001	40	10529
Flixborough, London, UK	Flixborough 1,2	Chemical factory explosion	1979	20	117
Oklahoma City, USA	Oklahoma1, 2	Terror bomb	1995	2.3	848
Ryongchon, North Korea	Ryongchon1,2,3,4,5	Train carrying flammable cargo exploded	2004	800	1461

Hemel Hempstead, UK	Hemel1,2	Oil terminal fire	2005	21.6	43
Docklands, London, UK	Docklands1, 2	Terror bomb	1996	0.5	41
Silvertown, London, UK	Silvertown1	Ammunitions factory explosion	1917	50	473
Beirut, Lebanon	Beirut1	Terror bomb	2005	0.3	110
Bali, Indonesia	Bali1	Terror bomb	2002	0.1	442

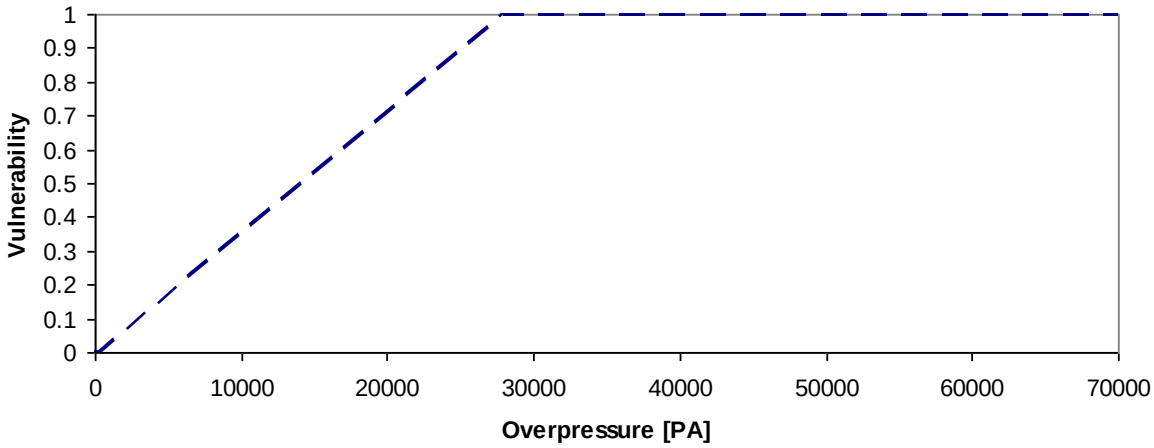

Figure 4.9: Plot of human vulnerability against felt overpressure.

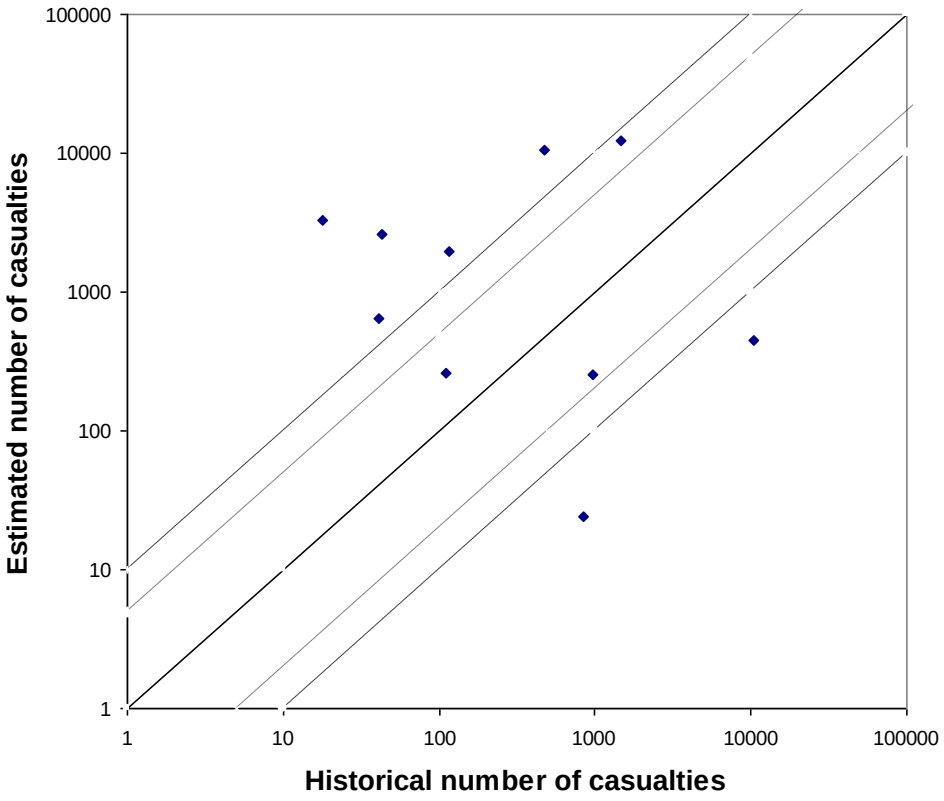

Figure 4.10: Estimated number of casualties compared with historical number of casualties. The dotted lines illustrate the one and one and a half uncertainty bounds.

A number of iterations to refine the model were performed and it was found that the main change in vulnerability lies between 300 Pa and 69000 Pa. The upper boundary has been moved up but it must also be taken into account that some will be sheltered from the effects. This was not initially taken into consideration in the original model. Figure 4.11 illustrates the new refined model while figure 4.12 show how well the estimated number of casualties for the historical events match with the historical data.

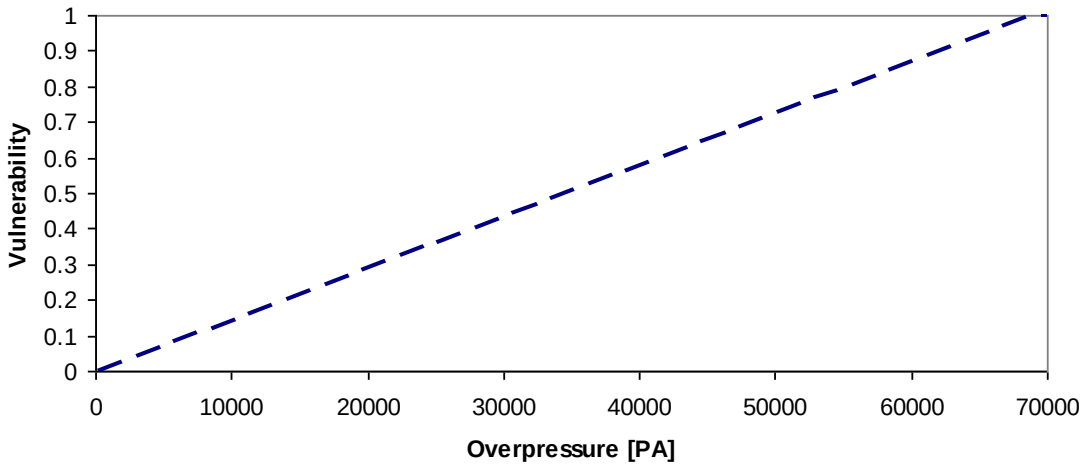

Figure 4.11: Plot of human vulnerability against felt overpressure.

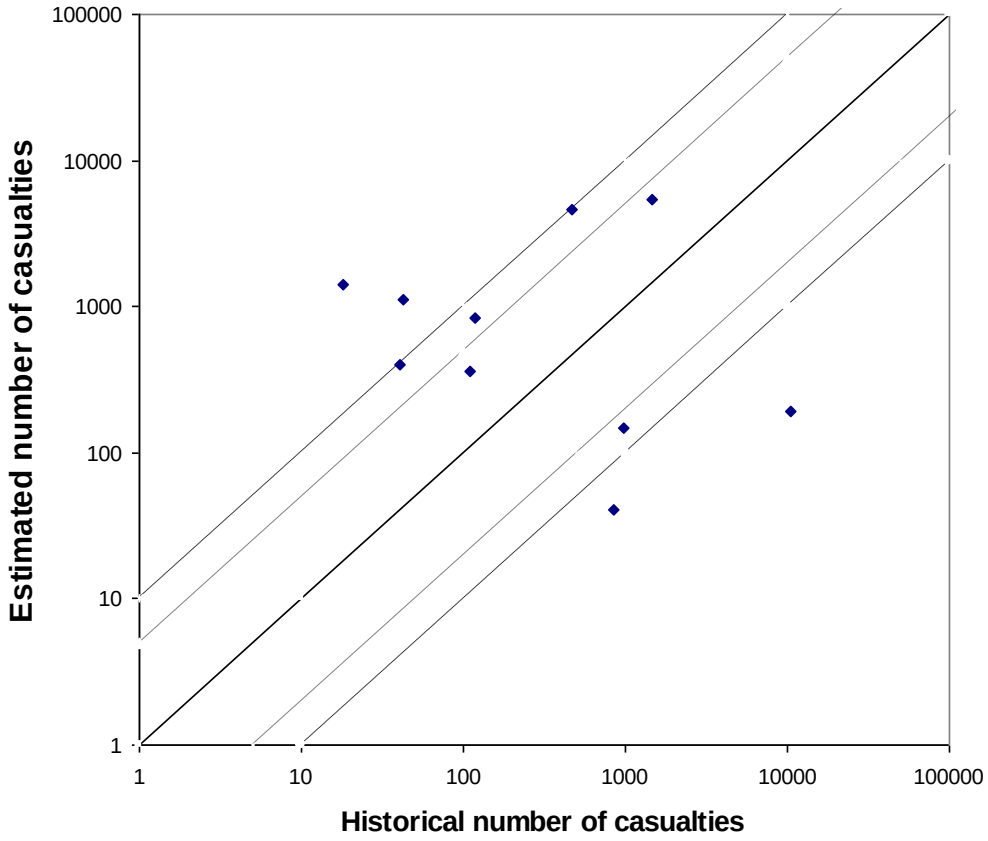

Figure 4.12: Estimated number of casualties compared with historical number of casualties for the final model. The dotted lines illustrate the one and one and a half uncertainty bounds.

The function for the overpressure model is as described in equation 4.9.

$$v_b = 0 \qquad \text{for } b \leq 300$$

$$v_b = 0.00001455 \quad 6 \times b - 0.00436681 \quad 2 \qquad \text{for } 300 > b \leq 69000 \qquad (4.9)$$

$$v_b = 1 \qquad \text{for } b > 69000$$

Where b is the air blast overpressure measured in Pascal.
All the historical events used to derive the vulnerability model due to air blasts are small compared to the potential blast caused by a NEO of a diameter of 50 m or more impacting the Earth. The energy released in such an event is measured in Megatons of TNT. The models derived here show how to estimate the casualties due to the overpressure on the outskirts of the region affected. The overpressure will cause full devastation closer to the impact location. Other effects from the impact will also affect the casualty numbers. The model should ideally take factors into account such as time of day, type of neighbourhood, demographics and number of people in full time work. All this information will be difficult to gather on a global basis.

4.2.3 Ejecta

Large amounts of material from the impact location will be ejected away from the impact location. Some fragments have the potential of damaging e.g. building stock, the local infrastructure and people while smaller fragments will cover everything in a layer of ejecta. The weight of this layer will vary and could result in roofs collapsing. It is also very likely that these loads will be unbalanced due to the wind speed (Taylor 1980). How heavy a layer of material a roof can withstand will depend on the roof design, building materials used and local building code. National building codes regarding roof load can vary within the country dependent on location and altitude (Strasser 2008). These building codes can be very different in different parts of the world, partly due to local climate and partly due to different approaches to risk. Currently no detailed dataset regarding local roof load exists, but the PAGER database provide an indicator for local building regulations in general.

The density of the ejecta particles from NEO impacts will depend on local geological features. As the top soil usually is five to twenty cm thick, the majority of

ejecta will come from the geological layers below the top soil. These layers will vary depending on region and can be everything from clay and limestone to more solid layers such as marble and granite. The density of these different layers varies from 1073 and 1121 kg m^{-3} for clay and chalk respectively to 2563 and 2691 kg m^{-3} for marble and granite. In comparison, the density of tephra particles from volcanic eruptions ranges from 400 kg m^{-3} to over 1600 kg m^{-3} for dry particles and 800 kg m^{-3} to 2000 kg m^{-3} for wet particles (Spence et al. 2005). The ejecta particles are broken fragments of the local geological layers so a reasonable assumption is to set the ejecta density to somewhere between clay and marble. The ejecta density is assumed to be 1600 kg m^{-3} in this thesis. Damage caused by ejecta from a NEO impact depends on the thickness of the ejecta layer, because its weight can cause roof collapse, and also on the particle size and energy, which will depend on distance from the impact location and weather conditions such as wind and rain.

Based on a study of the risks to human settlements by Pomonis et al. (1999) the casualty rates from collapsing roofs can be assumed to be:

1) low-rise buildings one third of occupants are trapped, of which 50% will be injured and 50% will be fatalities

2) multi-storey buildings: ten percent of occupants will be trapped, of which 50-75% will be fatalities and the remaining will be injured

As no global dataset of the average building height in different regions exists a more general assumption has been taken based on Pomonis' work:

Given a roof collapse twenty percent of the occupants will be trapped, of which 50% will be injured and 50% will be fatalities.

The local building code regarding roof live load was found for a number of countries. The roof live load is defined by the American Society of Civil Engineers (ASCE 2010) as:

"A load on a roof produced (1) during maintenance by workers, equipment, and materials and (2) during the life of the structure by movable objects, such as planters or other similar small decorative appurtenances that are not occupancy related. "

Table 4.7 shows a list of these countries, their roof building load standards and their building strength according to PAGER. Although it was only possible to collect the roof

building codes for a small number of countries it was possible to compare the collected data with the roof classification of European roof types from Spence et al. (2005b).

Table 4.7: Roof snow load and live load standards.

Country		Building strength	Roof snow- and live load standards psf	kg/m^2	kN/m^2	kPa	Reference
California	min	1	38.00	185.53	1.82	1.82	California
	max		220.00	1074.13	10.54	10.53	
United Kingdom	min	2	12.53	61.18	0.60	0.60	United Kingdom
	max		31.33	152.96	1.50	1.50	
Canada	min	2	30.00	146.47	1.44	1.44	Canada
	max		50.00	244.12	2.40	2.39	
Germany	min	2	12.53	61.18	0.60	0.60	Germany
	max		79.36	387.49	3.80	3.80	
Norway	min	2	20.89	101.97	1.00	1.00	Norway
	max		104.43	509.86	5.00	5.00	
Romania	min	3	31.33	152.96	1.50	1.50	Romania
	max		52.21	254.93	2.50	2.50	
Gibraltar		3	15.66	76.48	0.75	0.75	Gibraltar
Puerto Rico		3	40.00	195.30	1.92	1.92	Puerto Rico
The Philippines		3	41.77	203.94	2.00	2.00	The Philippines
Saudi Arabia	min	4	12.53	61.18	0.60	0.60	Saudi Arabia
	max		20.89	101.97	1.00	1.00	
Trinidad and Tobago	min	4	12.53	61.18	0.60	0.60	Trinidad
	max		20.89	101.97	1.00	1.00	
India	min	5	8.35	40.79	0.40	0.40	India
	max		31.33	152.96	1.50	1.50	

This comparison showed that areas with building strength 4 and 5 can be classified as areas with weak roof types. Areas with building strength 3 have medium roof types and areas with building strength 1 and 2 have strong roofs. Based on this observation, it was decided to use the tephra-fall roof vulnerability curves from Spence et al. (2005b) fig. 6. Here Spence has four s-curves describing the probability of roof collapse due to tephra fall on four roof strengths. Figure 4.13 illustrates these curves.

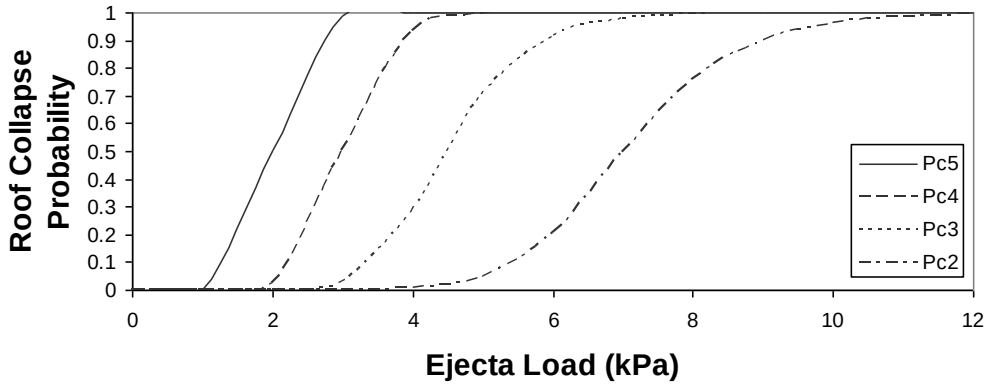

Figure 4.13: Probability of roof collapse due to ejecta load (Spence et al. 2005b).

The following four functions for calculating roof collapse probability have been fitted to these curves:

$$P_{c5} = \frac{1}{(1 + \exp(-4.32\,(\varepsilon - 1.61)))^{4.13}} \quad \text{weak} \quad (4.10)$$

$$P_{c4} = \frac{1}{(1 + \exp(-2.39\,(\varepsilon - 2.48)))^{2.74}} \quad \text{intermediate} \quad (4.11)$$

$$P_{c3} = \frac{1}{(1 + \exp(-1.37\,(\varepsilon - 3.14)))^{4.60}} \quad \text{intermediate} \quad (4.12)$$

$$P_{c2} = \frac{1}{(1 + \exp(-1.00\,(\varepsilon - 5.84)))^{2.58}} \quad \text{strong} \quad (4.13)$$

where ε is the ejecta load in kPa. Equation 4.10 is for areas with a weak building stock or PAGER building strength 5, equation 4.11 is for PAGER building strength 4, while equation 4.12 is for areas with PAGER building strength 3 and equation 4.13 is for areas with PAGER building strength 1 and 2. These four roof collapse probability models can be used along with the casualty assumption made to provide vulnerability estimates regarding the vulnerability to collapsing roofs.

Weak roofs have a probability of around 1 when ejecta with a density of 1600kg/m^3 reach a thickness of around 20cm on the roof. Likewise roofs with an intermediate building strength are likely to collapse when the ejecta thickness reaches 30-50cm and finally strong roofs are likely to collapse when the ejecta thickness reaches around 70cm when using the provided models.

4.2.4 Ignition exposure

The ignition exposure is proportional to the thermal energy released during impact and/or the NEO's decent through the Earth's atmosphere. This energy will radiate out in all direction from the impact location. The ignition exposure will reduce in magnitude with distance away from the impact location. Glasstone et al. (1977) show how buildings might protect people from the ignition exposure and how vulnerability differs between being outdoors and indoors. Data has been extracted from Glasstone et al. (1977) by Collins et al. (2005) and a quantitative relationship between ignition exposure and human vulnerability when located indoors and outdoors was derived by Morley (2005). Linear models were fitted to this data from Morley (2005) for indoors and outdoors separately, and the results can be found in figure 4.14.

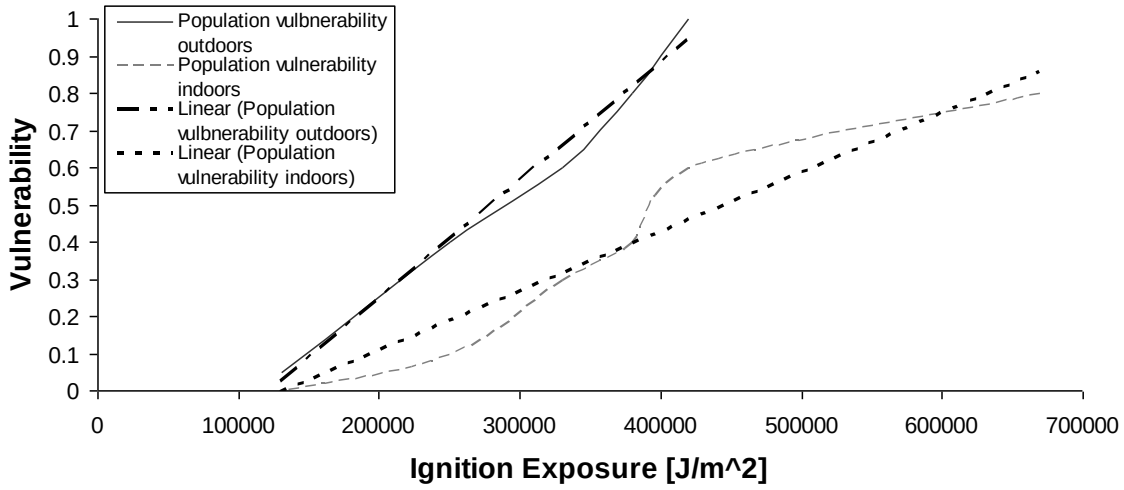

Figure 4.14: Ignition exposure vulnerability model (based on data from Morley 2005).

For the outdoor case the model is

$$v_i = 0.0000031613 \times i - 0.3847023361 \quad \text{for } 121692<i<438016 \qquad (4.14)$$

and for the indoors case the model is

$$v_i = 0.00000160 \times i - 0.21285657 \quad \text{for } 133035.4<i<758035 \qquad (4.15)$$

where i is the ignition exposure in J m^{-2}. The ignition exposure depends on the fireball radius and thereby the impact energy as described in section 2.2.2 and by Collins et al.

(2005). According to the NEO factsheet from the JPL Near Earth Object Program, the NEO mass is the dominant uncertainty. The mass is said to be *"accurate to within a factor of three"*[1] on the factsheet assuming the body is spherical and has a density of 2.6 g cm^{-3}. The impact energy is therefore dominated by an uncertainty factor of three.

4.2.5 Crater

The crater size and type depends on the size, energy and composition of the impactor and the material at the impact location. Some of the distinctive changes in an impact crater are the presence of rock such as shatter cones, melted rocks, and crystal deformations. Land craters can be divided into two types: simple- and complex craters.

It was not possible to find historical data about craters created by NEOs and any reported casualties. A different approach to modelling the vulnerability and the uncertainties was, therefore, applied to this hazard. The model is very similar to the one used in NEOSim, where there is a probability of 1 that the population within the crater radius will be casualties and a 0.9 risk of casualties at the edge of the crater. The model used here was modified slightly and can be seen in figure 4.15 (solid line). From the impact location and out to 90% of the crater radius the vulnerability is 1, but further out the vulnerability decreases to 0 at the rim. At the rim the other hazards, such as fireball, ejecta, air blast and earthquake, takes over, causing significant damage.

[1] JPL Near Earth Object Program: http://neo.jpl.nasa.gov/risk/

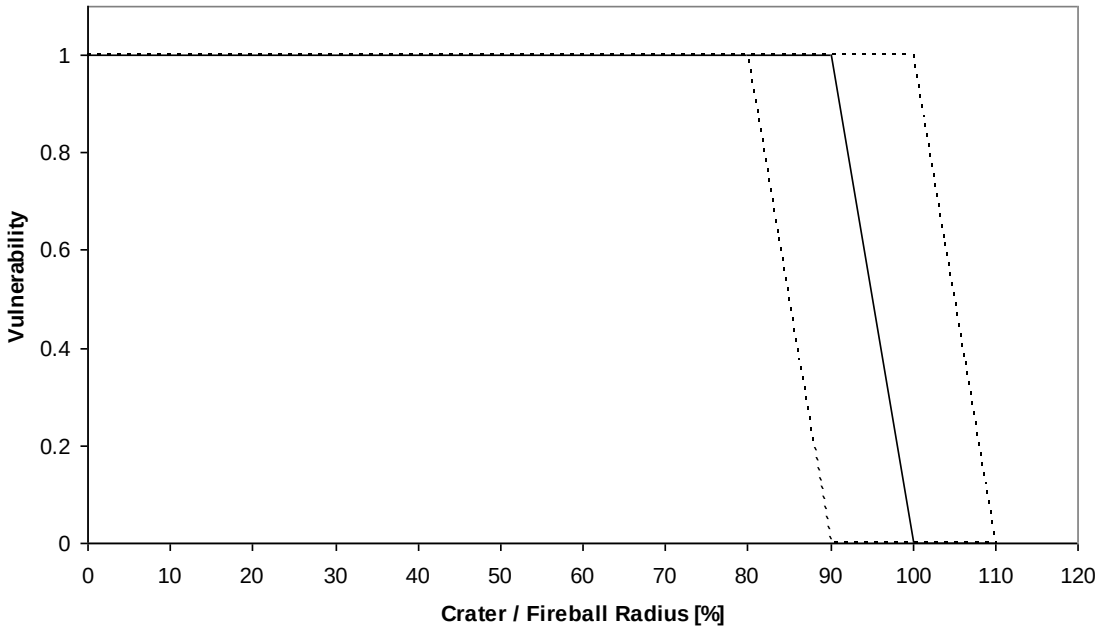

Figure 4.15: Crater and fireball vulnerability model.

The uncertainty in NEO mass was applied to the calculation of the crater radius by using Monte Carlo Simulation and the Polar method. See section 4.2.7 for more information. The uncertainty is illustrated in figure 4.15 as the finely dotted lines. These lines illustrate the upper and lower bounds of the crater radius.

4.2.6 Fireball (hot ball of gas / plasma)

Information about fireballs can be found in texts about nuclear weapons tests. The fireball that is generated after an impact expands rapidly. As the fireball expands, it radiates part of its energy away as thermal radiation and part of its energy goes into creating a blast wave (Sublette 1997). The vulnerability model that was developed for the fireball hazard is the same as for the crater vulnerability model and can be seen in figure 4.15. The fireball radius depends on the impact energy according to equation 11 in Collins et al. (2005). The uncertainty of the fireball radius is based on the NEO mass and its factor three accuracy. The dotted line in figure 4.15 shows the upper and lower bounds of the fireball radius due to the uncertainties in the available data.

4.2.7 Uncertainty modelling

The uncertainties in each vulnerability model were described using a probability density function (pdf). These were based on the mean and variance for the earthquake and air blast models and the factor of three in the NEO mass that dominates the uncertainties in crater, fireball and ignition exposure size. For the earthquake and air blast models the probability density function was based on historical data and how well the model was fitted to these.

Monte Carlo methods were used to propagate the uncertainty through to the model output (the number of casualties). Random numbers within the uncertainty boundaries at a given seismic magnitude or air blast overpressure were generated using the pdf of the earthquake and air blast models and the polar method. For the crater, fireball and ignition exposure models a random number was generated within the upper and lower limits of the crater radius, fireball radius and magnitude of ignition exposure. The corresponding vulnerability was found for the given radii.

4.2.8 Combined model

The previous sections provide human vulnerability models for six different physical effects: crater formation, fireball, air-blast, ignition exposure and ejecta. It can be assumed that in the region where the crater is formed human casualties can be the result of any of these six physical effects. It can also be assumed that further away from the fireball human casualties should be estimated based on the arrival time of each physical effect. A combined human vulnerability model has henceforth been developed. The main input into this model is information regarding the NEO such as energy, speed, radius, density and mass. The physical effects such as crater radius, fireball radius, air-blast, ignition exposure and ejecta are calculated using the code developed for NEOSim (Morley 2005). These are based on the physical models from Collins et al. (2005).

In the region inside the fireball radius there is though some uncertainty regarding which hazard arrives first so a hazard mixing model was developed calculating the human vulnerability to the six hazards in a random order at the impact location out to a

distance of 1.5 times the average fireball radius. This is the maximum expected fireball radius assuming that a factor of three dominates the uncertainty of the fireball radius. This is due to the uncertainty of the NEO mass according to the factsheet from the JPL Near Earth Object Program. Further out, the speed of the individual hazards leads to discernable differences in the timing of the arrival of the individual hazards, which was taken into account in the simulation.

The average velocity of a seismic wave is around 5 km s^{-1}, as the destructive transverse or shear secondary waves (S-waves) travel with a velocity of around 4 to 6 km s^{-1} in the Earth's crust (Wilcock 2013).

For the air blast the velocity model developed by Collins et al. (2005) was used. This was likewise the case for the ejecta speed.

The ignition exposure travels with the speed of light and the curvature of the Earth was taken into account in NEOSim when calculating the ignition-exposure. This was done by using the equations provided by Collins et al. (2005).

The time it takes for the crater to form and the speed with which the fireball travels were not considered since the area they cover is within the radius of the fireball and therefore within the mixing model zone, where each individual hazard is handled in random order.

The hazard magnitudes attenuate by distance and will become small enough not to cause any harm to the local population. As there was no reason to simulate the vulnerability in areas where the hazards no longer cause any human casualties a limit was established to how far away from an impact location the different NEO hazards were modelled. This limit was established by assuming that it is unlikely that there are any casualties when the seismic magnitude is less than 4.5 on the Richter scale, the wind velocity is less than 30 m s^{-1} (a category 1 hurricane) (Coch 1995), the ignition exposure is less than 100,000 J m^{-2} and the overpressure is less than 3000 Pa. An ignition exposure of 130,000 J m^{-2} will cause first degree burns on exposed skin for people outdoors, and an overpressure below 3000 Pa is unlikely to cause any injuries (Morley 2005).

The combined model also takes into account that as people becomes casualties from one hazard there are fewer to become casualties from the next hazard, i.e. a person can not become a fatality from two different hazards.

4.3 Human vulnerability software

For the human vulnerability software in NEOMiSS the physical impact simulators developed for NEOimpactor and NEOSim were reused, providing detailed information regarding the individual physical effects from individual sub hazards that can be expected from a NEO impact. In NEOSim these physical impact models were implemented in C++. The models derived for estimating the number of human casualties was likewise implemented in C++. The results are stored as Google Earth files and Virtual Earth files.

Figure 4.16 shows the structure of the NEOMiSS vulnerability simulator, while Table 4.8 show the main structure of the different human vulnerability models described in the previous sections. Input data is gridded data along with data regarding the different physical effects at different distances and output data is gridded data showing the casualty number for each affected grid cell. For each grid cell the number of casualties is calculated by

1) finding the distance between that particular grid cell and the impact location
2) finding the magnitude of each physical hazard based on the found distance
3) calculating the number of casualties based on the magnitude of each physical hazard, the total population number in that grid cell, building strength and the human vulnerability model(s) for that particular hazard
4) The total population number in that grid cell is reduced by the number of casualties

Monte Carlo Simulation was applied to the casualty estimation. This was done by using the polar method 5000 times in order to capture the uncertainty that has been identified within the models developed. The polar method was used for selecting a random number from a normal distribution, while Monte Carlo was used to provide a repeated random sampling from the probability distribution. The uncertainty in the crater and fireball radius means that the radius can be between 0.5 and 1.5 times bigger. Values between 0.5 and 1.5, from a normal distribution, are generated using the polar method. If an affected grid cell is within the first 90% of the radius, then the casualty model says

that the casualty rate is 100%. If the grid cell is within the last 10% of the radius, then the number of casualties will be somewhere between 0% and 100% as can be seen on figure 4.15. The same approach was used for calculating the number of casualties due to ignition exposure. In this case the polar method was used to select random number from a normal distribution within the ignition exposure uncertainty range. For the models describing the number of casualties due to seismic magnitude the polar method was applied on the models differently. Equation 4.6, 4.7 and 4.8 are here used to derive the variance, while equation 4.3, 4.4 and 4.5 describe mean. The polar method was used to select random numbers from a normal distribution within the variance of the vulnerability due to seismic magnitude. The polar method was not applied on the models describing the number of casualties due to ejecta load nor the overpressure. A number of assumptions have been taken with regards to e.g. the number of casualties due to collapsing buildings. It has here been assumed that 20% of people in collapsing houses are trapped and will become injured or fatalities; see section 4.2.3.

Table 4.8: Human vulnerability models.

Name	Equation	Input	Output
Crater Vulnerability	Figure 4.15	Crater diameter, population	Number of casualties for each grid cell
Fireball Vulnerability	Figure 4.15	Fireball diameter, population	Number of casualties for each grid cell
SeismicVulnerability	4.3, 4.4, 4.5, 4.6, 4.7, 4.8	Effective seismic magnitude, population	Number of casualties for each grid cell
EjectaVulnerability	4.10, 4.11, 4.12, 4.13	Ejecta thickness, population	Number of casualties for each grid cell
IgnitionExposure Vulnerability	4.14, 4.15	Magnitude of ignition exposure, population	Number of casualties for each grid cell
Overpressure Vulnerability	4.9	Size of overpressure, population	Number of casualties for each grid cell

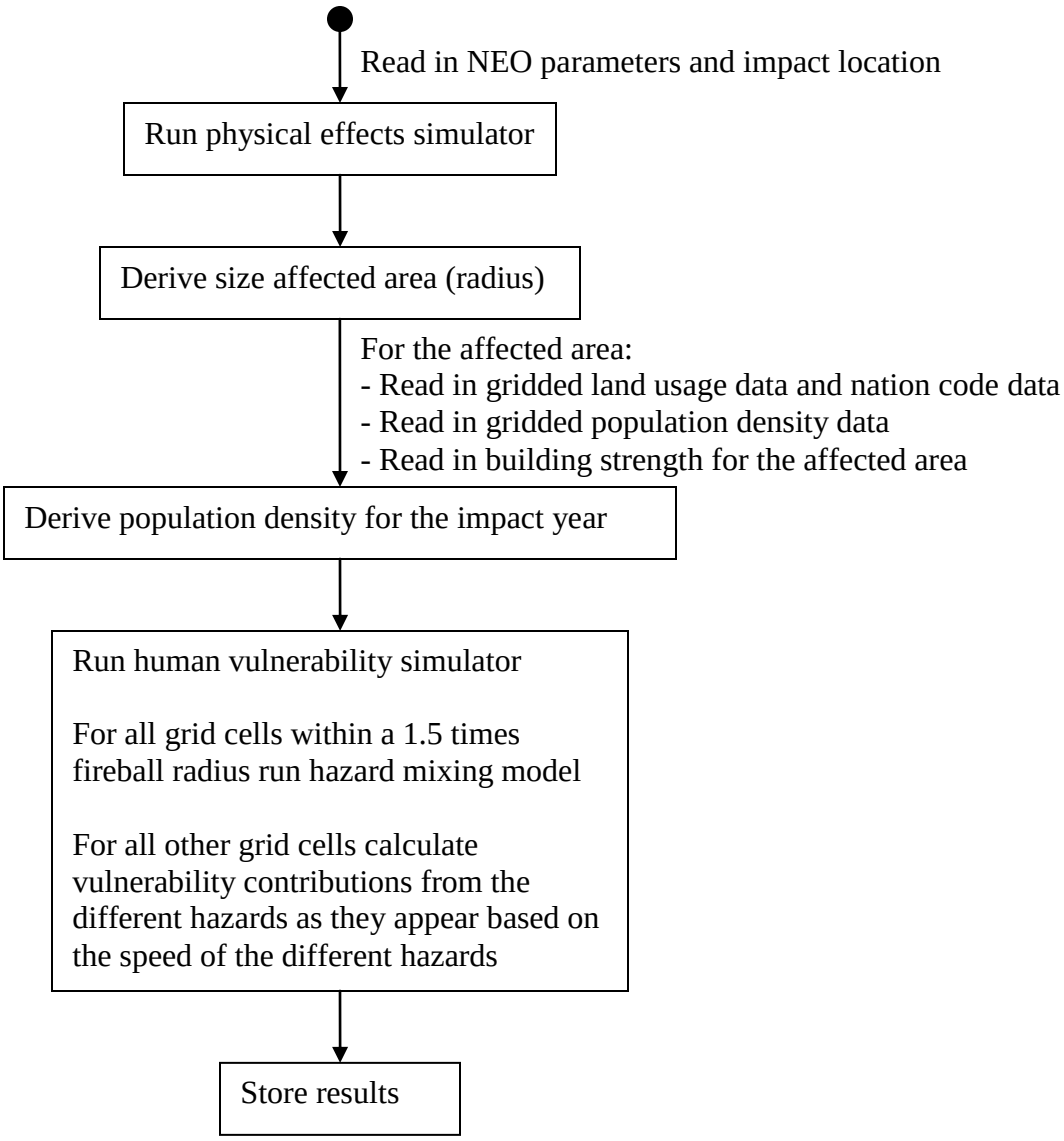

Figure 4.16: Human vulnerability software structure.

4.4 Case studies

One of the most discussed NEOs that could threaten Earth is asteroid 99942 Apophis. It is a 270 m diameter asteroid that could impact Earth on Friday 13th April 2036 with an impact probability of 2.2×10^{-5} (this value was recorded from the NEAR Earth Object Programme Impact Risk Page on the 16th July 2010). The technical data concerning this asteroid are available on the NASA Near Earth Object Program homepage. Impacts along the risk corridor for the year 2036 were modelled. A data file

containing an even distribution of possible impact locations along the centre of the risk corridor for Apophis for 2036 was kindly provided by Dr. Nick Bailey. A gridded population resolution of 2.5’ was used and a worst case of 90% of the affected population being outdoors was assumed. A total of 1556 impacts were sampled evenly along the centre of the risk corridor, but only the vulnerability to 405 land impacts was modelled using the developed multi-hazard model for NEO land impacts.

An additional case study was designed. In this case asteroid 2010 CA was selected. This asteroid has an estimated energy of 4.5 MT and a diameter of around 43 m according to the JPL Impact risk page. It was assumed that its composition is nickel-iron making it more likely to cause an impact and not an airburst. An impact on Earth from an asteroid of this size is much more likely to happen due to the larger number of these NEOs. This particular asteroid has an impact probability of 1.8×10^{-5} in August 2022. The risk corridor in this case study was hypothetical and stretched across parts of southern England, as illustrated in figure 4.17. The risk corridor stretches from just south of Bournemouth to just north of Winchester, UK. Impact locations along the risk corridor were found with intervals of 10 km. A grid cell resolution of 2.5’ was used. An Apophis impact was also simulated along the fictive risk corridor for comparison.

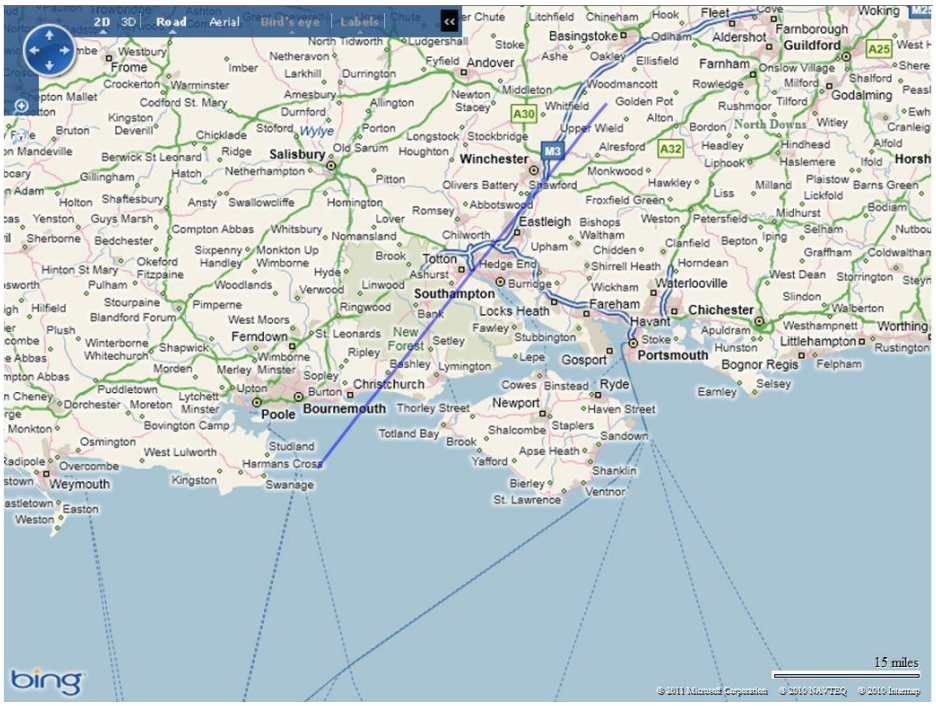

Figure 4.17: Hypothetical risk corridor for asteroid 2010 CA in August 2022.

4.5 Results

Three cases estimating the human vulnerability due to NEO impacts were investigated. Table 4.9 show the main model inputs and outputs for the selected case studies.

The overall result for Apophis shows that on average 0.14% of affected people are casualties, a maximum of 4% of affected people are casualties and a minimum of 0.0008% of affected people are casualties. The average number of casualties was 26,000 and the maximum was 990,000 casualties (figure 4.18).

A ratio of 0.0014 was observed between the number of casualties and the number of people affected for all the land impact simulations (figure 4.19) meaning that on average 14 in every 10,000 people will become a casualty.

(a) Maximum

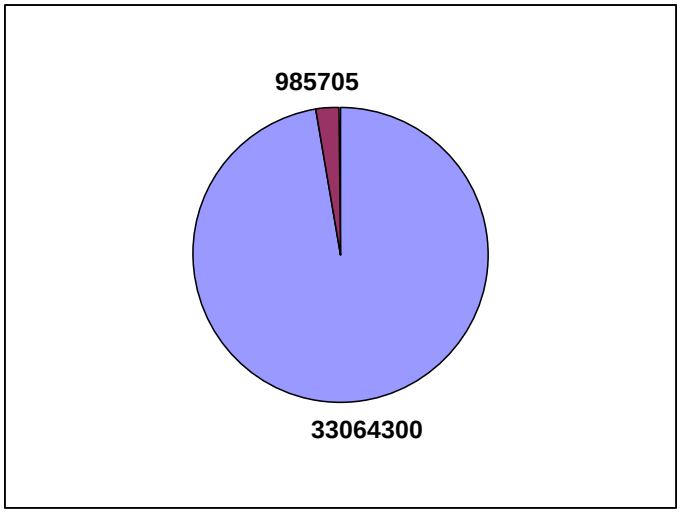

(b) Average

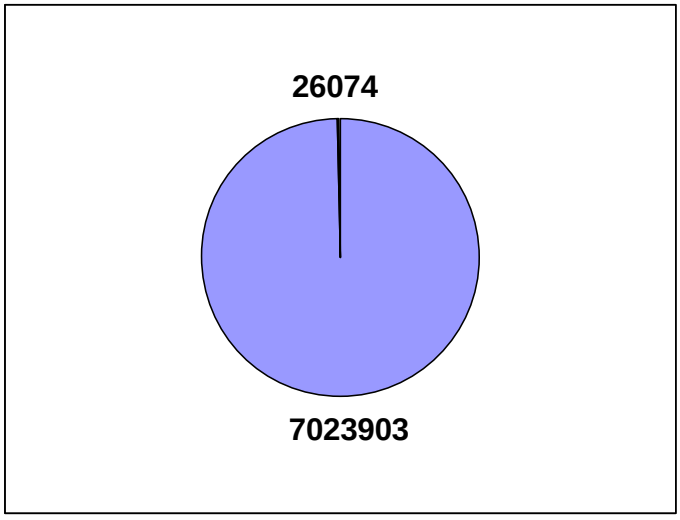

(c) Minimum

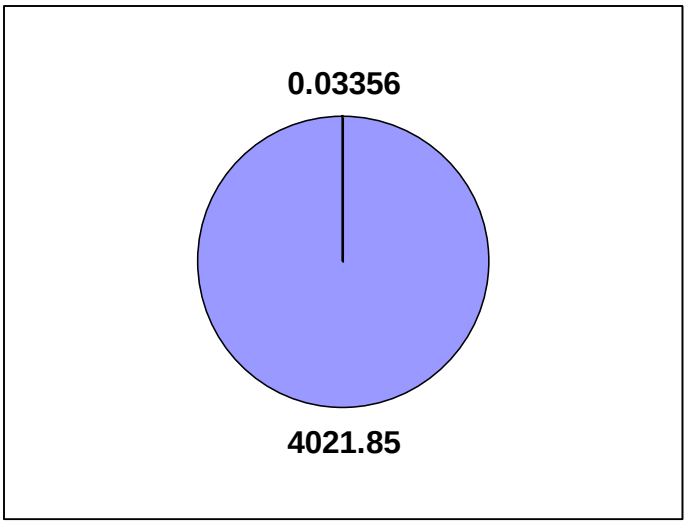

Figure 4.18: (a) Maximum, (b) average and (c) minimum number of casualties along the Apophis risk corridor for land impacts. Blue represents the number of people living in the affected area and red is the number of predicted casualties.

.

Table 4.9: Major input and outputs for the three case studies.

	Apophis 2036 impact	2010 CA 2022 Hampshire imp.	Apophis 2010 Hampshire imp.
Inputs			
Impact year	2036	2022	2022
Impact energy	750MT	4.5MT	750MT
Impact location	Along 2036 Apophis LoV	Along 2022 fictive LoV	Along 2022 fictive LoV
Outputs			
Crater diameter	5.36km	1.56 km	5.36km
Fireball radius	8.5km	1.28 km	8.5km
Radius of area at risk	467 km	181 km	467 km
Maximum number of casualties along LoV	986,000	175,000	563,000
Average number of casualties along the LoV	26,000	25,000	361,000
Minimum number of casualties along the LoV	0.03	3700	2900
Maximum human vulnerability along LoV	4.3%	0.6%	0.6%
Average human vulnerability along LoV	0.14%	0.08%	0.4%
Minimum human vulnerability along LoV	0.0008%	0.01%	0.03%

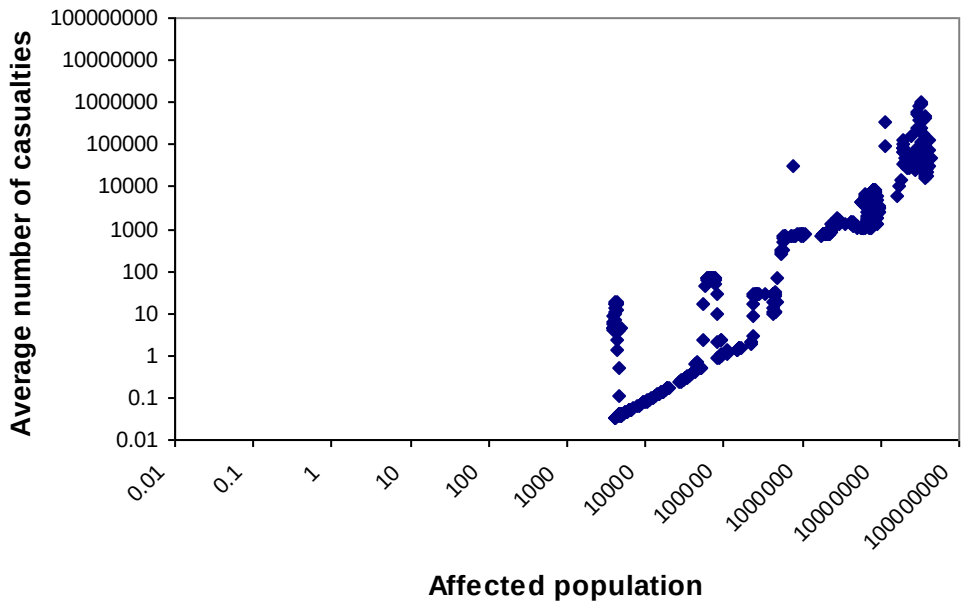

Figure 4.19: Average number of casualties plotted against affected population for land impacts along the risk corridor of Apophis.

Along the risk corridor for Apophis it was found that the highest proportion of casualties would be in the northern part of South America, with its densely populated coastal areas (~990,000 casualties or ~4%). In contrast, Siberia, which is very sparsely populated, will experience fewer casualties (~0.034 or 0.0008%). Figure 4.20 shows how people are worst affected close to the centre of the risk corridor and how towns and cities in the affected areas contribute many more casualties than the rural areas.

(a)

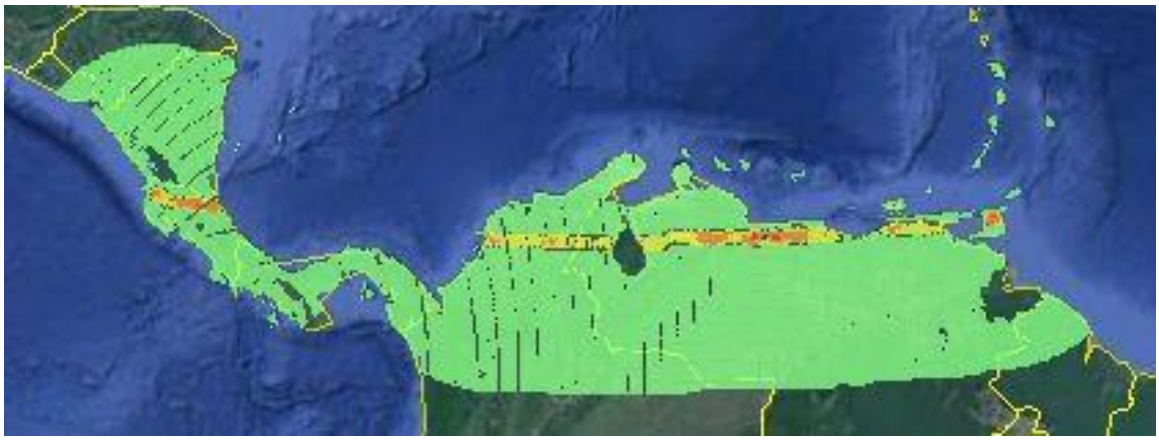

(b)

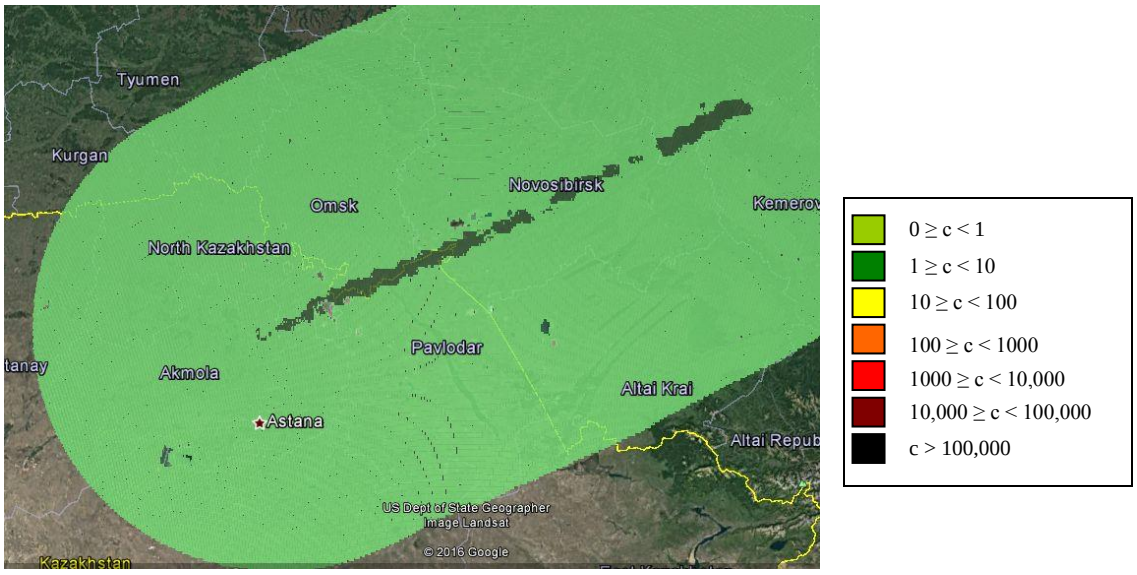

Figure 4.20: Average number of casualties along the Apophis risk corridor. (a) South America, (b) Russia.

One of the areas that potentially could be worst affected from an impact by asteroid Apophis was found to be close to the Costa Rican capital San José.

The hazard that leads to most casualties was found to be the ignition exposure closely followed by the ejecta, see table 4.10.

Table 4.10: Casualty contribution.

Hazard	Casualty contribution (%)
Ejecta	24.62
Ignition exposure	64.49
Air blast	0.41
Earthquake	0.16
Fireball	10.32
Crater	0.000034

For asteroid 2010 CA, the results show that an impact will create a crater with a diameter of 1.56 km. The seismic magnitude will be around 4.7 on the Richter scale at the impact location. The average proportion of casualties was found to be 0.08% of the affected people, whereas the maximum was 0.6% and the minimum was 0.01%, showing a difference of 47 times more casualties in the worst case compared to the best case.

Figure 4.21 show the maximum, average and minimum number of casualties along the risk corridor for asteroid 2010CA land impacts.

(a) Maximum

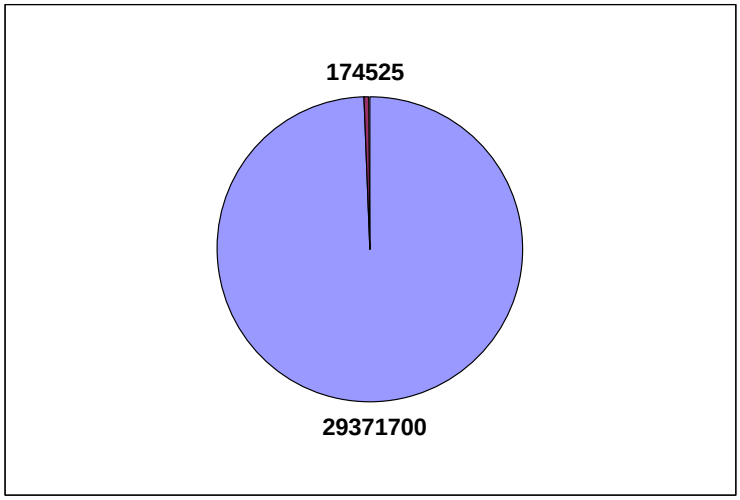

(b) Average

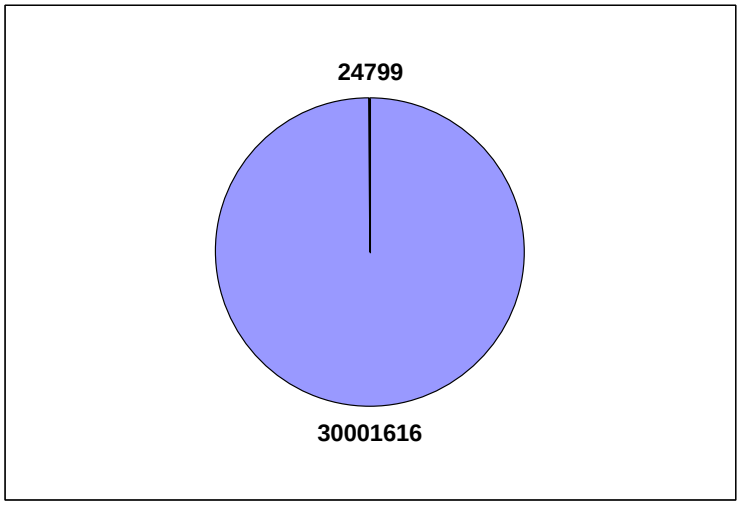

(c) Minimum

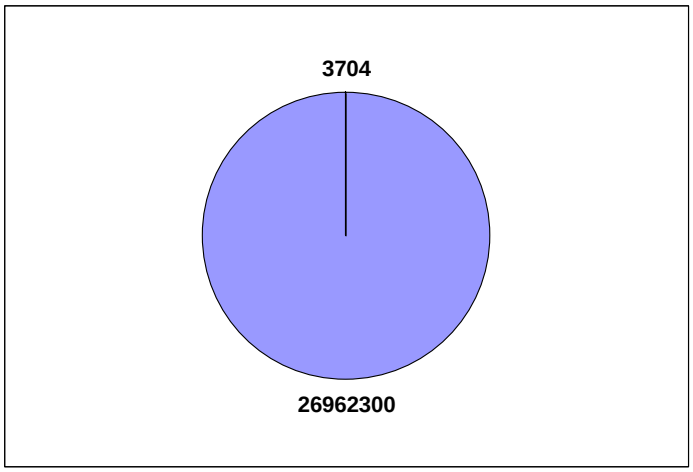

Figure 4.21: Maximum, average and minimum number of casualties along the risk corridor for asteroid 2010CA land impacts using average casualty estimates from the hazard models and assuming 90% of the population was outside. Blue is the number of people living in the affected area and red is the number of predicted casualties.

An average ratio of 0.0008 was observed between the number of casualties and the number of people affected for all the land impact simulations (Figure 4.22) meaning that on average 8 in every 10,000 people will become a casualty. But it could be as high as 60 and as low as 1 in every 10,000 people that will become a casualty.

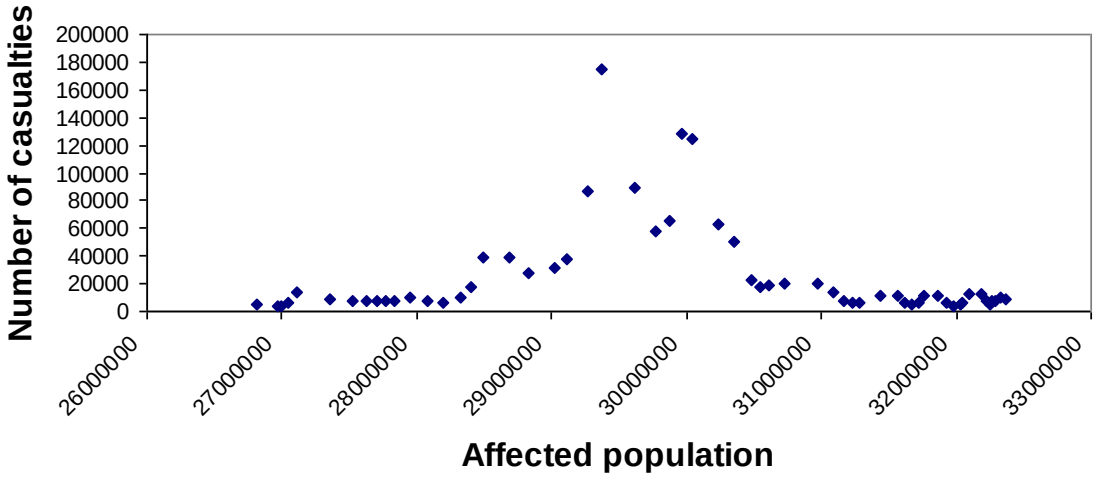

Figure 4.22: Average number of casualties plotted against affected population for land impacts along the risk corridor of 2010 CA .

Along the risk corridor for asteroid 2010 CA it was found that the worst affected land areas are in a Southampton suburb.

For the third case study the Apophis asteroid was used as impactor along the fictive LoV. Along the risk corridor the average proportion of casualties with respect to the number of people affected was found to be 0.4%, whilst the maximum was 0.6% and the minimum was 0.03% as seen in figure 4.23. With a crater size of 5.3km and an affected area radius of 467 km a far bigger area is affected by an Apophis impact compared with a 2010CA impact which only has an affected area radius of 181 km. Almost 100 million people live in the affected area, whereas the affected area for asteroid 2010CA only affects around 29 million people.

(a) Maximum

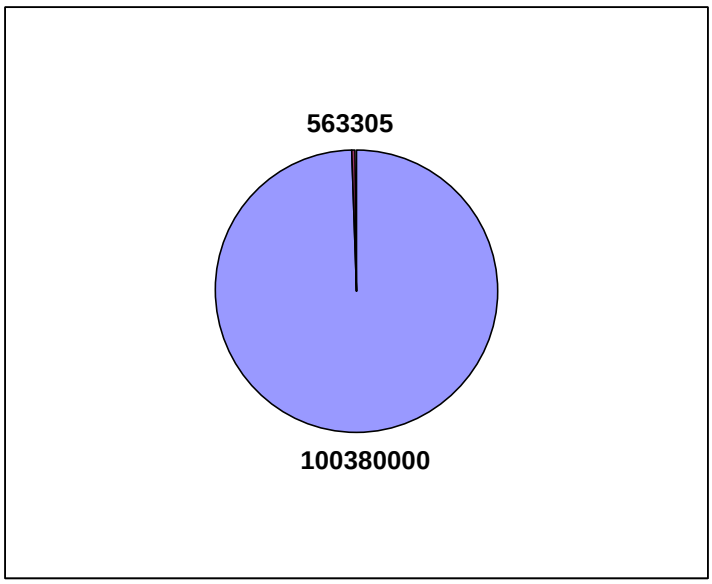

(b) Average

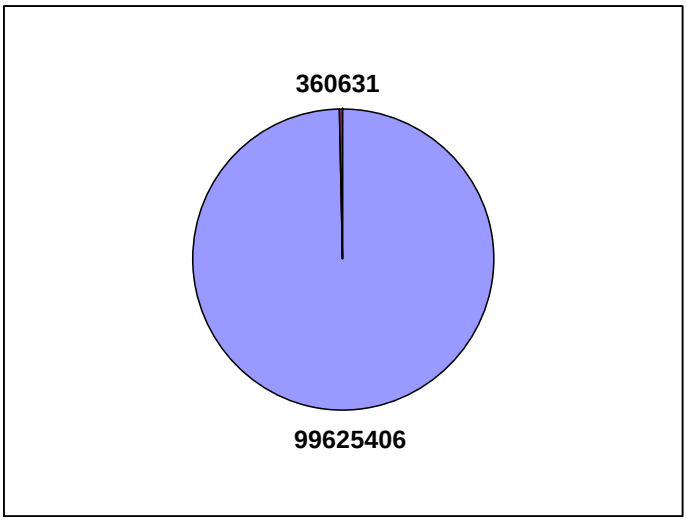

(c) Minimum

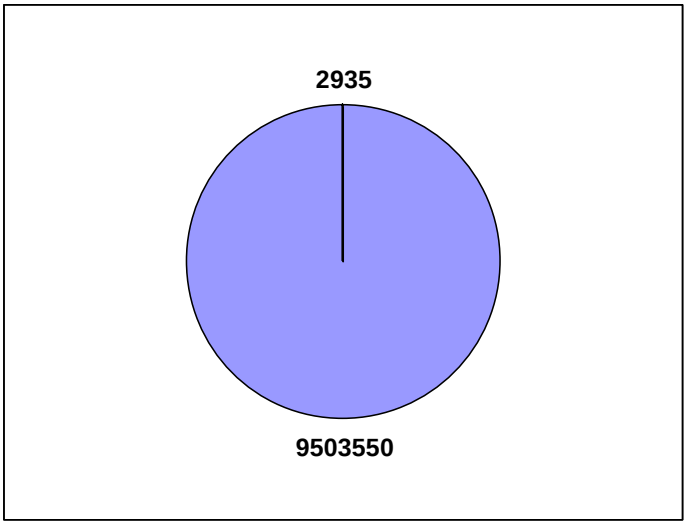

Figure 4.23: (a) Maximum, (b) average and (c) minimum number of casualties along the fictive risk corridor for asteroid Apophis land impacts. Blue is the number of people living in the affected area and red is the number of predicted casualties.

Figure 4.24 illustrate the average number of casualties plotted against affected population for land impacts along the fictive risk corridor for asteroid Apophis. An average ratio of 0.004 was observed between the number of casualties and the number of people affected for all the land impact simulations (Figure 4.24) meaning that on average 4 in every 1000 people will become a casualty.

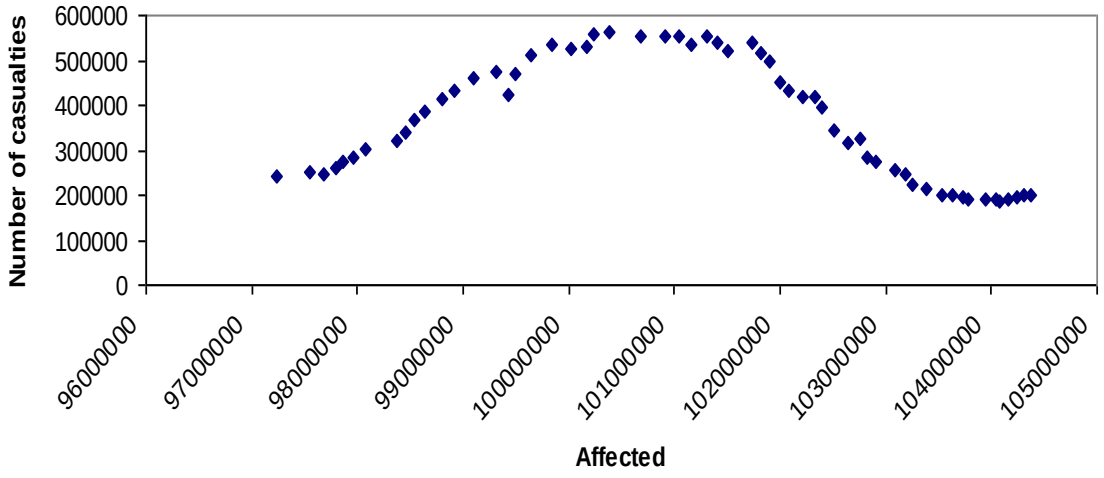

Figure 4.24: Average number of casualties plotted against affected population for land impacts along the fictive risk corridor for asteroid Apophis.

4.6 Discussion

Using historical earthquakes to model human vulnerability to earthquakes has been found to produce estimates that are closer to the historical estimates compared with previous models used in NEOImpactor and NEOSim. These models also take into account the local building strength, but do not take into account the time of day when the hazard occurs.

Similar approaches were used for the development of models describing the human vulnerability to air blasts and ejecta. More data would though be beneficial in order to ensure that these models produce estimates close to what has been observed in historical events.

The models describing the number of casualties due to ejecta were based on four models from Spence et al. (2005b) that estimate roof collapse probability. Additional models that capture casualties due to the ejecta itself have though not been derived. The ejecta could, based on its material and size, cause injuries to humans located outside along with causing health problems such as respiratory problems and heart problems.

The models that describe human vulnerability to the formation of a crater and due to the fireball are simple and more research into what happen at the crater rim and the edge of the fireball would be beneficial although not much is expected to survive within these perimeters.

The model that describes human vulnerability to ignition exposure is based on tests with nuclear weapons and takes into account whether people are located in a shelter or outside. Taking into account people location (indoors or outdoors) should ideally be added to the earthquake, air blast and ejecta models too.

Best and worst cases scenarios have been investigated by taking into account some of the uncertainties within the models and the data.

Uncertainties still need to be taken into account in vulnerability models for ejecta. For this more knowledge regarding the local building stock would be beneficial. Such information could also contribute to improvement of the remaining models. The ejecta models should also estimate casualties due to the potential injuries it can cause along with other health problems.

The developed human vulnerability model was used, together with a NEO impact simulator that simulated the physical effects of a NEO impact, to investigate the human vulnerability along the 99942 Apophis risk corridor for 2036 and for the 2010 CA along a fictive risk corridor. The result showed that the main contributor to the casualties is the air blast closely followed by ignition exposure and ejecta. More investigations into how different size NEOs affects human vulnerability in different regions should be investigated.

4.7 Summary

Although a large devastating NEO impact on the Earth is a rare event, such an impact could result is a range of devastating natural hazards. Six single hazard vulnerability models predicting the proportion of casualties were developed for a NEO land impact and the six models were combined into a multi-hazard model. The models are unique in accounting for uncertainty and three models (vulnerability earthquakes, ejecta and air blasts) were developed using historical data on earthquakes, snow load and

tephra fall and large explosions.

The earthquake model was tested against historical data. The other vulnerability models were not tested due to the lack of, or limited number of, historical events.

The results for the earthquake model generally showed that the estimated number of casualties was a factor of 115 larger than observed historically. This is a very high number but it is important to keep in mind that a NEO impact will create a shallow earthquake making. These types of earthquakes often cause much more damage than earthquakes originating deeper within the Earths crust.

The developed multi-hazard vulnerability model was used along the risk corridor of the asteroid 99942 Apophis. The case study shows that the worst affected area is along the densely populated coastal region of South America, whereas Russia, with its large unpopulated areas in Siberia, would experience fewer casualties. Along the risk corridor it was found that, on average, a proportion of 0.14% of the people living within the affected area are expected to be casualties, but this could vary between 0.0008% and 4% along the risk corridor.

The smaller asteroid 2010CA scenario showed a slightly lower average percentage of casualties (i.e. number of casualties divided by the number of affected people) of 0.08%. The physical effects were much smaller in the asteroid 2010CA scenario due to the NEO energy being more than 100 times smaller for 2010CA than for 99942 Apophis.

For asteroid 99942 Apophis impacting along the fictive risk corridor the result showed that on average, a proportion of 0.4% of the people living within the affected area are expected to be casualties.

Chapter 5
Coarse-scale evacuation flow simulator

This chapter describes the coarse-scale evacuation flow simulator created for NEOMiSS along with general assumptions used in this simulator. It also investigates a series of evacuation scenarios.

The coarse-scale evacuation simulator is a flow-based simulator, where the flows move between grid cells. These grid cells provide information regarding population numbers, land type (urban or rural) and available road network capacity and flow-time. This evacuation simulator should be categorised as a meso-simulator. It uses coarse global gridded data for its models and simulates flows of vehicles and the developed models are based on survey data regarding travel behaviour during hurricane evacuations.

This chapter provides an introduction to evacuation simulators and evacuation modelling followed by an explanation of how the gridded road network capacities and flow-times were estimated and how the different behaviour-based models were derived. Thereafter any additional models and assumptions made for this coarse-scale evacuation simulator will be discussed. The developed evacuation simulator is tested against a historical hurricane evacuation. Finally multiple case studies will be investigated followed by a discussion and summary.

5.1 Introduction

Traffic and evacuation simulators can be divided into three subgroups: macro-, micro- and meso-simulators based on the different approaches to describe how people or

vehicles move around in a network (Pidd et al. 1996). The movement of people and vehicles can be modelled using tools such as fuzzy logic, genetic algorithms, neural networks, artificial intelligence, agents, behaviour based models and many more.

Modelling and simulating normal daily travel behaviour is an area that is well described and investigated by the civil engineering community and is, among other things, used when looking into the potential issues that could arise due to new legislation and or new road builds and for forward predicting of future traffic loads. There exist many different tools that can enable people to apply their models to a simulator such as: Aimsum (Aimsum 2010), Paramics (QuadstoneParamics 2010), TRANSIMS (Early deployment of TRANSIMS, 1999), CUBE (Geodata Solutions Inc. 2010), VISTA (Vista Transport Group Inc. 2010) and CEMDAP (Bhat et al. 2003).

For evacuation simulation modelling many simulators has been developed in the past such as GES (Johnson 2006), ESM (Shen 2005), EVDEMON (Boulougouris et al. 2002), MASSVAC (Hobeika et al. 1998), CEMPS (Pidd et al. 1996), DYNASMART-P (Chiu 2004) and Robocup-Rescue (Adams et al. 2008). Many of the existing evacuation simulators are restricted to only simulate a small environment such as buildings (Shen 2005) (Murakami et al. 2002), ships (Vassalos et al. 2002) or airplanes (Poudel et al. 2005), but there are some that simulate larger areas (Chen et al. 2006, Chiu 2004).

5.2 Open Street Map data conversion

Due to the potentially large regions that would have to be evacuated in advance of a NEO impact the scale used in the evacuation simulator is coarse: 30'' grid cells (~1 times 1 km). Gridded data maps describing population number, which can be found in the GRUMP database were used along with road network capacities and flow-times through each grid cell. The road network capacity is necessary in order to be able to describe the number of vehicles that the road network within a grid cell can fit while the flow-time describes the average time it will take to travel through a grid cell. Gridded datasets describing the road network capacity and flow time were developed using Open Street Map (OSM) data with models that can describe the road network capacity and flow time

in regions where no Open Street Map data exist. These models are based on gridded population data and national OSM data.

5.2.1 Measuring road network capacity

Road network capacity in a grid cell describes the number of vehicles that can fit on the road network of cross cutting roads within a grid cell. A number of different vehicle types have been identified: cars, buses, motorbikes and trucks. These vehicles have different lengths and braking distances due to their size, weight and the local speed limits for these types of vehicles. Here vehicles are measured in average car lengths. It is assumed that a car has an average car length, whereas a motorbike is half an average car length and buses could be two to three average car lengths.

The road network capacity in each grid is

$$C_g = \sum_{i=0}^{R} (L_i l_i \frac{1}{c + b_i}) \quad (5.1)$$

where g is the grid cell, R is the number of roads within the grid cell, L_i is the length of road i, l_i is the number of lanes on road i in one direction, c is the average car length and b_i is the recommended braking distance on road i, assuming travel at the maximum speed limit. Only cross cutting roads within a grid cell are used for calculating the road network capacity.

Table 5.1 is based on the UK braking distance guidelines for cars. These values take into account both the reaction time needed and the time needed to bring the vehicle (cars) to a full stop. However, this table does not take into account the additional distance that should be kept on wet and slippery roads or during poor weather conditions. It is also not suitable for buses, large vans and trucks, which due to their weight will need a longer braking distance before bringing the vehicle to a full stop.

The UK braking distance guidelines can be described using the following model

$$b = 0.32S^{1.66} \quad (5.2)$$

where b is the braking distance in metres and S is the speed in m s^{-1}. Equation 5.2 has a RMSE of 1.065 metres.

Table 5.1: Braking distance for different speeds.

Speed (km/h)	Distance (m)
32	12
48	23
64	36
80	53
96	73
112	96

As a road becomes more congested distance between vehicles will reduce and the speed will have to be reduced by the drivers in order to keep the required braking distance. A maximum road network capacity can be found assuming that there must be at least one metre between each vehicle. At this point the speed on the road has almost come to a standstill with a speed of 2 m s^{-1} or 7.2 km h^{-1}. The maximum road network capacity is

$$C_{\max} = \sum_{i=0}^{R} (L_i l_i \frac{1}{c+1}) \tag{5.3}$$

5.2.2 Measuring road network flow-time

The road network flow-rate is the average rate at which the traffic will flow through the road network of cross cutting roads within a grid cell and the flow-time is the time it takes for one vehicle to travel through a grid cell.
The equation for flow-rate is

$$f_i = S_i L_i l_i , \tag{5.4}$$

where S_i is the speed in m s^{-1} on road *i*.

The time it takes on average to travel through a given area is defined as the flow-time:

$$t_f = \frac{\bar{L}}{\bar{S}} \tag{5.5}$$

where $\bar{L}$ is the average road length through a grid cell and $\bar{S}$ is the average speed. The average road length is

$$\overline{L} = \frac{\sum_{i=0}^{R} L_i}{R} \tag{5.6}$$

Road network data from OSM were converted into gridded road network capacity and flow-time maps for a number of countries. Additional information such as the average road length through a grid cell was also calculated. This was all done using a C++ program that uses as input the land usage (urban or rural land) and population density data for the particular country provided by GRUMP at a grid cell resolution of 30'' (~1 times 1 km), along with the available OSM road data for the country under investigation. This program also contained lists of national speed limits in km h^{-1} for different road types in each country investigated. This information was collected from a number of governmental homepages and travel advice pages and used when no speed limits were available in the available OSM data.

As the roads within a grid cell become more congested during an evacuation, the flow-rate will reduce and the travel time through a grid cell will increase. Knowledge about the reduction of speed due to congestion has been gathered from a variety of evacuation and congestion surveys. When more cars start to enter a grid cell and the capacity *C* is exceeded, the flow-time starts to go up and it will take longer for cars to travel through the grid cell as the speed slows down and congestion increases.

5.3 Road network capacity and flow-time models

Due to the lack of road data in OSM for some regions it is necessary to create models that estimate a grid cell's road network capacity and flow-time. These models take into account if the grid cell area is urban or rural as well as taking into account the population density in each grid cell. Other parameters could also be considered such as wealth and elevation. Such parameters might show trends such as areas with big differences in elevation, e.g. mountainous regions have fewer roads than flat plateau regions because of the costs and challenges involved in building roads in such regions. These additional parameters have not been investigated in this project.

The gridded road network capacity and flow-time maps generated for a selection of countries were used along with global gridded population data and land usage data for each country investigated at a resolution of 30''. For each urban grid cell where OSM data existed, the corresponding population density was found. The same was done for each rural grid cell. Graphs were produced illustrating the road network capacity and flow-time for each of these datasets and models were applied to the data using Microsoft Excel. It has been observed that as long the correlation function selected in Excel is NOT a polynomial function then the outcome is similar to correlation functions calculated using online tools such as alcula [alcula 2015] Figure 5.1 shows the road network capacity and flow-time for urban and rural grid cells in Costa Rica. Large fluctuations can be observed especially when the population density is low. Figure 5.1 (a) and (c) show that as population density in Costa Rica increases the road network capacity increases although there are large fluctuations. These fluctuations range between 0.04 and 602 vehicles in urban grid cells. For rural grid cells these fluctuations range between 0.03 and 771 vehicles. Figure 5.1 (b) and (d) show that the flow-time reduces as the population density increases. Whether the road network capacity and flow-time increases or decreases depends on the individual country and the area type and possibly a number of other factors such as wealth, elevation, etc. There may also be regional differences that could be of great importance for larger countries.

(a)

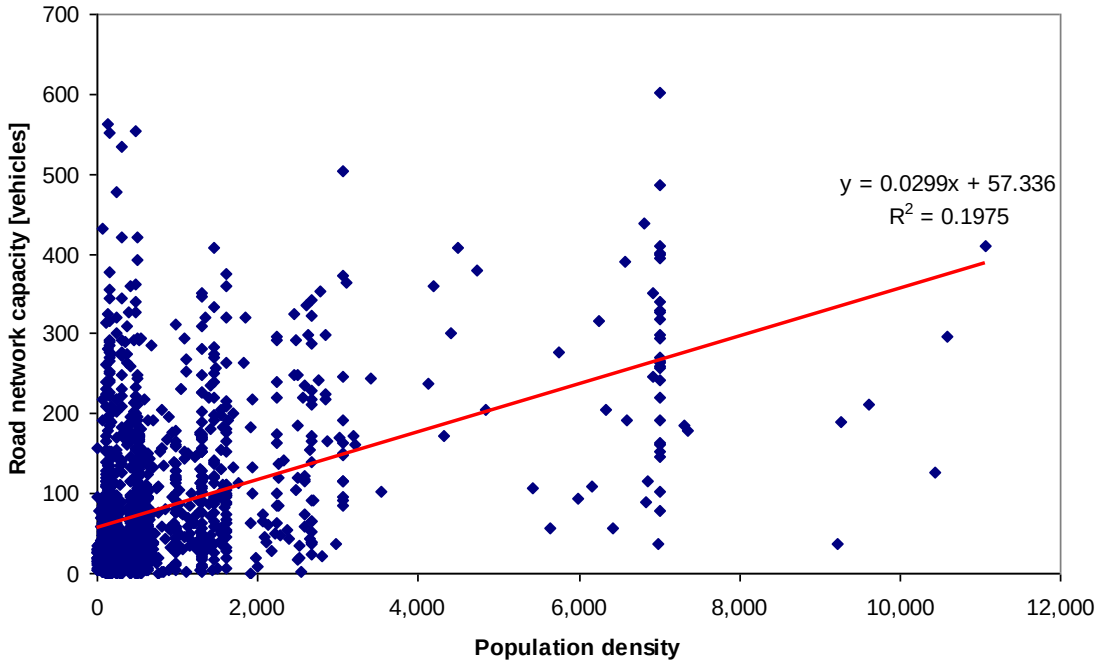
Road network capacity [vehicles]
700
600
500
400
300
200
100
0
0
2,000
4,000
6,000
8,000
10,000
12,000
Population density
y = 0.0299x + 57.336
R2 = 0.1975

(b)

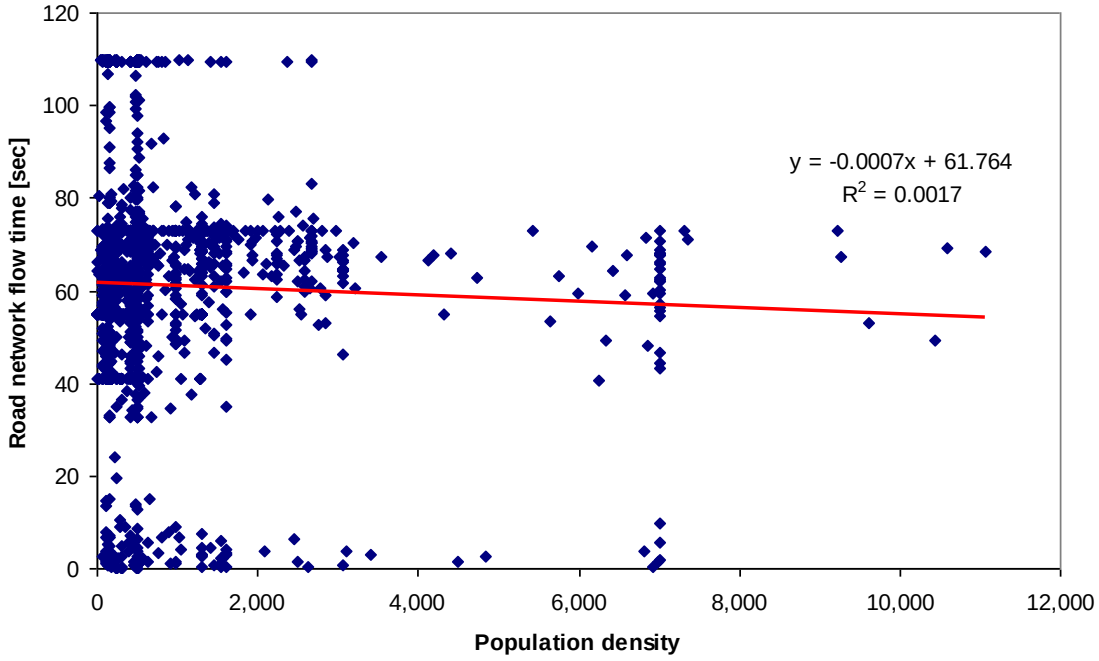
Road network flow time [sec]
120
100
80
60
40
20
0
0
2,000
4,000
6,000
8,000
10,000
12,000
Population density
y = -0.0007x + 61.764
R2 = 0.0017

(c)

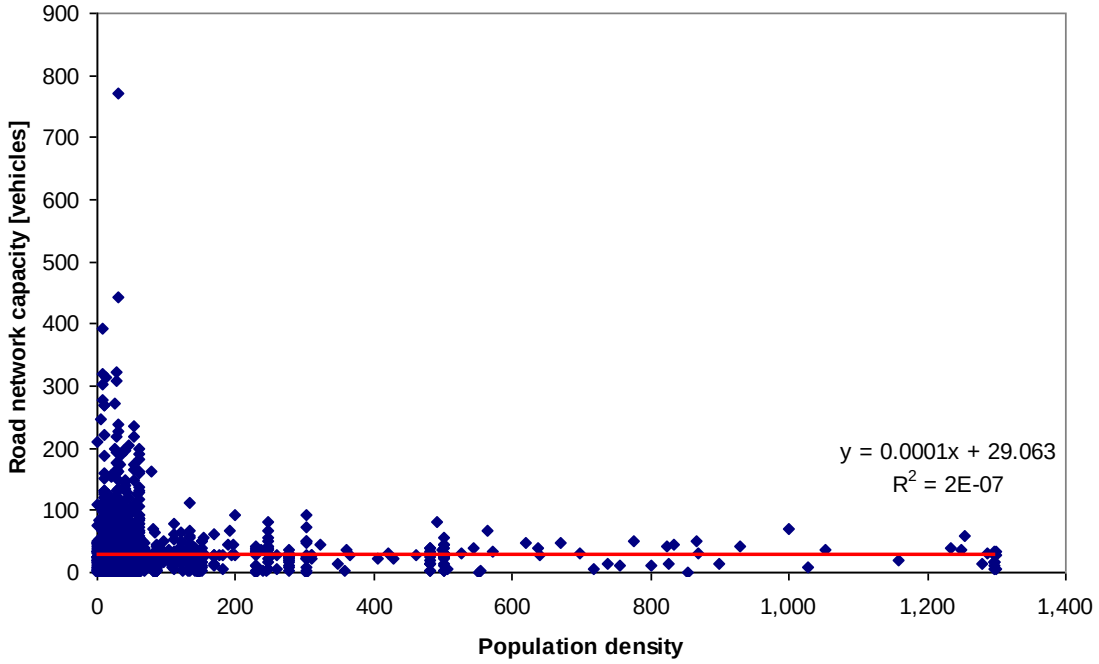

(d)

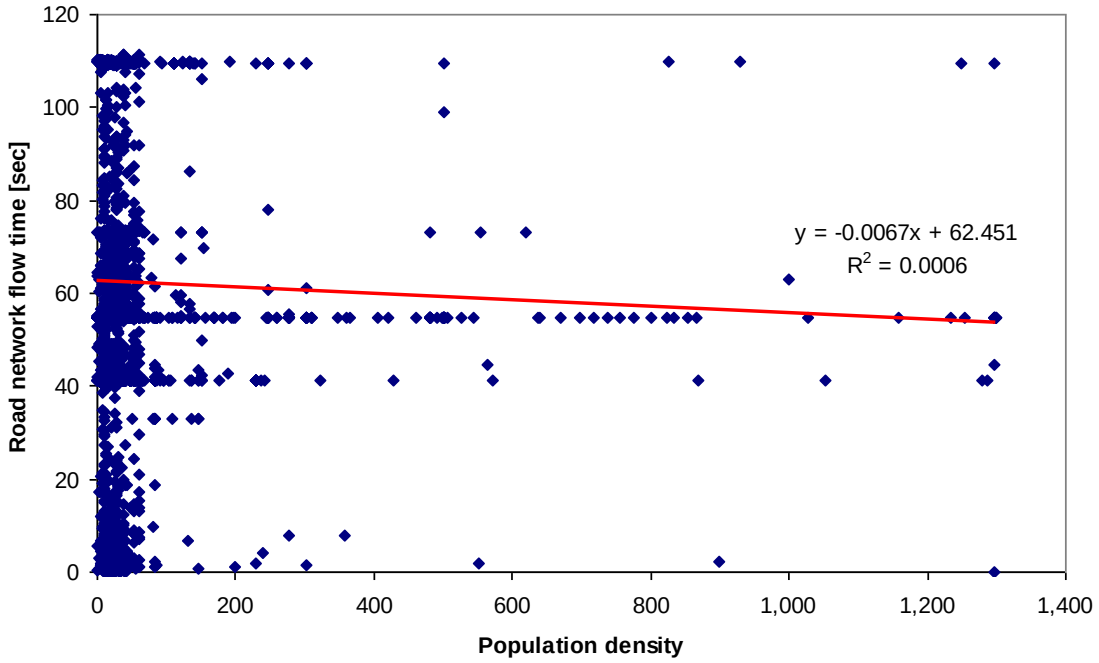

Figure 5.1: Costa Rica (a) road network capacity and (b) flow-time graphs for urban grid cells with respect to population density (number of people per km^2). (c) road network capacity and (d) flow-time graphs for rural grid cells with respect to population density.

The models fitted to the road network capacity and flow time results shown in figure 5.1 are linear and the RMSE was found to be 80 for figure 5.1a, 22 for figure 5.1b, 0.8 for figure 5.1c and 0.8 for figure 5.1c. The large variations in capacity and flow time as seen in the results for Costa Rica makes it difficult to develop any models that can be applied to grid cells where no OSM data is present. More factors such as elevation and wealth should ideally be investigated. The models developed here are simple linear models that can give a rough idea of the local road network capacity and flow time in grid cells with no OSM data.

The results regarding road network flow-time and capacity for a selection of countries were analysed and the quality of the available OSM data was determined. Table 5.2 shows the percentage of grid cells where a population exists. The table also describes the average road network capacity and flow-time for each country. For the road network flow-time the average flow-time lies at around 61 seconds which means an average speed of around 59 km h^{-1}.

Table 5.2: Statistical data for countries investigated regarding gridded road network capacity and flow-time. Grid cell resolution used: 30'' and 2011 OSM data.

Country	Percentage of grid cells with population but no OSM data [%]	Average capacity [cars/grid cell]	Average flow-time [sec/grid cell]
Panama	93	68	75
Costa Rica	84	42	62
Denmark	10	36	45
Average		**49 cars**	**61 sec ~ 59 km/h**

The purpose of developing models to describe the changes in road network capacity and flow-time is to improve the road network capacity and flow-time maps developed using OSM data. In section 5.4 models developed using OSM data from 2011 for three countries will be analysed and compared against OSM data from 2012 for these particular countries to investigate how good the models are.

5.4 Results and test of models

The following section investigates and tests the models and assumptions made in section 5.2.1 and 5.2.2 by comparing well documented road network surveys for two roads near Derby, UK with the results found using the equations provided in section 5.2.1 and section 5.2.2. Furthermore, the quality of a selection of road network capacity and flow-time models created for a number of countries in section 5.3 was investigated and tested against new OSM datasets collected nine months after the original OSM data were collected in 2011. The results can be found in section 5.4.2.

5.4.1 Capacity and flow-time equation test for single road

The following example illustrates the change in speed and flow-time on a road that is gradually being congested. It is also used as a simple way to test some of the many assumptions made regarding the road network capacity and flow-time. The equations tested in this section are equation 5.1, 5.2, 5.3, 5.4 and 5.5, but for single-roads only. Two roads in the UK were investigated the: A514 from Chellaston via Derby Ring Road to Derby City Centre and the A52 East from Derby Ring Road to Derby City Centre in the UK. The section of the A514 investigated is around 6.9 km long and the speed limit is 64 km h^{-1}. The section of the A52 investigated is around 1.8 km long, it has two lanes in each direction and the speed limit is 96 km h^{-1}. The braking distance and corresponding speed and flow-time were calculated for a growing number of vehicles (average length cars) on the road using equation (5.2) and (5.5). The flow was likewise calculated for the two road examples. Survey results from a 2008 traffic congestion survey regarding traffic routes in greater Nottingham, Derby, Leicester and towns in Leicestershire and South Derbyshire was used for illustration purposes (6Cs 2008).

Figure 5.2 a, b and c shows the flow-time, the speed and the speed as a function of flow-time for the A514. Figure 5.2 d, e and f show similar curves for the A52 road, when using the equations derived in section 5.2. The vertical green line illustrates the highest vehicle capacity that can be achieved with the minimum journey time, while the red vertical line shows the maximum vehicle capacity, given that there must be at least 1 m

between each vehicle. The yellow line shows the average capacity experienced in the 2008 survey for the particular road section during morning peak hours (8 am to 9 am) on normal weekdays. This value is based on the average travel delay per km, which is the journey time during peak hours minus the time taken to do the same journey at night under free flowing conditions. This travel delay was provided in the 6Cs 2008 report. The yellow line is only provided for illustration purposes. It shows the average number of vehicles on the road during morning peak hours in 2008.

The figures show that, as more vehicles enter the road, the number of vehicles exceeds the green line and the speed gradually reduces. The flow-time increases while the flow-rate grows. A limit is reached when the average speed reaches around 6 m/s and the number of vehicles that pass through the road decreases as shown in figure 5.2 c and f. For the A514 this limit it reached when there were 660 vehicles on the road. The braking distance was 6.3 m and the average speed was 22 km h^{-1}. At this speed, the optimal flow is achieved. For the A52 the limit is reached when there are 165 vehicles on the road, the braking distance is 6.3 m and the average speed is 21.9 km h^{-1}.

(a)

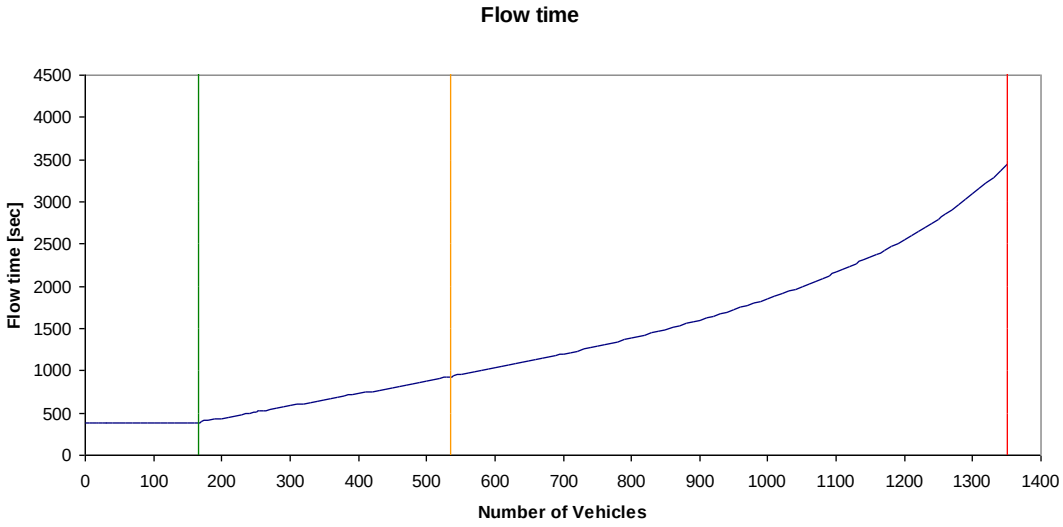

(b)

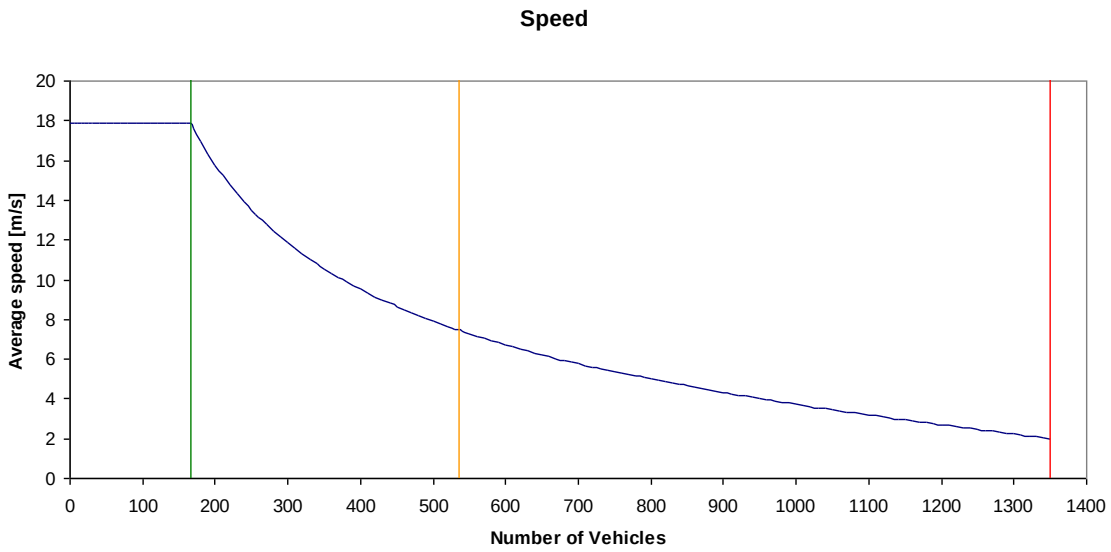
Speed
Average speed [m/s]
0
2
4
6
8
10
12
14
16
18
20
0
100
200
300
400
500
600
700
800
900
1000
1100
1200
1300
1400
Number of Vehicles

(c)

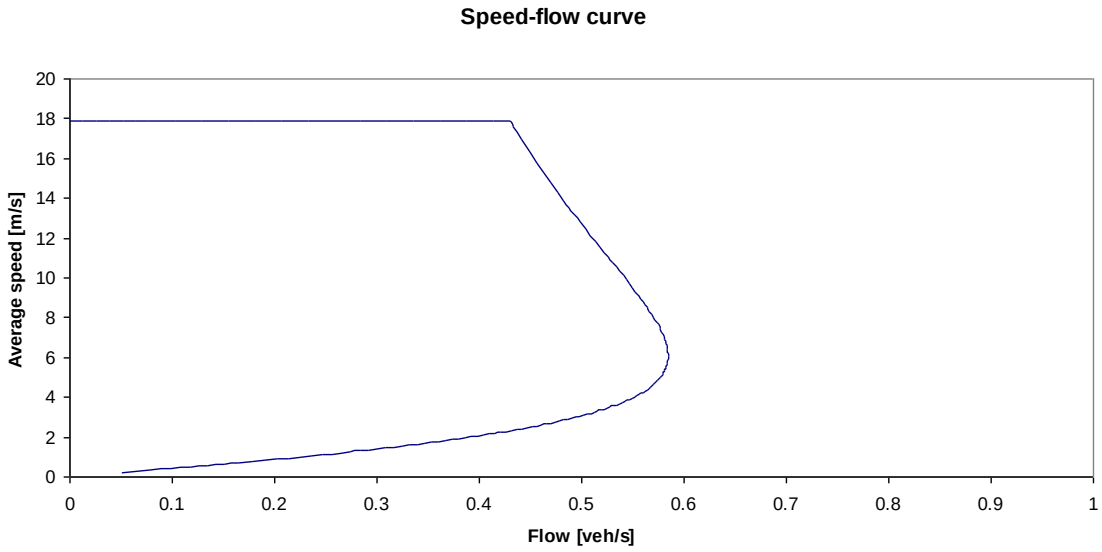
Speed-flow curve
Average speed [m/s]
0
2
4
6
8
10
12
14
16
18
20
0
0.1
0.2
0.3
0.4
0.5
0.6
0.7
0.8
0.9
1
Flow [veh/s]

(d)

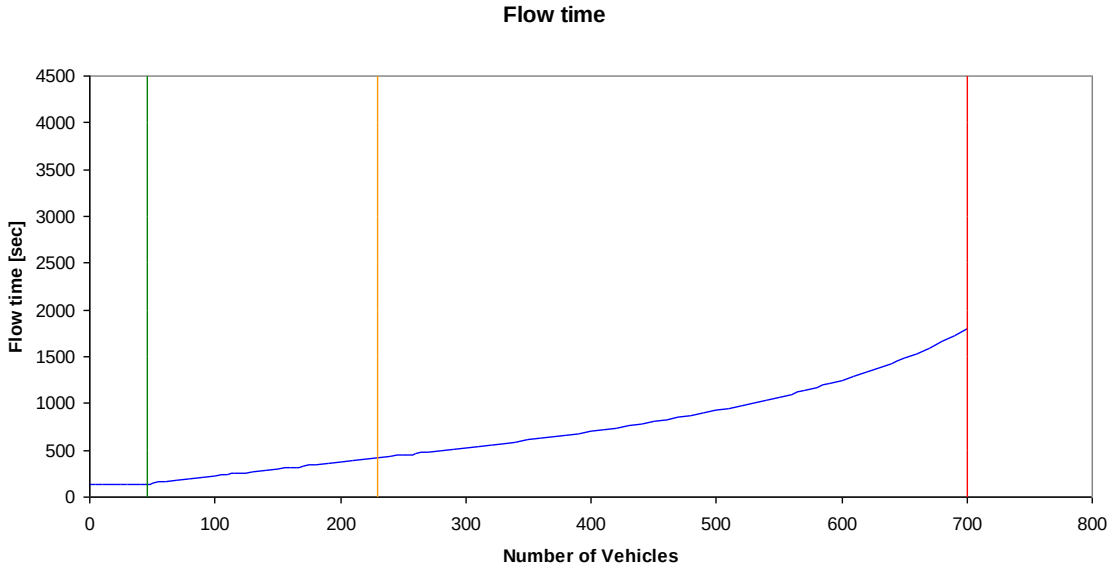
Flow time
Flow time [sec]
4500
4000
3500
3000
2500
2000
1500
1000
500
0
0
100
200
300
400
500
600
700
800
Number of Vehicles

(e)

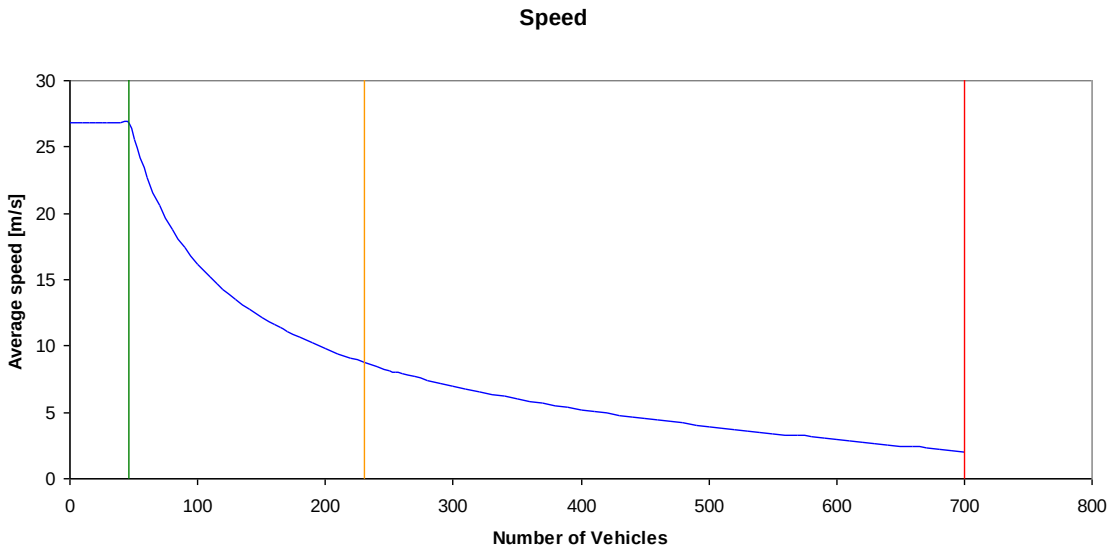
Speed
Average speed [m/s]
30
25
20
15
10
5
0
0
100
200
300
400
500
600
700
800
Number of Vehicles

(f)

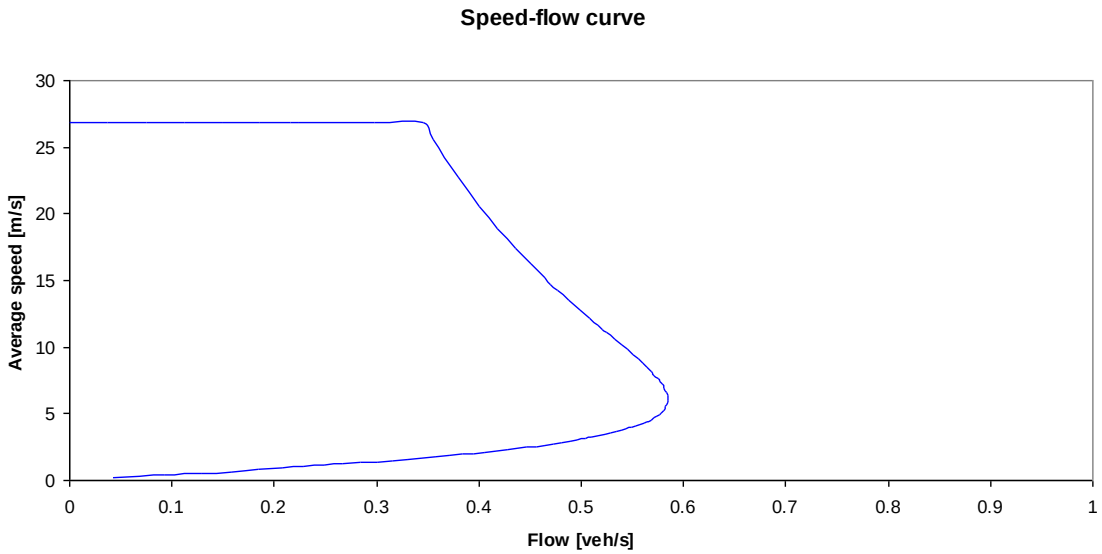

Figure 5.2: Change in (a) and (d) flow-time and (b) and (e) speed as number of car in a grid cell increases when $C_u > C$. (c) and (f) illustrates the speed-flow curve for A514 and A52 respectively.

The speed-flow curves show that by reducing the speed to 22 km h^{-1} or 6 m s^{-1} on the two roads investigated an optimal vehicle flow can be achieved. However, in the case where more than 650 vehicles are on the A514 road segment and 350 vehicles on the A52 road segment the flow will decrease.

Reducing the speed on congested roads has been used in order to reduce congestion and improve the flow. The UK highway agency use variable speed limits on motorways in order to reduce congestion and increase flow (Directgov b 2011).

To test the results derived using equation 5.1 to 5.5 for the two roads investigated, data were found regarding traffic counts for both roads. A traffic count for the A514 by the Head Mann Associates Ltd performed on Tuesday 18th May 2010 showed that during the peak hour, between 7:30 and 8:30, the number of vehicles counted was **1762** on the A514 north of the A5132/A514 junction and **1643** vehicles on the south of the junction, and "the junction would be considered as being near capacity in the weekday morning peak" (HMA 2010). For the A52 a traffic count was performed by the Highways Agency. Here a plot was created illustrating the hourly flows on the A52 on the Bardells Roundabout in Nottingham on Wednesday 15th March 2006. The plot shows that,

between 7:00 and 8:00, the number of vehicles counted was between **2200 and 2300** vehicles during that period. Between 8:00 and 9:00 it was between **1800 and 1900** vehicles and between 9:00 and 10:00 it was between **1550 and 1750** vehicles (Highways Agency 2006).

For the A514 example it was earlier found that between 8:00 and 9:00 on a normal weekday it took a car around 930 seconds to travel the 6.9 km and there were around 535 vehicles on the road segment investigated (figure 5.2 (a)). Over an hour, 2071 vehicles will travel through the investigated road segment. This is 309 more vehicles than the observed number from the traffic count between 7:30 and 8:30.

For the A52 road segment it was found that between 8:00 and 9:00 on a normal weekday it took a car 417 seconds to travel 1.8 km and there were 230 vehicles on the road segment investigated (figure 5.2 (d)). Over an hour, 1986 vehicles will travel through the investigated road segment. This is between 86 and 186 more vehicles than the 1800-1900 vehicles counted by the Highways Agency between 8:00 and 9:00.

The above results show that the models used for deriving road network capacity and flow-time provides results that are between 4.5% and 17.5% higher than the counted number of vehicles from the two surveys from Derbyshire, UK.

The tests performed in this section are for single roads only, and do not illustrate the much more complex multi-road scenarios. They results show that the assumption that the flow-time will increase as the road network becomes more congested can be used. They also show that the equations derived for describing the change in flow-time can be applied to the evacuation simulator.

5.4.2 Road network capacity and flow-time improvement and model testing

All the countries listed in table 5.2 had gridded capacity and flow-time maps created using the conversion software developed using the gridded population density and land usage data from GRUMP and the available OSM data. Models were developed based on these results and used for estimating the road network capacity and flow-time in areas where a population is present, but where no OSM data were available. This section describes the individual steps used to create these gridded maps. Tests were performed on

the data generated for three of the countries investigated: Costa Rica, Panama and Denmark. The quality of the estimated gridded road network capacity and flow-time data generated using the models generated in section 5.2 was investigated by comparing the results with a newer OSM dataset converted into gridded road network capacity and flow-time maps for the individual countries.

The three datasets were downloaded from OSM nine month apart and a difference in data size was observed. The OSM data file for Costa Rica grew from 55,910 kb to 82,370 kb, for Panama the file grew from 60,422 kb to 61,731 kb and for Denmark the file size grew from 2,280,799 kb to 2,983,836 kb. An increase in number of grid cells where road network data was available was observed. The number of grid cells where road network data were available grew by 4324 grid cells for Costa Rica, 850 for Panama and 12353 grid cells for Denmark.

Figure 5.3, 5.4 and 5.5 shows the different steps in generating gridded capacity and flow-time maps and improved capacity and flow-time maps for Costa Rica, Panama and Denmark, respectively, using the models derived from the initial gridded maps. Figure 5.3 (a) shows the gridded population density for Costa Rica as a map overlay on Google Earth. Figure 5.3 (b) shows the road network capacity found using the available OSM data while Figure 5.3 (c) shows the improved road network capacity using the models developed for the country. A newer set of OSM data was downloaded and the gridded road network capacity and flow-time was found for this dataset as can be seen in Figure 5.3 (d) and (g). Grid cells that did not have any OSM data in the previous dataset had road network capacity and flow time estimates applied to them. These were based on the models developed in section 5.3. The models developed in section 5.3 were based on the exiting knowledge regarding road network capacity and flow time and the corresponding population density in grid cells where a road network was provided by OSM. The grid cells where the road network capacity and flow time was based on the models were finally compared with the grid cells in the new dataset where OSM data was available and henceforth a road network capacity and flow time could be calculated. Figure 5.3 (e), (f) and (g) show the road network flow-time maps. Figure 5.3 (h) and (i) provide the road network capacity and flow-time estimates generated when only using the models for the particular country on the grid cells where a population is present. Finally

Figure 5.3 (h) shows that the models are able to identify larger settlements and to provide reasonable estimates for these. However, the models are not able to identify the major road network connections binding these settlements together. The dataset available from OSM show these main roads between the bigger settlements.

A comparison between the road network capacity grid cells generated from the available new OSM data and the equivalent grid cells where the road network capacity previously had been calculated using the developed models showed that the average difference is around 5 vehicles per grid cell between the model-based capacity estimate and the new OSM based capacity value. In some grid cells this difference was as large as 337 vehicles. For the flow-time, the average difference was around 18 seconds per grid cell and, in some grid cells, as large as 51 seconds (table 5.3). The root-mean-square error for the between the new capacity values and the values calculated using the models developed is 32 vehicles. For the two flow-time dataset the root-mean-square error is likewise 32 seconds per grid cell.

(a) Population density map

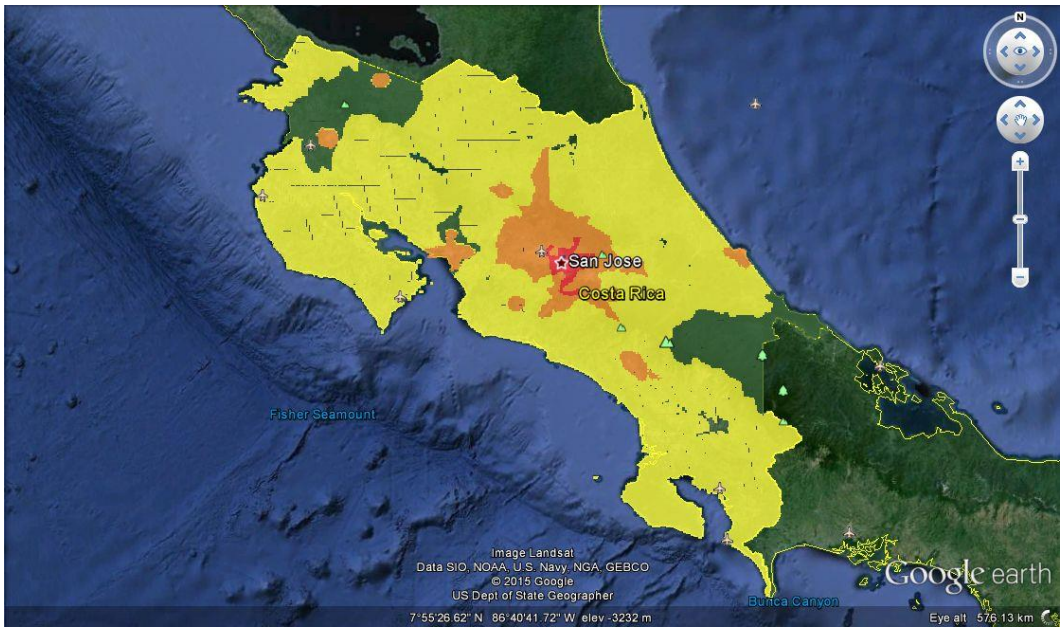

(b) Original capacity map

(c) Improved capacity map

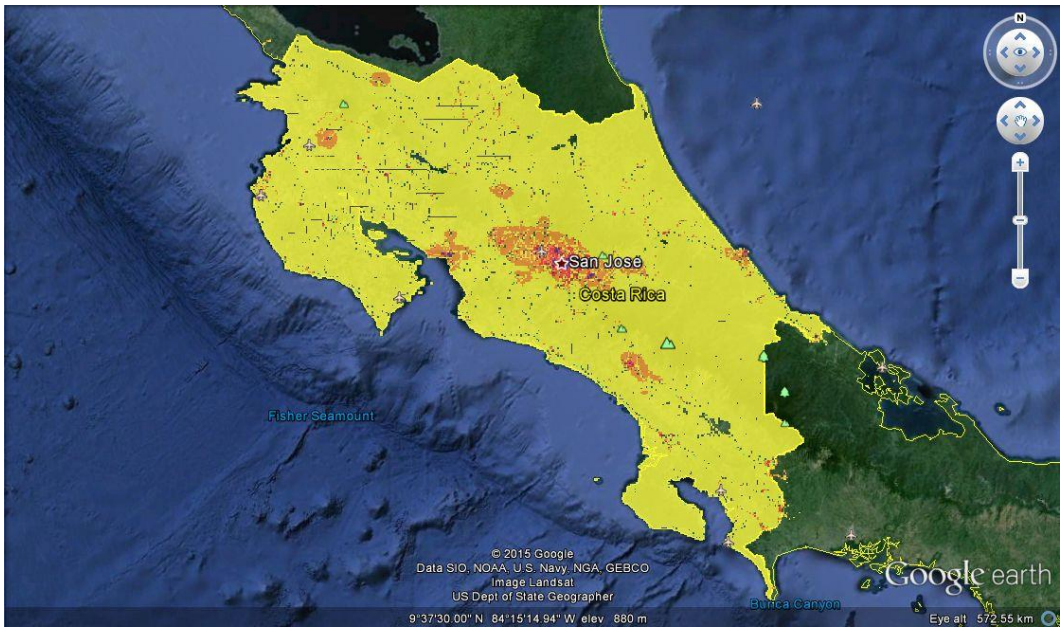

(d) New OSM capacity map

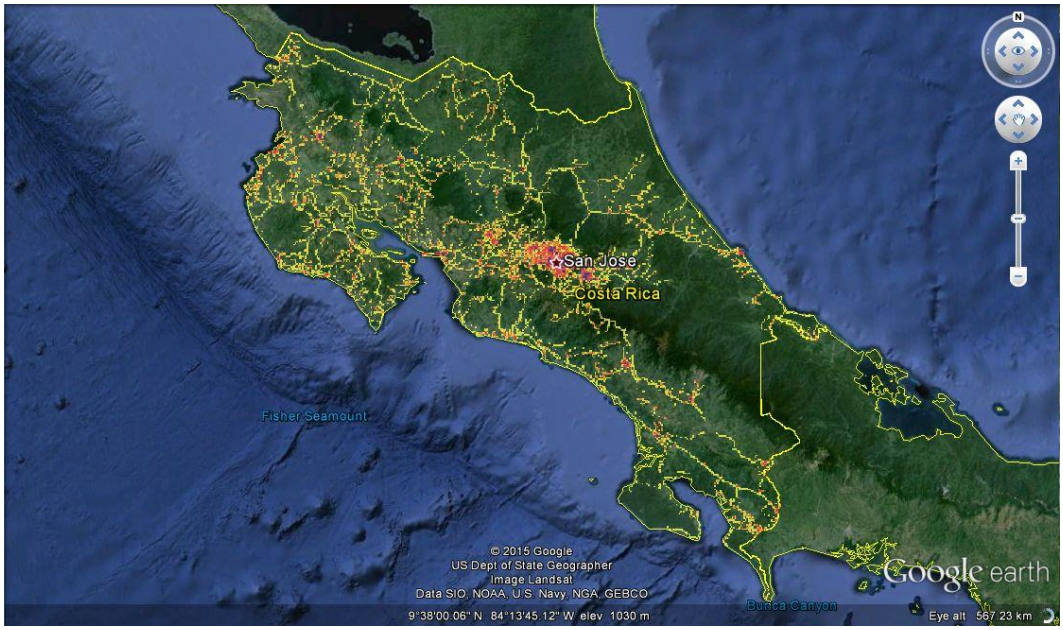

(e) Flow-time map

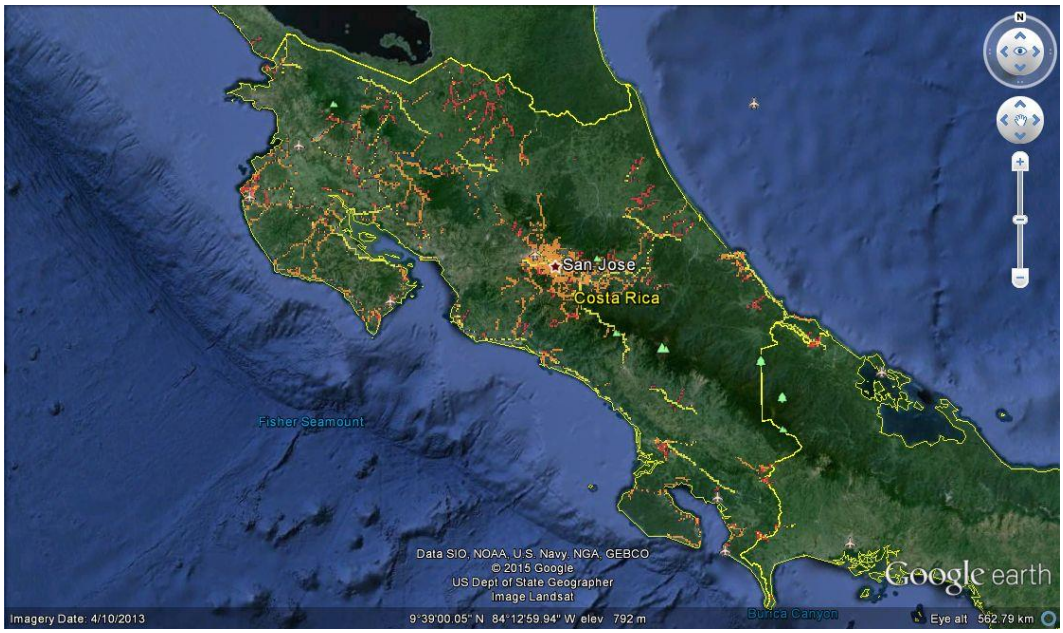

(f) Improved flow-time map

(g) New OSM flow-time map

(h) Models only capacity map

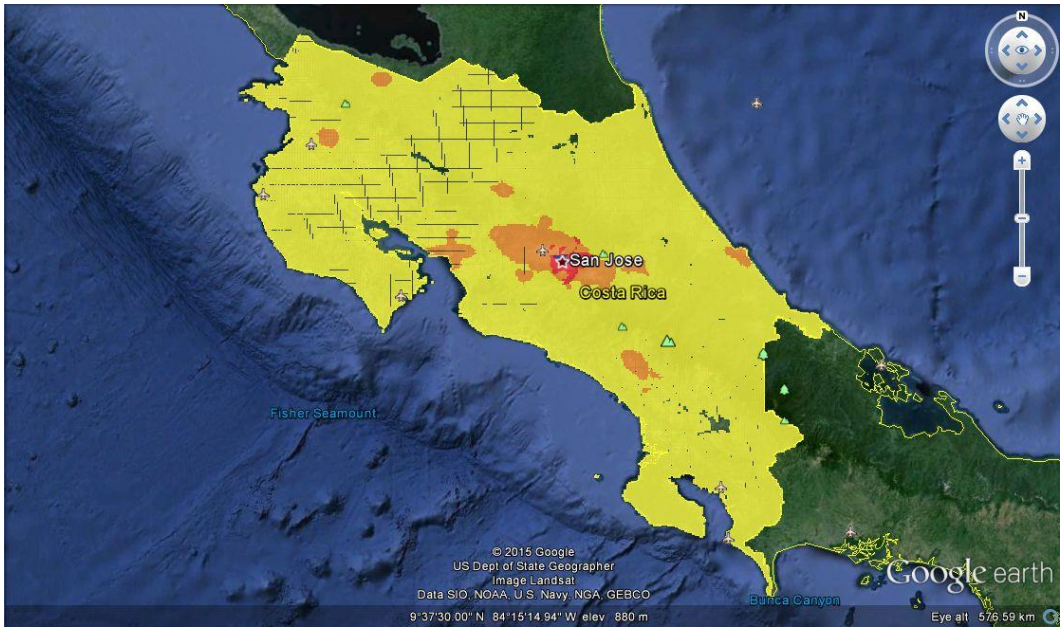

(i) Models only flow-time map

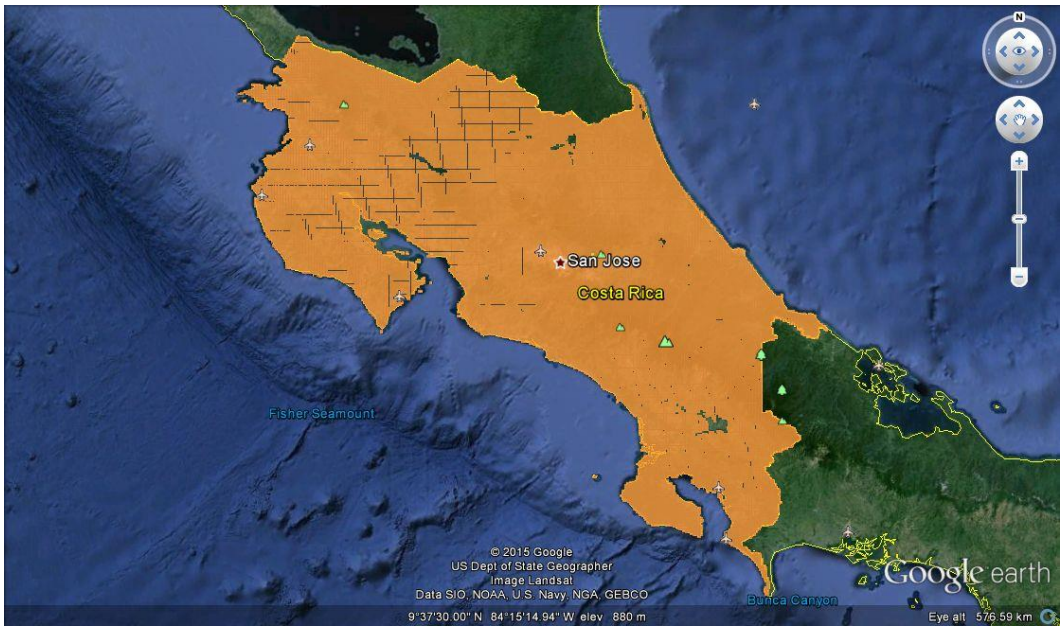

(j) Colour coding

Population density	Capacity [cars] and Flow time [sec]
0≤p<1	0≤c<1
1≤p<10	1≤c<10
10≤p<100	10≤c<50
100≤p<1000	50≤c<100
1000≤p<10,000	100≤c<250
10,000≤p<100,000	250≤c<500
100,000≤p	500≤c

Figure 5.3: Gridded data maps for Costa Rica. (a) gridded population density map overlapping Google map for the area investigated in Costa Rica (b) gridded capacity map of the area investigated (c) improved gridded capacity map using urban and rural models developed for Costa Rica (d) gridded capacity map of the area investigated using new data (e) gridded flow-time map (f) improved gridded flow-time map using models in grid cells where no OSM data are available, but where a population was present (g) gridded capacity map of the area investigated using new data. Finally (h) and (i) show the capacity and flow-time maps, respectively, using only models to generate road network capacity on all grid cells where a population is present. (j) provides the legend.

For Panama, 93% of grid cells had a population present, but no OSM data.

(a) Population density map

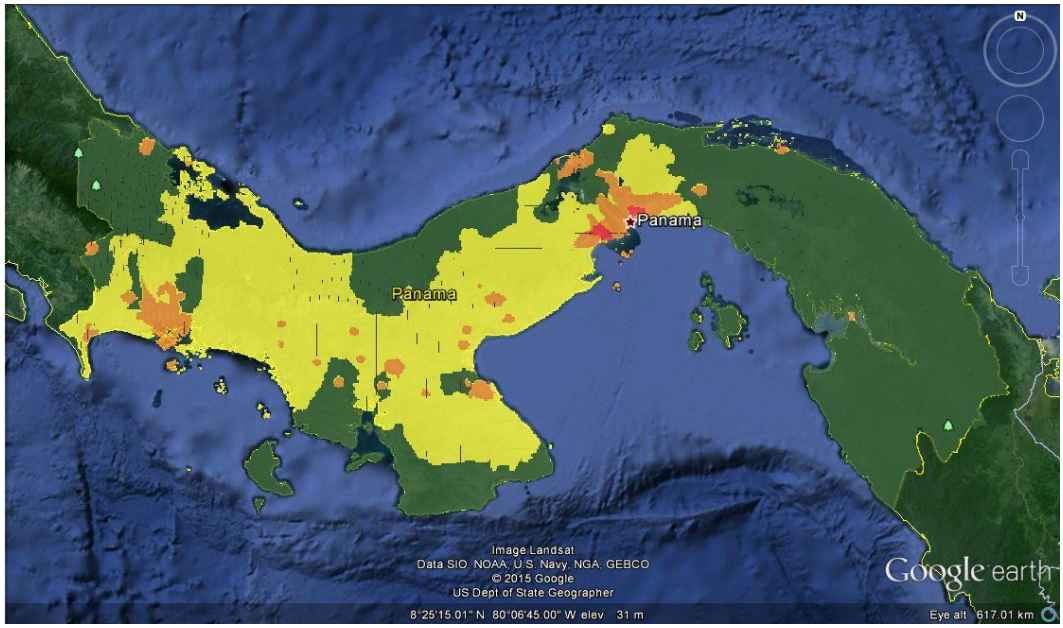

(b) Original capacity map

(c) Improved capacity map

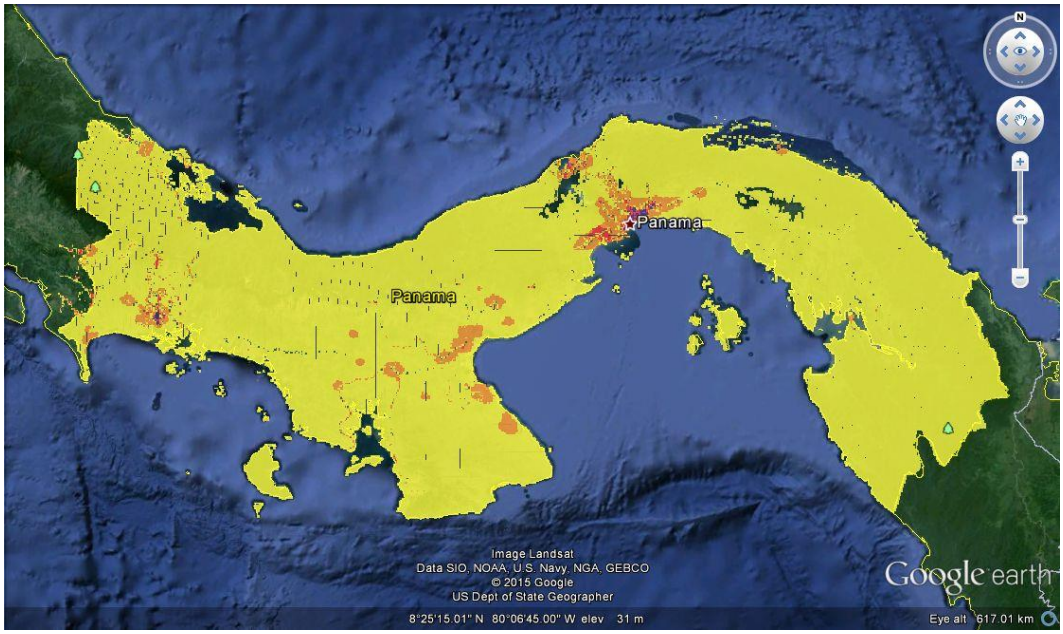

(d) New OSM capacity map

(e) Flow-time map

(f) Improved flow-time map

(g) New OSM flow-time map

(h) Models only capacity map

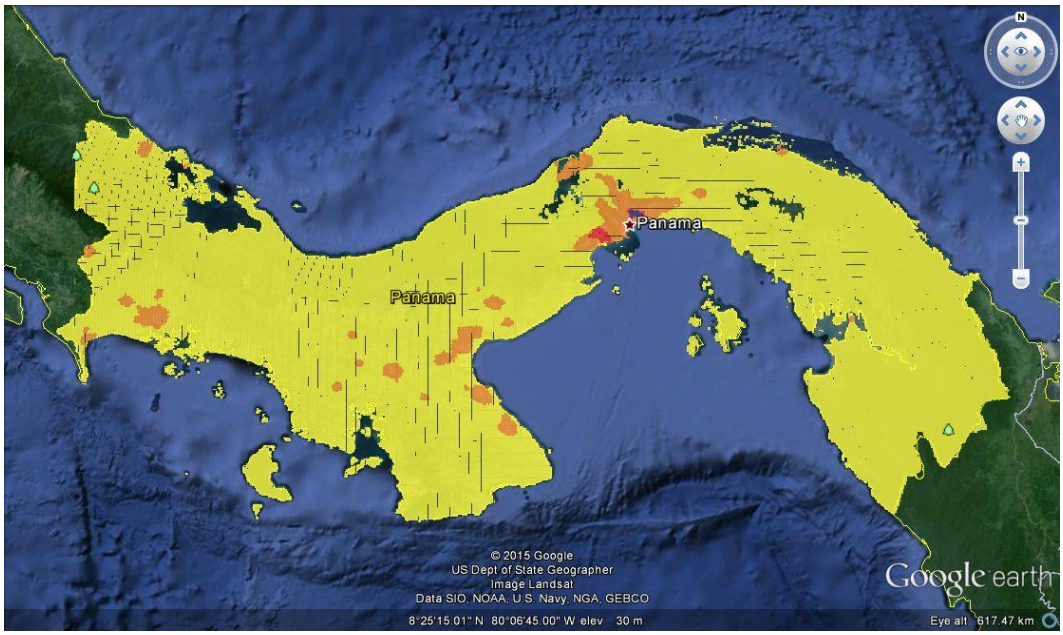

(i) Models only flow-time map

(j) Colour coding

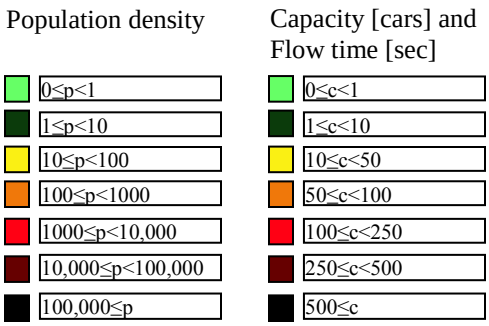

Figure 5.4: Gridded data maps for Panama. (a) gridded population density map overlapping Google map for the area investigated in Panama (b) gridded capacity map of the area investigated (c) improved gridded capacity map using urban and rural models developed for Panama (d) gridded capacity map of the area investigated using new data (e) gridded flow-time map (f) improved gridded flow-time map using models in grid cells where no OSM data are available, but where a population was present (g) gridded capacity map of the area investigated using new data. Finally (h) and (i) show the capacity and flow-time maps, respectively, using only models to generate road network capacity on all grid cells where a population is present. (j) provides the legend.

Table 5.3 shows that the average difference between new road network capacity grid cells and the estimated capacity using the models generated is 7 vehicles per grid cell. However, in some grid cells this difference can be as large as 94 vehicles per grid cell. For the flow-time, the average difference is 12 seconds per grid cell and can, in some grid cells, be as large as 37 seconds. The root-mean-square error for the between the new capacity values and the values calculated using the models developed is 29. For the two flow-time datasets the root-mean-square error is 25.

For Denmark only 10% of grid cells with a population do not have any OSM data available. The population density is also much higher than it is in Costa Rica and Panama as can be seen in Figure 5.5 (a).

(a) Population density map

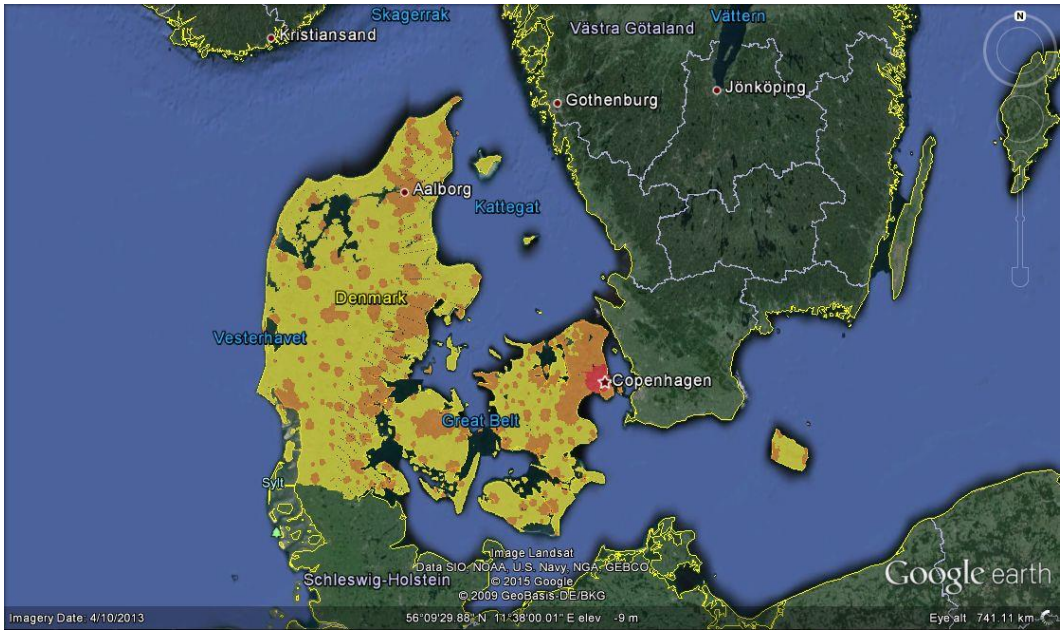

(b) Original capacity map

(c) Improved capacity map

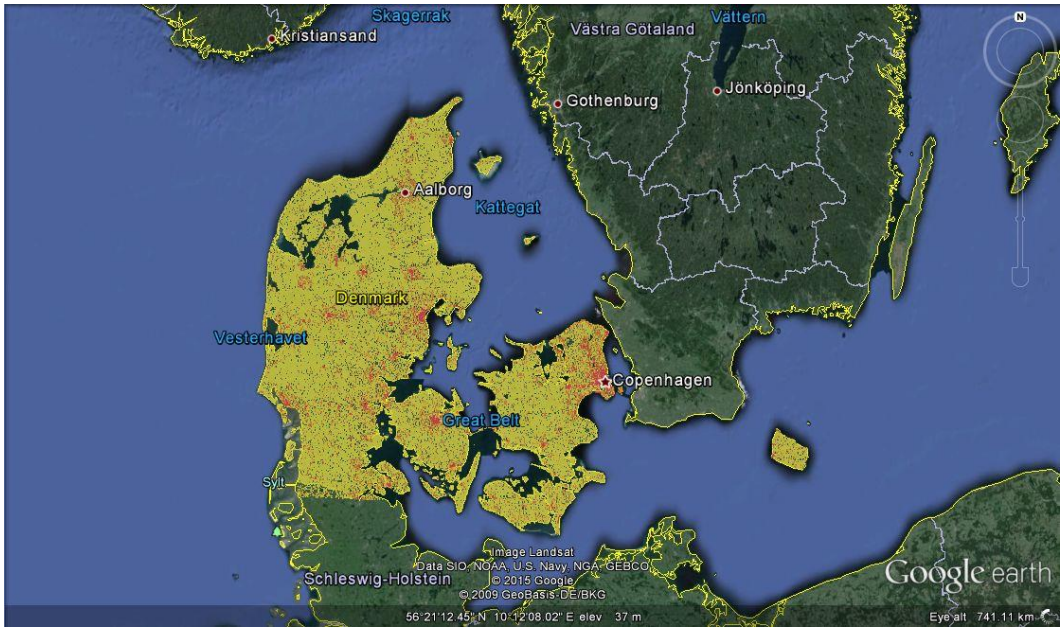

(d) New OSM capacity map

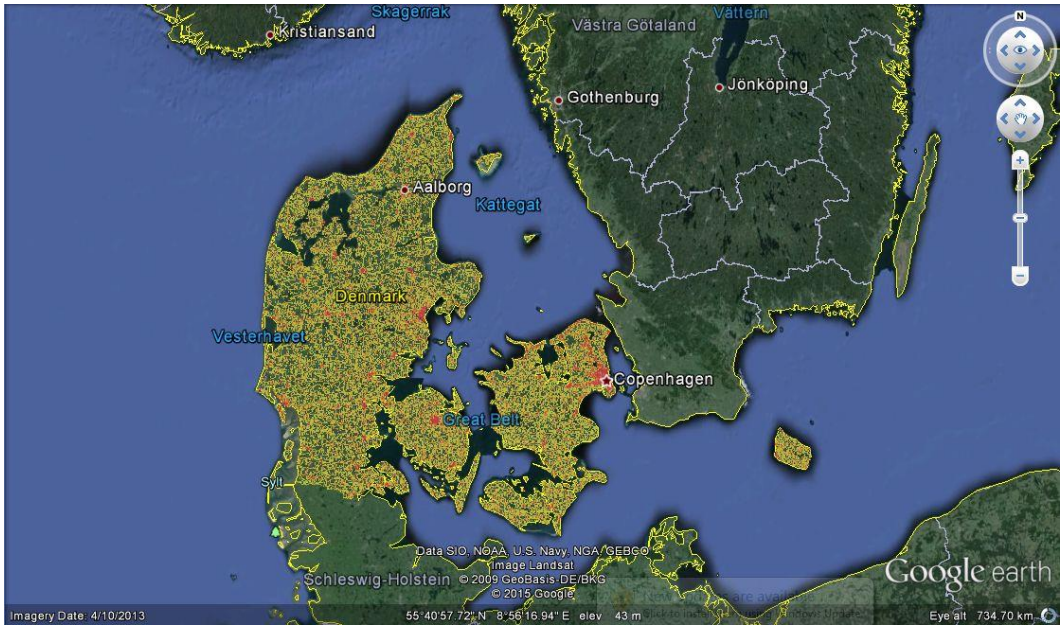

(e) Flow-time map

(f) Improved flow-time map

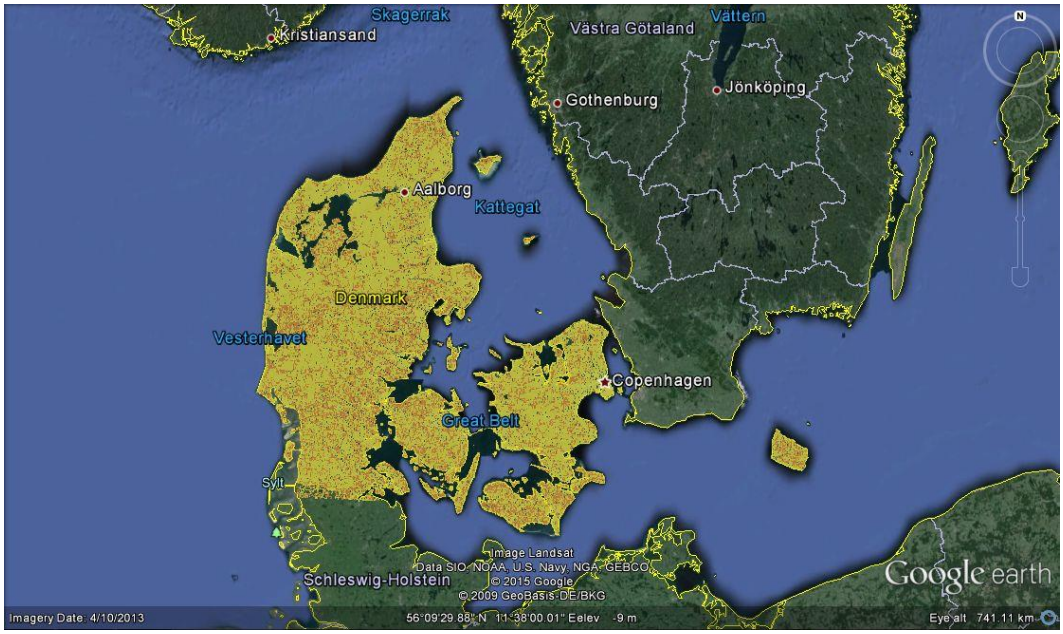

(g) New OSM flow-time map

(h) Models only capacity map

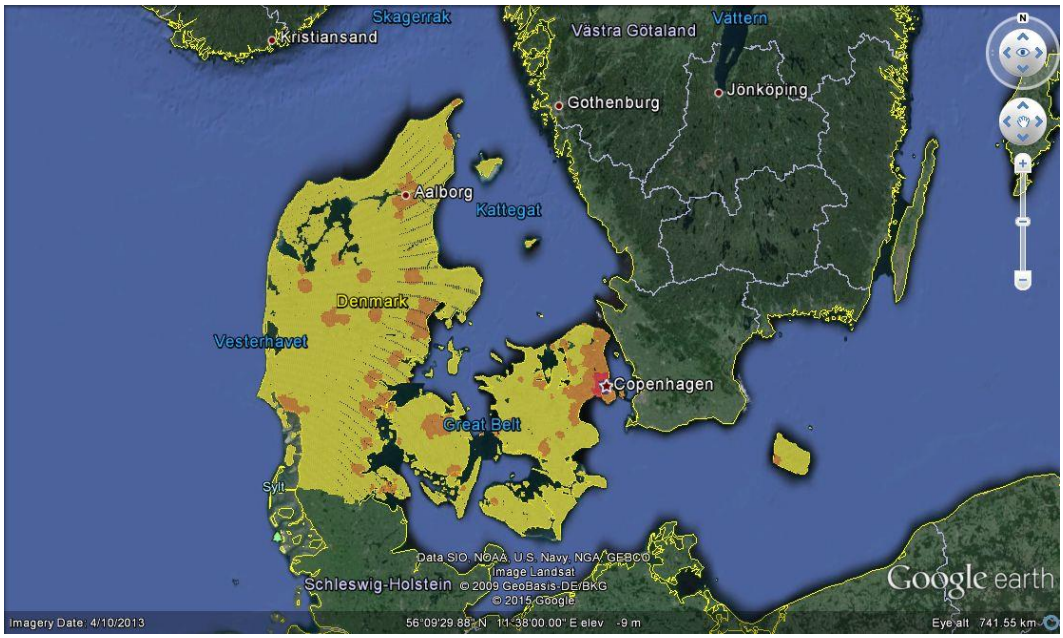

(i) Models only flow-time map

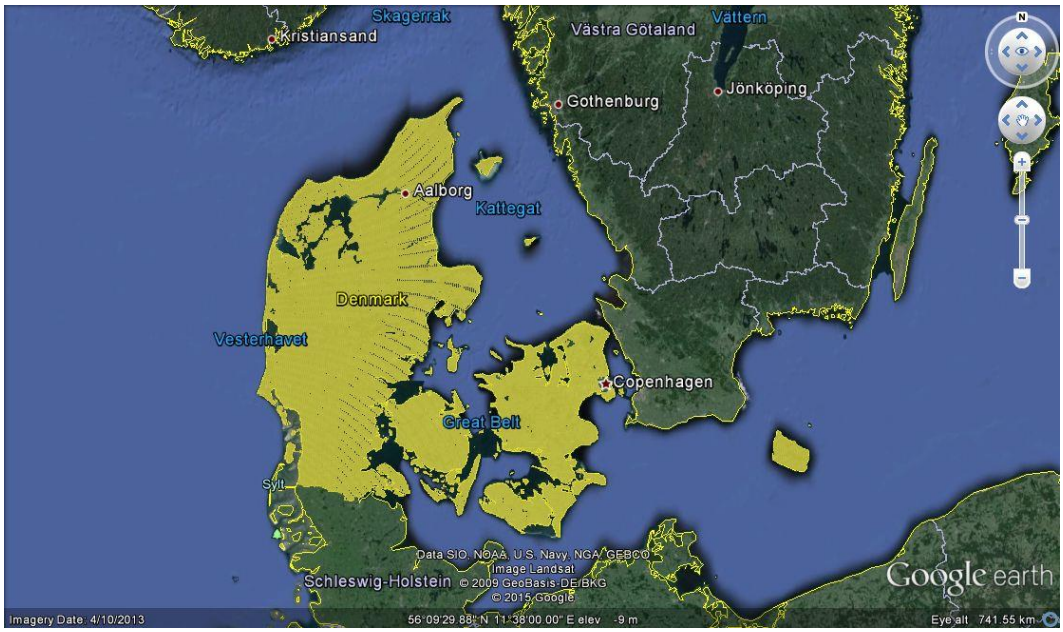

(j) Colour coding

Population density	Capacity [cars] and Flow time [sec]
0≤p<1	0≤c<1
1≤p<10	1≤c<10
10≤p<100	10≤c<50
100≤p<1000	50≤c<100
1000≤p<10,000	100≤c<250
10,000≤p<100,000	250≤c<500
100,000≤p	500≤c

Figure 5.5: Gridded data maps for Denmark. (a) gridded population density map overlapping Google map for the area investigated in Denmark (b) gridded capacity map of the area investigated (c) improved gridded capacity map using urban and rural models developed for Denmark (d) gridded capacity map of the area investigated using new data (e) gridded flow-time map (f) improved gridded flow-time map using models in grid cells where no OSM data are available, but where a population was present (g) gridded capacity map of the area investigated using new data. Finally (h) and (i) show the capacity and flow-time maps, respectively, using only models to generate road network capacity on all grid cells where a population is present. (j) provides the legend.

Table 5.3 shows that the average difference between new road network capacity and the estimated capacity using the models generated was 5 vehicles per grid cell. However, in some grid cells this difference can be as large as 161 vehicles. For the flow-time, the

average difference is around 7 seconds per grid cell and can, in some grid cells, be as large as 72 seconds. The root-mean-square error for the between the new capacity values and the values calculated using the models developed is 24. For the two flow-time dataset the root-mean-square error is 25.

Table 5.3: Average difference between original gridded road network capacity and flow-time data and modelled road network capacity and flow-time data for the countries investigated.

Country	Average capacity difference (vehicles)	Root–mean-square error for capacity results	Average flow-time difference (seconds)	Root–mean-square error for flow-time results
Costa Rica	5	32	18	32
Panama	7	29	12	25
Denmark	5	24	7	25

5.5 Behaviour-based evacuation models

New models to be used for modelling of the human decision-making and travel behaviour during an evacuation were developed to provide realistic models that reflect individual travel behaviour as well as household decisions.

In Chapter 2, it was recognized that hurricanes are natural hazards that, in several ways, are similar to the NEO hazard in that their arrival, magnitude and path of destruction can be predicted. Therefore evacuations due to an approaching hurricane can be similar to an evacuation due to an approaching NEO.

In this section, models for hurricane evacuation decision-making and travel behaviour were derived using travel behaviour data gathered from a range of evacuation surveys in the United States. For these surveys, people had been interviewed regarding their behaviour during one, or more, evacuations or their plans in the event of an evacuation due to an approaching hurricane. Based on these surveys, hypothetical models were derived for the modelling of travel behaviour during an evacuation due to an approaching NEO.

This section is structured as follows: Section 5.5.1 is a short introduction into behaviour-based modelling. Section 5.5.2 describes the survey data used to develop

behaviour-based evacuation models. These behaviour-based evacuation models are described in section 5.5.3 along with trends observed and uncertainties.

5.5.1 Introduction to behaviour-based modelling

When an evacuation order is issued the travel patterns of those evacuating will gradually change. New trips are being performed while preparing for the evacuation whereas normal, daily trips are cancelled by the individuals in each household (Baker 1995). Being able to capture these daily travel patterns, together with the changes to them due to an approaching hazard and an issued evacuation warning enables the simulation of evacuations and thereby prediction of evacuation clearance times and changes to transportation network load.

The decision to evacuate is not taken at the same time for everybody and will, among other things, depend on knowledge regarding the approaching hazard, the information received from official sources and previous experience with that type of hazard. Demographic characteristics such as age, gender, ethnicity, and income can also influence the decision (Post et al. 1993) (Dash et al. 2007). Some decide to evacuate very early in the duration of time set aside for the evacuation, while others decide to evacuate shortly before the arrival of the hazard. Being able to capture this gradual change from normal travelling to evacuation among a population is important in order to know the changes in load on a transportation network, the evacuation rates and expected clearance times. It is also important to take into account shadow evacuees. These evacuees are households that are located outside the area that is going to be evacuated but who either think they live within the evacuation zone and start to evacuate or just decide that they want to evacuate. Such an extra load could potentially bring the evacuation to a standstill in some areas.

5.5.2 Survey data

The survey data used for the development of behaviour-based evacuation models was collected from fourteen individual surveys carried out after evacuations due to approaching hurricanes. These survey reports contained information regarding:

- percentage of people evacuating prior to official evacuation notification and after official notification,
- percentage of people **believing** to have heard different types of notifications such as voluntary and mandatory,
- likelihood of choosing to evacuate based on gender, ethnicity, income and many more derivatives,
- chosen type of shelter and chosen destination,
- response rate (i.e. how fast do people respond to the warning, how much time do they need to prepare for evacuation and how long are their clearance times),
- percentage that use cars for evacuation.

The survey size varied from 120 to 7000 households but not all surveys contained all the above information.

5.5.3 Evacuation simulation models

The evacuation behaviour surveys collected show some trends. For example, more people evacuate if the approaching hurricane category is large, see Figure 5.7 and 5.9. Based on such observations, a series of decision and travel behaviour models have been derived in order to answer the following questions:

1) Did a household decide to evacuate prior to a warning (early evacuation)

2) Did the household hear the warning notice?

3) The probability of evacuating based on:

- notice heard or not
- the notice type heard (voluntary or mandatory)

- is the household located in the area that is to be evacuated or outside (shadow evacuees)?
- the magnitude of the approaching hazard, for hurricanes this is the hurricane category and for NEOs the different physical effects that are expected in the area
- gender

4) The evacuation destination (neighbourhood, own parish or out of parish)
5) The duration of the evacuation preparation

5.5.3.1 Households that decide to evacuate prior to a warning

A number of evacuation surveys were used for the development of a pre-warning evacuation model. The findings regarding how many that started evacuating prior to an evacuation warning in the evacuation surveys are summarised in table 5.4. The predicted hurricane category is the category that the hurricane was predicted to have at landfall. The actual category was on several occasions smaller. One of the surveys was a hypothetical survey while the remaining was surveys following actual hurricane in the United States of America.

Figure 5.6 shows the percentage of the population that evacuated prior to a warning for a number of hurricane evacuation surveys along with a model. This percentage varies between 4 and 61% with an average of 21.4% evacuating prior to a warning being issued. The small number of surveys makes it difficult to apply a model to the data so a conservative simple linear model was applied. This model shows an increase in the percentage of people that evacuate prior to an issued warning when the hurricane category increases. The model provides an adequate description of how the number of early evacuees will increase when the magnitude of the approaching hazard increases.

Table 5.4: Pre-warning evacuation survey results.

Hurricane	Hurricane magnitude in survey area	Location	Evacuation percentage [%]	Reference
Hypothetical	2.5	Lower Southeast Florida	5	Nelson 1989
	2.5		10	
Floyd	2.5	South Carolina	5	Dow et al. 2002
Opal and Erin	4	Alabama	20	Federal Emergency Management Agency 1995
Isabel	2	Maryland	10	Baker 2006
Andrew	4	Southeast Florida	15	Post et al. 1993
	4		20	
Georges	4	Lower Keys	61	Post et al. 1999b
	4	Alabama	35	
	4	Mississippi	26	
	4	Louisiana	36	
Ivan	3	South-eastern Louisiana	4	The Southeast Louisiana Hurricane Taskforce 2005
	3		11	
Lily	4	Louisiana & Texas	40	Post et al. 2003
Isabel	2	North Carolina	42	Post et al. 2005
Isabel	2	Virginia	10	
Isabel	2	Maryland	10	
Hugo	3	South Carolina	10	Post et al. 1990
	3		50	
Bonnie	2.5	North Carolina	8	Post et al. 1999

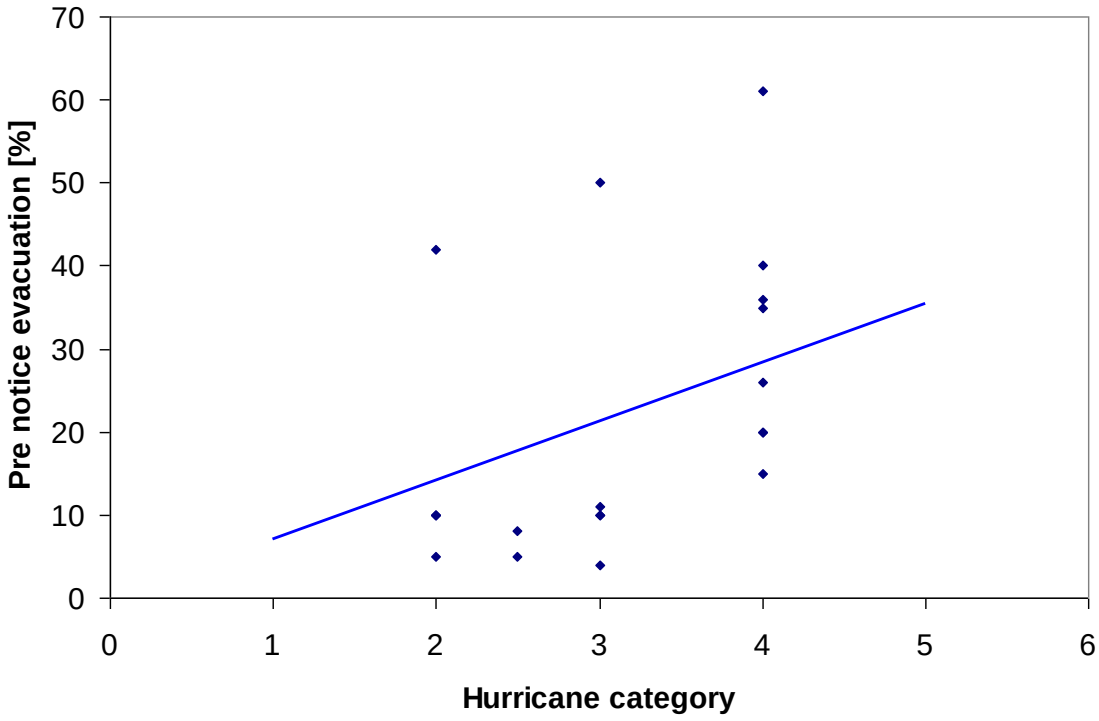

Figure 5.6: Decision to evacuate prior to a warning model (solid line) along with collected survey. data illustrated as dots

The model fitted to these observations can be described as follows:

$$p_w = 7h \tag{5.13}$$

p_w is the percentage of the population that will evacuate during the watch period, due to an approaching hazard, with predicted hurricane intensity, h, on the Saffir-Simpson hurricane scale. The fitted model was found to have a root mean square error of 14%. The average percentage of people evacuating using equation 5.13 is:

$\bar{p} = \frac{\sum_{h=1}^{5} 7h}{5} = 21\ \%$. This result is almost the same as the average calculated using the survey data, which is 21.4%. The outcome from a student t-test reveals that the model fit is **not significant**, P(T<=t) one-tail is 0.35. It must here be said that modelling human behaviour is a major challenge. Factors such as previous experience, how the warning

was presented, distance from predicted landfall area, gender, ethnicity and wealth should ideally be taken into account. The surveys used in this section do not provide such detailed information. It will likewise be a challenge to find such detailed information globally to use when running the model. It would though be useful to have such detailed models to use in a micro-simulator, where detailed descriptions of the local community exist.

5.5.3.2 Did the household hear the warning notice?

Two models were developed to describe the probability of a household hearing the public notice, informing the public that an evacuation has been issued: one for households located inside the evacuation area and one for households located outside the evacuation area. Figure 5.7 illustrates the survey results along with the models that were applied to the survey results. The figure shows that the probability of a household hearing a warning is higher for households living in the area that is being evacuated than for households living outside the area. The models applied are simple linear models, but they show how the number of people hearing a notice increases with respect to an increasing hurricane category. This behaviour has been observed in several evacuation behaviour surveys.

The proportion, p_{in}, of households within the evacuation area hearing a warning can be described as:

$$p_{in} = 13\ h + 13 \tag{5.14}$$

and the proportion of households outside the evacuation area (shadow evacuees) hearing a warning is,

$$p_{out} = 10\ h - 6 \tag{5.15}$$

The fitted models were found to have a root mean square error of 22% (5.14) and 17% (5.15) with respect to survey data. The average percentage of people hearing a notice is

52% for inside the evacuation area and 24% for outside the evacuation area when using the developed models. This is very close to the average using the survey data, 44.5% for inside the evacuation area and 21.1% for outside the evacuation area. A student t-test reveals a P(T<=t) one-tail of 0.42 and 0.48 for the models where people are hearing a notice inside the evacuation area and outside the evacuation area respectively. The model fits are once again not significant, but they do illustrate the rise in awareness with respect to the hurricane category.

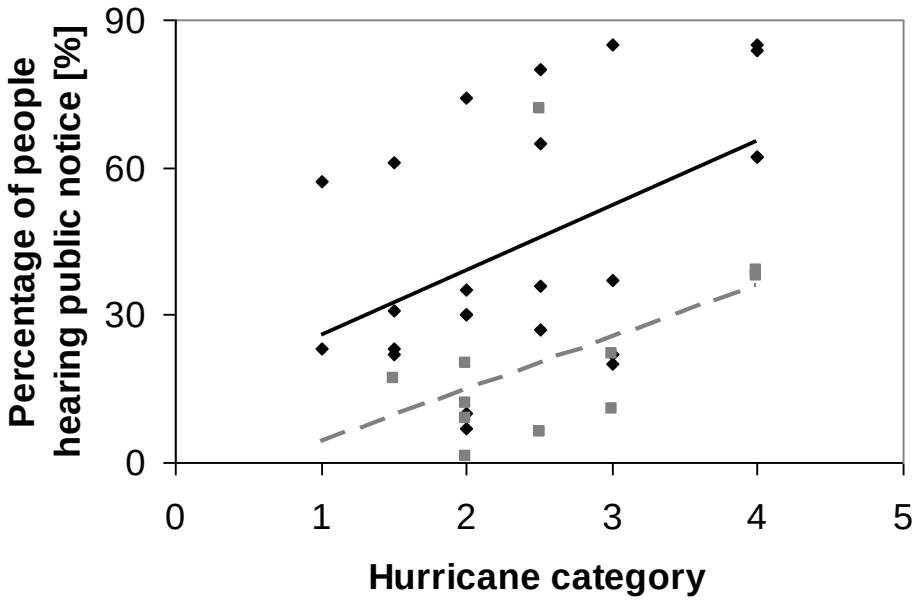

Figure 5.7: Percentage of people hearing a public notice in the area that was evacuated (solid line) and percentage outside evacuated area (dashed line) along with the survey results for inside (dots) and outside evacuated area (squares).

5.5.3.3 The probability of evacuating

It was found that the probability that a household decided to evacuate depended upon the notice type heard. Based on this observation, three models were derived describing the probability of a household evacuating for each of the following warnings:

- a mandatory warning
- a voluntary warming
- no official warning.

These models are shown in Figure 5.8. The three models show that the probability of evacuating is higher for households which believed they heard a mandatory warning than households that believed they heard a voluntary warning or did not hear a warning. The probability of evacuating also increases with respect to the hurricane category. These three models are for households located in an area where a warning has been issued. Households outside the area that is being evacuated could also decide to evacuate. They usually evacuate because they have heard a warning and think that this warning also applies to them. The probability of being a shadow evacuee is based on the probability of hearing an evacuation notice as illustrated in Figure 5.7 and the probability of evacuation based on hearing either a mandatory or voluntary warning as in Figure 5.8. Households outside the evacuation area were assumed to have a probability of evacuating if they heard an evacuation notice.

People are more likely to evacuate after hearing an official mandatory evacuation order, than a voluntary order, and people are least likely to evacuate if they do not hear an evacuation order.

The models describing the proportion deciding to evacuate after believing they heard an official, mandatory evacuation order was found to be:

$$p = 3h + 66 \quad \text{for } h \geq 1 \tag{5.16}$$

whereas the proportion that evacuates after believing they had heard a voluntary evacuation order is

$$p = 4h + 40 \quad \text{for } h \geq 1 \tag{5.17}$$

Finally, the proportion evacuating in spite not hearing an official evacuation order is

$$p = 6h + 19 \quad \text{for } h \geq 1 \tag{5.18}$$

These models were found to have a root mean square error of 17% (5.16), 19% (5.17) and 20% (5.18) with respect to survey data.

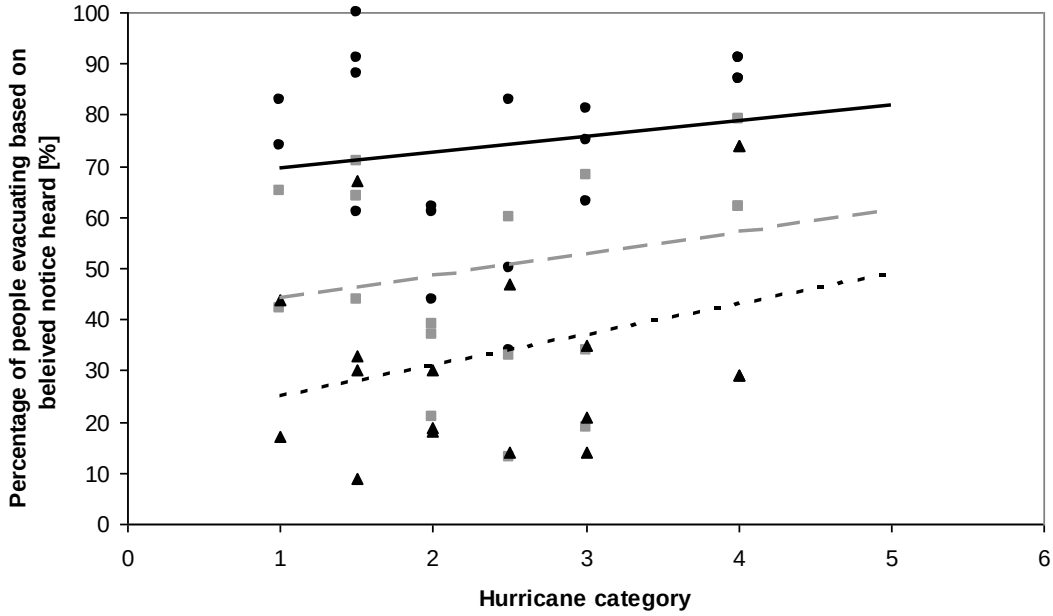

Figure 5.8: Models describing the probability of evacuating when believed hearing a mandatory warning (solid line), voluntary warning (coarse dashed line) and no warning (fine dashed line). The survey data is described as dots (mandatory), squares (voluntary) and triangles (no notice heard).

A student t-test reveals a P(T<=t) one-tail of 0.47, 0.46 and 0.40 for the models where people are hearing a mandatory notice, a voluntary notice and are not hearing any notice respectively. The model fits are once again not significant but they do illustrate the rise in awareness with respect to the hurricane category.

5.5.3.4 Evacuation start time models

The time at which people start to evacuate depends on when the warning is issued and the time provided to evacuate. Surveys show that people prefer to start evacuating between 05:00 and 23:00 hrs. A peak in the number of evacuees is expected at approximately 14:00. Consequently, two types of models were used in NEOMiSS to describe the proportion of people beginning their evacuation at each time step: a Normal distribution and a Pearson distribution, the example in Figure 5.9. The Pearson model is used to address the skewness (asymmetry) that can be expected in some scenarios, due to

the peak in number of evacuees at around 14:00. This peak can be modelled using Pearson model in examples where the evacuation starts or ends close to the peak.

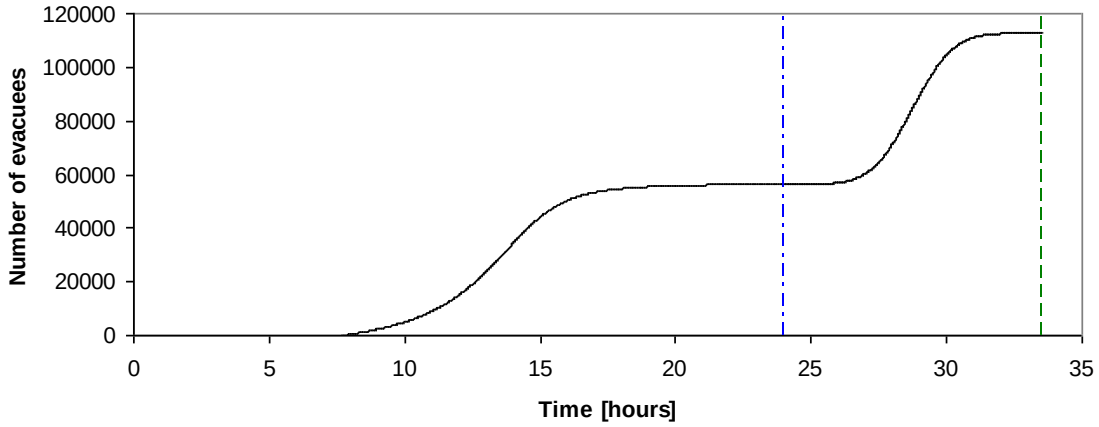

Figure 5.9: Example of Pearson and normal distribution showing the cumulative percentage of people starting to prepare for evacuation (solid line).

In the scenario in Figure 5.10, people start evacuating at 7:30 and the evacuation finished around 9:30 the following day. A Pearson distribution was used to model the cumulative number of evacuees starting to evacuate on the first day while a normal distribution was used to model the cumulative number of evacuees on day 2.

If several days are provided for evacuation, a proportion of evacuees will delay their departure by one or more days. This proportion is based on the number of days available and will be equally distributed across the individual days, for example out of a total of 1000 evacuees 10% evacuate before an official evacuation is issued. Thereafter 18% evacuate every day over the following 5 days while the evacuation is running.

Two models have been developed describing this behaviour depending on the time available in the scenario. An example showing the cumulative percentage of evacuees evacuating during a one day evacuation scenario is illustrated in Figure 5.10 while Figure 5.11 provides an example of a longer evacuation scenario. Two types of evacuees have been identified: those who start evacuating prior to a warning being issued and those who start evacuating after a warning has been issued.

Pre-warning evacuation start times

It is unknown how early households start evacuating prior to an issued warning. Some might start prior to a watch while others start when a watch has been issued. It is therefore assumed that in NEOMiSS households that start evacuating prior to a warning start evacuating between an issued watch and a warning.

Post-warning evacuation start times

People prefer to start evacuating between 5:00 and 23:00 according to the outcomes from surveys regarding people's evacuation behaviour during hurricane Lili (Post et al. 2003), Isabel (Post et al. 2005), Bonnie (Post et al. 1999), Opal and Erin (Florida 1996) and Opal (Alabama 1996). A peak in number of evacuees would be expected between these two times, around 14:00 and the standard deviation would be 9 hours. The model developed for the evacuation simulator in NEOMiSS reflects the above habits.

"One-day" scenario model

The "one-day" scenario model predicts when a household will start evacuating during the day of the evacuation. It uses Normal and Pearson distributions to model the cumulative number of evacuees starting to evacuate. The Polar method was used for selecting a random number from a normal distribution in order to generate random numbers, to be used when deriving the time of day when a household starts evacuating. The normal distribution is applied on a normal 24 hour day, with an average of 14 hours and a standard deviation of 9 hours. This represents the peak in the number of households starting to evacuate around 14:00. Figure 5.10 illustrates the cumulative percentage of households starting to prepare for evacuation during the day. In this example it shows that almost 40% of households start preparation prior to a warning which in this example was issued at 7:00. The remaining households start preparing for evacuation after the warning is issued and before the hazard arrival time at 22:30.

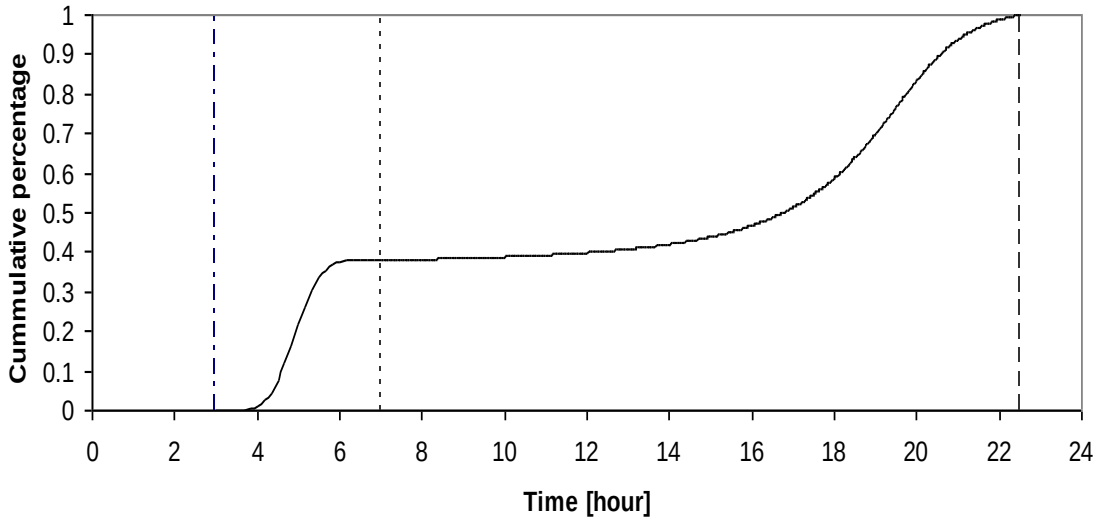

Figure 5.10: Single day evacuation start model case study showing the cumulative percentage of people starting to prepare for evacuation (solid line). In this scenario, the watch was issued at 3:00, a mandatory warning was issued at 7:00 and the hazard arrived at 22:30 (dashed vertical lines). The hazard was in this example a category 3 hurricane.

"Multiple days" scenario model

For the multiple day scenario the number of evacuees was assumed to be spread evenly across multiple days. The evacuation surveys show that the spread is not evenly distributed across the days, but the results are inconclusive and this simplification has been found to be the best representation of the spread. Post et al. (1999b) provide an example of the spread of people evacuating over a 6 day period in 5 different survey areas. The hurricane in question was Hurricane Georges which resulted in 604 casualties in 1998. Table 5.5 is a recreation of the table provided in Post e al. (1999b). It shows how people living in Lower Keys in Florida start evacuating a day earlier than elsewhere, this is due to a watch being issued in this area already on the Wednesday and an evacuation warning on the Thursday whereas the remaining regions first had a watch issued in the Friday and a warning Saturday. It is important to notice that there must be a minor error regarding the data for NW Florida. The total percentage of evacuees for NW Florida is 113%. When looking at table 5.5 it becomes clear that how early people start evacuating and how many evacuates on the different days varies. Factors such as how the

information regarding the approaching hurricane was delivered, the probability of making landfall and previous experience influenced the outcomes in the different survey areas.

Table 5.5: Date evacuated in Georges, by state.

	Louisiana	Mississippi	Alabama	NW Florida	Lower Keys
Tuesday	0	0	0	0	17
Wednesday	4	4	5	19	44
Thursday	8	4	8	6	30
Friday	24	18	22	38	6
Saturday	51	49	47	38	1
Sunday	12	26	17	12	0

The model developed for the evacuation simulator first found the day when a given household will start evacuating. This was done by generating random numbers between 1 and the number of minutes between watch start time and warning start time for pre-warning evacuees and between warning and impact for post-warning evacuees. The corresponding day is then found. Thereafter, it uses the same polar method as for the one-day scenario to find the time of day when the household will start evacuating. Assuming the scenario is a three day evacuation: for the first day the generated time must lie within are between watch time (pre-warning evacuees) / warning time (post-warning evacuees) and end of day in minutes. For the following days the time must lie within the start of day and the end of day and for the last day the time must lie between start of day and warning / impact time. Figure 5.11 shows the cumulative percentage of households starting to evacuate during a 6 day evacuation scenario. Between the issued watch and warning only a small percentage of households start evacuating. It is first after the issued warning that the majority of households start evacuating.

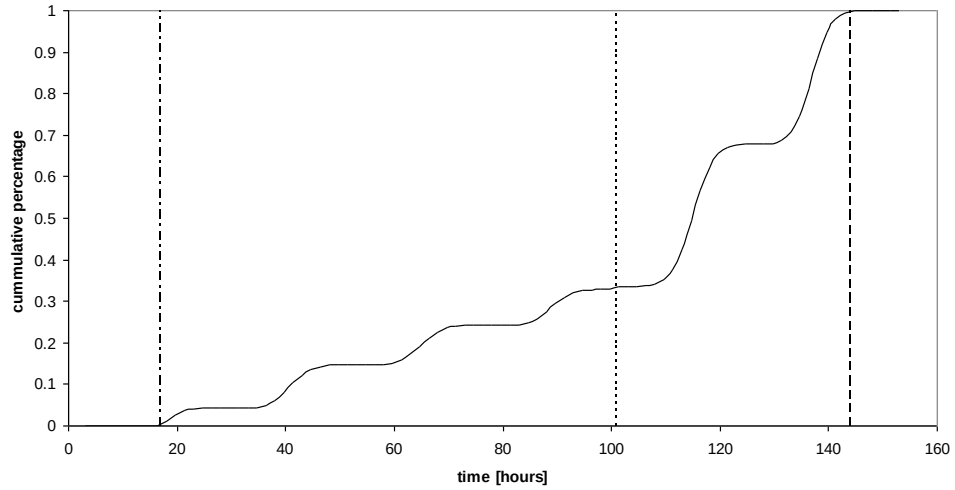

Figure 5.11: Multiple days evacuation start model, cumulative percentage of evacuees starting to **evacuate** (solid line), the watch was issued at 17:00 on the first scenario day, a mandatory warning was issued at 5:00 on the 5th day and arrival of hazard was at 23:59 on day 6 (dotted lines). A hurricane of magnitude 3 was used in this scenario.

5.5.3.5 Duration of the evacuation preparation model

The model describing the duration that a household spends on preparing for an evacuation is based on results from Kang et al. (2007). In Kang's survey the results include a table with expected time needed to perform different evacuation preparation tasks and actual time used when evacuating from hurricane Lili in 2003. These actual times show that on average a household spends 150 minutes on evacuation preparation. The corresponding standard deviation is 87 minutes. The model derived describes the time used to prepare for evacuation and uses the polar method with an average of 150 and a standard deviation of 87.

5.5.3.6 Number of vehicles used

It was found in the hurricane evacuation surveys that on average 68% of vehicles available were used for evacuating. There are, however, large fluctuations in the data collected. The percentage of vehicles used for evacuation lies between 53% and 79%. These fluctuations are in part due to variations in peoples' evacuation behaviour due to

wealth and ethnicity among other factors. For example, many households in the wealthy town of Charleston evacuated using two or more cars during the hurricane Floyd evacuation in 1999.

5.5.3.7 NEO evacuation decision and travel models

Many of the models used for describing household decision-making and travel behaviour during an evacuation due to an approaching NEO can be assumed to be similar to those developed for evacuations due to approaching hurricanes. The developed hurricane evacuation models are based on hurricane magnitude. These categories are from the Saffir-Simpson Scale and are based on wind-speeds. The wind-speeds due to a NEO land impact blast wave can be converted into hurricane categories and the models developed in the previous sections can be used for areas where wind speeds of hurricane magnitude can be expected. Closer to the impact location other models are needed.

It can be assumed that the model predicting whether a household heard a notice is unchanged as well as the preparation duration model. The model predicting whether a household evacuates early will also remain unchanged along with the evacuation start time models.

The model predicting whether a household evacuates was changed to reflect that previous experience cannot be expected in such a rare event and that given a good information campaign many more will evacuate due to this hazard than due to a Hurricane. It can be expected that anything from 0% to 100% of households will evacuate from an area stretching from the impact location out to where there are wind speeds similar to hurricane category 5 force winds. From there the evacuation decision model for hurricane evacuations is used. A sensitivity analysis will be required in order to investigate how the outcome will change if for example 0%, 20%, 40%, 60%, 80% or 100% evacuate in this inner region of the area at risk of an NEO impact.

5.6 A coarse-scale evacuation flow simulator

This section describes the coarse-scale evacuation flow simulator developed for NEOMiSS. The road network capacity and flow time models described in section 5.4 along with the evacuation behaviour models from section 5.5 are used in this simulator. A number of additional models and assumption are described in section 5.6.1. This is followed by evacuation software in section 5.6.2, model testing and sensitivity analysis in section 5.6.3 and case studies in section 5.6.4.

5.6.1 Additional models and assumptions

New behaviour-based evacuation models were described in section 5.5. These were used for the modelling of human decision-making and travel behaviour during an evacuation. The models for hurricane evacuation decision-making and travel behaviour were derived using travel behaviour data gathered from a range of evacuation surveys from the United States, where people had been interviewed regarding what they did during either one or more evacuations or what they were planning to do in the event of a evacuation due to an approaching hurricane. Based on these models more hypothetical models were derived for the modelling of peoples' travel behaviour during an evacuation due to an approaching Near Earth Object, NEO. The evacuation area due to a potential NEO impact was assumed to include all regions where the ignition exposure was high enough to ignite paper, an ignition exposure of 330,000 Jm^{-2}. Within this area, everybody is assumed to evacuate. Beyond this boundary the wind speed (due to overpressure) was converted into hurricane intensity and the hurricane evacuation behaviour models were used. In this coarse-scale evacuation simulator the following behaviour-based models were used to mimic people's decision-making and behaviour during an evacuation:

a. Probability of evacuating prior to a warning model, equation 5.13
b. Warning notice heard models, equations 5.14 and 5.15
c. Probability of evacuating models, equation 5.16, 5.17 and 5.18, but without taking gender into account.

d. Evacuation start time models as described in section 5.5.3.4
e. NEO evacuation decision and travel models as described in section 5.5.3.7

Change in travel time

During an evacuation it is likely that the roads will become congested. This would cause a reduction in the speed that can be achieved on a given road. In this simulator, congestion was modelled as an increase in transit time through a grid cell. This increase in flow-time was modelled using UK guidelines on braking distance, which can be modelled using equation 5.2. The speed can be found knowing the number of vehicles in a given grid cell, measured in number of cars, c, the average car length, c_a, N_c is the number of cars and the total road length of cross cutting roads, l_t, in a given grid cell. This provides the average distance between each vehicle and the speed is then

$$S = [(\frac{l_t}{N_c} - c_a) \times \frac{1}{0.3}]^{1/1.6}. \quad (5.28)$$

The flow-time, f, is then

$$f = \frac{l_a}{S}, \quad (5.29)$$

where l_a is the average road length through a given grid cell. In addition, an upper limit on road capacity was set. This was based on the assumption that there must be a minimum one meter separation between each car. When the maximum capacity is reached no more vehicle flows can enter the grid cell and the flow will be brought to a standstill until there is road capacity available again. There are no capacity limits on walking flows and mopeds will be assumed to be ½ car length. l_t and l_a were calculated for each grid cell at the same time as the gridded road network capacity and flow-time were calculated in section 5.2 and N_c is the total number of car evacuation flows within a grid cell. It is important to mention that the calculation of car speed and flow-time using

equation (5.28) and (5.29) are different from the descriptions in section 5.2. In this section the values are made on a grid cell basis whereas in section 5.2 individual roads had their capacity and flow-time calculated and the results were used to estimate the road network capacity and flow time in the individual grid cells.

Three modes of transport were simulated in this simulator: cars, mopeds and pedestrians. This decision is based on the available data from Worldmapper regarding number of cars and mopeds in each country. Other modes should be added to the simulator such as buses, ferries and airplanes, but the lack of knowledge on a global scale regarding public transportation currently limits the simulation. Evacuating by car is usually seen as being fastest, but there are cases where travelling on foot might be just as efficient. This can be the case when the maximum capacity of the local road network has been reached.

The simulation treats evacuees as flows that move from one grid cell to the next with the aim of simply leaving the affected area or moving to neighbouring settlements outside the evacuation area. A flow is in this simulator defined as a decimal number larger than 0.0 and there are three types of flow: car-flow, moped-flow and pedestrian-flow.

Several other assumptions were made in the evacuation simulation such as number of people per car, average walking speed and average car length (see Table 5.6). These assumptions were based on research, although some should ideally be improved, for example, to reflect differences in wealth and demographic composition. It has, for example, been observed that in Charleston many households used more than one vehicle when evacuating (Dow et al. 2002). Households usually prefer to evacuate together using only one vehicle. The high wealth in this area is believed to be the main reason for such behaviour and such behaviour will cause more traffic congestion.

Table 5.6: General assumptions used in coarse-scale evacuation flow simulation.

	Assumption
Number of people per car	4 people
Number of people per moped	1 person
Moped average speed	45 km h^{-1}
Average walking speed	5 km h^{-1}
Shadow evacuation area	5 km
Average car length	4.12 m
Average moped length	½ car length

Evacuation types

Two types of evacuation can be run using the Evacuation simulator in NEOMiSS.

- One where the evacuees travel to just outside the evacuation area
- One where they travel to the nearest settlement with available shelter space.

This last approach is more realistic since people are more likely to evacuate to an area where there is access to drinking water, shelter and health services.

The initial evacuation scenarios will only simulate that evacuee's travel to just outside the evacuation area. Future work should investigate the second type of evacuation, where evacuees travel to the nearest settlement with available shelter space.

Attractiveness

When flows move from one grid cell to a neighbouring grid cell, the direction is based on "attractiveness". An attractiveness score, *a*, for each neighbouring grid cell is calculated. This is based on:

- grid type; grid cells outside the evacuation area are given a high score. This is to ensure that the evacuation flow leaves the evacuation area.
- distance to edge of evacuation area; shorter distance gives a higher score. This is to encourage the evacuation flows to move towards the edge of the evacuation area.
- flow-time; if flow-time in a grid cell is low then the score improves. This is to encourage evacuation flow to travel through the fastest grid cells.

Equation 5.30 describes how attractiveness is calculated.

$$a = n + \frac{1}{f} + \frac{1}{d} \times 1000 + A \times 10 \qquad (5.30)$$

where n is a negative number if the grid cell is one that has recently been visited by the flow, else it is positive. n is set to -5000 if the grid cell recently has been visited by the flow. This is to discourage any flows to travel back and forward between two grid cells and to maintain the flow away from the evacuation area. Each flow will keep a record of the previous grid cell that they have visited. The flow time f is only of minor importance whereas d, the distance to the edge of the affected area measured in number of grid cells, is of very high importance in this model, leading to a factor of 1000 being used. A is the grid cell type. A factor of 10 has been used to make this part of the model of more medium importance. Four grid cell types exist in the simulator: evacuation, shadow, rural and urban cells. Each area type has been given a value: evacuation areas are 0, shadow areas are 1, rural areas are 2 and urban areas are 3. Hence, grid cells with short flow-time and in close proximity to the edge of the affected area are preferred by the evacuation flows, if the first evacuation strategy is used (the "just get out of the evacuation area" strategy), and urban areas outside the evacuation area are preferred if the second strategy is used.

Shadow evacuees

When modelling shadow evacuees in hurricane evacuation scenarios it is uncertain how far out this group of evacuees stretches from the area that is to be evacuated, so the following assumption was taken:

The Shadow evacuation area is set to be 5 km wide (this area is a band 5 km wide outside the actual evacuation area stated in the scenario).

This assumption seems to be reasonable since some people living within this distance are likely to be uncertain about whether they live within or outside the area that

is to be evacuated. People living further away should know that they live outside the area to be evacuated.

Nearest cities/settlements to evacuate to

Another element to the model is the extra capacity a settlement has for evacuees. It can be assumed that this will depend on the size of a settlement. Larger settlements such as towns and cities have more schools and community centres and are more likely to have more hotels/motels than smaller settlements such as villages. It was found that in Hampshire each town and city has an excess capacity of around 19%, which means that if a town has a population of around 10,000 people then this town has space for around 1900 evacuees. Hereon, an average of 2-16% can be accommodated in public shelters and the remaining with family/friends or hotels/motels. But it can also be as low as 0.5% as seen in Southampton, UK and as high as 90% in Oak Bluff, Massachusetts. These observations are based on the Hampshire county council public shelter map along with shelter capacity information from Connecticut and Massachusetts (US Army Corps of Engineers et al. 1994) (US Army Corps of Engineers et al. 1997).

A correlation between the number of people using public shelters and time of day has been observed by the Hazard Management Group, Inc. (1988), with more using public shelters if it is a late night evacuation.

Based on these observations it was assumed that each settlement has space for a population increase of 19%.

Number of vehicles used

It was found in section 5.5 that on average 68% of vehicles available were used for evacuating. There are though large fluctuations in the data collected. This is among other things due to variation in people's evacuation behaviour due to wealth. Data regarding number of vehicles available are available from The World Bank. They provide estimates of how many cars exist in each country. These data are presented as the number of passenger cars per 1000 people and mopeds per 1000 people.

5.6.2 Evacuation simulator software

The coarse-scale evacuation simulator uses gridded data and a bucket flow model. It is a meso-simulator and the main structure of the simulator is as follows:

1) A scenario is read into the simulator. This scenario provides information about:
   - the centre location of the evacuation area
   - the radius of the evacuation area (only used in hurricane evacuation scenarios)
   - the type of evacuation: managed or self managed (currently only self managed is supported by the software)
   - the type of warning: mandatory or voluntary
   - the hazard type: hurricane or NEO impact
   - hurricane category, if it is a hurricane scenario
   - start of watch time, start of warning time and time when the hazard is expected to arrive
   - the country codes for the affected countries involved in the evacuation

   Additional information regarding how the simulator should run is added to it:
   - in how big time-steps should the simulator operate: 30 seconds time-steps have been used
   - whether evacuees evacuate to just outside the evacuation zone or to a settlement outside the evacuation zone (currently only cases to just outside the evacuation zone has been tested)
   - how long the simulator should continue to simulate after the hazard has arrived, this was set to 4 hours in the simulations run for this thesis
2) Load in gridded road network capacity gridded data for the area to simulate
3) Load in gridded road network flow-time gridded data for the area to simulate
4) Load in gridded population data and urban/rural data for countries within the area that is being simulated
5) Load in car data for countries within the area that is being simulated
6) Evacuation area is identified. This area depends on hazard type. For hurricanes an area is specified in the scenario file. For NEO impacts an area is identified using

the results from the physical impact simulator. The area goes out to where wind speeds of hurricane category 2 can be expected.

7) Identify area types: evacuation area, shadow area and outside evacuation area (urban area if that evacuation type has been selected). Grid cells where wind speeds of hurricane category 1 can be expected are marked as shadow evacuation grid cells for NEO impact evacuations. Grid cells beyond category 1 are the exit zone. Then calculate the attractiveness for each grid cell as described in section 5.6.1 using equation 5.30. A recursive function has been developed to perform this task.
8) Calculate the proportion of people within the different grid cells that will evacuate prior to a warning and after a warning has been issued using equation 5.13 to 5.18
9) Initiate evacuation models regarding when households will start evacuate based on section 5.5.3.4. For the normal distribution following equation is used to describe the probability density function for when people will start evacuating:

$$f(x,\mu,\sigma) = \frac{1}{\sigma\sqrt{2\pi}} e^{-\frac{(x-\mu)^2}{2\sigma^2}}, \tag{5.31}$$

where σ is the standard deviation and μ is the mean. For the Pearson distribution the following equation is used:

$$p(x) = \frac{\left|\frac{\Gamma(m+\frac{v}{2}i)}{\Gamma(m)}\right|^2}{\alpha B(m-\frac{1}{2},\frac{1}{2})}\left[1+\left(\frac{x-\lambda}{\alpha}\right)^2\right]^{-m}\exp\left[-v\left(\arctan\left(\frac{x-\lambda}{\alpha}\right)\right)\right] \tag{5.32}$$

This is a type IV distribution, where *m* and *v* are the shape parameters, α is the scale parameter and λ is the location parameter,

$\langle x \rangle = \lambda - \frac{av}{2(m-1)}$ is the mean, (5.33)

$\mu_2 = \frac{a^2}{r^2(r-1)}(r^2+v^2)$ is the variance, (5.34)

$\sqrt{\beta_1} \equiv \frac{-4v}{r-2}\sqrt{\frac{r-1}{r^2+v^2}}$ is the squared skewness, (5.35)

$$\beta_2 \equiv \frac{3(r-1)\left[(r+6)(r^2+v^2)-8r^2\right]}{(r-2)(r-3)(r^2+v^2)} \text{ is the kurtosis,} \quad (5.36)$$

$$r = \frac{6(\beta_2 - \beta_1 - 1)}{2\beta_2 - 3\beta_1 - 6} \quad (5.37)$$

$$v = -\frac{r(r-2)\sqrt{\beta_1}}{\sqrt{16(r-1)-\beta_1(r-2)^2}} \quad (5.38)$$

$$\alpha = \frac{\sqrt{\mu_2\left[16(r-1)-\beta_1(r-2)^2\right]}}{4} \quad (5.39)$$

$$\lambda = \langle x \rangle - \frac{(r-2)\sqrt{\beta_1}\sqrt{\mu_2}}{4} \quad (5.40)$$

10) Start the simulation:

For each time step:

For each grid cell inside the evacuation area:

For each existing flow in the grid cell:

If the flow transit time set for the flow has been reached at this particular time step or a previous time step and if neighbouring grid cells closer to the edge of the evacuation area (using the attractiveness measure generated in 7) can facilitate the flow then move the flow to the identified neighbouring grid cell with the highest attractiveness that can facilitate the flow. Set the flow transit time for the flow in the new grid cell.

If the flow has reached a grid cell outside the evacuation area then the flow size is added to the overall number of flows that managed to evacuate within the simulation time. The time is also stored.

Note: at initialisation there will be no flows in any of the grid cells.

If there is remaining space for flows in the grid cell and there are still evacuees that need to start evacuating in that particular grid cell:

- Add evacuation flows (cars, mopeds and pedestrians) to the grid cell based on the evacuation time models described in 9) and the number of evacuees that have not yet started evacuating. The models are used to calculate the flow size to add at each time step to a grid cell. The national information about number of cars and mopeds is used to derive whether a flow is a car flow, a moped flow or a pedestrian flow.
- Add flow transit time for each evacuation flow. For car flows this time is either the flow time calculated for each grid cell during the creation of this gridded data as in section 5.3 plus the time step the flow was added to the grid cell or a reduced time due to congestion in the grid cell where the flow is added to, as described in equation 5.29 plus the time step the flow was added to the grid cell. For moped flows in a non-congested grid cell this time is based on the road length through the grid cell divided with the average moped speed. Finally for pedestrians in a non-congested grid cell this is based on the road length through the grid cell divided with the average walking speed.

The evacuation simulation will stop after the simulated time has been reached.

It is important to note that in the case where people are evacuating to neighbouring settlements evacuation flows exits the simulation on arrival in an urban grid cell and as urban areas fill up evacuation flows travel towards urban areas further away. This case has though not been tested.

A coarse-scale evacuation simulator was developed in C++. The structure of this program is as described in figure 5.12

Each grid cell has attractiveness, a capacity and a flow time (the time it will take a flow to travel through the grid cell) along with total grid cell population, total number of evacuees, number of evacuees expected to evacuate prior to a warning, number of evacuees expected to evacuate after a warning has been issued and total number of shadow evacuees (if the grid cell is of the type shadow area). This is all generated prior to

initialisation of the simulator or at start up of the simulator. The grid cell handles all incoming flows using vectors to store flow size and transit times.

When a flow enters a grid cell the transit time is set based on the grid cell flow time plus the current time step or if there is congestion based on a reduced flow time as described in equation 5.29 plus the current time step. A flow can either enter a grid cell from a neighbouring grid cell or a new flow can be created within the grid cell.

A new flow is created using the evacuation models described in section 5.5.3.4 When a new flow is created then the number of evacuees waiting to evacuate will be reduced for that grid cell.

Neighbouring grid cells will be analysed when a flow in the grid cell has stayed until the transit time has been reached. The neighbouring grid cell that can accommodate a flow of the size needed and with the highest attractiveness is chosen and the flow is moved. If no neighbouring grid cell is available e.g. due to congestion then the flow will have to wait for another time step in its current grid cell and the neighbouring grid cells will be re-analysed at the next time step. Note: neighbouring grid cells that are exit grid cells will have the highest attractiveness and it is assumed that they always have capacity available. This assumption should be refined in a later version of the simulator.

The simulator also has the ability of dividing a flow into two smaller flow. This only happens if a flow is unable to move to a neighbouring grid cell because all neighbouring grid cells have lover capacity compared with the flow size.

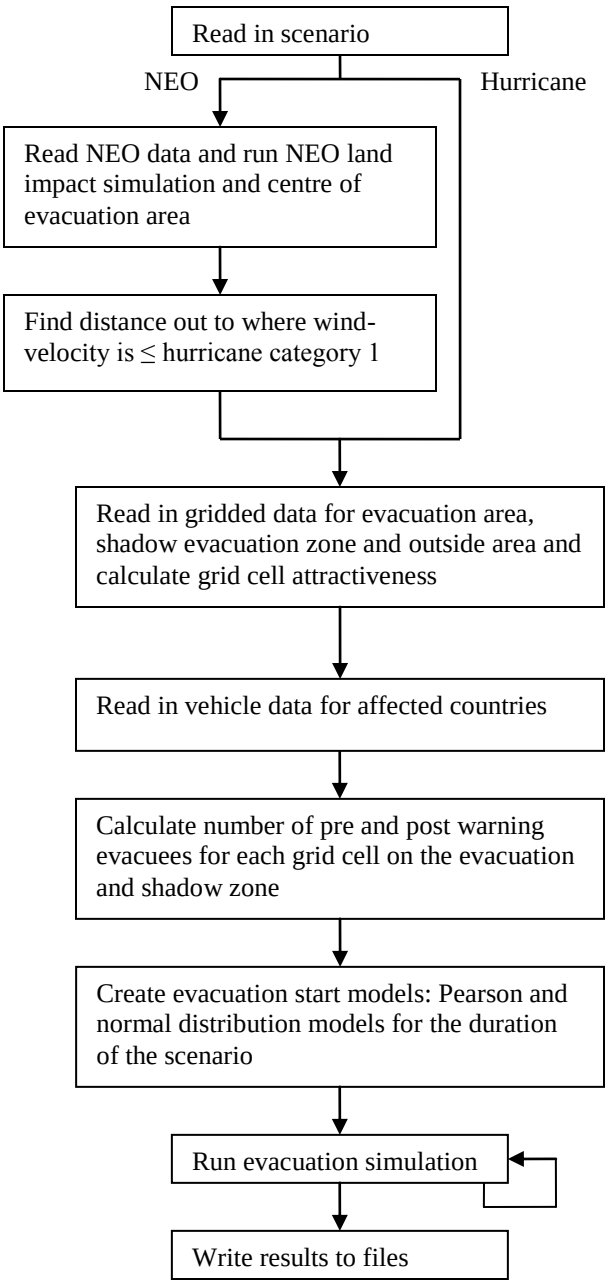

Figure 5.12: Coarse-scale evacuation simulator.

5.6.3 Model tests

A number of tests were performed in order to identify how the evacuation simulator would perform when the total number of evacuees for a simple 1 day scenario grew from 10% of the affected population to 100% of the affected population. This sensitivity analysis was also used to identify how sensitive an area is to evacuations. That

is, the time when the local road network is no longer able to handle the evacuation traffic. In these scenarios the complicated models estimating the number of evacuees based on the natural hazard were skipped and it was simply assumed that an even spread of e.g.10% of the affected population throughout the evacuation area would evacuate. The following watch, warning and evacuation end times were selected for this scenario:

1 day:	Watch start time:	5:00 = 300 minutes
	Warning issued at:	8:00 = 480 minutes
	Evacuation end time:	20:00 = 1200 minutes

It was assumed that a surrounding zone of 5 km would contain shadow evacuees. Southampton was chosen as the impact location. Two NEOs (2010CA and Apophis) were used in order to identify at what percentage of evacuees the road network would start to be unable to handle the large number of evacuees. The evacuation area is 11 km and 56 km respectively resulting in noticeable rise in number of expected evacuees as well as a much longer distance for the Apophis evacuees to travel in order to get out of the evacuation area. Table 5.7 and 5.8 shows the number of expected evacuees for the two NEO scenarios, when the percentage of evacuees grew from 10% of the affected population to 100% of the affected population. They show the expected number of shadow evacuees, expected number of early evacuees, expected number of evacuees starting to evacuate after a warning is issued, the actual number of evacuees that started to evacuate as well as the final number of evacuees that managed to complete their evacuation. The results for the 2010CA NEO scenario show that most of the expected evacuees manage to evacuate along with many shadow evacuees when 10%, 20% and 30% of the affected population evacuates. When 40% of the affected population want to evacuate, the road network starts to become so congested that many are unable to evacuate in the time provided. Figure 5.13 shows the number of evacuees that have started evacuated along with the number of evacuees that have finished evacuating at each evacuation time-step. This also shows how at around 40% the road network starts to be insufficient when evacuating such large numbers of evacuees over such a short period of time.

Table 5.7: 2010CA NEO impact evacuation results.

Percentage of evacuees	Total number of evacuees	Shadow evacuees hereof	Evacuees pre warning	Evacuees post warning	Total number started to evacuate	Total number finished evacuating
10%	50,500.7	3186.13	4731.45	45,769.2	50,500.7	50,500.7
20%	97,815	3186.13	9462.9	88,352.1	97,815	97,815
30%	145,130	3186.13	14,194.3	130,935	145,130	145,130
40%	192,445	3186.13	18,925.8	173,519	187,394	187,303
50%	239,759	3186.13	23,657.2	216,102	223,187	223,020
60%	287,073	3186.13	28,388.6	258,685	260,097	259,873
70%	334,386	3186.13	33,120.2	301,266	292,081	291,705
80%	381,701	3186.13	37,851.6	343,849	323,338	322,547
90%	429,016	3186.13	42,583	386,433	352,923	352,614
100%	476,329	3186.13	47,314.5	429,015	383,657	382,758

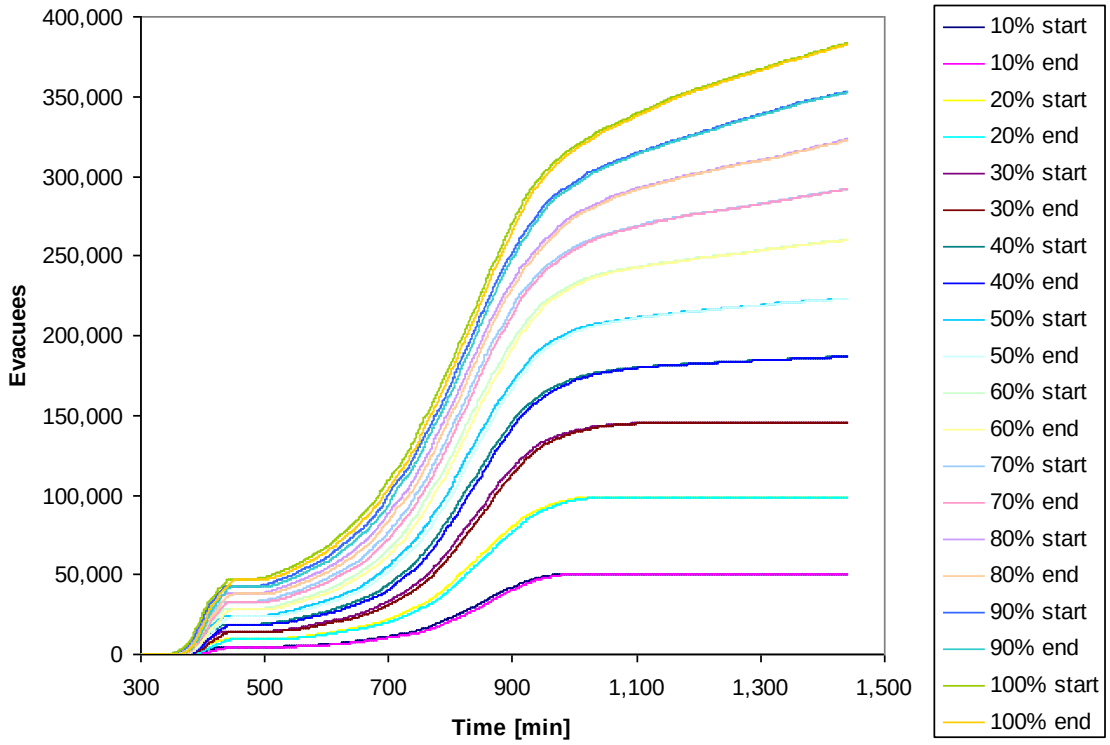

Figure 5.13: Evacuees started and finished evacuating during a 1 day evacuation scenario for asteroid 2010CA.

For the Apophis evacuation scenarios it is clear from table 5.6 that the road network is unable to handle that large number of evacuees due to the much larger evacuation area, the longer time it takes to travel to outside the evacuation area and the larger number of evacuees. Almost all evacuees that start evacuating also manage to finish evacuating for

the 10%, 20%, 30% and 40% scenario. Hereafter there is a clear reduction in how many evacuees that manage to finish evacuating in the time provided, see figure 5.14.

Table 5.8: Apophis NEO impact evacuation results.

Percentage of evacuees	Total number of evacuees	Shadow evacuees hereof	Evacuees pre warning	Evacuees post warning	Total number started to evacuate	Total number finished evacuating
10%	616,578	3399	22,066	594,522	515,128	503,643
20%	793,600	3399	44,132	749,481	708,854	696,882
30%	970,672	3399	66,197	904,487	891,773	878,542
40%	1,147,670	3399	88,264	1,059,440	1,065,830	1,043,960
50%	1,324,770	3399	110,330	1,214,450	1,227,620	1,140,530
60%	1,501,790	3399	132,395	1,369,420	1,392,400	1,238,000
70%	1,678,840	3399	154,461	1,524,400	1,530,820	1,315,440
80%	1,855,830	3399	176,528	1,679,350	1,671,280	1,370,810
90%	2,032,930	3399	198,591	1,834,370	1,822,750	1,440,360
100%	2,210,010	3399	220,661	1,989,340	1,953,820	1,518,130

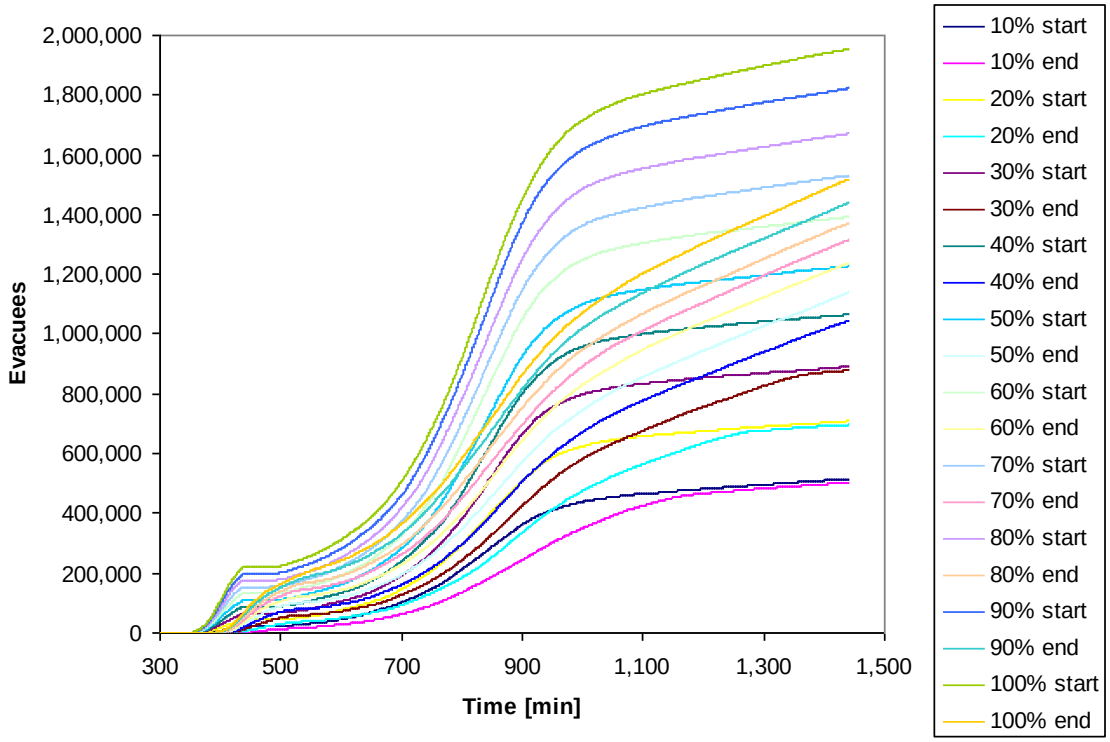

Figure 5.14: Evacuees started and finished evacuating during a 1 day evacuation scenario for asteroid Apophis.

A historical evacuation due to an approaching hurricane was used as an example to test the coarse-scale evacuation simulator. The selected hurricane was hurricane Rita

which was one of the major hurricanes during the hurricane season in 2005. This hurricane made landfall in the US at 7:40 on September 24. Landfall was between Sabine Pass in Texas and Johnsons Bayou in Louisiana. It was originally predicted to be a category 5 hurricane, but as it approached land it weakened and was only a category 3 hurricane when it made landfall. A mandatory evacuation warning of the greater Houston area was issued at 9:30 on the 21st September. The evacuations prior to this hurricane resulted in significant traffic jams in the broader Houston area. Seven people died directly from this hurricane, while many others died in evacuations in Texas and Louisiana and from indirect effects (Zhang et al. 2007). Severe traffic gridlocks and heat led to between 90 and 118 deaths during the evacuation and an estimated 2.5 – 3.7 million people were believed to have evacuated prior to landfall. 40% of people living outside, but near the evacuation area, decided to evacuate and were a major contributor to the congestion experienced during the evacuation (Science Daily 2009). Only 1.1 million were expected to evacuate from the storm surge zones, but with Hurricane Katrina making landfall less than a month earlier and the devastation it caused in New Orleans, an additional 1.9 million residents living outside these zones decided to join the evacuation resulting in congestion, fuel and food shortage (Soika 2006) (Siebeneck et al. 2008) (Harris County). Figure 5.15 shows the different evacuation zones in Houston Texas and the surrounding counties depending on hurricane category. With the prediction of Rita being a category 5 hurricane the affected area is of a considerable size.

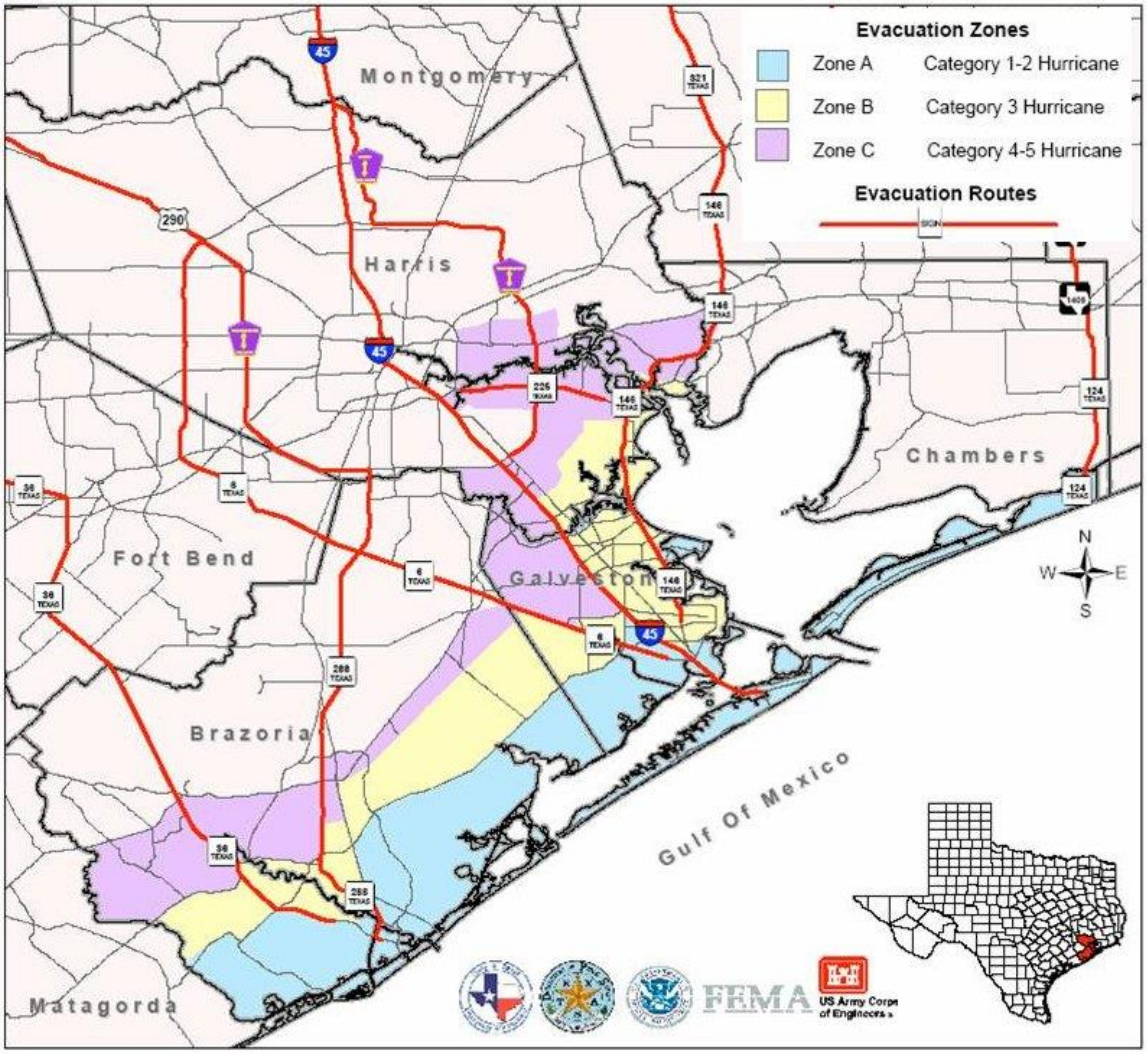

Figure 5.15: Evacuation zones for Houston and Galveston Texas (GlobalSecurity.org 2012).

Figure 5.16 illustrates the predicted path of hurricane Rita as predicted on the 22nd September 2005 by the National Hurricane Center. This prediction shows that the hurricane would make landfall very close to Houston, Texas and a long stretch of Texas and Louisiana coast was on hurricane warning.

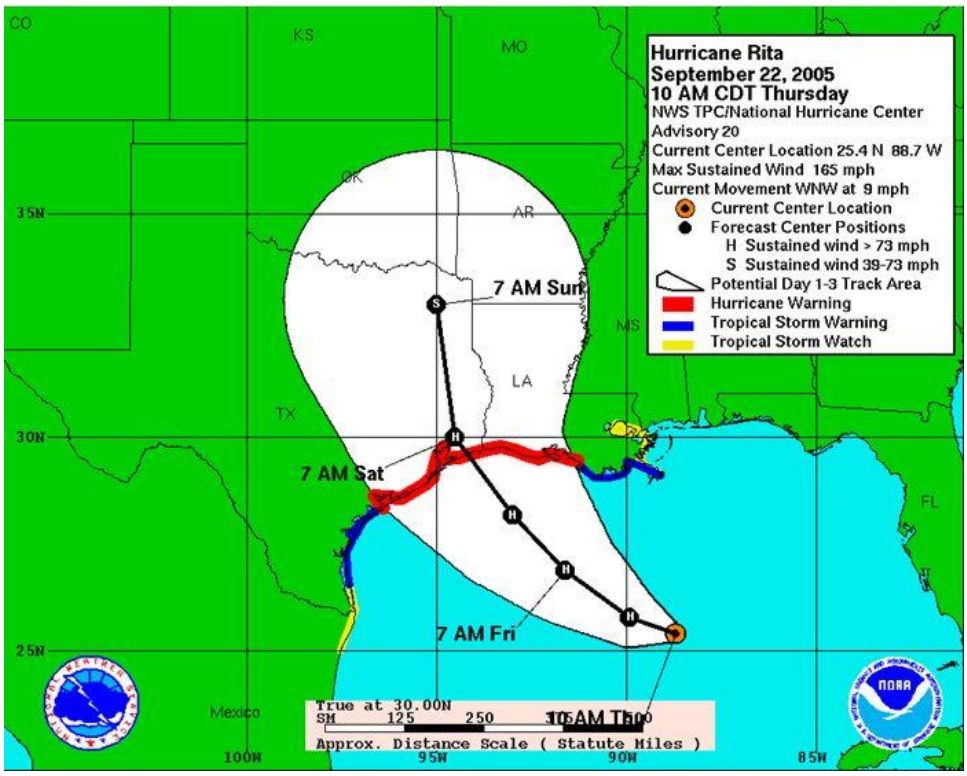

Figure 5.16: Predicted path of Hurricane Rita (National Hurricane Centre 2005).

5.6.3.1 Scenario

The hurricane scenario that was run in the coarse-scale evacuation simulator mimicked the evacuation in the broader Houston area due to the approaching hurricane Rita and had the following parameters:

Hurricane magnitude: 5 (since this was the believed hurricane magnitude when the evacuation warning was issued). Five scenarios were investigated. One where the evacuation radius was 85 km and the shadow evacuation radius was 4 km, one where evacuation radius was 86 km and shadow radius was 3 km, etc. up to evacuation radius 89 and shadow radius 0 km.

Area to evacuate:

Centre location:	94.9699 W and 29.189N
Evacuation radius:	85 km, 86 km, 87 km, 88 km, 89 km
Shadow evacuees radius:	4 km, 3 km, 2 km, 1 km, 0 km
Evacuation type:	Mandatory

Evacuation times:

Watch start time:	7:40 on the 20th September = 460 minutes
Warning start time:	9:30 on the 21st September = 2010 minutes
Hurricane arrival time:	7:40 on the 24th September = 6220 minutes

5.6.3.2 Test of hurricane scenario

The number of people expected to evacuate, by using the evacuation simulator, is shown in table 5.9

Table 5.9: Hurricane Rita evacuation scenario results.

Evacuation radius [km]	Shadow evacuation radius [km]	Expected number of evacuees	Shadow-evacuees	Evacuees started evacuating	Evacuees finished evacuating
85	4	2,319,670	136,758	2,319,670	2,302,860
86	3	2,357,030	103,810	2,357,030	2,341,540
87	2	2,390,520	74,284.9	2,390,520	2,369,370
88	1	2,436,960	33,347.6	2,436,960	2,420,850
89	0	2,474,790	0	2,474,790	2,454,640

It was found that up to 2.47 million people were to evacuate in the scenarios run, of which 1.14 million were expected to evacuate prior to the issued warning, while 1.33 million were believed to evacuate after the warning was issued. Figure 5.17 illustrates the area around Houston where the evacuation was simulated for the first scenario. The evacuation radius was 85 km and the shadow evacuation radius was 4 km. Figure 5.17 (a) shows the number of people living within this area in each grid cell while figure 5.17 (b) illustrates the number of people expected to evacuate from each grid cell. Figure 5.17 (c) shows the number of people who were not planning to evacuate within the evacuation area and the shadow evacuation area and finally figure 5.17 (d) illustrates the colour coding used for these maps. The densely populated City of Houston contributes a very large number of evacuees along with settlements like Galveston, Baytown and League

City. The shadow evacuation area can be seen on figure 5.17 (c) as a curved strip around the actual evacuation area. The number of people that started evacuating versus the number of people that reached outside the evacuation area during the evacuation is illustrated in figure 5.18 along with the cumulative model used. This figure shows that all who were planning to evacuate started their evacuation, but not all evacuees managed to evacuate before the evacuation end time at 7:40 on the 24th September. Almost 17,000 evacuees were still evacuating when the scenario stopped. At peak time during the day, when many started evacuating the ratio between the number of people finishing their evacuation and the number of people still evacuating grew. There is also a delay from when people start evacuating till when they reach outside the evacuation area.

(a) Population density map

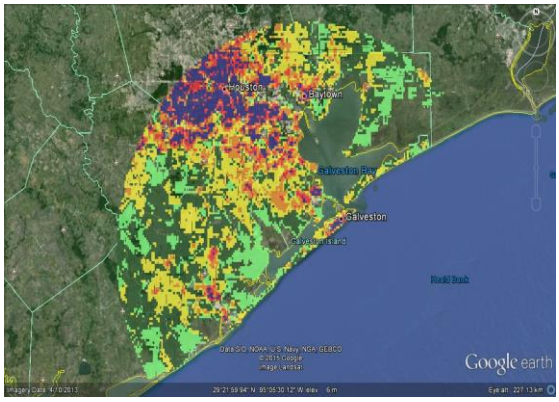

(b) Evacuees map

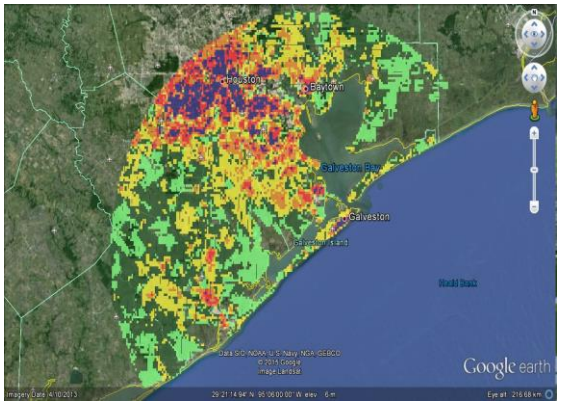

(c) Not evacuating map

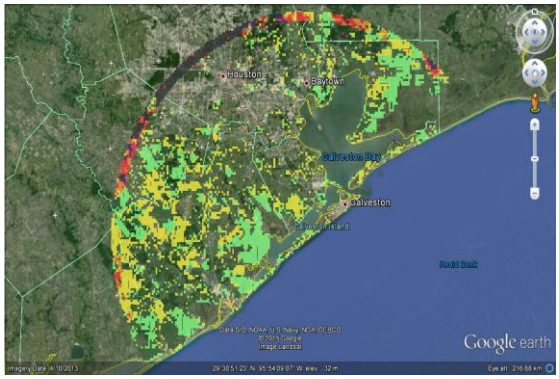

(d) Colour coding

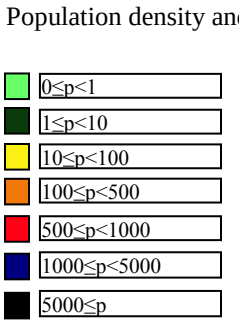

Figure 5.17: Hurricane Rita evacuation simulation area: (a) population density, (b) expected number of evacuees, (c) expected number of people staying, (d) illustrates the colour coding used.

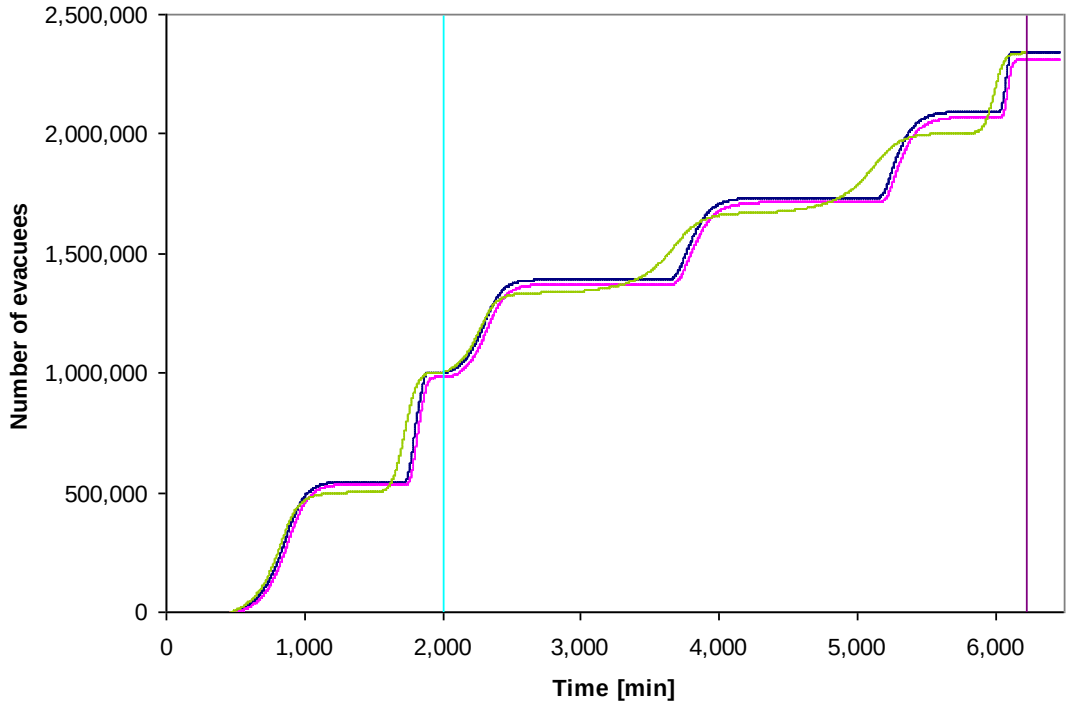

Figure 5.18: Cumulative evacuation model (green line), actual number of evacuees started (blue line) and finished (pink line), warning issued (yellow line) for Houston, Texas, evacuation radius 85 km, shadow evacuation radius 4 km.

5.6.3.3 Hurricane Rita evacuation comparison

The 2.47 million people expected to evacuate using the evacuation simulator is not far from the estimated 2.5 to 3.7 million that are believed to have evacuated prior to landfall. The number of shadow evacuees predicted in all five scenarios was much smaller than the actual number experienced during this major evacuation. Changes to the scenario and the main assumptions, such as the shadow evacuation area, could change the evacuees to shadow evacuees' ratio.

5.6.3.4 Comments and conclusions

A number of evacuations due to two NEOs Asteroid 2010CA and Apophis were tested. In these evacuation simulations the number of evacuees was slowly increased

from 10% of the affected population to 100% of the affected population. The results show that for asteroid 2010CA the road network in Southampton was able to handle up to when 30% of the population evacuated when giving 1 day for the evacuation to be performed in. If more than 30% of the affected population attempted to evacuate within one day then the road network would start to become too congested and not everyone will be able to evacuate. For the Apophis scenarios the number of evacuees that started to evacuate was lower than the expected number of evacuees showing that the road network was unable to handle the many evacuees already when only 10% of the affected population evacuated. It was though possible for many of the evacuees that started to evacuate to complete their evacuation. This was only up to around 40% of the affected population. Above this more and more evacuees were unable to complete their evacuation.

The coarse-scale evacuation simulation of the historical evacuation ahead of the arrival of Hurricane Rita in Houston Texas showed that the models used for predicting the number of expected evacuees in a specified area due to an approaching hurricane provide realistic numbers of evacuees. Although the predicted number in the test case was below the believed number of evacuees it was still closer to the actual number than the number of evacuees predicted by the emergency services. The shadow area could potentially be extended to improve the evacuees to shadow evacuees' ratio, but more historical cases would be needed to be simulated in order to find the correct ratio of evacuation area to shadow evacuation area. This ratio is very likely to depend on the hurricane magnitude and other factors such as previous experience with evacuating and cultural differences. More historical hurricane evacuations should also be investigated in order to improve the simulator along with the behaviour-based evacuation models and the road network and flow-time models used.

5.6.4 Case studies

Multiple evacuation cases were investigated. The selected cases was designed to investigate evacuations due to both larger Apophis sized NEO impacts in Costa Rica and Hampshire and smaller Tunguska sized NEO impacts in Hampshire. They also

investigate how the time provided to evacuate affects the evacuation outcome along with how the location and local infrastructure can result in very different evacuation outcomes.

The first case study is the 99942Apophis NEO and the impact location chosen is latitude 10.5511 N and longitude 84.4733 W, which is the location where most casualties could be expected based on the previous casualty investigation in Chapter 4. Three scenarios were created, a one-day scenario, a 3 ½ day scenario and a five day scenario. The five day scenario is similar to the test case scenario for hurricane Rita. This was done in order to capture the difference it makes when providing more evacuation time than just a day. The following watch, warning and evacuation end times were selected for the three scenarios:

1 day:	Watch start time:	5:00 = 300 minutes
	Warning issued at:	8:00 = 480 minutes
	Evacuation end time:	20:00 = 1200 minutes
3½ days:	Watch start time:	15:00 = 900 minutes
	Warning issued at:	7:00 on day 2 = 1860 minutes
	Evacuation end time:	16:00 on day 3 = 3840 minutes
5 days:	Watch start time:	7:40 = 460 minutes
	Warning issued at:	9:30 on day 2 = 2010 minutes
	Evacuation end time:	7:40 on day 5 = 6220 minutes

The warning type is a mandatory warning and the simulation area radius is 56 km plus 5 km shadow area. The time step size is 30 seconds and an additional 240 minutes were added to the simulation to investigate the 4 hours after the evacuation should have ended.

The second case study is based on a smaller Tunguska sized NEO. The chosen NEO is the 2010CA, a 43 m diameter asteroid which also was investigated in Chapter 4 using a fictive risk corridor across Hampshire. Four impact locations in Hampshire were selected: Southampton, Portsmouth, Basingstoke and The New Forest. This was done to investigate how location and local infrastructure can affect an evacuation. Portsmouth is a separate island located next to the mainland. There are very few roads connecting this island to the rest of England to the north. Southampton is likewise located next to the English Channel but on the mainland and has good road connections to the north, east and west. Finally, Basingstoke is located further inland and has good roads connecting it

in all directions. The New Forest is unlike the other three locations: not a large settlement, but a National Park with small villages and small winding roads. It is located to the west of Southampton. Once again, the 1 day, 3 ½ and 5 days scenarios were used. One additional scenario, a half day scenario was created due to the smaller area affected by the NEO. The scenario watch, warning and evacuation end times are as follows:

½ day:	Watch start time:	3:00 = 180 minutes
	Warning issued at:	6:00 = 360 minutes
	Evacuation end time:	15:00 = 900 minutes

The selected NEO impact locations for Asteroid 2010ca are presented in table 5.10.

Table 5.10: Asteroid 2010ca impact locations.

Location	Latitude	Longitude
Southampton	50.933333 N	1.39389 W
Portsmouth	50.796111 N	1.073889 W
Basingstoke	51.268056 N	1.088056 W
The New Forest	50.833333 N	1.65 W

The simulation area radius was 11 km. The time step size is 30 seconds and an additional 240 minutes were added to the simulation to investigate the 4 hours after the evacuation should have ended.

A third case study investigates how the impact energy will affect the evacuation scenario where Southampton is being evacuated over one day. A number of NEO impacts have been selected. Table 5.11 show the NEO name, along with the estimated diameter and energy.

Table 5.11: NEOs with different energies.

NEO Name	Estimated Diameter [m]	Energy [MT]
2010 CA	43	4.5e+00
2002 TX55	63	9.2e+00
2004 ME6	93	3.4e+01
2011 VG9	121	2.2e+02
2010 XA68	151	6.7e+02

The final case study investigates how by performing an evacuation the human vulnerability in the area at risk can be decreased. In this case study the area investigated is Southampton in the UK. The threatening NEOs are the 2010CA and 2004 ME6 respectively. Due to the higher resolution of 30'' used in the Evacuation simulator the same resolution was used when estimating the human vulnerability. Three steps were performed in these case studies: Calculate the human vulnerability in 2000 in the identified risk location. Run a 1 day evacuation simulation scenario similar to the one day scenarios used in the first case studies. Finally calculate the human vulnerability in the identified risk location based on the population that remain in this area.

5.6.5 Results

The first two scenarios investigated an area's ability to evacuate due to the 99942Apophis NEO. The impact location was in Costa Rica and the simulator predicted that around 211,575 people would evacuate from the affected area. 127,775 people are expected to evacuate prior to the issued warning, while 83,799 are predicted to evacuate after the warning is issued. Around 3620 shadow evacuees are predicted to join the evacuation. Table 5.12 shows the main results from the three scenarios. This table shows that for the selected area one-day is not enough warning time to allow everyone wanting to evacuate to start. For the 3 ½ day scenario the results are similar. Just over 100 more evacuees manage to start and finish their evacuation. For the 5 days scenario all expected evacuees managed to start evacuating and all except 42 evacuees managed to finish their evacuation.

Table 5.12: 99942Apophis scenarios results.

Location	Scenario	Expected evacuees	Started evacuating	Finished evacuating
Costa Rica	1 day	211,575	195,088	195,029
Costa Rica	3.5 day	211,575	195,210	195,156
Costa Rica	5 days	211,575	211,575	211,533

Figures 5.19, 5.20 and 5.21 show the cumulative number of evacuees that have started and finished evacuating at the different time steps. The green line shows the time when

the official warning is issued and the red line shows when the evacuation should have ended. All scenarios were set to run for an additional 4 hours.

Figure 5.19 shows the results for the one-day scenario. This figure shows that already before an official warning is issued evacuees are trying to evacuate, but are slowed down due to congestion. At the time when a warning is issued only 82% of the expected pre-evacuation evacuees have started evacuating. At the end of the evacuation 92% of the expected evacuees have started evacuating and 92% have finished evacuating.

The 3 ½ day scenario, shown in figure 5.20, show that at the time when the warning is issued 88% of the expected early evacuees have started evacuating and at the end of the evacuation 90% of the expected evacuees have started their evacuation and 85 % of the expected evacuees have finished their evacuation.

For the 5 day scenario, illustrated in figure 5.21, the number of pre-warning evacuees that have started at the time when the warning is issued compared with the expected number of pre-warning evacuees is 88%. By the end of the simulation all expected evacuees have started evacuating and 99.9% have finished their evacuation.

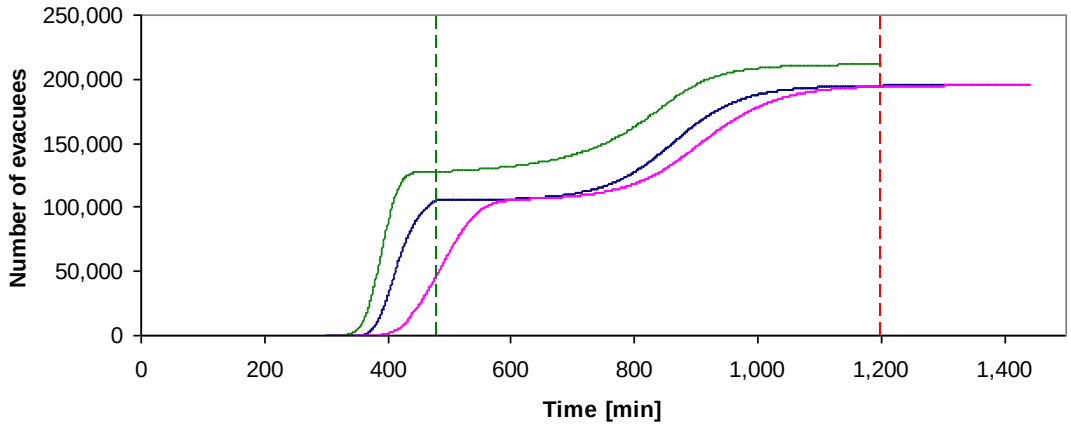

Figure 5.19: Cumulative evacuation model (black line), actual evacuation started (blue line) and finished (pink line), warning issued (green line), evacuation end time (red line) 1 day Apophis.

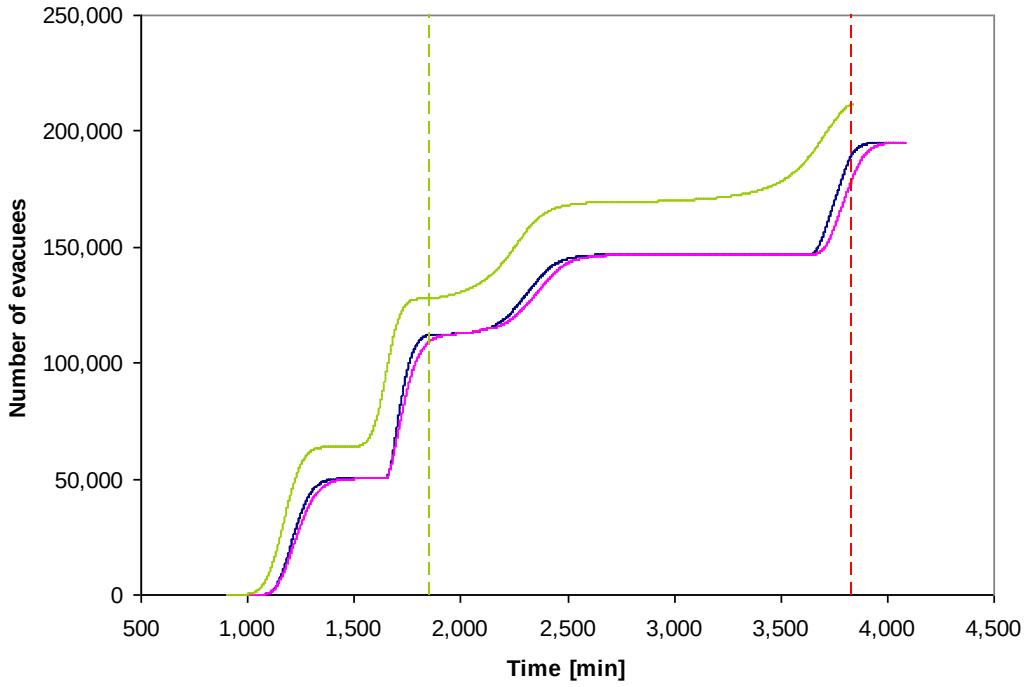

Figure 5.20: Cumulative evacuation model (black line), actual evacuation started (blue line) and finished (pink line), warning issued (green line), evacuation end time (red line) 3 ½ day Apophis.

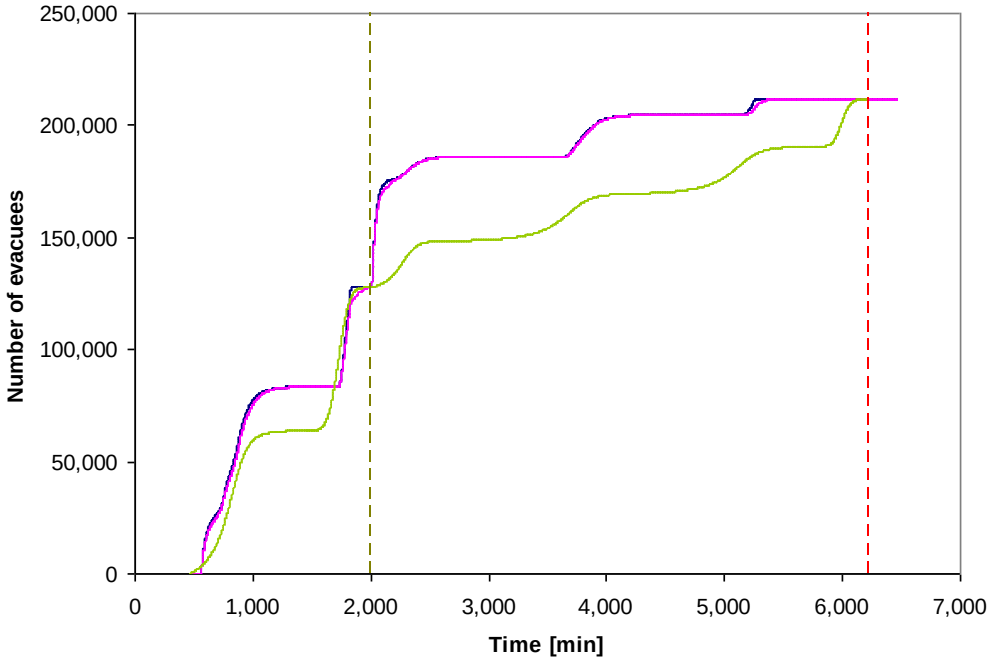

Figure 5.21: Cumulative evacuation model (black line), actual evacuation started (blue line) and finished (pink line), warning issued (green line), evacuation end time (red line) 5 days Apophis.

The second case study is the 2010ca NEO. The effects of location and local infrastructure on how well an area can evacuate are investigated. The number of expected evacuees and the categories of evacuees are presented in table 5.7. Hampshire can accommodate a total number of 30,620 evacuees in public shelter spaces spread across Hampshire. With a minimum of 35,327 expected evacuees in the New Forest scenario alone many evacuees would have to find alternative shelter solutions such as hotels/motels, stay with relatives and friends or shelters in neighbouring counties. The main results from the evacuation simulations are presented in table 5.8. It was found that a total of 486,444 people live within the evacuation area of Southampton, whereas 444,415 people live within the Portsmouth evacuation area, 120,328 people live within Basingstoke's evacuation area and 86,887 people live in the New Forest evacuation area. The expected number of evacuees range from 30,334 in the New Forest scenario to 221,437 in the Southampton scenario as can be seen in table 5.13. Shadow evacuees take up between 1 and 14% of these evacuees depending on the scenario, with 14% of the evacuees being shadow evacuees in the New Forest scenario. The number of evacuees who started evacuating and finished evacuating for the four ½ day scenarios, four 1 day scenarios, four 3½ days scenarios and four 5 days scenarios are illustrated in Figures 5.22, 5.23, 5.24 and 5.25.

Table 5.13: 2010ca evacuation numbers.

Location	Expected evacuees	Expected pre-warning evacuees	Expected post-warning evacuees	Expected shadow evacuees
Southampton	221,437	155,944	65,493	3186
Portsmouth	199,579	132,760	66,819	4566
Basingstoke	54,325	38,773	15,552	1221
The New Forest	30,334	12,254	18,080	4434

For the half-day scenario, only in the New Forest and Basingstoke scenarios do all expected evacuees start evacuating and all evacuees manage to finish their evacuation for the New Forrest scenario while almost all evacuees manage to evacuate in the Basingstoke scenario. 91% of the expected evacuees managed to start in the Southampton and the Portsmouth scenario and 91% of expected evacuees managed to finish their evacuation in the two scenarios. Figure 5.21 shows that at the time where the evacuation

should have finished several evacuees are still evacuating in both the Portsmouth and the Southampton scenarios. More time is needed in order to clear the areas. Congestion was a major issue in both the Southampton and the Portsmouth scenarios. 46% of the expected pre-warning evacuees in Southampton managed to start evacuating before the official warning was issued, while 41% of the expected pre-warning evacuees in Portsmouth managed to start evacuating before the warning was issued, as can be seen in Figure 5.24.

Table 5.14: 2010ca scenario results.

Location	Scenario	Expected evacuees	Started evacuating	Finished evacuating
Southampton	½ day	221,437	202,198	201,795
Portsmouth	½ day	199,579	182,250	182,076
Basingstoke	½ day	54,325	54,325	53,720
The New Forest	½ day	30,334	30,334	30,334
Southampton	1 day	221,437	205,754	205,604
Portsmouth	1 day	199,579	190,435	190,343
Basingstoke	1 day	54,325	54,325	53,969
The New Forest	1 day	30,334	30,334	30,334
Southampton	3.5 days	221,437	221,437	221,437
Portsmouth	3.5 days	199,579	199,579	199,579
Basingstoke	3.5 days	54,325	54,325	54,325
The New Forest	3.5 days	30,334	30,334	30,334
Southampton	5 days	221,437	221,437	221,437
Portsmouth	5 days	199,579	199,579	199,579
Basingstoke	5 days	54,325	54,325	54,325
The New Forest	5 days	30,334	30,334	30,334

For the 1 day scenario the results have improved for Southampton. Just over 3,000 more start evacuating. Most of these evacuees also manage to finish their evacuation. For the Portsmouth scenario almost 8000 more evacuees start to evacuate.

The 3½ day scenarios show further improvement in the number of evacuees that start and finish evacuating with all expected evacuees starting evacuating and all finishing their evacuation.

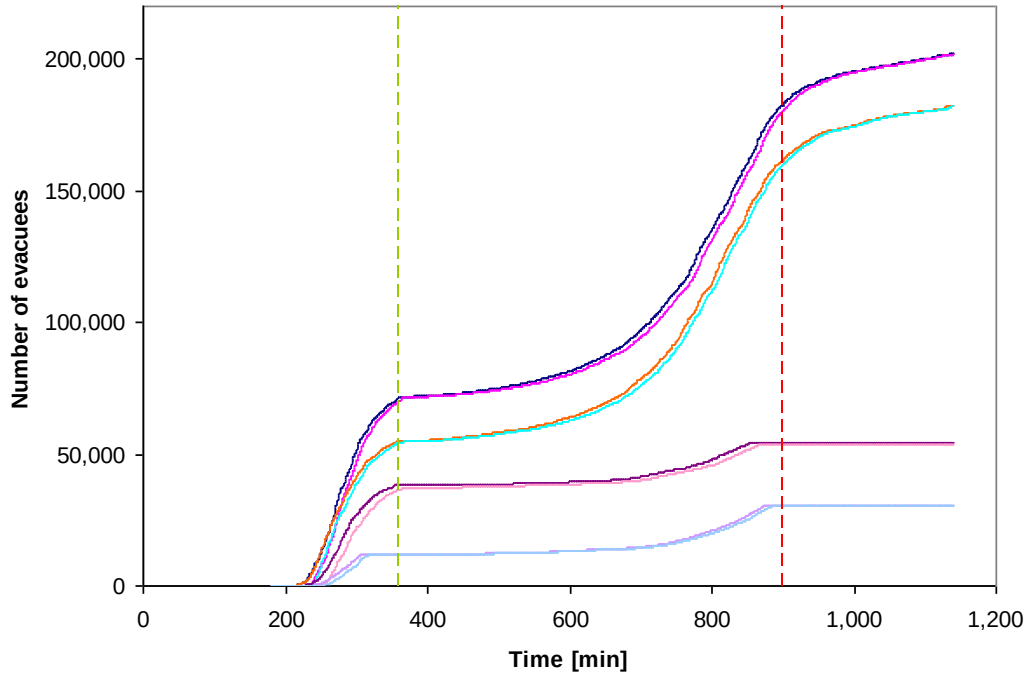

Figure 5.22: Actual evacuation started (blue) and finished (pink) Southampton, evacuation started evacuation started (orange) and finished (turquoise) Portsmouth, (purple) and finished (Bourgogne red) Basingstoke, evacuation started (lavender) and finished (pale blue) The New Forest, warning issued (green line) ½ day.

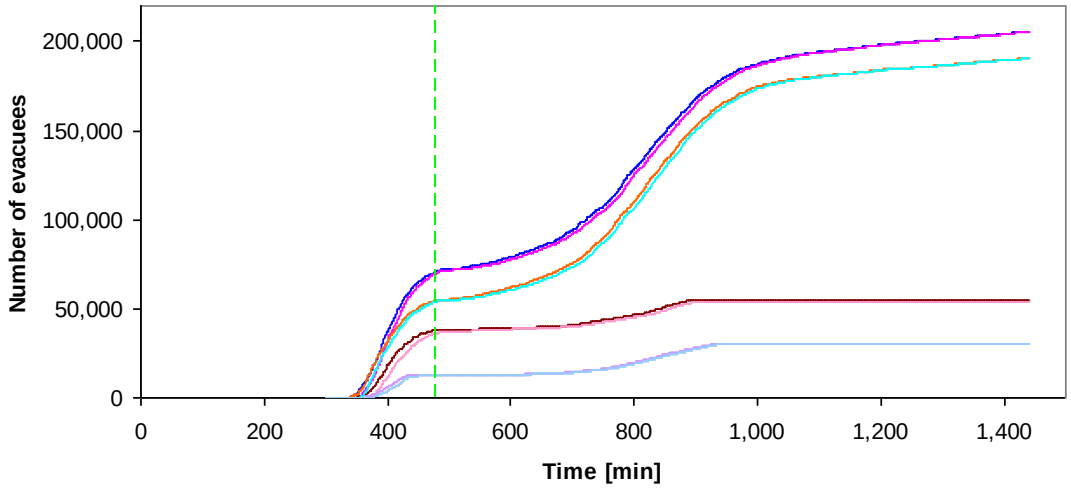

Figure 5.23: Actual evacuation started (blue) and finished (pink) Southampton, evacuation started evacuation started (orange) and finished (turquoise) Portsmouth, (purple) and finished (Bourgogne red) Basingstoke, evacuation started (lavender) and finished (pale blue) The New Forest, warning issued (green line) 1 day.

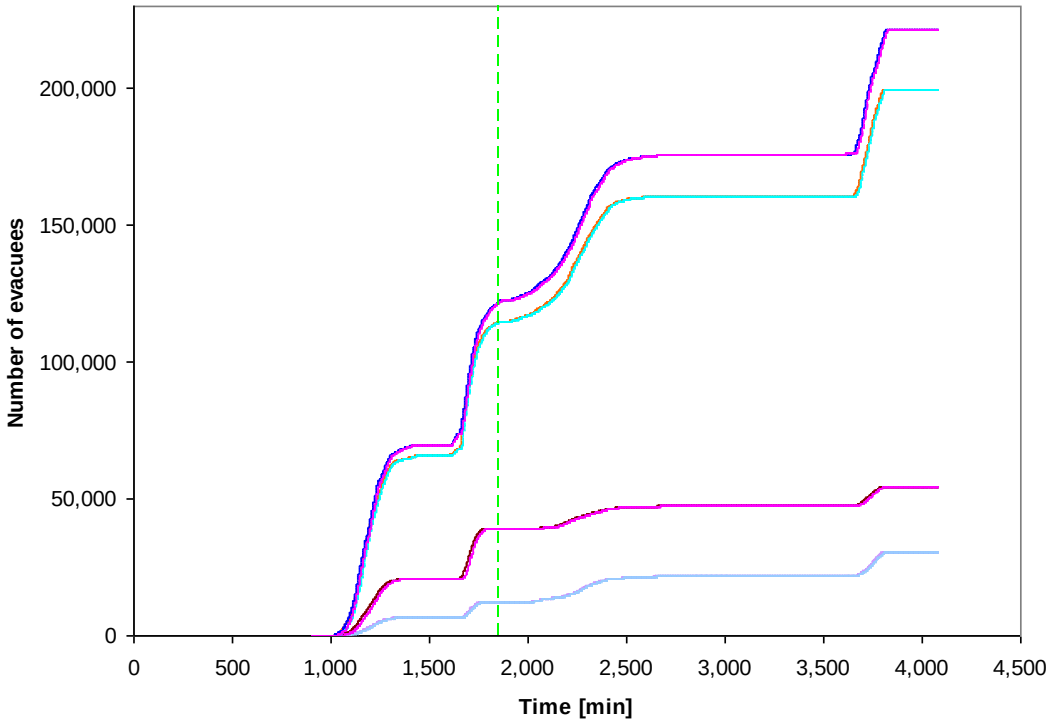

Figure 5.24: Actual evacuation started (blue) and finished (pink) Southampton, evacuation started evacuation started (orange) and finished (turquoise) Portsmouth, (purple) and finished (Bourgogne red) Basingstoke, evacuation started (lavender) and finished (pale blue) The New Forest, warning issued (green line) 3.5 days.

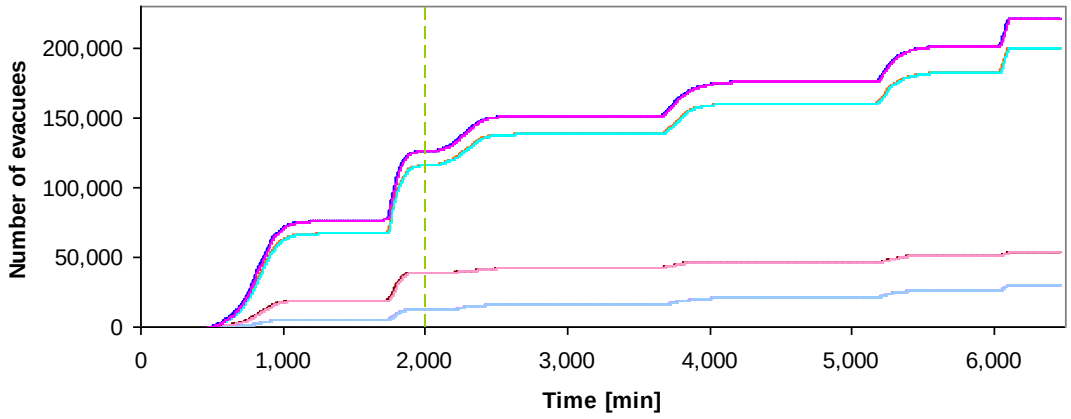

Figure 5.25: Actual evacuation started (orange) and finished (turquoise) Southampton, evacuation started (purple) and finished (Bourgogne red) Portsmouth, evacuation started (blue) and finished (pink) Basingstoke, evacuation started (lavender) and finished (pale blue) The New Forest, warning issued (green line), evacuation end time (red line) 5 days.

An investigation into how the increased NEO energy affects the evacuation outcome, have been performed. Table 5.15 show the outcome. As the energy increases a larger area will be affected from a potential impact and a larger number of people will have to evacuate. For the first four cases: 2010 CA, 2002 TX55, 2004 ME6 and 2011 VG9 most of the expected evacuees will be able to evacuate within the 1 day that these cases run for, but for the 2010 XA68 case it is clear that the local road network starts to struggle to cope with the many evacuees and around 450,000 evacuees will not be able to evacuate by 20:00.

Table 5.15: NEO energy effects on evacuation outcome for the 1 day Southampton scenario.

NEO name	Energy	Predicted number of evacuees	Evacuees started evacuating at end of simulation	Evacuees finished at 20:00	Evacuees finished evacuating at end of simulation
2010 CA	4.5e+00	221,437	205,754	197,947	205,604
2002 TX55	9.2e+00	269,587	253,976	244,460	253,736
2004 ME6	3.4e+01	392,884	381,921	366,750	380,968
2011 VG9	2.2e+02	959,771	948,784	911,431	941,817
2010 XA68	6.7e+02	1,338,110	1,338,110	881,847	1,117,260

In the final case studies the initial human vulnerability for Southampton for a NEO impact by 2010 CA was found to be an average number of casualties of 56,564 people. This graph shows that around 197,947 of the 221,437 people that want to evacuate are expected to be able to evacuate during this one day. After such an evacuation the expected average number of casualties has dropped to 2150. This is twenty six times fewer casualties than if no evacuation was performed. For 2004 ME6 the average number of casualties was found to be 190,843. During the 1 day evacuation 366.750 of the 392,884 expected evacuees manage to evacuate. After the 1 day evacuation the average number of casualties drops to 5325, a thirty five times reduction in the average number of casualties.

5.7 Discussion

A coarse-scale evacuation simulator was developed and used to investigate the effects on road networks and an area's ability to evacuate when an evacuation is initiated prior to an approaching hazard such as a NEO impact. Before being able to develop such a coarse-scale evacuation simulator models were needed to be developed for measuring the local road network capacity and flow time along with models describing the evacuees travel behaviour during such an evacuation. The outcomes from the scenarios run on the developed simulator showed that local infrastructure and geography affects an area's ability to evacuate. The outcomes from the evacuation simulator were also used in the developed human vulnerability estimation tool to estimate how by performing evacuations the human vulnerability can be reduced.

5.7.1 Gridded road network capacity and flow-time

Methods were developed to derive gridded datasets describing the local road network capacity and flow time within a grid cell. OSM data and models regarding recommended breaking distance were used to develop these gridded datasets. Additional models were developed to make up for the shortfall in the available OSM data. These models are simple models based on the outcome from the derived gridded datasets and gridded data regarding population density. The models are used when a gridded population can be identified through the gridded population dataset from CEDAC but no OSM roads were available. Graphs were derived showing the road network capacity, flow time and population density in each grid cell where OSM data was available in urban and rural grid cells. These graphs show fluctuations in road network capacity and flow time in area with a low population density. The models fitted to this data are simple and do not reflect this. A number of factors should be considered in order to improve these models such as:

Wealth, number of cars, road quality, elevation, bendiness of the roads, location of airports, harbours, industry, regional differences, roundabouts, traffic signals, insurance claims, time of year, speed limits, etc.

As many of these factors should be analysed against each other in order to identify any correlations that can be used to improve the existing models. Ideally a micro-simulation of each grid cell should be performed in order to improve and calibrate the models.

It can be assumed that OSM in many countries cover major roads between cities and larger settlements along with a good coverage of the urban road network.
When modelling an evacuation using the developed gridded road network capacity and flow time maps there are a number of factors that are not being taken into account such as:

Weather conditions, road works, accidents and hourly, daily and seasonal variations in traffic volume

Such factors all contribute to the uncertainty in the simulation results and should ideally be investigated using a micro-simulator.

5.7.2 Evacuation behaviour models

Although the collected hurricane evacuation surveys contained a lot of information regarding people's decision-making and behaviour before and during evacuations there still are questions that needs to be answered in order to improve the evacuation models.

- When do people start to evacuate if they decide to evacuate prior to a warning?
- What are people's travel patterns during the preparation period?
- What is the travel pattern of non-evacuees?

These are some of the unanswered questions. During the preparation there might be trips down to the local petrol station and shops or maybe the school to pick up the children? Non-evacuees might do additional trips to prepare their houses for the coming hazard and the potential lack of, for example, electricity and water in the aftermaths. Having additional factors to influence the models such as wealth, age and type of home could also improve the models, but more survey data are needed to base the models upon.

One potential issue with the surveys collected is the large variation in sample size. With survey size varying between 120 to 7000 households, some of the smaller surveys

might not capture the variation in people's behaviour due to, for example, wealth and ethnicity. Since the surveys were on a voluntary basis some types of household might not take part. Better knowledge with regards to uncertainties and quality of the results could be provided by adding the uncertainties in the developed models. The developed models also do not reflect the large fluctuations in the gathered survey data. More survey data along with additional factors such as wealth, demographics, building stock, etc. should be considered to be used in order to improve the current models. A micro-simulator could also be considered to be used for calibration purposes.

A number of models that have been identified to be useful when describing the travel behaviour during an evacuation, but where not enough data has been found available are:

1) Model the travel behaviour during the evacuation preparation period

2) Model travel behaviour by non-evacuating households. These households might do some preparation shortly before the arrival of the hazard

5.7.3 Evacuation simulation

The results from the hurricane Rita test case on the coarse-scale evacuation simulator showed that the simulator can be used to mimic how an evacuation can be expected to unfold. It was found that the ratio of shadow evacuees versus evacuees should be changed in order to better mimic the historical data. This can be done by changing parameters such as the shadow evacuation radius and by running more cases that mimic historical evacuations. Such cases can also be used to improve the various models used within this simulator such as behaviour-based models and road network capacity and flow-time models. Finding well documented historical evacuations is a challenge. There are many reasonably well documented evacuations from the United States, but from the rest of the world this has been found slightly more difficult. Historical evacuations from the rest of the world could provide useful information regarding social and cultural differences in how people address an evacuation and behave during an evacuation. The ratio between shadow evacuation area and evacuation area might not only depend on the expected hazard magnitude but also on previous experience

with evacuations due to natural hazards as well as cultural differences and how warnings are issued.

The sensitivity analysis of the local road networks showed that the road network in and around Southampton is able to handle the expected evacuation of up to 40% of the local population. Similar sensitivity analyses should be performed for other areas enabling decision makers to gain early knowledge regarding the sensitivity of road network sensitivity for different areas.

The first set of evacuation scenarios was based on the assumption of a potential impact by asteroid Apophis in Costa Rica. Three cases were investigated showing, how one day and 3 ½ days are insufficient durations for an evacuation of such a scale. By increasing the time available to evacuate to five days an improvement in the number of people who managed to start and finish evacuating was observed. All expected evacuees managed to start and finish evacuating during the 5 day scenario.

The second set of evacuation scenario that was simulated considered the difference in area types such as rural and urban areas along with differences in geography and infrastructure. Four different locations in Hampshire were selected:

- Portsmouth, an island city with a few large roads leading to mainland England
- Southampton, a neighbouring city with good road connections to the North, East and West
- Basingstoke, a smaller town with good road connection in all directions
- The New Forest, a nature reserve containing many small villages and small and winding roads.

A smaller asteroid named 2010CA was selected as the impactor and at each impact location ½ day, 1 day, 3½ days and a 5 days scenario were investigated. It was found that the smaller settlements such as the New Forest and Basingstoke can evacuate fairly quickly (1/2 day is enough) due to their smaller number of evacuees and because they have a reasonably good infrastructure in all directions. Larger settlements require more time to perform their evacuation. In both the Southampton and Portsmouth scenarios the evacuation was slowed due to congestion that started already prior to an official warning being issued. The infrastructure and the road connections need to be taken into consideration. A decrease in the number of evacuees that managed to start evacuating

was noticed when comparing the evacuation results for the ½ day scenario with the 1 day scenario. Both Southampton and Portsmouth required ~3 ½ days to evacuate.

The third set of case studies that were performed investigated different size NEOs and how the size affects the evacuation results. These simulation results showed that for the largest NEO 2010 XA86 there was a noticeable drop in the number of evacuees that managed to finish evacuating compared to the other simulations.

Finally the results for the final set of case studies, where the local human vulnerability was changed due to evacuation, revealed 26 to 35 times reductions in vulnerability.

Additional case studies that also look at areas with different elevations such as mountainous regions versus flat regions along with scenarios that investigate regions with different wealth distributions would improve the knowledge regarding expectations if an evacuation was issued in these different areas.

Adding other means of transportation to the simulator such as buses and trains would likewise be beneficial for the simulation of evacuations along with investigating the difference between fully managed evacuations and more self managed evacuations. Adding normal background traffic, from people who are planning to stay, to the simulation and adding the possibility of traffic accidents and the delays they may cause would improve realism. The agent-based simulator described in Appendix E benefits from the ability of both simulating normal travel traffic along with evacuation traffic. Results from the agent-based simulator could potentially be used to improve the models used in the coarse-scale evacuation simulator.

Some of the outcomes from the evacuation simulator were used for estimating the human vulnerability after an evacuation had been performed in Southampton and in Costa Rica. A reduction in expected number of casualties was observed.

5.8 Summary

An area's ability to evacuate, along with the pressure that is put on local road networks during an evacuation, was investigated using a coarse-scale evacuation simulator. This evacuation simulator uses gridded maps describing local road network

capacity and flow time along with population and land usage. Models describing the expected evacuation behaviour, due to a number of circumstances, such as type of evacuation, time and duration of the evacuation etc. were used to mimic the travel behaviour during an evacuation.

Four sets of case studies were investigated using the evacuation simulator.

The first case study investigated an areas ability to evacuate for 3 different evacuation scenarios, a 1 day, a 3 ½ day and a 5 day scenario. Asteroid 99942Apophis was used and the impact location chosen was in Costa Rica.

The second case study investigated different areas ability to evacuate. A smaller Tunguska sized NEO asteroid 2010CA was used and four impact locations in Hampshire were selected: Southampton, Portsmouth, Basingstoke and The New Forest.

A third case study investigates how NEOs with different impact energies will change the evacuation outcome. An evacuation scenario where Southampton is being evacuated over one day was used along with 5 different NEOs.

The final case study investigates how by performing an evacuation the human vulnerability in the area at risk can be reduced.

5.9 Conclusions

The coarse-scale evacuation simulator does not provide optimal evacuation plans, but provides realistic evacuation estimates based on behaviour-based evacuation models and road network models. A test of the evacuation simulator showed that it can provide realistic results when comparing to a historical event. Several case studies involving asteroid 99942 Apophis and asteroid 2010ca showed how different areas require different times in order to clear the affected area. They also showed how geographical location, local infrastructure and size of NEO are of vital importance when estimating the required evacuation time needed.

Additions to the simulator such as public transportation, non-evacuee traffic and accidents could improve the simulator, along with greater investigation into how the recreation of historical evacuations can improve the existing assumptions and models.

The use of the agent-based micro-simulator to be described in Appendix E may also be used to modify and improve the existing models and assumptions.

Chapter 6
General discussion and future work

In order to reduce the threat from natural hazards such as NEOs, governments and emergency decision-makers need information regarding the threat and the potential loss due to such a hazard in order to be able to make the best decisions regarding mitigation, which could either be in the form of active or passive mitigation.

Decision-makers need to know when such an event could occur and the uncertainty in this knowledge. This information will be provided from space agencies, which are running orbital predictions of every known asteroid based on the observation data available. Spatial estimates regarding the physical effects of a NEO impact can be calculated using information regarding the potential impact locations along a risk corridor along with knowledge such as NEO energy and composition. Several tools exist that can provide this information, such as NEOSim, NEOimpactor, Impact Earth (Impact Earth) and the Earth Impact Effects Program. Initial work on calculating human and financial loss due to a NEO impact was done by Bailey (2009). These initial models have, in this thesis, been refined using historical data and knowledge regarding uncertainty in the models derived and the NEO data available. This resulted in human vulnerability models that can provide decision-makers with information regarding human casualties due to NEO land impacts.

Developing human vulnerability models for a range of natural hazards that could be expected in a potential NEO land impact was found difficult and the uncertainty is noticeable. Inspiration was taken from other similar, but more regularly occurring hazards such as earthquakes, large explosions and snow- and tephra-fall as well as tests

with nuclear bombs. This provided information regarding expected numbers of human casualties due to crater, fireball, ejecta fall, blast wave, ignition exposure and earthquake, which are some of the expected hazards that could be experienced due to a NEO impacting the Earth. Models were developed based on collected historical data as well as textual description regarding the effects from individual hazards on humans, buildings and infrastructure. Section 6.1 provides a more in-depth discussion regarding these vulnerability models, the outcome from simulating the physical impact effects from a NEO impact and the following damage in the form of human vulnerability along with possible further improvements.

Decision-makers might also find it useful to know how prepared an area can be expected to be regarding active mitigation in the form of evacuation. For this two behaviour-based evacuation simulators (a coarse- and a fine-scale evacuation simulator) were developed with the goal in mind to be able to simulate evacuations across the Earth.

Before developing a coarse-scale evacuation simulator, gridded maps describing the available road network capacity and corresponding average flow-time through a grid cell were generated. It was found important to distinguish between land usages and develop models on a country or regional basis. A more in-depth discussion regarding the development of such models can be found in section 6.2.

Behavioural evacuation models along with other models needed in a behaviour-based evacuation simulator were created using survey data regarding evacuations due to approaching hurricanes in America. These models were then implemented in both a coarse-scale flow-based evacuation simulator and a fine scale agent-based simulator. These behaviour-based models along with the two evacuation simulators are discussed in section 6.3.

6.1 Human vulnerability

Six single hazard human vulnerability models predicting the number of casualties were developed for NEO land impacts and combined into a multi-hazard model. Physical models describing the air blast, ejecta fall and earthquake related to a NEO land impact were used along with historical data on earthquakes, snow- and tephra-fall and large

explosions for the development of the earthquake, ejecta and air blast human vulnerability models. Both the ejecta and earthquake models depend on the local building strength as well as the physical effects. The remaining vulnerability models, describing the human vulnerability with regard to crater, fireball and ignition exposure, were based on previous models developed for NEOimpactor and NEOSim. The uncertainties in the earthquake and air blast models were described by how well the models fit historical data. In both models, the predicted human vulnerability was smaller than for existing vulnerability models for these types of hazards developed in NEOimpactor and NEOSim.

The three earthquake vulnerability models developed distinguish between areas with predominantly weak, intermediate and strong buildings. By creating these models, which are based on historical data, it was assumed that factors such as time of day, social aspects such as public emergency preparedness training and secondary hazards are reflected in the historical data.

The earthquake models were tested against historical data. The results for the earthquake model generally showed results between the upper and lower one and a half uncertainty bounds. This shows that the model predictions are very close to the historical numbers. With most predictions slightly larger than the historical number of casualties the over predictions were acceptable. This is because a NEO land impact is believed to create shallow earthquakes, which are the most devastating, and it is important that the model reflects this. The model was also compared with similar models developed for the NEOimpactor project and NEOSim. The number of casualties calculated using the NEOimpactor simulator was found to be on average a factor of 27 larger than for the present model and for NEOSim the results were on average a factor of 1000 larger.

For the other three vulnerability models (crater, fireball and ignition exposure) the uncertainty modelling was based on the uncertainty in the NEO data such as NEO diameter and mass, where the mass is the dominant uncertainty. These three models and the air blast vulnerability model and ejecta vulnerability model were not tested due to the lack of, or limited number of, historical events. The case studies that were run showed the main contributor to casualties is the ignition exposure closely followed by the ejecta fall.

Results were illustrated by generating maps that can be shown on Google Earth as well as Virtual Earth (now called “Bing Maps”). Results are also stored as detailed tables

and summary tables showing the uncertainty in the results and the extremes that could be expected due to these uncertainties.

Using the output from these models which, in detail describe physical effects of a NEO land impact as well as the human vulnerability to these hazards, decision-makers are provided with a clear overview regarding what to expect and which regions potentially are worse off. This can enable decision-makers to start planning for mitigation.

A number of areas that should be improved or considered are: taking into account the time of day when the hazard occurs, investigating the human vulnerability to secondary and tertiary hazards along with how these hazards mix. How some hazards such as earthquakes weaken buildings so that they can't withstand other hazards such as the ejecta or air blast. Finally better and more data for models, such as the model estimating the number of casualties due to the air blast, should be collected.

6.2 Gridded road network capacity and flow-time

Due to the large size of an area that potentially would have to be evacuated due to the threat from an approaching NEO it is useful to develop a coarse-scale evacuation simulator that within a reasonable time can provide good realistic evacuation clearance times and other useful information regarding what to expect when evacuating a given area anywhere on the globe. In order to keep simulation time short, but still being able make realistic evacuation simulations, a gridded data approach was used. This also enables the simulator to work across the planet using global gridded data along with models that reflect the diversity in population density, land usage and infrastructure, and it enables the evacuation simulator to run simulations in regions where there is only very little road network data available. These regions might be at much higher risk. There might be a lack of governance and emergency plans to support the local population. Having an evacuation simulator that can inform decision-makers and institutions such as the UN about such issues would enable them to estimate what type of help is needed. This could provide a much smoother evacuation in these areas and a better distribution of aid.

Global gridded population and land usage data are available from SEDAC, while gridded road network capacity and flow-time data were generated using data from Open Street Map. Road networks capacity and flow time were found to vary from region to region and they were also found to depend on land type, such as urban and rural areas and population density. The models were generated, using data regarding population density, land usage, national speed limits and road network data, and reflect the regional diversity in road network capacity and flow-time.

Models were also developed to simulate the change in road network flow-time as the road network flow-time changes due to congestion. These models were tested against actual road congestion surveys and results from using these models were found to mimic the observations from these surveys well.

The road network capacity and flow-time models developed for three of the 26 countries investigated were tested against newer datasets from OSM that were downloaded nine months after the first models were developed.

The available OSM data from these countries was found to have grown between 2% and 47% in size during this time interval, showing how the OSM dataset is an ever-growing road network database. The predicted road network capacity and flow-time predicted using the original models were found to be close to the actual road network capacity and flow-time found in the new datasets.

The models were found to provide good predictions regarding the available road network capacity and flow-time for the individual grid cells, although factors such as wealth, elevation and more detailed land usage information should be considered to be taken into account for future improved road network capacity and flow-time models. Results from the fine scale agent-based evacuation simulator would also provide more in-depth detail regarding how to improve the gridded road network capacity and flow-time models.

6.3 Evacuation simulation modelling

The two evacuation simulators developed both use behaviour-based evacuation models developed using survey data regarding evacuation behaviour. These behaviour-

based models benefit from being able to simulate the change in behaviour due to various demographic factors along with the magnitude of the approaching hazard and the evacuation strategy used by decision-makers such as: mandatory or voluntary. An important issue identified is that the evacuation behaviour surveys used are relatively small and that demographic factors such as ethnicity might play a role in who takes part in such surveys. This means that variation within a community might not be captured in these surveys. These surveys also rely on people's memory, which might not always be as correct as it ideally should be. Several steps within an evacuation were also found to not be captured in the evacuation behaviour surveys collected, such as:

- how do people who are not evacuating behave (this behaviour could increase the number of vehicles on the roads).

- how do people behave during evacuation preparation time.

The uncertainty in the developed behaviour-based evacuation models should also be taken into account and will be a task to do in the future.

The Coarse-scale evacuation simulator used a gridded data flow approach, where evacuation flows are generated based on the behaviour-based evacuation models. Traffic then moves from grid cell to grid cell simulating the evacuation. Using this coarse-scale approach does unfortunately mean that the more detailed behaviour-based evacuation models that depend on, for example, gender are not used. Only the more general models are used. Using statistics regarding regional or national demographics could provide the necessary information so that some of these more detailed models can be taken into account. The coarse-scale simulator benefits from being fast and it does not require as much detailed information as a micro-simulator would need, enabling it to work across the Earth using global gridded data. The areas to run evacuation simulation on can also be much bigger than for a micro-simulator, but the size will still be limited due to time and computing power constraints. It benefits though from being an easy to use tool that can quickly provide realistic evacuation clearance times. Various improvements to the simulator and the models and assumptions used were identified in Chapter 5 and would be beneficial in order to capture cultural and geographic differences along with even more realistic evacuation simulations.

The fine scale evacuation simulator, CEMEvac, developed in collaboration with University of Wisconsin-Madison, benefits from using very detailed demographic data. It also used the detailed evacuation behaviour models generated from evacuation surveys from the US. The simulator simulates daily travel patterns on a household and individual level as well as evacuation travel patterns based on the behaviour-based evacuation models developed. With such detail in data, running this simulator is much more time consuming than the coarse-scale flow simulator and the size of the areas to run will be limited due to time and computing power constraints. The main purpose of the CEMEvac simulator was to use the outcomes from this simulator to validate and calibrate the coarse-scale evacuation simulator. This has though not been done due to a current lack of appropriate data, but should be considered as a future task.

6.4 Fine scale evacuation simulation modelling

A new improved version of the Comprehensive Econometric Micro-Simulator for Daily Activity Travel Patterns (CEMDAP) originally, developed previously by Chandra R. Bhat, Jessica Y. Guo, Sivaramakrishnan Srinivasan, and Aruna Sivakumar at Department of Civil Engineering, University of Texas, was modified by the author of this thesis. The new version of this agent-based simulator is able to generate behavioural travel patterns for multiple days during an evacuation. New evacuation travel behaviour models were developed to describe the local population's travel behaviour during such an event (Chapter 5). The new addition to CEMDAP has been named Comprehensive Econometric Micro-Simulator for EVACuations (CEMEVAC). This simulator is capable of modelling the daily average travel behaviour as well as the travel behaviour during an evacuation for individuals and households. To update the travel times, that are expected to change from the daily average due to the evacuation being performed, TRANSIMS, a sophisticated traffic micro-simulator, was used to simulate the trips generated by CEMEVAC and provide new travel times that reflect the changes in traffic on the road-network.

CEMEVAC is capable of modelling the mixture of normal day-to-day travel behaviour along with the gradually increasing number of evacuees. This provides a more

realistic description of the expected loads on the transport network and more realistic knowledge regarding number of expected evacuees and expected clearance time. CEMEVAC models evacuations due to approaching hazards, such as hurricanes and NEO impacts on the Earth. Both types of hazards can be tracked and a landfall/impact location and time can be predicted with some uncertainty.

New models to be used for modelling human decision-making and travel behaviour during an evacuation have been developed and are described in detail in Chapter 5. These models provide a way of simulating a realistic evacuation behaviour that reflects individual travel behaviour as well as household decisions made. The models for hurricane evacuation decision-making and travel behaviour were derived using travel behaviour data gathered from a range of evacuation surveys from the United States, where people had been interviewed regarding what they did during either one or more evacuations or what they are planning to do in the event of a evacuation due to an approaching hurricane. Based on these models more hypothetical models were derived for the modelling of people's travel behaviour during an evacuation due to an approaching NEO.

The main purpose with this micro-simulator is to use it for running micro-evacuation-simulations and to use the outcome from these to validate and calibrate the coarse-scale flow based evacuation simulator described in Chapter 5.

A more detailed description of the work done till date, regarding the development of an agent based evacuation micro-simulator can be found in Appendix E.

6.5 Future work

The NEOMiSS software provides some useful tools for decision-makers and the public to use to learn more about the threat from NEOs impacting the Earth in the form of physical effects and human vulnerability. It can provide decision-makers with knowledge regarding how different areas along a potential risk corridor would be affected and the ability to evacuate different areas.

In NEOMiSS, previous vulnerability models were improved and several are now based on historical data instead of a more vague description of how specific physical

effects might cause injury to humans and damage to nature and infrastructure. The outcome from running these models highlights the spatial differences in human vulnerability. There is space for improvements to all the developed models to reflect aspects such as local wealth, elevation and more detailed information regarding land usage. Collaborating with geologists to improve the modelling of the earthquakes due to a NEO land impact could be useful. Climatologists might also be able to help improve the knowledge regarding the short- and long-term climatic changes due to the large amounts of material that would be catapulted into the atmosphere. Such effects could cause weather changes and famine.

The behaviour-based models developed for the two evacuation simulators are limited by the surveys they are based upon and several areas of the evacuation process have been found not to be covered by the evacuation surveys, such as the evacuation preparation period and travel behaviour by people not evacuating but preparing for the arrival of the hazard. Investing time and money in additional evacuation surveys that can provide better knowledge regarding people's behaviour and travel patterns during the evacuation preparation time could improve existing models by also enabling the simulator to simulate the evacuation preparation. Investigating peoples' evacuation travel behaviour in other parts of the world would likewise broaden the knowledge regarding how people react in such dramatic circumstances and how previous experience and cultural differences might affect such behaviour. Finally looking more into the uncertainties in the models developed for NEOMiSS would be beneficial. These uncertainties could among other be due to large data fluctuations due to limited survey data.

Various areas of improvement within the coarse-scale evacuation simulator were also identified as discussed in Chapter 5. Table 6.1 provides a detailed list of subjects where further research in the future could improve the NEOMiSS software. Some of the subjects have already been mentioned.

Table 6.1: List of possible future project and investigations that could improve NEOMiSS.

Area of research	Subject
Physical simulator	Use geology and building knowledge to improve simulation of blast wave and ignition exposure
	Use geology to improve earthquake simulation
	Implement new physical asteroid impact model by Gisler regarding ocean impact.
	Use weather and climate models to simulate the short and long-term climatic changes due to the infusion of large amounts of material and water into the atmosphere.
Vulnerability modelling	Improve vulnerability models due to air blast, ejecta, ignition exposure, crater and fireball.
	Improve earthquake vulnerability models to reflect the time of day issues that is applicable in areas with a weak building stock.
	Investigate long-term secondary and tertiary hazards and the vulnerability to these.
	Create human vulnerability models due to the different ocean impact hazards
	Investigate the potential use of additional parameters when modelling human vulnerability such as wealth, demographics and elevation
	Investigate reduction in vulnerability to e.g. evacuation
Road network capacity and flow-time modelling	Use parameters such as wealth, road bendiness, accident statistics, elevation and land usage to improve models in order to try and identify major traffic routes between settlements
	Include uncertainty to models using standard deviation and Monte Carlo
Survey data	Run surveys of evacuees that highlights some of the areas that are lacking in current surveys and has been identified on my wiki
Evacuation simulation	Add buses and other transportation means to the simulator
	Improve models by including uncertainty
	Convert simple assumptions into models where possible and increase level of detail
	Make it possible to run different evacuation strategies (i.e. the managed UK evacuation strategy versus the US help yourself evacuation strategy)
	Investigate the use of other types of transportation such as ferries and air planes in the simulator
	Generate data for CEMEvac case study and test case and run these cases
	Improve coarse-scale simulator based on CEMEvac results

Chapter 7
Conclusions

This thesis investigates how human vulnerability in the form of casualties can be estimated using models that describe the physical impact from a NEO on the Earth and how the different physical hazards will cause destruction. Uncertainties in the developed models and the available data have been taken into account providing a much broader insight into these casualty estimates.

A coarse-scale behaviour based evacuation simulator was used to investigate different areas ability to evacuate and how factors such as the evacuation, the infrastructure and the local geography can affect such evacuations. The outcome from this simulator was used to investigate the reduction in human vulnerability after an evacuation.

The NEOMiSS software, which was developed as a toolbox to help decision-makers and the public gaining better knowledge regarding the physical effects and human vulnerability to NEO land impacts on the Earth along with assisting a potentially affected areas' ability to undertake mitigation in the form of evacuation. This knowledge could be used by decision-makers when deciding on mitigation strategies and planning for mitigation.

The NEOMiSS software consists of four simulators:

- a physical impact simulator developed by Morley and based on models developed by Collins et al. (2005)
- a human vulnerability simulator for estimating the number of expected casualties (i.e. fatalities and injured)

- a coarse-scale behaviour-based evacuation simulator
- a fine scale behaviour and agent-based evacuation simulator

The fine scale evacuation simulator needs further work in order to be used for validation and calibration of the coarse-scale evacuation simulator and is therefore only described in Appendix E.

7.1 Human vulnerability

Although a large devastating NEO impact on the Earth is a rare event, such an impact could result in a range of devastating natural hazards. Six single hazard vulnerability models predicting the number of casualties were developed for a NEO land impact and the six models were combined into a multi-hazard model. The models are unique by accounting for uncertainty and three models (vulnerability to earthquakes, ejecta fall and air blasts) were developed using historical data on earthquakes, snow load, tephra fall and large explosions. The ejecta models are based on tephra fall roof vulnerability curves developed by Spence et al. (2005b), while the earthquake models are based on historical earthquakes, and the air blast models are based on large explosions. Both the earthquake and ejecta fall models also take into account the local average building strength while the ignition exposure model takes into account if people are located indoors or outdoors.

The earthquake model was tested against historical data. The other vulnerability models were not tested due to the lack of, or limited number of, historical events. The results for the earthquake model test showed that the predicted number of casualties generally was within the one and a half uncertainty band of the historical data. These results correspond well with the assumption, that a NEO land impact will create shallow earthquakes.

The developed multi-hazard vulnerability model was used along the risk corridor of the asteroid 99942 Apophis. This case study shows that the worst affected area is along the densely populated coastal region of South America, while Russia with its large unpopulated areas in Siberia would experience fewer casualties. Along the risk corridor it was found that on average a proportion of 0.9% of the people living within the affected

area are expected to be casualties, but depending on the final impact location this could vary between 0.0002% and 20% along the risk corridor. It was also found that the ejecta was one of the major casualty contributors being responsible for around 25% of the casualties.

An additional case study was performed using the much smaller asteroid 2010CA. This asteroid size is a much more likely scenario given the larger number of these objects being potentially hazardous. A fictive risk corridor was created across Hampshire and it was found that that on average 3% of people living in the affected area would become casualties. For the same scenario but with asteroid 99942 Apophis the average number of casualties was found to be 1.6 %.

7.2 Evacuation simulation modelling

Two evacuation simulators were developed. A coarse-scale evacuation simulator that uses global gridded data and a flow approach, and an agent-based micro-simulator, that simulates individuals and households both prior to and during an evacuation. Both simulators use behaviour-based models that were developed using survey data regarding people's behaviour during evacuations, especially hurricane evacuations. This natural hazard is similar to NEO impacts in that its land fall location can be predicted with some uncertainty and affected areas can be evacuated ahead of the arrival of the hazard.

The behaviour-based evacuation models and the survey observations regarding evacuation behaviour showed interesting trends depending on the magnitude of the hazard, wealth and gender. The coarse-scale evacuation simulator was tested against an actual hurricane evacuation event, hurricane Rita and the evacuation of the broader Houston area in Texas, and it was found that the simulator was able to mimic this evacuation reasonably well. The ratio between the number of normal evacuees and shadow evacuees could, however, be improved.

A sensitivity analysis was performed investigating how well local road networks were able to cope with an increasing number of vehicles during a 1 day evacuation scenario. This analysis showed that when the number of people evacuating started to

reach 40% of the total local population then the road network started to be unable to handle the large amounts of evacuees and fewer evacuees were able to evacuate.

Multiple case studies were run using the coarse-scale evacuation simulator for a number of different asteroids, primarily asteroid 99942 Apophis and 2010 CA. These cases studies were designed to investigate the change in evacuation results depending on the time available to perform the evacuation, geographical location and asteroid size (energy). The results for the 99942 Apophis test cases showed that the selected area in Costa Rica needs more than 3 ½ days for all expected evacuees to be able to evacuate. For asteroid 2010ca the results showed that smaller settlements and rural areas with reasonably good road connections in all directions can evacuate relative quickly, within ½ day for the New Forest and the Basingstoke scenarios. Larger settlements such as Southampton and Portsmouth will take longer to evacuate and the road connections will also have an impact in the needed clearance time. For these two location 3 ½ days was enough time to be able to evacuate all the expected evacuees.

An investigation into how well Southampton would be able to handle 1 day evacuation scenarios where the size of the impacting NEO grew showed that for the largest of the investigated NEOs, asteroid 2010 XA68 with an energy of 6.7e+02 MT TNT, a noticeable drop in number of evacuees that managed to evacuate was observed.

Finally two case studies were performed with the objective of investigate how the human vulnerability will decrease after a 1 day evacuation was performed in Southampton with Asteroid 2010 CA and 2004 ME6 respectively. For the 2010 CA case study the human vulnerability dropped by a factor of 26 after an evacuation was performed compared to the scenario where no evacuation was performed. For asteroid 2004 ME6 there was a 35 times drop in the number of human casualties compared to the previously predicted number.

Appendix A

NEO deflection and fragmentation strategies

Type	Method(s)	Limits	Possi-bility
Solar collectors / Solar mirror [1][2]	A spacecraft carrying a large solar collector. Sunlight is focused onto the NEO surface vaporizing the surface. This will result in a continued transfer of momentum to the object.	The collector has a very limited lifetime of a few minutes. The method is only applicable on objects with a diameter < 250 m.	U
Electric propulsion [1]	Attach an electric propulsion system on the NEO	How to attach the system onto the rotating NEO? When to use the propulsion on the rotating NEO? Need very	M
Chemical propulsion [1]	Attach a chemical propulsion system on the NEO	How to attach the system onto the rotating NEO? When to use the propulsion on the rotating NEO?	M
Mass driver engine [1][11]	Provide a steady thrust by mining the NEA		U
Lasers [1]	Ground or space based laser system, that will vaporize parts of the NEO surface and thereby provide a thrust	Need a very good target system in order to provide momentum at the right part of the rotating NEO	U
Solar sails [1][3]	1. Using solar sails to deliver a projectile to a NEO with enough kinetic energy to deflect the NEO [3] 2. A solar sail could be attached to the NEO and use the impulse delivered from the solar wind to deflect the object [1]	1. Need a long lead time to reach the object with enough velocity 2. The impulse is low and the sail has to be very large which means heavy and difficult to manufacture + difficult to attach on a rotating object + limited launch payload	1. P 2. M
Yakowsky effect [1][3][4]	Cover the surface of the NEO with a coat in order to change the Yakowsky effect	Need large amounts of coating. Ex 1km diameter NEO with 1 cm cover need 250000 tons coating (~90 fully loaded Saturn V launchers). How to spread the coating?	U
Kinetic energy impact [3]	Using solar sails to deliver a projectile to a NEO with enough kinetic energy to deflect the NEO	Need a long lead time to reach the object with high enough velocity.	
Gravitational tractor [5][6][8]	20 T massive spacecraft tow the asteroid by using its force of gravity	Need long warning time. Launch limitations.	M
Impactor [1][2]	A spacecraft hit the NEO at a high velocity. The energy transferred will either provide enough momentum to change the orbit or to fragment the NEO	NEO size, orbit and composition. Danger of an uncontrolled fragmentation.	P
Tug boat [7][9]	A spacecraft dock to the asteroid.	Issues about how to do the	M

	Reorient the asteroid and then provide a continuous parallel thrust to the asteroid.	docking, especially on to a rubble pile asteroid.	
Fragmentation [10]	Use nuclear bombs to fragment the NEO and create a large amount of harmless debris.	There is a big risk that not all fragments will be harmless debris. It might cause a greater damage to Earth and to the satellites orbiting Earth than a single NEO would.	P
NEO collisions [1]	Change the orbit of smaller NEO to make them collide with bigger NEO.	Need a lot of knowledge about both NEOs and need another deflection method to use on the smaller NEO.	
Nuclear explosives [1][2]	3 types: 1) Stand off explosion a distance away from the object 2) Surface explosion creating a crater and the ejected mass creates an impulse 3) Explosion under the surface creating a larger amount of ejected material and a higher impulse	Political issues Nuclear explosions are banned in space Danger of an uncontrolled fragmentation.	1) P 2) P 3) M
Nuclear propulsion [1]	Use nuclear fusion or fission to heat up hydrogen. This is then released creating a thrust.	In the 1950s to 1970s tests with fusion where performed [1]. Fission energy is still being tested on a small scale [12].	M

Table A1: Suggested NEO deflection and fragmentation methods

P stands for possible with the technology currently available, M means that more research and improved technology is needed and U stands for currently unrealistic.

References:

1. Gritzner, G.: NEO – MIPA Near Earth Object Hazard Mitigation Publication Analysis: Eurospace: http://www.tu-dresden.de/mwilr/space/rfs/Dokumente/Publikationen/NEO-MIPA-report.pdf: 2001
2. Gritzner, C., Dürfeld, K., Kasper, J., Fasoulas, S.: The asteroid and comet impact hazard: risk assessment and mitigation options: Naturwissenschaften (2006) 93: 361--373
3. McInnes, C. R.: Deflection of Near-Earth asteroids by kinetic energy impacts from retrograde orbits: Planetary and Space Science, 52 (2004) 587--590
4. Spitale, J. N.: Asteroid Hazard Mitigation Using the Yarkovsky Effect: Science Vol. 296 pp. 77 5 April 2002
5. Svoboda, E.: "Gravity Tractor" Super Telescopes Enlisted to Battle Killer Asteroids: National Geographic: February 17. 2007: http://news.nationalgeographic.com/news/2007/02/070217-asteroid-impact.html
6. Jaggard, V.: "Killer Asteroid" Debate Pits Gravity Tractors Against Bombs, Projectiles: National Geographic, March 8. 2007: http://news.nationalgeographic.com/news/2007/03/070308-asteroids.html
7. Gugliotta, G.: Science's Doomsday Team vs. the Asteroids: Washington post, April 9, 2005: http://www.washingtonpost.com/ac2/wp-dyn/A38306-2005Apr8?language=printer
8. Schweickart, R., Chapman, C., Durda, D., Hut, P.: Threat Mitigation: The Gravity Tractor: white paper 042: 2007: http://www.aero.org/conferences/planetarydefense/documents/wpGT%20(Schweickart).pdf
9. Schweickart, R., Chapman, C., Durda, D., Hut, P.: Threat Mitigation: The Asteroid Tugboat: white paper 041: 2007: http://www.aero.org/conferences/planetarydefense/documents/wpAT%20(Schweickart).pdf
10. Project Icarus: The MIT Press Cambridge, Massachusetts, and London, England
11. Space Studies Institute, SSI: Asteroid Deflection: http://spacestudiesinstitute.wordpress.com/papers/asteroid-deflection/
12. McGrath, M.: Fusion falters under soaring costs: BBC news, 17. June 2009: http://news.bbc.co.uk/1/hi/sci/tech/8103557.stm

Appendix B

Global datasets

The tables below describe the individual global datasets found during this PhD. The tables are divided into topics and contain information such as name, a short description of the dataset, data availability and data quality is available in these tables, providing a quick overview of available data and where to find it.

General world data:

Name	CIA World factbook
Made by	CIA, USA
Description	Contain information about the world in general and about each individual nation. Rank order lists are also available. In these lists the data of each country is put into rank order making it possible to get complete lists of example Population, Population growth rate, GDP growth rate, Roadways in km, Net migration rate(migrant(s)/1,000 population) and Area in square km. The book is reviewed annually, but it was reviewed semi annually until 1980. It provides 3 types of intelligence basic, current, and estimative [https://www.cia.gov/library/publications/the-world-factbook/docs/history.html], where basic is fundamental and factual reference material on a country or issue, current intelligence is reports on new developments, these are continual updates on the inventory of knowledge and estimative intelligence show estimates on probable outcomes, and revises overall interpretations of country and issue.
History	The factbook started out in 1955 as an annual summary of The National Intelligence Survey. In 1962 the first classified factbook was published and in 1971 it became unclassified. In 1997 the factbook became available on the Internet and data back to 1981 is currently available.
Data available	Facts about population, geography, government, GDP, infrastructure/transportation, resources, communication and military for each nation. It provides data for 232 countries according to the Rank Order - Population growth rate table https://www.cia.gov/library/publications/the-world-factbook/rankorder/2002rank.html
Data quality	Data last updated in 2008.
Data access	The factbook is in the public domain and may be copied freely without permission of the Central Intelligence Agency (CIA). A complete version of the book can be downloaded from https://www.cia.gov/library/publications/download/ Data from 2008 and back to 1981 is online available.
Data used by	NEOimpactor
Data used for	
Issues	It contains no granular data distribution across countries only country by country facts.
Links	https://www.cia.gov/library/publications/the-world-factbook/. https://www.cia.gov/library/publications/the-world-

	factbook/docs/contributor_copyright.html
Other notes	

Name	Global Peace Index (GPI)
Made by	Institute for Economics and Peace, Australia
Description	Show ranking lists for peacefulness on a country-by-country level for 149 nations. It also contains plots illustrating - Political Democracy Index and overall GPI - Functioning of government and over overall GPI - Perception of corruption and overall GPI - The extent of regional integration and overall GPI - Mean years of schooling and GPI measure of internal "peace" - …
History	Launched in 2007 and provide a yearly country ranking list for peace based on 23 qualitative and quantitative indicators, using 'respected' sources.
Data available	Available in tables in a pdf document and on http://www.visionofhumanity.org/gpi-data/#/2010/scor/
Data quality	
Data access	http://www.visionofhumanity.org/ and http://www.visionofhumanity.org/wp-content/uploads/PDF/2010/2010%20GPI%20Results%20Report.pdf
Data used by	
Data used for	
Issues	Data show a combination of countries internal and external peace witch does punish relative internally peaceful nations such as the UK whose military is stationed in at least 2 other independent nations.
Links	http://www.visionofhumanity.org/ and http://www.visionofhumanity.org/wp-content/uploads/PDF/2010/2010%20GPI%20Results%20Report.pdf
Other notes	

Name	UN data
Made by	The United Nations Statistics Division (UNSD) of the Department of Economic and Social Affairs (DESA)
Description	General statistics databases
History	The UN data database service was launched in 2005 as a part of the "Statistics as a Public Good" project. The purpose with this project was to: • Provide free access to global statistics • Educate users about the importance of statistics for evidence-based policy and decision-making • Assist National Statistical Offices of Member Countries to strengthen their data dissemination capabilities.
Data available	Provide global data sets for up to 243 countries between 1970 and 2007. Data that is provided is divided into following sub types: • Commodity Trade Statistics Database • Energy Statistics Database • FAO Data, Food and Agriculture Organization

	• Gender Info 2007 • Greenhouse Gas Inventory Data • ILO Data, International Labour Organization • Industrial Commodity Statistics Database • Key Global Indicators • Millennium Development Goals Database • National Accounts Estimates of Main Aggregates • National Accounts Official Country Data • The State of the World's Children 2008 • UNESCO UIS Data, UNESCO Institute for Statistics • UNSD Demographic Statistics, United Nations Statistics Division • WHO Data World Health Organization • World Population Prospects: The 2006 Revision • World Tourism Organization Statistics Database and Yearbook
Data quality	Very varying quality. In some cases data are only available for very few countries and the years data are available from also varies a lot.
Data access	Online access from the UN database homepage [http://data.un.org/Browse.aspx?d=SNAAMA] Data are easy to export and there are filters that make it possible to group the countries.
Data used by	Data Distribution Centre, DDC [http://www.ipcc-data.org/]
Data used for	Crating climate, socio-economic and environmental data
Issues	Data are only for each country. It is not divided into more local grids.
Links	http://data.un.org/Browse.aspx?d=SNAAMA
Other notes	Provide some useful growth rates.

Wealth / poverty:

Name	G-Econ
Made by	William Nordhaus, Sterling Professor of Economics, Yale University.
Description	A geophysical scaled global economic dataset showing economic activity for the world.
History	
Data available	Economic data such as gross cell product and demographic and geophysical data such as mean temperature, average rain fall, latitude, longitude, elevation, population and quality of data. 2006 and 2008 datasets contain data from the years 1990, 1995 and 2000.
Data quality	Data quality is described in the dataset for each grid cell
Data access	All data are publicly available to all not-for-profit researchers, and can be found on the G-Econ home page, see links.
Data used by	
Data used for	The data can "be helpful in environmental and economic studies of energy, environment, and global warming." [http://gecon.yale.edu/short.html]
Issues	Data quality varies very much between regions and some regions such a Greenland, Antarctica, Northern Canada, Alaska and Siberia are economic deserts. There is also missing data for some years from countries such as Zimbabwe.

Links	http://gecon.yale.edu/
Other notes	27,500 terrestrial grid cells Resolution 1 degree longitude by 1 degree latitude which is approximately 100 km by 100 km grid cells

Name	PovcalNet
Made by	The World Bank
Description	PovcalNet is a computational tool that can estimate the extent of absolute poverty in the world. It replicates the calculations made by the World Bank's researchers. It looks at 116 developing countries. The data can be calculated for a specific user defined poverty lines and reference year. Another way is to group the countries and calculate for the specific group.
History	
Data available	Get tables from requested country and requested years containing country name, year, used poverty line, Monthly per capital mean in 2005 Purchasing Power Parity (PPP)$, Headcount index, Poverty gap index, FGT2 index, Watts index, GINI index and MLD index
Data quality	The Bank's official estimates use unit record household data whenever possible and PovcalNet uses grouped distributions. Due to this difference, there are some minor discrepancies between official World Bank estimates and online PovcalNet results.
Data access	Online available and downloadable
Data used by	
Data used for	
Issues	It only looks at 116 developing countries not at any countries in Western Europe, North America or Eastern Asia. The years where data are available varies from country to country.
Links	http://web.worldbank.org/WBSITE/EXTERNAL/EXTDEC/EXTRESEARCH/EXTPROGRAMS/EXTPOVRES/EXTPOVCALNET/0,,contentMDK:21867101~pagePK:64168427~piPK:64168435~theSitePK:5280443,00.html
Other notes	A major feature worth mentioning is that PovcalNet both provide a duplicate the World Bank's regional poverty estimates and also makes it possible to form groups of countries and providing estimates for these groups.

Name	Decomposing World Income Distribution Database
Made by	The World Bank
Description	Look at national income and expenditure distribution data from 119 countries. The total income is decomposed inequality between the individuals in the world, by continent and by countries grouped by income level.
History	
Data available	Population size and PPP per country for 1988 and 1993
Data quality	
Data access	
Data used by	

Data used for	
Issues	This database only looks at each individual country and not at different regions inside the country. It also only looks at 119 countries.
Links	http://econ.worldbank.org/WBSITE/EXTERNAL/EXTDEC/EXTRESEARCH/0,,contentMDK:20713100~pagePK:64214825~piPK:64214943~theSitePK:469382,00.html
Other notes	

Name	FAOSTAT
Made by	United Nations Food and Agriculture Organisation (FAO)
Description	The database contains time-series and cross sectional data related to food and agriculture for up to 210 countries.
History	
Data available	Data on a national level about: production, trade, consumption, food security, prices, resources, forestry and fisheries. Data are available from 1961 to 2007. The available data comes in many different formats from tables in pdf documents, csv file and xls files.
Data quality	Use questionnaires in order to gather the information. Some countries might not provide high quality data and some of it might be based on low quality estimates.
Data access	Online asses from the FAO homepage.
Data used by	Data Distribution Centre, DDC [http://www.ipcc-data.org/]
Data used for	Creating climate, socio-economic and environmental data
Issues	Only provide data on a country basis. Data quality will be of varying quality.
Links	http://faostat.fao.org/default.aspx
Other notes	

Gridded population databases:

Name	Global Population of the World, GPW
Made by	Socioeconomic Data and Applications Center, SEDAC
Description	This database shows the spatial distribution of human populations across the globe along with information about location of the different nations, their boundaries and coastlines. Data from 232 countries are included in this database. Provided future population estimates for the years 2005, 2010 and 2015 using growth rates from the United Nations Food and Agriculture Programme (FAO).
History	The Idea for the development of a Gridded Population of the World database started in 1994 at the Global Demography Workshop at the Center for International Earth Science Information Network (CIESIN) of the Earth Institute, Columbia University.
Data available	Population grid, resolution 2.5', 1/4°, 1/2° and 1°, from year 1990, 1995, 2000, 2005, 2010 and 2015 Population density grid, resolution 2.5', 1/4°, 1/2° and 1°, from year 1990, 1995, 2000, 2005, 2010 and 2015 Land / Geographic Unit Area Grids, resolution 2.5', 1/4°, 1/2° and 1°, from circa 2000 National Identifier Grid, resolution 2.5', from circa 2000 Centroids, from circa 2000 Coastlines, from circa 2000

	National Boundaries, from circa 2000
Data quality	Varying, depends on the available national or subnational spatial units
Data access	Online available from SEDAC's homepage, see links
Data used by	
Data used for	
Issues	Use national or subnational spatial units of varying resolutions these unites are usually administrative units.
Links	http://sedac.ciesin.org/gpw/
Other notes	

Name	Global Urban-Rural Mapping Project, GRUMP
Made by	Socioeconomic Data and Applications Center, SEDAC
Description	An addition to the GPW database. Here population is spatially distinguished by urban and rural areas. The resolution is also noticeably higher than in GPW.
History	The Idea for the development of a Gridded Population of the World database started in 1994 at the Global Demography Workshop at the Center for International Earth Science Information Network (CIESIN) of the Earth Institute, Columbia University.
Data available	Population grid, resolution 30'', from year 1990, 1995 and 2000 Population density grid, resolution 30'', from year 1990, 1995 and 2000 Land / Geographic Unit Area Grids, resolution 30'', from circa 2000 Settlement points, from circa 2000 Urban extend grid, resolution 30''
Data quality	Varying, depends on the available national or sub national spatial units
Data access	Online available from SEDACs homepage, see links
Data used by	The European Commission's Joint Research Centre and the World **B**ank
Data used for	Map of global accessibility [http://bioval.jrc.ec.europa.eu/products/gam/sources.htm]
Issues	Use national or sub national spatial units of varying resolutions these unites are usually administrative units.
Links	http://sedac.ciesin.org/gpw/
Other notes	

Name	United Nations Environment Programmes Global Resource Information Database (UNEP/GRID)
Made by	United Nations Environment Programme in partnership with U.S. Geological Survey (USGS), and the National Aeronautics and Space Administration (NASA, United States Environmental Protection Agency (US EPA) and United States Forest Service (USFS)
Description	Global gridded population density data from 1960 to 2000
History	Founded in 1991
Data available	Population density data for the different continents and a global distribution dataset.
Data quality	1x1 latitude/longitude resolution, here they probably mean 1^{o} x 1^{o} resolution.

Data access	Online access. Data are free to download.
Data used by	
Data used for	
Issues	Global dataset only available for 1990
Links	http://na.unep.net/datasets/datalist.php
Other notes	Provide links to other global databases

Elevation data:

Name	SRTM 90m Digital Elevation Data
Made by	The Consortium for Spatial Information (CGIAR-CSI)
Description	SRTM 90m Digital Elevation Data (DEM) for the entire world
History	The SRTM 90m Digital Elevation Data for the entire world was originally made by NASA. The data comes from the NASA Shuttle Radar Topographic Mission (SRTM), whose mission was to provide digital elevation data for over 80% of the Earth.
Data available	Digital elevation models (DEM) for the entire world with a resolution of 90m at the equator and use 5^{o} x 5^{o} grids on CGIAR-CSIs homepage and the SRTM data are available as 3 arc second (approx. 90m resolution) DEMs, from USGS. A 1 arc second data product has also been produced for some countries.
Data quality	The vertical error of the DEM's is reported to be less than 16m.
Data access	Downloadable from the CGIAR-CSI homepage and from the National Map Seamless Data Distribution System, or the USGS ftp site and is free of charge.
Data used by	
Data used for	
Issues	
Links	http://srtm.csi.cgiar.org/
Other notes	

Name	GTOPO30 (Global 30 Arc-Second Elevation Data Set)
Made by	US Geological Survey, USGS
Description	Global 1-km digital raster data describing the elevation on Earth.
History	The GTOPO30 database was completed in 1996. It was produced in collaboration with U.S. Geological Survey's EROS Data Center (EDC), the National Aeronautics and Space Administration (NASA), the United Nations Environment Programme/Global Resource Information Database (UNEP/GRID), the U.S. Agency for International Development (USAID), the Instituto Nacional de Estadistica Geografica e Informatica (INEGI) of Mexico, the Geographical Survey Institute (GSI) of Japan, Manaaki Whenua Landcare Research of New Zealand, and the Scientific Committee on Antarctic Research (SCAR).
Data available	Global land elevation data with a 30'' (~1km) resolution.
Data quality	Uses an acceptable resolution, providing a good quality. The entire earth is covered.
Data access	Online access from the USGS web site and the data are free of charge. Download data in minor portions. Earth is divided into 33 tiles and each tile can be downloaded.

Data used by	The European Commission's Joint Research Centre and the World **B**ank
Data used for	Map of global accessibility [http://bioval.jrc.ec.europa.eu/products/gam/sources.htm]
Issues	Uncertainty about the quality of data, When opening the tiles in ArcMap data in some regions where clearly wrong. This might be due to the conversion of the data when opening it into ArcMap. No Ocean data available.
Links	http://eros.usgs.gov/products/elevation/ and http://edc.usgs.gov/products/elevation/gtopo30/README.html
Other notes	Data are viewable in GIS software

Road network data:

Name	VMAP0
Made by	
Description	VMAP0 is a slightly more detailed reiteration of the DCW. It contains worldwide coverage of vector-based geospatial data describing major road and rail networks, hydrologic drainage systems, utility networks, major airports, elevation contours, coastlines, international boundaries, populated places and a list of geographic names. Scale (1:1,000,000).
History	Developed after the DCW was made. A VMAP1 was also developed with a higher resolution, but only partly available in the public domain according to [http://en.wikipedia.org/wiki/Vector_Map]
Data available	Data about: country regions, water depth, coastlines, roads, rail roads (very outdated!!!) , cities, elevation, vegetation, rivers and streams, …
Data quality	Varying quality. Has been criticised by CODATA to be incomplete.
Data access	Data are downloadable from the VMAP0 homepage
Data used by	The European Commission's Joint Research Centre and the World **B**ank
Data used for	Map of global accessibility [http://bioval.jrc.ec.europa.eu/products/gam/sources.htm]
Issues	Some of the data seems to be very outdated, e.g. the railroad maps. In some cases the tracks actually still exists, but has not been in use for the last 20 to 50 years, but in other cases the tracks were removed and there are no plans to reinstall the railroad.
Links	http://www.mapability.com, http://en.wikipedia.org/wiki/Vector_Map
Other notes	Data are viewable in GIS software

Name	Global Roads Open Access Data Set (gROADS)
Made by	Global Roads Data Development Working Group under CODATA, the Committee on Data for Science and Technology, which is an interdisciplinary Scientific Committee of the International Council for Science (ICSU)
Description	Should provide global roads data but will be focusing on roads between settlements
History	The group was started at a workshop on Global Roads Data at the Lamont Campus of Columbia University in October 2007.
Data available	Not yet available, under construction, is planned to be ready in March 2010
Data quality	~50m positional accuracy

Data access	Should be freely available on an “attribution only” basis
Data used by	
Data used for	
Issues	Not yet available, is planned to be ready in March 2010
Links	http://www.ciesin.columbia.edu/confluence/display/roads/Global+Roads+Data http://www.codata.org/taskgroups/WGglobalroads/ www.ciesin.columbia.edu/confluence/download/attachments/.../CODATA+Global+Roads+Implementation+Plan_FINAL_25nov08.pdf?
Other notes	

Name	OpenStreetMap, OSM
Made by	Steve Coast
Description	Founded in July 2004
History	The database was built by volunteers. They perform systematic ground surveys using a handheld GPS unit and a notebook or a voice recorder. This data are then entered into the OpenStreetMap database. Aerial photography and other data sources from commercial and government sources are also being used to improve the quality of the data.
Data available	Road data as images showing the road system and the data as xml files containing roads latitude, longitude and elevation. On the image the roads are coloured in order to describe the type of road.
Data quality	The database is still being improved but there is areas that might be badly covered such as Mozambique [Users diary note Posted by katpatuka at Tue Jan 13 07:05:10 +0000 2009 http://www.openstreetmap.org/diary] This can be due to lack of volunteers in the region and last of necessary equipment.
Data access	Accessible from the OpenStreetMap home page where requested maps can be exported. OpenStreetMap data are licensed under the Creative Commons Attribution-ShareAlike 2.0 license.
Data used by	Is used at a large variety of mapping services such as: • OpenStreetMap general, cyclists, debugging (Worldwide) http://www.openstreetmap.org/ • FreeMap walkers (parts of the UK) http://www.free-map.org.uk/freemap/index.php? • OpenCycleMap cyclists (Worldwide) http://www.opencyclemap.org/ • OpenRouteService routing (Germany) http://openrouteservice.org/ • OpenPisteMap skiing (some European and USA resorts) http://openpistemap.org/ • CloudMade general, mobile (Worldwide) http://cloudmade.com/
Data used for	
Issues	The quality might be very low in especially developing countries.
Links	http://www.openstreetmap.org/ http://en.wikipedia.org/wiki/OpenStreetMap
Other notes	It is worth noticing that in some towns the location of hospitals, pubs and public

	building are placed on the map but the quality of this information is still very low.

Climate:

Name	Population, Landscape, and Climate Estimates, PLACE
Made by	Socioeconomic Data and Applications Center, SEDAC
Description	The PLACE database contains global, geospatially calculated values of population and land area in specific zones of population density, coastal proximity, climate, elevation and biomes. It looks at 228 nations for the years 1990 and 2000.
History	
Data available	Maps illustrating the geographical and spatial data and two dataset files PLACE I and PLACE II containing the data.
Data quality	
Data access	Data and maps can be downloaded from the PLACE homepage
Data used by	
Data used for	
Issues	
Links	http://sedac.ciesin.columbia.edu/place/
Other notes	

Name	Köppen Climate Classification data of the world
Made by	Institute for Veterinary Public Health, University of Veterinary Medicine Vienna.
Description	Global climate classification data in a 0.5 degree latitude/longitude grid (= 92416 grid boxes) for the period 1951 to 2000. The data are based on data from Climatic Research Unit (CRU) of the University of East Anglia and the Global Precipitation Climatology Centre (GPCC) at the German Weather Service.
History	
Data available	Global climate classification data for each grid cell. The data contains 3 columns. Column 1 and 2 are information about grid box centre coordinates (latitude, longitude), while column 3 is the corresponding climate class abbreviated following the official climate classification made by Köppen and Geiger.
Data quality	
Data access	Online access from the koeppen-geiger homepage. Data can be downloaded as a ASCII file, GIS file or Google Earth KMZ file
Data used by	Beck et al, koeppen-geiger.vu-wien.ac.at/pdf/beck_et_al_ksb_2006.pdf
Data used for	Characterization of global climate change
Issues	
Links	http://koeppen-geiger.vu-wien.ac.at/
Other notes	

Name	Climatic Research Unit (CRU)
Made by	Climatic Research Unit (CRU), University of East Anglia (UEA), Norwich
Description	Global climate data. Hemispheric and global averages as monthly and annual values are available as separate files.
History	The Climatic Research Unit (CRU) started in 1972 in the School of Environmental Sciences (ENV) at the University of East Anglia (UEA) in Norwich. CRU is recognised as a world leading institution in the area of natural and anthropogenic climate change.
Data available	Temperature data, resolution: 5^{o} by 5^{o} grid, data from 1850 to 2008 Global Land Precipitation, resolution: 2.5^{o} latitude by 3.75^{o} longitude or 5^{o} latitude/longitude grids, data from 1900 to 1998. Grid-Point Pressure Data for the Northern Hemisphere, resolution: 5° latitude by 10° longitude grid-point, data from 1873 to 2000 Other pressure data
Data quality	Large variety of data resolution and data coverage available.
Data access	All data are publicly available from the CRU homepage and can be freely downloaded from there.
Data used by	Köppen Climate Classification data of the world
Data used for	Creating the Global climate classification map
Issues	For some countries the older data are missing and for the Global Land Precipitation the latest data are from 1998.
Links	http://www.cru.uea.ac.uk/
Other notes	The temperature dataset is updated at regular interval.

Name	ISLSCP Initiative II data collection
Made by	The International Satellite Land Surface Climatology Project, Initiative II
Description	The data available in 50 global time collections from a time period between 1986 and 1995 and is collected for investigating the global carbon, water and energy cycle.
History	The project started out in 1983 with the Initiative I data collection. In 1999 Initiative II was started. In this initiative the spatial resolution of the data were improved, from one degree to 0.5 and 0.25 degrees.
Data available	Data available is categorised info following groups • Carbon • Hydrology, Soils, and Topography • Near-Surface Meteorology • Radiation and Clouds • Snow, Sea Ice, and Oceans • Socioeconomic • Vegetation • Ancillary Data
Data quality	
Data access	Online available for downloading from the ISLSCP homepage.
Data used by	Köppen Climate Classification data of the world
Data used for	Creating the Global climate classification map

Issues	
Links	http://islscp2.sesda.com/ISLSCP2_1/html_pages/islscp2_home.html
Other notes	

Name	Global Land Cover Characterisation, GLCC
Made by	U.S. Geological Survey (USGS), the University of Nebraska-Lincoln (UNL), and the European Commission's Joint Research Centre (JRC)
Description	The database is containing global land cover characteristics with a 1-km resolution. The data are based on 1-km Advanced Very High Resolution Radiometre (AVHRR) data collected in a period between April 1992 and March 1993.
History	The first version of the 1-km resolution global land cover characteristics data base was created by the U.S. Geological Survey's (USGS), the University of Nebraska-Lincoln (UNL) and the Joint Research Centre of the European Commission, and was completed and released to the public in November, 1997. An improved second version was ready in 1999.
Data available	Tables and images containing information about: Seasonal Land Cover Regions, Ecosystems, Land Cover, Biosphere, Atmosphere Transfer and Running Vegetation Life forms. The data are available on continental basis but also as a global dataset. The global dataset is 21,600 lines (rows) and 43,200 samples (columns). Data are provided as a raster image.
Data quality	Some of the data used for deriving this dataset is data from 1992 to 1993.
Data access	Online access from the USGS homepage [http://edc2.usgs.gov/glcc/] and from an ftp server [ftp edcftp.cr.usgs.gov]. Data from each continent is separately available.
Data used by	
Data used for	
Issues	Data are slightly out of date.
Links	http://edc2.usgs.gov/glcc/
Other notes	Image raster data are viewable in GIS software

Other:

Name	Digital Chart of the Word, DCW
Made by	Was developed by the Environmental Systems Research Institute, Inc. back in 1992
Description	DCW is a 1:1,000,000 scale geographic database containing information about • Populated places • Railroads • Roads • Land cover • Vegetation • Physiography • Utilities • Transportation structures • Drainage • Supplemental drainage • Hypsography • Supplemental hypsography

	• Ocean features • Aeronautical features • Cultural landmarks The data are divided into grids of size 5^{o} by 5^{o}, which gives 2,094 terrestrial grid cells.
History	From 1991 to 1993 DCW was produced by the National Imagery and Mapping Agency (NIMA) for the US Defence Mapping Agency (DMA)
Data available	Political data, Oceans data, Populated places, Railroads, Roads, Land cover, Vegetation, Physiography, Utilities, Transportation structures, Drainage, Supplemental drainage, Hypsography, Supplemental hypsography, Ocean features, Aeronautical features, Cultural landmarks and Data Quality
Data quality	
Data access	Online access from the GEO community web site [http://data.geocomm.com]. Can here download the datasets after crating a user account.
Data used by	SEDAC and The European Commission's Joint Research Centre and the World **B**ank
Data used for	Human footprint database and other databases [http://sedac.ciesin.columbia.edu/data.html] and global map of accessibility [http://bioval.jrc.ec.europa.eu/products/gam/sources.htm]
Issues	The data are quite old. It has not been updated since 1992. Can only download one small national dataset at a time ex dataset about roads in Afghanistan.
Links	http://www.lib.ncsu.edu/gis/dcw.html, http://en.wikipedia.org/wiki/Digital_Chart_of_the_World http://bobby.york.ac.uk/services/cserv/sw/gis/dcw.htm, http://www.lib.ncsu.edu/gis/dcw.html,
Other notes	

Name	Natural Disaster Hotspots: A Global Risk Analysis
Made by	Center for Hazards and Risk Research (CHRR) at Columbia University
Description	The database containing global gridded data about natural disaster hotspots for different types of disasters. Resolution: 2.5' by 2.5'. The data used for crating the disaster hotspot datasets comes from various sources such as the Advanced National Seismic System (ANSS) Earthquake Catalogue of actual earthquake events and the Emergency Events Database (EM-DAT).
History	
Data available	The data looks at the: • Hazard Frequency and/or Distribution • Hazard Mortality Risks and Distribution • Hazard Total Economic Loss Risk Deciles • Hazard Proportional Economic Loss Risk Deciles For following hazards: • Global Cyclone Hazard • Global Drought Hazard • Global Earthquake Hazard • Global Landslide Hazard • Global Volcano Hazard
Data quality	
Data access	Online downloadable from the Center for Hazards and Risk Research homepage.

Data used by	
Data used for	
Issues	
Links	http://www.ldeo.columbia.edu/chrr/research/hotspots/coredata.html
Other notes	This database might provide useful information about what areas regularly get hit by natural hazards such as hurricanes and earthquakes. These areas can be expected to be more resilient towards specific hazards than other, and some also have proper tested evacuation plans.

Name	PAGER: Global building inventory database
Made by	U.S. Geological Survey, USGS
Description	Global building stock database and their earthquake vulnerability
History	
Data available	Global building stock on a national level for 247 countries using 89 building type categories and their vulnerability to earthquakes (vulnerability code between 0 and 5, where 0 is low vulnerability (strong building stock) and 5 is high vulnerability (weak building stock)).
Data quality	The year data are found at varies from 1979 to 2007 and a PAGER rating of the data sources gives an indication of the quality.
Data access	Online as a PDF document
Data used by	USGS
Data used for	Earthquake Loss Assessment and Risk Management
Issues	Only national data not global gridded.
Links	http://pubs.usgs.gov/of/2008/1160/ http://pubs.usgs.gov/of/2008/1160/downloads/OF08-1160.pdf http://pubs.usgs.gov/of/2008/1160/downloads/PAGER_database/PAGER_database.pdf http://earthquake.usgs.gov/eqcenter/pager/prodandref/Jaiswal_Wald_(2008)_14WCEE_PAGER_Inventory.pdf http://earthquake.usgs.gov/eqcenter/pager/
Other notes	Prompt Assessment of Global Earthquakes for Response (PAGER) Vulnerability code: Region 1: Countries with few inherently lethal pre-code buildings. Region 3: Countries with poor engineered construction. Region 5: Countries where the building stock predominance of adobe and rubble masonry buildings. Region 2 and 4: intermediate regions

Name	EM-DAT
Made by	Centre for Research on the Epidemiology of Disasters (CRED)
Description	Global database containing data about medium and large scale disasters. At least one of following criteria's must be present: - more than 10 or more deaths - 100 or more people affected - a declaration of emergency

	- a call for international assistance
History	
Data available	Data about natural and technological disasters and their occurrences and effects / impact on affected countries. Data available from 1900 to 2008.
Data quality	Data are country level data. Public available data are updated every 3 months.
Data access	Online database search and access to trend graphs and global maps
Data used by	United Nations Development Programme, UNDP.
Data used for	Look at global vulnerability to 3 natural hazards (earthquakes, tropical cyclones and floods)
Issues	Some countries are not very open resulting in missing data.
Links	http://www.emdat.be/Database/terms.html
Other notes	

Name	Significant Earthquakes of the World
Made by	U.S. Geological Survey, USGS
Description	Global database containing data Earthquakes of magnitude 6.5 or greater or ones that caused fatalities, injuries or substantial damage
History	
Data available	Data from 1977 to 2010.
Data quality	
Data access	Online database
Data used by	
Data used for	
Issues	Some inconsistencies between data from EM-DAT and this database
Links	http://earthquake.usgs.gov/earthquakes/eqarchives/significant/
Other notes	Uncertainties about the actual number of e.g. fatalities. Use wording like “at least”, “some” and “several hundred”.

Name	Worldmapper
Made by	The university of Sheffield, University of Michigan, The Leverhulme trust and Geographical Association
Description	Global country information. A collection of world maps, where territories are re-sized on each map according to the subject of interest.
History	
Data available	Multiple map categories among other disaster, communication, transport, housing and resources
Data quality	Look at around 200 countries
Data access	Data available as maps and excel files downloadable from the Worldmapper homepage

Data used by	
Data used for	
Issues	Not all countries are described
Links	http://www.worldmapper.org/textindex/text_index.html
Other notes	

Name	The World Bank
Made by	The World Bank
Description	Global data describing each country
History	
Data available	The topics available is: agriculture and rural development, Aid Effectiveness, Economic Policy and external debt, Education, Environment, Financial Sector, Health, Infrastructure, Labour and social Protection, Poverty, Private sector, Public sector, Science and technology, Social development, Urban development
Data quality	Look at 209 countries
Data access	Data files available to download
Data used by	Worldmapper
Data used for	Worldmapper
Issues	Not all countries are described for all types of data
Links	http://data.worldbank.org/indicator
Other notes	

Name	Gridded bathymetry data (GEBCO)
Made by	British Oceanographic Data Centre
Description	Global gridded bathymetry data.
History	1 arc-minute data: Data initially released in 2003, but was updated in 2008 30 arc-second data: Data released in 2009
Data available	Resolution: 1 arc-minute grid and 30 arc-second grid
Data quality	
Data access	Online on http://www.gebco.net/data_and_products/gridded_bathymetry_data/
Data used by	
Data used for	
Issues	
Links	http://www.gebco.net/data_and_products/gridded_bathymetry_data/ and http://www.bodc.ac.uk/
Other notes	

Name	Emporis
Made by	Emporis, a real estate data mining company with headquarters in Frankfurt, Germany
Description	Data about and pictures of Buildings in Cities worldwide with focus on high rise buildings (35-100 metres tall) and skyscrapers (at least 100 metres tall)
History	
Data available	Buildings from 221 countries and territories
Data quality	
Data access	Online at http://www.emporis.com/en/wm/
Data used by	Michael Batty “The dynamics of skyscrapers” European Conference on Complex Systems 2009
Data used for	Ranking building height, city population, firm revenues, individual incomes,.. with focus on building scaling and allometry. Look at the development of cities.
Issues	Difficult to extract the data from the homepage. No coordinates. The use of numbers of floors as a height in some cases could potentially make the data difficult to use.
Links	http://www.emporis.com/en/wm/
Other notes	Data about structural material and usage is available.

Name	Travel time to major cities
Made by	The World Bank and the European Commission's Joint Research Centre
Description	A geographic projection of the estimated travel time to the nearest city of 50,000 or more people in year 2000.
History	
Data available	Free to download. Used the integer ESRI™ grid format with pixels representing the travel time in minutes. Also available as a poster.
Data quality	30’’ resolution, global map
Data access	http://bioval.jrc.ec.europa.eu/products/gam/download.htm
Data used by	
Data used for	
Issues	
Links	http://bioval.jrc.ec.europa.eu/products/gam/index.htm
Other notes	

Name	OneGeology
Made by	165 organisation from 117 different countries
Description	A dynamic geological survey map of the world
History	Launched in 2007.
Data available	
Data quality	

Data access	Online from http://portal.onegeology.org/
Data used by	
Data used for	
Issues	No consistency in naming of datasets and data available in the individual countries. Various languages used.
Links	http://www.onegeology.org/
Other notes	

Name	Global soil regions map
Made by	United States Department of Agriculture, Natural Resources Conservation Service
Description	Global map showing different soil regions across the world
History	First produced in 1997. Later revised in 2005.
Data available	Available to download in .jpg or binary raster format
Data quality	Data is rasterized on a 2 minute grid cell
Data access	http://soils.usda.gov/use/worldsoils/mapindex/order.html
Data used by	
Data used for	
Issues	
Links	
Other notes	

Appendix C

Prepare for coarse-scale evacuation simulation

This Appendix provides a guide in how to prepare for running coarse-scale evacuation simulations. It will provide list of what to do and what to remember before running the different preparation software developed in this project.

1) download OSM country data from example http://downloads.cloudmade.com and store these in the "..\ OSMDataPreparation\inputdata" folder and unzip the file.

2) Open the OSMDatapreparation program and change the country code (as given in the GRUMP data) and country name (as given in the OSM data) to the country investigated before running the program.

3) Open the OSM_capacity_and_flow_one program

- Check that speed limits exist for the country investigated. If not then add these to the code
- Download "UrbanRural" data from Cemdap for the country investigated and store this in the "..\OSM_capacity_and_flow_one \inputdata" folder
- Change the 3 digit country code
- Run the program

4) Open the CapacityAndFlowAnalysis program. Change the 3 digit country code. Check that the correct continent is choosen for the GRUMP population data. Run the program.

5) Load results from the "..\OSM_capacity_and_flow_one\outputdata" folder into MATLAB and find appropriate models:

6) Open the ImproveCapacityAndFlowMaps program. Change the country code. Add the models to the code. Run the program.

7) Open the CoarseScaleEvacuationModel program. Ensure that the needed country data is available. Ensure models and scenarios are added and available. Run scenario.

Note: the first 6 steps might only be used given that the country investigated has not previously been investigated.

Note: in some cases it has been found that the downloaded population data and urban/rural data from SEDAC for specific country are of different sizes. If that is the case a small program named “ChangeGridMapSize” and written in C++ is used to reduce the bigger grids dataset to the same size as the smaller dataset. This program loads in the two datasets, reduces the bigger datasets size to the same size as the smaller dataset and returns this new small dataset.

Appendix D

Terms and definition

Several terms such as risk and vulnerability have been mentioned in the previous sections and will also be used in later section without providing any clear definition and description of these terms. This section looks at the different definitions used for describing both natural and manmade hazards and the consequences.

D.1 Hazard

The hazard in this project is a NEO impact on the Earth. In (Blaikie et el. 1994) the term hazard is defined as:

"The extreme natural events which may affect different places single or in combination at different times."

This definition only looks at natural events and is missing out on risk caused by man and technology. This is included in the definition from (Cross 2001), where a hazard is

a *"variety of natural and technological phenomenon that have the potential to generate loss."*

This definition not only covers natural and technological events but also tells that what a hazard generates is loss. This could be loss of lives, loss of infrastructure and loss of income. It could also be damage that can be repaired such as a broken leg.

D.2 Likelihood

Likelihood is in this project a term that is used to describe various probabilities such as the probability that a NEO is going to impact with the Earth and for describing, in the event of an impact, the likelihood of impacting at a specific location and the likelihood that the NEO will reach the Earth creating a crater and not explode in the atmosphere. Two official definition found on (Reverso dictionary) are:

"1. The condition of being likely or probable; probability
2. Something that is probable"

D.3 Risk

The risk of an impact is often being used in close connection with the Torino and Palermo scales (NASA 2005c) (NASA 2005b). These scales look at the chance of an impact and the size of the impact. In (Kumpulainen 2006) risk is defined as:

The *"likelihood of a hazard event"*

This is a fairly simple definition and is related to whether the hazard will happen or not, and the probability of it happening. This type of risk can be refined to look at the risk of a specific area being affected by a NEO impact. A likewise simple definition comes from Mitchell (1999).

"The probability of experiencing an extreme natural event"

When looking at the possible damage to people, economy, infrastructure and property, risk is used to define the probability of loss. (Dilley et al. 2005) defines risk as:

"Risk of individual element losses can be stated as the probability of loss or as the proportion of elements that will be damaged or lost over time."

Whereas the definition from (Coburn et al. 1994) is as follows:

Risk is the *"expected losses from a given hazard to a given element of risk, over a specified future time period."*

The introduction of loss is in the previous two definitions very vague, but in the UNDP's definition of risk some examples of loss are included in the definition (United Nations Development Programme 2004):

"The probability of harmful consequences, or expected loss of lives, people injured, property, livelihood, economic activity disrupted (or environmental damage) resulting from interactions between natural or human induced hazards and vulnerable conditions."

This definition also takes into account *"vulnerable conditions"* which broadens the definition to look into vulnerability.

Risk is conventionally expressed by following equation:

$R = H \times V$

where R is the risk, H the Hazard and V the vulnerability according to (United Nations Development Programme 2004), (Kumpulainen 2006) and (Blaikie et al. 1994). (United Nations Development Programme 2004) has two other ways of how to express risk:

$R = PE \times V$

where PE is the physical exposure.

or

$R = H \times P \times V$

P is the population.

The physical exposure or hazard can be calculated when predicting the different physical effects from an impact. The different definitions of risk are very similar and throughout this thesis will risk be defined as in UNDP.

Another quite different type of risk that should be mentioned is Voluntary risk:

"Voluntary risk is People's acceptance of risk."

Voluntary risk could, for example, be daily activities such as driving a car. Involuntary risk is usually associated with the risk from natural disasters. There is generally a higher acceptance of risk posed from technological systems such as airplanes. The tolerance of voluntary risk is as much as 1000 times higher than that of involuntary risk (Coburn et al. 1994).

D.4 Exposure

Exposure is by Mitchell (1999) defined as:

"The degree to which human population are at risk"

The degree people are at risk will depend on the physical effects from the hazard experienced in different exposed areas. It also depends on building strength, shelter availability and disaster response.

D.5 Vulnerability

Vulnerability means "to experience harm during a crisis" (Dilley et al. 2001). Vulnerability provides knowledge about the affected area and how it will be affected in the event of a specific hazard. How many lives could be lost, how many could be injured, how many building and how much infrastructure would be damaged and to what degree.

Vulnerability is by (Coburn et al. 1994) defined as:

Vulnerability is the *"percentage of loss for a given hazard of specified intensity."*

And Mitchell (1999) defines it as:

"The potential for loss"

These definitions are both quite vague but it also means that they are applicable across various sciences such as social-, environmental- and computer science.

Another definition can be found on (OECDs glossary)

"Vulnerability is a measure of the extent to which a community, structure, service or geographical area is likely to be damaged or disrupted, on account of its nature or location, by the impact of a particular disaster hazard."

This definition is clearly directed towards social- and environmental sciences. It provides information about the different types of vulnerability such as structural vulnerability, human or social vulnerability, environmental vulnerability and economic vulnerability.

Social vulnerability describes the vulnerability of different groups of people (Cutter et al. 2003). This type of vulnerability can be described using information such as age, gender, race, health, income, type of dwelling, family structure and other social and economical factors. Social vulnerability is by (United Nations Development Programme 2004) defined as:

"A human condition or process resulting from physical, social, economic and environmental factors, which determine the likelihood and scale of damage from the impact of a given hazard."

In (Kumpulainen 2006) several definitions of vulnerability are mentioned. One definition is:

"The degree of fragility of a person, a group, a community or an area towards defined hazards"

where fragility is a measure of how easily something can be damaged. (Blaikie et al. 1994) defines vulnerability as:

"The characteristics of a person or group in terms of their capacity to anticipate, cope with, resist, and recover from the impact of a natural hazard."

But this definition sounds more like the definition of resilience and is a good example on how people use terms differently across different disciplines.

None of the above definitions have mentioned time although the time of year and time of day could influence the vulnerability.

The vulnerability definition that will be used throughout this project is inspired by the definition from (OECDs glossary) and is as follows:

Vulnerability is an objective measure of the effects and damage on people, infrastructure, building, economy and the environment due to a specific hazard at a given time.

D.6 Resilience

Resilience describes how well an area is able to cope with and recover from a specific natural hazard. Resilience is very similar to vulnerability, but it is also about how well prepared the society is. It can be used when looking at improving structures in an area that might be affected by a hazard. E.g. improve nuclear power plants, chemical factories, wooden buildings, bridges, dams and so on and how to improve infrastructure so that evacuation goes smoother (FEMA 2004). One of the earliest definitions of resilience was presented by (Holling 1973):

Resilience is *"a measure of persistence of systems and their ability to absorb change and disturbance and still maintain the same relationships between populations or state variables."*

The official OECD definition of resilience (OECDs glossary) is as follows:

"Resilience refers to the capacity of a natural system to recover from disturbance."

This definition only looks at a natural system. A broader definition that takes into account the social system would be appreciated. The definition of resilience from the UNDP does that and is as follows (United Nations Development Programme 2004):

"The capacity of a system, community or society to resist or to change in order that it may obtain an acceptable level in functioning and structure. This is determined by the degree by which the social system is capable of organizing itself, and the ability to increase its capacity for learning and adaption, including the capacity to recover from a disaster."

(The Infrastructure Security Partnership 2006) goes even further by both mentioning multi hazards and economy. The definition is:

"The capability to prevent or protect against significant multihazard threats and incidents, including terrorist attacks, and to expeditiously recover and reconstitute critical services with minimum damage to public safety and health, the economy, and national security."

Resilience is about how systems (natural-, social- and economic systems) are able to resist, adapt, prevent and protect against hazards and recover from hazards, and the definition used in this project will be:

Resilience is the ability for a system to resist, adapt, prevent and protect against hazards and recover from hazards.

D.7 Response

Response is the

"measures adopted by formal public and private institutions and adjustments adopted by private individuals" (Mitchell 1999)

Such measures could be training of emergency services and educating the public, detailed planned procedures and management of emergency services, cross collaboration between different services, active and passive mitigation and recovery.

D.8 Evacuability

Evacuability is used to describe the ability of evacuating an area at risk. The equation for it is (Shen 2005) as follows:

$$E = \frac{N}{TN} * 100\ \%$$

where E is the evacuability, N is the number of successful evacuees and TN the total number of occupants in the areas that is evacuated. This equation is does not take into account the time involved in an evacuation. Presenting the progress as a rate per hour could be one way to evaluate an evacuation model.

D.9 Mitigation

(Kumpulainen 2006) defines mitigation as:

A *"measure to reduce risk and/or its impact."*

Reducing the impact from a hazard can be done by reducing vulnerability by improving things like building structures. For many man-made hazards the risk can be

reduced. This can be done by improving safety measures, applying laws to protect people and the environment and by developing better techniques in order to obtain a sustainable and safer environment.

Another definition comes from (OECDs glossary). It says that mitigation is:

"Actions taken to reduce damage and loss."

In a NEO impact event both definition are valid. Reduce risk and/or its impact can be done by launching a deflection mission. Reduce damage and loss can be done by evacuating the people at risk and by reducing vulnerability by reinforcing structures, buildings and improving infrastructure.

The definition used in this project will be:

Mitigation is measures taken to reduce risk and/or its impact and to reduce damage and loss.

D.10 Coping

Coping is in (Blaikie et al. 1994) defined as:

"The manner in which people act within existing resources and range of expectation of a situation to achieve various ends."

The definition only looks at people, not at nature or economy and how these systems are able to overcome the difficulties caused by a hazard.

Appendix E

CEMEVAC: An Evacuation Travel Behaviour Micro-simulation Software

A new improved version of the Comprehensive Econometric Micro-Simulator for Daily Activity Travel Patterns (CEMDAP) originally, developed previously by Chandra R. Bhat, Jessica Y. Guo, Sivaramakrishnan Srinivasan, and Aruna Sivakumar at Department of Civil Engineering, University of Texas, was modified by the author of this thesis. The new version of this agent-based simulator is able to generate behavioural travel patterns for multiple days during an evacuation. New evacuation travel behaviour models were developed to describe the local population's travel behaviour during such an event (Chapter 5). The new addition to CEMDAP has been named Comprehensive Econometric Micro-Simulator for EVACuations (CEMEVAC). This simulator is capable of modelling the daily average travel behaviour as well as the travel behaviour during an evacuation for individuals and households. To update the travel times, that are expected to change from the daily average due to the evacuation being performed, TRANSIMS, a sophisticated traffic micro-simulator, was used to simulate the trips generated by CEMEVAC and provide new travel times that reflect the changes in traffic on the road-network.

CEMEVAC is capable of modelling the mixture of normal day-to-day travel behaviour along with the gradually increasing number of evacuees. This provides a more realistic description of the expected loads on the transport network and more realistic knowledge regarding number of expected evacuees and expected clearance time. CEMEVAC models evacuations due to approaching hazards, such as hurricanes and NEO impacts on the Earth. Both types of hazards can be tracked and a landfall/impact location and time can be predicted with some uncertainty.

New models to be used for modelling human decision-making and travel behaviour during an evacuation have been developed and are described in detail in Chapter 5. These models provide a way of simulating a realistic evacuation behaviour that reflects individual travel behaviour as well as household decisions made. The models for hurricane evacuation decision-making and travel behaviour were derived using travel behaviour data gathered from a range of evacuation surveys from the United States, where people had been interviewed regarding what they did during either one or more evacuations or what they are planning to do in the event of a evacuation due to an approaching hurricane. Based on these models more hypothetical models were derived for the modelling of people's travel behaviour during an evacuation due to an approaching NEO.

E.1 Introduction

This chapter describes the use of an agent-based micro-simulator, CEMDAP, to model the detailed travel behaviour of individuals and households in an area that is undergoing an evacuation.

The work described in this chapter is an expansion of the CEMDAP software combined with the TRANSIMS software. The expansion of the existing CEMDAP is able to model the behavioural travel patterns for individuals during a normal day along with the gradual change in travel behaviour during an evacuation. TRANSIMS is used to generate new travel times between locations during an evacuation.

The models developed describe the decision-making and the travel behaviour during an evacuation due to an approaching hurricane or NEO were developed by the PhD candidate at University of Wisconsin-Madison during a 3 month visit. Chapter 2 describes the survey data that the models are based on. The derived models are described in Chapter 5.

This chapter describes the software used for modelling and simulating the expected travel behaviour. General assumptions used in this agent-based micro-simulator for simulating evacuation are described in section E.2. Section E.3 describes the original CEMDAP software. Section E.4 describes the TRANSIMS software. In Section E.5

CEMEVAC, the new additions to CEMDAP, is described followed by a brief discussion regarding the new tool, the models and future work in section E.6. Section E.7 contains the conclusions.

E.2 Assumptions

The models describing the decision-making and the travel behaviour during an evacuation was developed based on survey data from primarily evacuations due to approaching hurricanes and NEOs. Several assumptions were made due to limited knowledge regarding the decision-making and limitations to the behavioural evacuation travel models that were derived.

1) The evacuation decision is only taken by adults in a household.
2) The likelihood that a woman decides to evacuate is higher than for men (odds 1.3).
3) If one adult in a household wants to evacuate and another wants to stay the decision is taken by flipping a coin.
4) Households evacuating prior to a warning are assumed to start evacuating between the watch time and the warning time.
5) All households that believe they hear a warning hear the same warning (not enough data were available to model the warning type heard).
6) Household outside the evacuation area is assumed only to have a probability of evacuating if they heard an evacuation notice.
7) All evacuation preparation is done at home. Not enough data were available to make detailed models regarding travel patterns during this period, but future surveys might fill this gap.
8) Households primarily evacuate together, but if the household size is larger than four persons and the household owns more than one car and more than one adult owns a drivers' license, more than one car is used to evacuate (wealth could also result in more cars being (Dow et al. 2002) but nor enough information is available to model this currently).

9) Households that do not evacuate are assumed to perform normal travel behaviour during the entire scenario duration. Not enough data were found to model potential preparations performed prior to the hazard's arrival, but future surveys could potentially fill this gap in knowledge.

The decision to evacuate can only be taken by adults. For each adult in a household the probability of evacuating is found and the decision whether to evacuate is derived by generating a random number between 0 and 1. If this random number is within the probability that the person wants to evacuate the person has decided to evacuate. If a household has more than one adult and some adults want to evacuate while others want to stay then a coin is flipped. This is done by generating a random number between 0 and 1. If the number is below 0.5 the household evacuates.

For each evacuating household it is determined if a household evacuates to its neighbourhood. If not then if it evacuates to its own parish. If not, then the household evacuates out of parish, so only two probability models are actually being used.

E.3 CEMDAP

CEMDAP is an activity-based travel demand simulator that was developed at the University of Texas at Austin, Department of Civil Engineering (Bhat et al. 2003). CEMDAP uses agents to simulate individuals and is capable of modelling the activity travel patterns of both workers and non-workers in a household on a micro-simulation level enabling it to forecast the response in transportation demand on a normal working day. It was designed to be very easy to use, enabling the user to make fast changes to existing behavioural travel models to reflect new areas where the travel behaviour is slightly different due to demographics, ethnic make-up and different proportions of age groups. CEMDAP has been used to simulate daily travel patterns for the entire population in the Dallas–Fort Worth area, in Texas (Bhat et al 2004). Work has also been done regarding repercussions of evacuation on a regional transportation network (Lin et al. 2009). The major limitations within CEMDAP are its ability only to simulate normal

travel patterns for one-day and its use of Level of Service (LoS) tables to describe the perceived travel time between each segment during a normal day. In Lin's (2009) work these tables were updated so that they reflected the new circumstances using VISTA, a Data Traffic Assignment (DTA) system from VIST Transport Group Inc.. A major issue in Lin's (2009) work is that the used scenarios only look at one-day evacuations and assumes that everyone evacuates. It also uses a set of "intuitive" rules to model the travel assignment. An evacuation of a major city or area will often take several days to evacuate and depending on the magnitude of the approaching hazard, the way official information is provided to the public and the public preparedness for such an event, different evacuation rates can be expected.

E.4 TRANSIMS

TRANSIMS is a micro-simulation transportation simulation and analysis tool. It was developed by Los Alamos National Laboratory in the 1990s and is based on a cellular automata micro-simulator. Today it is not only used for traffic simulations, but also for travel modelling and as an air quality analysis tool (Early deployment of TRANSIMS, 1999) (TIMS, 2010). TRANSIMS is only able to simulate 24 hours, but it does provide detailed traffic simulations on a given network, simulating each trip performed by the individuals in the area.

The evacuation clearance time and individual travel times depend on traffic demand and road capacity and when the demand exceeds the capacity the travel speed declines. By using TRANSIMS such bottlenecks can be spotted and new more realistic travel times can be simulated.

E.5 CEMEVAC

The new expansion to CEMDAP enables the software to model and simulate peoples travel behaviour during an evacuation. In the original CEMDAP three major limitations were found:

2) Its ability to model normal daily travel patterns
3) Its ability to model travel behaviour for a 24 hour period
4) Its use of LoS tables to describe the perceived travel time between two segments during a normal day

In order to model and simulate an evacuation four additions were added to the software, enabling it to handle such events:

1) Be able to handle multiple days
2) Handle different evacuation scenarios. These scenarios should contain data such as watch start time, warning start time, warning type, hazard type and hazard magnitude
3) Handle evacuation models that should be used to simulate whether a household evacuates or stays and people evacuation travel patterns during the evacuation preparation and the evacuation itself
4) Be able to update the LoS table so that they reflect the changes in traffic loads during the evacuation scenario.

E.5.1 Additions to CEMDAP

The new additions to CEMDAP were given the name CEMEVAC, illustrating that this part is a Comprehensive Econometric Micro-simulator for EVACuation. The original CEMDAP is working along with the new evacuation addition and both can be run separately in the CENDAP user interface. CEMEVAC uses the original CEMDAP software to model a person's travel behaviour on a normal day until the decision is taken to evacuate, then a new set of behavioural models are used to model the travel behaviours during evacuation preparation and evacuation. The main additions to CEMDAP were:

- the ability to model the travel behaviour for several days
- to read in and use an evacuation scenario
- to read in and use evacuation decision and travel models.

Figure E.1 illustrates the original CEMDAP class architecture along with the new evacuation classes marked in red. Six new classes were added to the existing software and are described in table E.1.

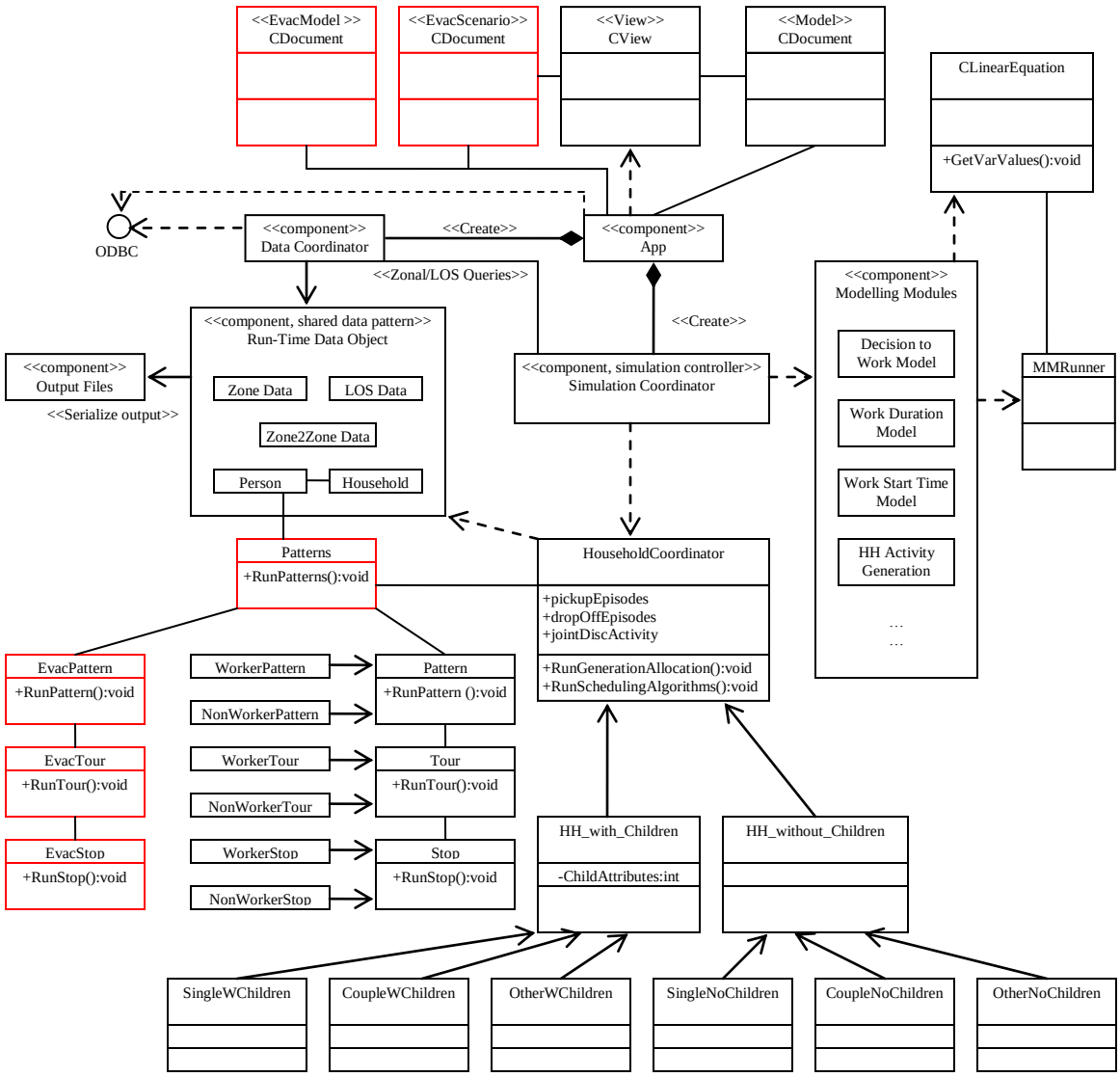

Figure E.1: Classes in CEMDAP and CEMEVAC additional classes shown in red

The six new classes enable the software to create several days with normal daily travel patterns as well as evacuation travel patterns for each individual in a household. In the event where a household decides to evacuate the given day where that decision is made is likely to have two patterns, one normal day pattern and one evacuation pattern. The remaining days only have one pattern per day.

New functions have also been added to the existing CEMDAP classes enabling them to handle multiple days and to run an evacuation scenario.

Table E.1 CEMEVAC classes

Class name	Description
EvacScenario	Used for reading in and storing an evacuation scenario
EvacModel	Used for reading in and storing evacuation models. It also runs the different evacuation decision and travel models
Patterns	Used for handling multiple patterns
EvacPattern	Used for handling evacuation patterns
EvacTrip	Used for handling evacuation preparation trips and the final evacuation trip
EvacStop	Handles evacuation preparation stops and the final evacuation stop

E.5.2 Run Evacuation

This section describes what happens when an evacuation scenario is run. The following pseudo code shows how the Run_evacuation function works

```
Run_evacuation()
{
read in normal CEMDAP input data (demographic- and zone data)
read in evacuation scenario
read in evacuation models
read in normal day travel models
go through each household
        model if a household hear an official warning or not
        model if a household evacuates or not
        if household evacuates
                derive start time of evacuation
                derive preparation duration
                derive preparation start time
                for each person in the household
                        derive normal travel patterns for the entire scenario until
                         evacuation preparation starts, then the person returns home if
                         not already at home
                        add evacuation travel pattern to the evacuation pattern
        else
                for each person in the household
```

derive normal travel patterns for the entire scenario duration

Store travel results. Data is stored in one file for each day in the scenario

}

It is important to note that people living outside the area where an evacuation has been issued could potentially also decide to evacuate. These evacuees are called shadow evacuees. These households add additional strain to the transportation network and could potentially delay the evacuation. Models have been derived to simulate these evacuees along with the normal evacuees.

E.5.3 Run TRANSIMS from CEMDAP

After running an evacuation scenario it is important to update the LOS tables to reflect more realistic travel times during the scenario. For that purpose TRANSIMS is used. TRANSIMS takes the tables describing the individual trips as an input together with a detailed description of the transportation network. Several iterative loops are run until equilibrium is achieved. This is necessary to provide new realistic travel times during the evacuation scenario. TRANSIMS can be run directly from the CEMDAP user interface using a batch file that starts the TRANSIMS python scripts. The updated LoS tables are used to modify the trip assignment times for the individual trips.

E.5.4 Scenario creator

The user interface in CEMDAP was expanded to accommodate the creation of evacuation scenarios and to enable the user to run these evacuation scenarios and TRANSIMS. Figure E.2 is a screenshot of the “Create Evacuation Scenario” window where the user can set watch start time, warning start time and the warning type. The watch is a period where a potential hazard is followed closely by the officials, but where it is still too early to start an evacuation due to the uncertainties regarding where the hazard might hit. During the watch it has been found that there are a small number of people who decide to evacuate. Warning is the official warning from the officials where

they inform that an evacuation has started. Two types of warning were found to be used by officials: voluntary and mandatory. A voluntary warning usually is used in areas that are believed to only experience a small part of the forces from the hazard. A mandatory warning is used in areas that must evacuate prior to the hazards' arrival. The hazard impact time is the time where all evacuees should have left the area at risk. Three evacuation strategies can be used. Free, controlled and mixed, where the free strategy is where people leave the area in their cars. The controlled evacuation strategy is one where people are evacuated using public transportation. No private cars are allowed. This strategy is used in Hampshire in the UK. The mixed strategy is where some evacuate using cars and other using public transportation. Only two hazard types can be chosen currently: hurricanes and NEO impacts, but future versions could also model, for example, tsunamis, volcanic eruptions and flooding.

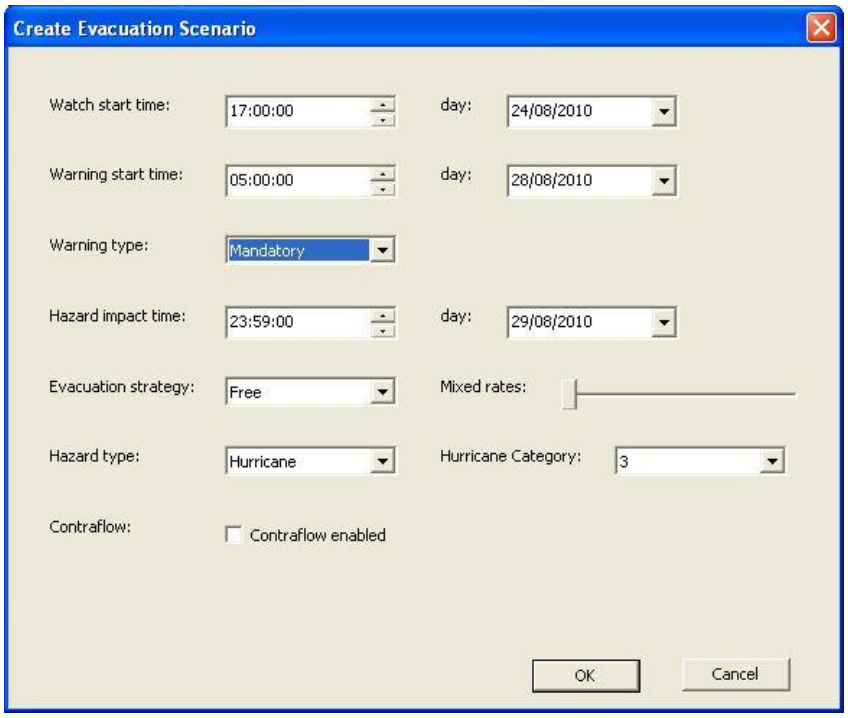

Figure E.2: Create Evacuation Scenario user interface

E.6 Discussion and future work

The new additions to CEMDAP enable the software to read in new evacuation decision and travel behaviour models, read in evacuation scenarios and simulate an

evacuation scenario. The flexibility from the original CEMDAP have been kept making it easy to change daily travel behaviour models and evacuation scenarios to reflect the cultural and domestic differences in travel behaviour across the world. A user interface that can be used for making and changing evacuation decision models and travel behaviour models still need to be made. These models are currently read in from a simple test file. Other useful future features are the ability to use public transportation during an evacuation and enable contra flow on some main roads in the area investigated.

The ability to capture the gradual change in travel behaviour provides a more realistic description of the evacuation and potential issues such as clearance time needed. The current limitation with CEMDAPs usage of LoS tables results in the necessity to use a micro-simulation transportation simulation tool like TRANSIMS to generate more realistic travel time tables. A new plug and play platform that can be used for short- and long-term travel/evacuation simulation and planning would be a major improvement to aim for in the future.

Several assumptions had to be taken due to limitations in the available evacuation decision and travel models. Improving these models using survey data that focus on the preparation and the decision-making would reduce the number of assumptions needed. The current model developed describes evacuation due to an approaching hurricane and a NEO impact. Future evacuation decision and evacuation travel models could describe the evacuation behaviour due to, for example, approaching tsunamis.

With the ability to model and simulate multiple days comes also the need for models that describe people's weekend travel behaviour. Such models could be derived from detailed travel behaviour surveys.

E.7 Conclusions

CEMEVAC is a novel new addition to the original CEMDAP software. CEMEVAC enables the user to quickly and easily change both models describing normal as well as evacuation travel behaviour and evacuation decision models as well as creating evacuation scenarios. This new improved software has the ability to simulate the gradual change in travel behaviour due to an approaching hazard and official evacuation notices,

providing a more realistic description of people's expected travel behaviour. By updating normal travel time tables using TRANSIMS enables potential transportation bottlenecks to be spotted and more realistic evacuation clearance times to be found. This information can, together with the uncertainty in landfall/impact location and the changes in this uncertainty over time, provide key knowledge about where and when an evacuation warning should be issued.

Appendix F

The Influence of Time of Day on Human Vulnerability during Earthquakes

This chapter investigates how the timing of an earthquake influences injury and fatality numbers, by analysing correlations between earthquake timing and human vulnerability. Investigations in this chapter include, whether earthquakes cause more fatalities at night than during the day, and how factors such as local building strength and earthquake magnitude should be taken into account when estimating casualties. Earthquake magnitude and the building strength in the affected area are taken into account when testing the basic hypotheses and this yields a complete and quantitative analysis.

F.1 Introduction

Being able to calculate casualty rates due to earthquakes is of great importance, especially in the aftermath of an earthquake where relief organizations and emergency services need to provide help, but also to provide evidence for policy improvement (e.g., improved building regulations). The time of day of an earthquake event can influence the vulnerability of a population and, if this effect is sufficiently large, it should be taken into account by models estimating casualty rates.

Intuitively, there might be compelling reasons why a correlation between human vulnerability and the time of day when a hazard occurs should exist. For example, more human activity occurs during daylight hours, when the majority of the population is awake. Individuals who are asleep when an earthquake occurs are likely to be slower getting out of bed and leaving a building than individuals who are awake. The time of day will also affect the whereabouts of people. It determines whether the majority of individuals are at home, at work (or in school), partaking in other functions (such as

shopping), or in transit. The day of week and time of year also holds information about individuals' weekend and holiday patterns. However, the building stock in many earthquake prone areas has improved greatly over the years with the introduction of tougher building regulations, so in some regions of the world the correlation between time of day and human vulnerability might be diminished or not exist.

In the early 1970s a correlation was found between the timing of an earthquake and human vulnerability (i.e. fatalities and casualties). Results from Lomnitz (1970) and Scawthorn et al. (1978) showed that if an earthquake occurred during the night, more casualties could be expected. This assumption is still used today when creating earthquake vulnerability models (Porter et al. 2007, Jaiswal et al. 2008, Wagner 1994, Hess et al. 2006) and mitigation plans (Ramirez 2005, Emergency Planning Consultants 2004).

Lomnitz (1970) and Scawthorn (1978) used historical datasets regarding earthquakes to investigate how foreshocks affected the number of casualties in Chilean earthquakes and how time of day affected earthquake casualties. Lomnitz (1970) used 22 historical earthquakes from Chile from 1570 to 1960, describing the number of casualties and the time of day when each earthquake occurred. A model was fitted to these data and it was found that time of day strongly affected the number of casualties in Chilean earthquakes, with more casualties occurring at night. It also showed that foreshocks lower the number of casualties. Scawthorn (1978) used historical earthquake events from the 20th century from across the globe. His figure 2 (Scawthorn et al. 1978), shows the total number of fatalities for all these historical events collected. This figure shows large fluctuations in the collected data making the fitting of a model difficult. The trend line fitted showed an average fluctuation of ±62% in fatality rate depending on the time of day. The quality of both of these historical earthquake datasets is of some concern due to their age, the lack of census data and appropriate reporting systems.

The ±62% fluctuation in fatality rate was used in the model developed by Porter et al. (2007).

Allen (2009) questioned the assumption that the time of day is of high importance when calculating the casualty number due to an earthquake. The results hint towards the

effect of time of day on the expected number of casualties: “earthquakes in the early morning may contribute more to the observed losses”, but the results were inconclusive.

Simmons et al. (2007) found that time of year influences the casualty numbers for tornado victims, where “off season” tornados resulted in more casualties. One possible explanation for this was the greater public awareness during the tornado season resulting in better response to warnings. Time of year can also have a large effect on the number of casualties due to secondary hazards that occur after a natural hazard. Many people died due to the cold weather conditions in the mountains during the winter month following the Pakistan earthquake in 2006. This was because many survivors of the earthquake had become homeless and lived in tents that were not suitable for the cold winter in the mountains (Rivers 2006). Another example, where the time of year influenced the number of casualties, was in the aftermath of the 2010 Haiti earthquake. Here an outbreak of cholera caused many additional fatalities during the rainy season due to the limited local health services available and damaged sanitation system (BBC 2010).

de Ville de Goyet et al. (2006) showed that the time of day along with the structural vulnerability of housing, factories and public buildings and the location of the victims within the buildings, were significant factors in determening the number of casualties to expect from some hazards, such as earthquakes. Age and gender were found to be significant factors affecting vulnerability for hazards such as tsunamis, where physical fitness can be important to avoid becoming a victim.

Taubenböck et al. (2008) used time of day along with remote sensing in their approach for estimating the geographical shift in population during the day in different types of build-up areas within a city. This shift can be of vital importance when estimating potential casualties due to a hazard such as an earthquake or tornado.

Other parameters that should be taken into account when modelling the number of casualties due to earthquakes are geological features and composition. Geological features can accelerate and de-accelerate the seismic waves. The depth at which the earthquake originates will be of high importance to the effects experienced on the Earth’s surface. The seismic waves which are created at the Earth’s surface in the event of a shallow earthquake cause most destruction (Cascadia 2009).

F.2 Data and Models

Data regarding natural and the manmade hazards has been gathered by the Center for Research on the Epidemiology of Disasters (CRED) and stored in the EM-DAT database since 1973 (Ward et al. 2011). Another source of data regarding earthquakes and their effects on the affected area is the Earthquake database provided by USGS.

F.2.1 Data

The historical earthquake data used for this analysis were collected from USGS earthquake database (USGS 2010) and the EM-DAT database at The International Disaster Database of the CRED (EM-DAT 2009).

Data in the EM-DAT database contain information about the country, date and year of the earthquake, number of fatalities and number of people affected, whereas the USGS data contain additional information such as the time of day, location of the earthquake epicentre in latitude and longitude, the seismic magnitude and, in many cases, a breakdown of casualties into fatalities, injuries as well as homeless estimates in text form. Wording such as: “at least 50 people injured/killed”, “124 missing“ and “several hundred injured” is used to describe these numbers, showing that there are some uncertainties regarding the actual number of fatalities and injuries.

The casualty estimates are usually provided by emergency aid organisations or officials from the countries affected. There is, however, the potential for under-reporting for countries where the emergency services are stretched or where no clear reporting system exists, and potential for error where there are large uncertainties regarding local demographics such as population numbers. There has, by the author of this chapter, been found to be some inconsistency between the two databases for quantities such as day of the event and number of fatalities.

An initial dataset of 95 historical earthquakes was collected from the USGS database ranging from 1980 to 2009. This dataset contains variables such as country, location, day and year, time of day described using the Coordinated Universal Time (UTC), seismic magnitude, number of fatalities and number of injured individuals. The

time of day was converted into local time without taking into account any local summer time. An additional dataset of 381 historical earthquake events was collected from the EM-DAT database, ranging from the 1970s to 2010. As the time of day was not available in EM-DAT the time of day for the event in question was found in the USGS database and converted into local time. Epicentre location and seismic magnitude were likewise found in the USGS database and used with the EM-DAT earthquake data.

The 95 USGS earthquakes were originally collected for the purpose of developing human vulnerability models that could provide estimates regarding expected number of casualties due to an earthquake. These models were used in NEOMiSS along with human vulnerability models for other natural hazards that could be expected in the event of a NEO land impact. The earthquakes were selected to give as broad a distribution of earthquake locations as possible along with a broad distribution of earthquake magnitudes. Earthquakes were also selected based on the criteria that they caused at least one casualty. The same criteria were used for the selection of earthquakes from EM-DAT. This set of data was collected with the sole purpose of being used for statistical analysis to determine whether people are more at risk if an earthquake occurs during the night than during the day. Earthquakes that generated tsunamis were not selected. These earthquakes should be analysed separately because the casualties during such events not only are casualties due to e.g. collapsing building and trees but some are due to e.g. drowning.

Additional data used in this research were the global gridded population data from SEDAC with a grid resolution of 2.5' (SEDAC 2010). These data are available for the years 1995, 2000, 2005, 2010 and 2015 and provides gridded information regarding the number of people living in each grid cell across the Earth and, therefore, the population density. From these data, population estimates were obtained for the individual regions affected by earthquakes for the particular year of the disaster. Building strength data from the USGS PAGER project (Porter et al. 2008) were used to distinguish between countries with different building strengths and building regulations. This dataset provides a measure of building strength in each country, presented as a number between one and five where one represents countries with a generally strong build stock and five represents countries with a weak building stock.

F.2.2 Models

Two different models were used. The first model used the seismic magnitude and earthquake models implemented in the NEOSim asteroid impact simulator (Morley 2005). This model derives the seismic shock magnitude as a function of distance from the earthquake epicentre. The second model used global gridded population data with a spatial resolution of 2.5' from SEDAC to calculate the population living in the affected area out to where the seismic magnitude is 4.0 on the Moment magnitude scale used by the USGS. For calculating the proportion of fatalities (P_F), injuries (P_I) and casualties (P_C) equation F.1 was used.

$$P_F = \frac{F}{A} \tag{F.1}$$

where F is the total number of fatalities, injuries or casualties depending on the proportion calculated and A is the total number of people living in the affected area.

F.3 Test Cases, Hypotheses and Definitions

This section introduces several definitions used in this chapter, and sets out the hypotheses to be tested regarding correlations between time of day of earthquake and human vulnerability and whether there are times during the day when earthquakes occur more often than at other times.

F.3.1 Day, Night and Working Hours Definitions

Describing when it is day and night is not straightforward. There are some unavoidable cultural issues along with the change between normal and summer time. On weekdays it can be assumed that school starts between 7 and 9 in the morning and most people work between 8 and 17 these assumption will off course depend on children's age, individual workers' professions and national/cultural variations in work patterns. Nevertheless, based on a number of cultural observations it was assumed that night is the time when most people are likely to sleep, which in most countries is between 23:00 and

9:00 while day includes the hours between 9:00 and 23:00. Within the day, the majority of the population was assumed to be at work or in school between 10:00 and 18:00.

The earthquake magnitude was separated into two categories (weak and strong earthquakes), where weak earthquakes have a seismic magnitude less than 6.0 on the Moment magnitude scale (M) used by the USGS and strong earthquakes have a seismic magnitude larger than or equal to 6.0. The Moment magnitude scale was originally designed to be consistent with the Richter scale, so the numerical values are approximately the same and textual descriptions regarding the earthquake effects at different magnitude earthquakes on the Richter scale can be used for defining when an earthquake is weak or strong. One could also use the already existing earthquake magnitude classes provided by the USGS (Great; M>=8, Major; 7<=M<7.9, Strong; 6<=M<6.9, Moderate; 5<=M<5.9, Light; 4<=M<4.9; Minor; 3<=M<3.9 and Micro; M<3), but this was found to lead to too many subgroups given the limited set of historical earthquake data used.

F.3.2 Test Cases and Hypotheses

The main hypothesis investigated in this chapter is whether earthquakes at night cause more casualties than earthquakes during the day. Additionally, the injury and fatality numbers during standard working hours were investigated. This will determine whether an individual's risk is greatest when in bed, at work/school or elsewhere when an earthquake occurs.

Multiple test cases were developed to analyse whether a correlation between time-of-day and number of fatalities, injuries or casualties exists:

1) Is there a difference between the proportions of casualties in the affected area depending on the time of day the earthquake occurred such as day versus night? The casualties should also be divided into fatalities and injuries and investigated individually.

2) Is there a difference between the proportion of casualties, fatalities and injured in the affected area depending on the time of day the earthquake occurred in areas with strong, intermediate and weak building stock?

3) Is there a difference between the proportion of casualties, fatalities and injured in the affected area depending on the time of day the earthquake occurred and the earthquake magnitude (strong versus weak earthquakes)?

4) Is there a difference between the proportion of casualties, fatalities and injured in the affected area depending on the time of day the earthquake occurred, the building strength in the affected area and the seismic magnitude?

One additional case was found based on the following question:

5) How does building strength influence the injury and fatality numbers overall?

These different cases were all investigated using the collected historical earthquake events along with the gridded data and national building strength data from PAGER and *t*-tests were performed on the data, investigating if any significant correlations existed.

F.4 Results

F.4.1 Day, Night and Working Hours

The first of the four experiments investigated the impact of time of day on the number of casualties, fatalities and injuries independent of seismic magnitude and building strength.

A statistical analysis was performed on the two historical sets of earthquake data from USGS and EM-DAT. Three different time intervals were selected, day, night and working hours, and tests were performed on each dataset: night versus day, day versus working hours and working hours versus night. For each of these three intervals, four different comparisons were made: (1) the proportion of fatalities (2) the proportion of injuries (3) the proportion of casualties (fatalities and injured) (4) the ratio of fatalities to injuries.

The overall results from these tests showed no significant difference between night-day, day-working hours and working hours and night for the USGS dataset, whereas a significant difference was observed for the EM-DAT dataset between fatalities

and the time of day. Figure F.1a presents the average proportion of fatalities with respect to the time of day for the EM-DAT data used. The red lines in the plot illustrate the boundaries between day-time and night-time hours. This plot shows much higher fatality rates during night-time hours than during day-time hours. Figure F.1b shows the proportion injured with respect to the time of day for the EM-DAT data. The number injured is larger from early evening to late morning. The number injured is a factor of 490 greater than for fatalities, so for each fatality approximately 490 injured can be expected.

The results show that the average fatality rate is 0.0000309 during the day-time, 0.0000408 during working hours and 0.000179 at night. This means that out of 100,000 people 3 people would die if an earthquake strikes during the day, whereas around 18 people would die for each 100,000 people if an earthquake strikes during the night. For the number of injured then 3 in 100 are on average expected to be injured during the day while 7 in 100 are expected during an earthquake at night. It means that more than twice as many people can be expected to be injured during a night-time earthquake than during a day-time earthquake and six times more fatalities can be expected for a night-time earthquake than for a day-time earthquake. These numbers are the average numbers irrespective of location and the magnitude of the earthquake. The numbers can be expected to be significantly higher in densely populated areas or for severe earthquakes.

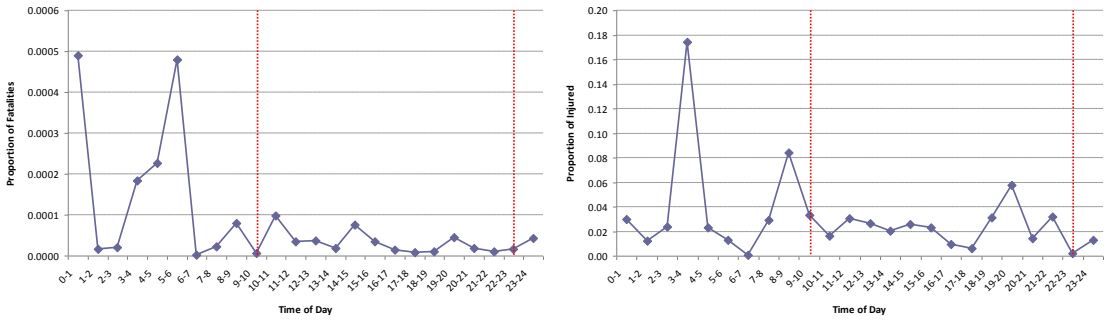

(a) (b)

Figure F.1: The average proportion of fatalities (a) and injured (b) out of the total number of people for all the historical earthquakes from EM-DAT in a 24 hour time interval.

This is a noticeable worsening compared to the equivalent number found in Porter et al. (2007), where the difference was 1.62. Similarly, there is a significant difference between the fatalities during working hours and at night, where there are 4.5 times more fatalities at night. There is also a difference between day and working hours, but not

sufficient to be statistically significant.

The results of the above tests showed that earthquakes at night lead to significantly more fatalities than during the day, but not for the number of injuries and casualties. Similarly, earthquakes that occur during working hours are statistically comparable to earthquakes that occur during the day (i.e. significantly fewer fatalities than during the night).

F.4.2 Day, Night and Working Hours - Building Strength

In the second experiment the national building strength was taken into account when answering whether people are more vulnerable if an earthquake strikes during the night than during the day, or during working hours. As for the previous experiment, for each of these three intervals, four different comparisons were made:

1. the proportion of fatalities (vulnerability)
2. the proportion of injuries
3. the proportion of casualties
4. the ratio of fatalities to injuries

For category 1 and 2 buildings there were no differences in the fatality, casualty or injury proportions between day, night and working hours. For buildings with building strength 3 and 4, there was a weak statistically significant difference in injury and casualty numbers between day and night and a significant difference in fatality numbers between day and night. In the USGS dataset, there was a significantly higher fatality rate in areas with a weak building stock during the night. This means that the risk of death or serious injury is greater at night than during the day or during working hours. Previous EM-DAT results showed that overall there are significantly more fatalities at night than during the day or during working hours. The following table F.1 shows the tendencies in the EM-DAT data when investigating areas with different building strength. It shows the average proportion of injured individuals and fatalities, by time of day, for the three different building strengths. Table F.1 shows the likelihood of becoming a fatality or

injured during the day, night and working hours for areas with a weak, intermediate and strong building stock.

Table F.1: EM-DAT, average proportion of fatalities and injured in areas with strong, intermediate and weak building strength and WH means Working Hours.

	Cat. 5 Buildings	Cat. 3+4 Buildings	Cat. 1+2 Buildings
Proportion of Fatalities (Night)	$1.90 \cdot 10^{-4}$	$1.72 \cdot 10^{-4}$	$1.18 \cdot 10^{-5}$
Proportion of Fatalities (Day)	$2.48 \cdot 10^{-5}$	$3.99 \cdot 10^{-5}$	$3.05 \cdot 10^{-6}$
Proportion of Fatalities (WH)	$2.95 \cdot 10^{-5}$	$5.62 \cdot 10^{-5}$	$3.72 \cdot 10^{-6}$
Proportion of Fatalities (All day)	$9.58 \cdot 10^{-5}$	$9.60 \cdot 10^{-5}$	$6.89 \cdot 10^{-6}$
Proportion of Injured (Night)	$5.61 \cdot 10^{-2}$	$8.23 \cdot 10^{-2}$	$1.30 \cdot 10^{-3}$
Proportion of Injured (Day)	$6.99 \cdot 10^{-2}$	$1.56 \cdot 10^{-2}$	$1.01 \cdot 10^{-3}$
Proportion of Injured (WH)	$3.19 \cdot 10^{-2}$	$1.80 \cdot 10^{-2}$	$3.72 \cdot 10^{-3}$
Proportion of Injured (All day)	$6.40 \cdot 10^{-2}$	$4.37 \cdot 10^{-2}$	$1.14 \cdot 10^{-3}$

The probability of becoming injured during a night-time earthquake is much larger in areas with a weak building stock than in areas with an intermediate and strong building stock as mentioned previously. The probabilities for weak and intermediate buildings are, however, not particularly large in some cases. For example, the probability of becoming a fatality in areas with weak buildings during the day is slightly lower than the probability of becoming a fatality in areas with intermediate buildings during the day or during working hours. This is not the case during the night where more people can be expected to become fatalities in areas with a weak building stock than in areas with an intermediate building stock. This could be due to the way the three building strengths are defined. Table F.1 also shows that by building strong buildings the probability of becoming a fatality during an earthquake reduces by a factor of 14 compared to areas with weak or intermediate buildings while the numbers of injured individuals reduces by a factor of 56 when improving the local building strength from weak to strong buildings and slightly less when improving from intermediate to strong buildings.

Table F.1 shows the probability of becoming injured in the specified time periods: day, night, working hours and all day. When looking in more detail, for example, at the probability of becoming a fatality or injured on an hourly basis, the results show large variations. This is mainly due to the limited number of historical events being analysed. There are, however, also trends which were observed already in table F.1. Figure F.2a

shows the average proportion of fatalities for areas with strong, intermediate and weak building strength for the collected EM-DAT data for each hour over a 24 hour period, whereas figure F.2b illustrates the average proportion injured for areas with strong, intermediate and weak building strength for the collected EM-DAT data for each hour over a 24 hour period. There are several time intervals with no data for areas with a strong building stock. This is due to the limited number of historical cases. For areas with a strong building stock the plot in figure F.2a does not show any significant changes in the average proportion of fatalities during each hour. In areas with an intermediate building stock is an apparent increase in proportion of fatalities in the morning hours, but statistically there is no significant difference in fatality numbers between day and night. Finally, for areas with a weak building stock the plot shows clearly a significant increase in fatalities during the night. This was also identified statistically. In figure F.2b areas with a strong building stock do not show any significant changes in the average proportion injured during each hour, while for intermediate building stock there seem to be significant changes in the average proportion injured during the night compared to during the day. For areas with a weak building stock there is a significant increase in the proportion injured from early evening to late morning.

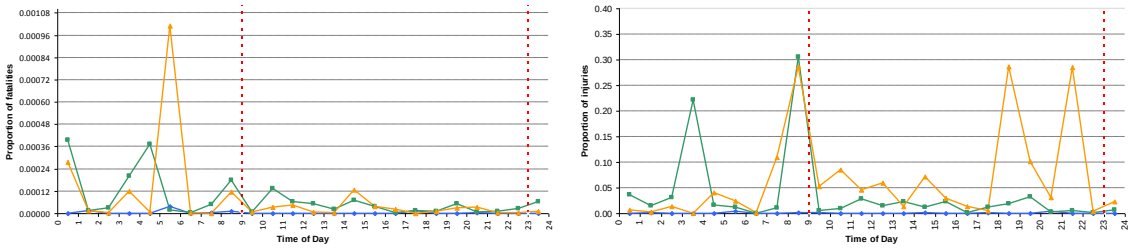

(a) (b)

Figure F.2: The average proportion of fatalities (a) and injured (b) out of the total number of people in the affected area for areas with strong (blue line), intermediate (green line) and weak (yellow line) building strength.

The outcome of this case study shows that there are significantly more fatalities in areas with a weak building stock than in areas with intermediate and strong building stock. People living in areas with a weak building stock are also much more likely to become casualties if an earthquake strikes during the night than during the day. This is not the case for people living in areas with a strong and intermediate building stock.

F.4.3 Day, Night and Working Hours – Seismic Magnitude

In this set of experiments the seismic magnitude was taken into account to determine whether people are worse off if the earthquake is of a strong or a weak seismic magnitude and occurs during the day, night or working hours. The seismic magnitude is measured as a number between one and ten on the Moment magnitude scale. This is a logarithmic scale, where one can barely be measured with seismographs and ten is a massive earthquake that would cause widespread devastation across a very large area. It was decided based on the textual descriptions regarding the damage due to earthquakes of different magnitudes, that weak earthquakes are earthquakes that can cause minor damage and up to more moderate sized earthquakes that can cause major damage to poorly constructed buildings over small regions. These weak earthquakes were defined to have a seismic magnitude of less than six on the Moment magnitude scale. Strong earthquakes were assumed to have a magnitude greater than or equal to six.

This experiment showed that for weak earthquakes there was no significant correlation between fatalities, casualties, and injured and the time of day that the earthquake occurs, except for the proportion injured in the day versus the night. For weak earthquakes people are slightly more likely to become injured if the earthquake happens during the night than during the day. For strong earthquakes the results are largely the same, but there is a weak correlation between fatalities and the time of day. People are 7 times more likely to become a fatality if a strong earthquake occurs during the night compared to during the day.

Table F.2 shows the proportion injured and proportion of fatalities, by time of day, for the two groups of seismic magnitude defined earlier. This table shows that the probability of becoming a fatality is almost three times bigger during strong earthquakes than during weak earthquakes while the probability of becoming injured is 4.5 times higher during weak earthquakes than during strong earthquakes. The probability of becoming a fatality during the night compared to during the day for strong earthquakes is around seven times bigger and the probability of becoming injured during the night compared to during the day for weak earthquakes is around three times bigger. By illustrating the events on an hourly basis throughout the day the same trends as observed

using the *t*-test and in table F.2 can be observed although there are large fluctuations due to the limited number of historical events.

Table F.2: EM-DAT, proportion of fatalities and injured for strong and weak earthquakes, WH means Working Hours.

	Strong Earthquakes	Weak Earthquakes
Proportion of Fatalities (Night)	$2.43 \cdot 10^{-4}$	$6.20 \cdot 10^{-5}$
Proportion of Fatalities (Day)	$3.40 \cdot 10^{-5}$	$3.07 \cdot 10^{-5}$
Proportion of Fatalities (WH)	$4.42 \cdot 10^{-5}$	$3.67 \cdot 10^{-5}$
Proportion of Fatalities (All day)	$1.10 \cdot 10^{-4}$	$4.03 \cdot 10^{-5}$
Proportion of Injured (Night)	$1.78 \cdot 10^{-2}$	0.16
Proportion of Injured (Day)	$1.59 \cdot 10^{-2}$	$4.70 \cdot 10^{-2}$
Proportion of Injured (WH)	$1.55 \cdot 10^{-2}$	$4.79 \cdot 10^{-2}$
Proportion of Injured (All day)	$1.65 \cdot 10^{-2}$	$7.50 \cdot 10^{-2}$

Figure F.3a illustrates the proportion of fatalities for earthquakes with a weak seismic magnitude (light blue) and strong seismic magnitude (dark blue) for the collected EM-DAT data for each hour over a 24 hour period. Figure F.3b illustrates the proportion injured for earthquakes with a weak seismic magnitude and strong seismic magnitude. The plot in figure F.3a shows much higher fatality rates during the night than during the day especially for strong magnitude earthquakes. In figure F.3b the proportion injured during the night is likewise higher than during the day for weak earthquakes.

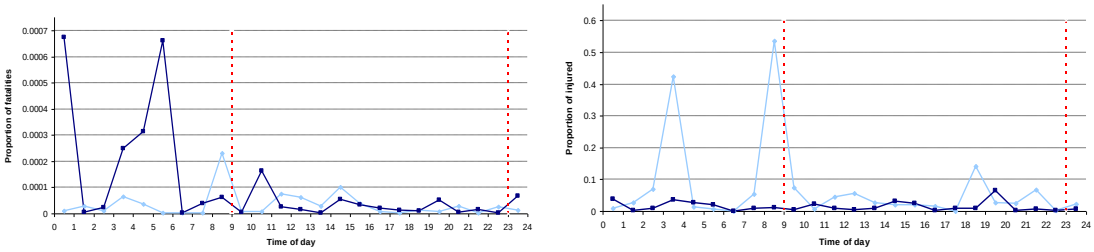

(a) (b)

Figure F.3: The average proportion of fatalities (a) an injured (b) out of the total number of people in the affected area for strong seismic magnitude earthquakes (dark blue line) and weak seismic magnitude earthquakes (pale blue line).

The results were found to be significant for the EM-DAT historical events only, not for the USGS historical events.

F.4.4 Day, Night and Working Hours – Seismic Magnitude and Building Strength

This final test investigates how the proportion of casualties, fatalities and injuries depends on the time of day of the earthquake, building strength and seismic magnitude. The same type of statistical analysis as used in the previous tests was used for these tests and table F.3 summarises the main results from this analysis both regarding casualties, fatalities, injuries and the fatality to injury ratio. It is important to note that the number of weak historical earthquakes in areas with a strong building strength is only eight; two during the day, five during the night and one during working hours. This makes it impossible to make any *t*-test between day and working hours and night and working hours. This lack of events highlights how weaker earthquakes rarely cause any casualties in areas with a strong building stock. The statistical results between day and night showed no significant correlation between day and night for weak earthquakes in areas with a strong building stock, but more historical events should be collected before any final conclusions can be provided. For strong earthquakes in areas with a strong building stock there was likewise no significant correlation. For weak earthquakes in areas with an intermediate building strength, the results show that a greater proportion of fatalities and injured can be expected during the night than during the day or work hours. For strong earthquakes in areas with an intermediate building stock the number of fatalities is likely to be larger if the earthquake occurs during the night compared to during the day and work hours. Finally, for weak earthquakes in areas with a weak building stock and strong earthquakes in areas with a weak building stock more injuries can be expected at night from earthquakes. In areas with weak building stock significantly more fatalities can be expected during a strong night-time earthquake. Table F.3 shows the likelihood of becoming a fatality or injured during the day, night and working hours for areas with a weak, intermediate and strong building stock and for weak and strong earthquakes. For strong earthquakes the probability of becoming a fatality or becoming injured in areas with a strong building strength is less than for areas with a weak building strength as was also found in test case 2. For weaker earthquakes this is mostly the case too: the data do, however, show that that the probability of becoming a fatality in areas with an intermediate building strength is larger than for areas with a strong or weak building

strength. This can, however, be due to statistical uncertainties. Once again the hourly probability of becoming a fatality or becoming injured was investigated down to an hourly basis, see figure F.4.

Table F.3: EM-DAT, average proportion of fatalities and injured in areas with strong, intermediate and weak building strength and for strong an weak earthquakes, WH means Working Hours.

	S E & S BS	S E & I BS	S E & W BS	W E & S BS	W E & I BS	W E & W BS
Proportion of Fatalities (Night)	$1.55 \cdot 10^{-5}$	$2.29 \cdot 10^{-4}$	$2.90 \cdot 10^{-4}$	$5.23 \cdot 10^{-6}$	$1.15 \cdot 10^{-4}$	$9.68 \cdot 10^{-6}$
Proportion of Fatalities (Day)	$3.07 \cdot 10^{-6}$	$3.95 \cdot 10^{-5}$	$3.61 \cdot 10^{-5}$	$2.89 \cdot 10^{-6}$	$4.06 \cdot 10^{-5}$	$1.54 \cdot 10^{-5}$
Proportion of Fatalities (WH)	$4.02 \cdot 10^{-6}$	$5.18 \cdot 10^{-5}$	$3.97 \cdot 10^{-5}$	$1.12 \cdot 10^{-7}$	$5.96 \cdot 10^{-5}$	$1.07 \cdot 10^{-5}$
Proportion of Fatalities (All day)	$7.54 \cdot 10^{-6}$	$1.28 \cdot 10^{-4}$	$1.67 \cdot 10^{-4}$	$4.57 \cdot 10^{-6}$	$6.61 \cdot 10^{-5}$	$1.35 \cdot 10^{-5}$
Proportion of Injured (Night)	$1.50 \cdot 10^{-3}$	$1.90 \cdot 10^{-2}$	$2.06 \cdot 10^{-2}$	$9.45 \cdot 10^{-4}$	0.25	0.12
Proportion of Injured (Day)	$6.02 \cdot 10^{-4}$	$1.32 \cdot 10^{-2}$	$3.44 \cdot 10^{-2}$	$4.27 \cdot 10^{-3}$	$1.94 \cdot 10^{-2}$	$9.92 \cdot 10^{-2}$
Proportion of Injured (WH)	$7.19 \cdot 10^{-4}$	$1.47 \cdot 10^{-2}$	$2.57 \cdot 10^{-2}$	$2.85 \cdot 10^{-5}$	$2.20 \cdot 10^{-2}$	$4.57 \cdot 10^{-2}$
Proportion of Injured (All day)	$9.27 \cdot 10^{-4}$	$1.59 \cdot 10^{-2}$	$2.73 \cdot 10^{-2}$	$1.89 \cdot 10^{-3}$	$9.64 \cdot 10^{-2}$	0.11

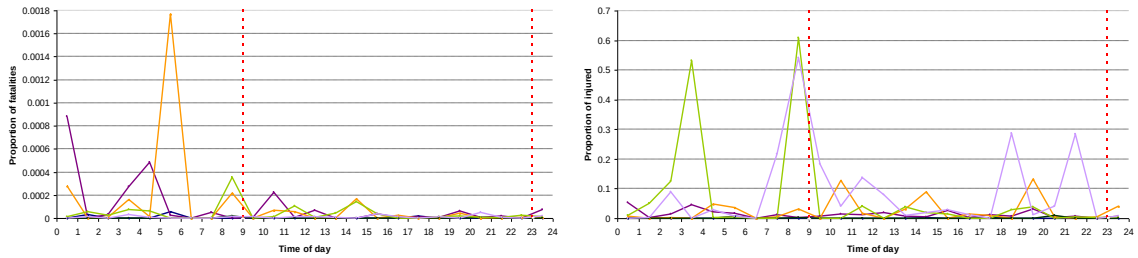

(a) (b)

Figure F.4: The average proportion of fatalities (a) and injured (b) out of the total number of people in the affected area for strong seismic magnitude earthquakes and strong building strength (dark blue line), strong seismic magnitude earthquakes and intermediate building strength (purple line), strong seismic magnitude earthquakes and weak building strength (orange), weak seismic magnitude earthquakes and strong building strength (dark green), weak seismic magnitude earthquakes and intermediate building strength (light green) and weak seismic magnitude earthquakes and weak building strength (pale purple line).

Figure F.4a shows that areas with a weak building strength have many more fatalities if the earthquake is strong and happens during the night compared to a weaker earthquake during the night. This is the same for areas with intermediate buildings. The results also reflect that stronger buildings protect better and that for weak and intermediate buildings people are more likely to become fatalities or injured during a night-time earthquake than during a day-time earthquake.

Another interesting observation from the EM-DAT dataset is that a casualty is more than twice as likely to become a fatality in a strong building, than in a weak building. This is intuitively not a surprise given that stronger buildings are generally built using stronger and heavier materials than, for example, huts and clay buildings. This means that generally during an earthquake it is safer to be in a strong building. If, though, the strong building should collapse then those people located in the building are more likely to become casualties, and especially fatalities, than if they were in a weaker building that collapsed.

F.5 Discussion

Results, based on historical earthquake data, show that there is a correlation between fatality and injury rates and the time of day when an earthquake happens, with more casualties during night time earthquakes, but building strength is a factor. It was shown that the time of day only influences the number of casualties in areas with a weak building stock. These results show that it is worthwhile strengthening building regulations and improving local building stock in areas where earthquakes occur on a regular basis. It was also found that people are more likely to become fatalities in areas with strong building stock than being injured. This is believed to be due to the stronger and heavier building materials used to achieve the higher building standards. The probability of becoming a fatality is though overall much lower than for becoming injured.

The results showed that stronger earthquakes produce more fatalities than weaker earthquakes if the earthquake occurs during the night. This result was expected since stronger earthquakes can be expected to cause more buildings to completely collapse. Weaker earthquakes produce a greater proportion injured than stronger earthquakes if the earthquake happens during the night. When investigating any possible correlation between time of day and both building strength and earthquake magnitude the results revealed once again that building strength matters. The effect of earthquake magnitude is reflected in the proportion of fatalities and injured: weaker earthquakes cause more

injured and stronger earthquakes cause more fatalities in areas with intermediate and weak building strength given that the earthquake occurs during the night.

The earthquake vulnerability models used in HAZUS are believed to be based on the work done by Porter et al. (2007), whose models assume a ±62% fluctuation in fatality rate depending on the time of day.

This study showed that when modelling fatality and injury numbers for earthquakes it is important to take into account the building strength and the seismic magnitude along with the correlations that exist between the time of the day when an earthquake occurs in areas with an intermediate and weak building stock. Other factors that could be taken into account when creating the models is the depth at which an earthquake occurs, local geological features, and cascading natural hazards that occur because of the earthquake, such as landslides and tsunamis. The models should ideally also take into account secondary and tertiary hazards such as fires due to bursting gas pipes and epidemics such as cholera due to an overstretched health care system and a broken down infrastructure.

F.6 Summary

This chapter examined two historical earthquake datasets collected from the: USGS and EM-DAT databases dating between 1970 and 2010. An earthquake simulator developed at the University of Southampton as a part of the NEOSim tool was used to identify the number of people living within the individual areas affected by earthquakes out to a seismic magnitude of four. The proportion of casualties, injured and fatalities was estimated and four test cases were identified and tested using the statistical *t*-test. The first of these test cases examined whether there is a temporal correlation between the time of day of an earthquake and the number of casualties, injured and fatalities and if earthquakes are more likely to happen during particular times of the day. In test case two the local building strength was taken into account along with the time of day while in test case three the effect of seismic magnitude an the time of day was investigated. The final test case investigated whether both the local building strength and the seismic magnitude

have an influence on the correlation between time of day and casualty, injury and fatality rates.

Overall, a correlation between time of day and the number of casualties, injured and fatalities was found. During the night, people are more likely to become injured or become fatalities. When taking into account the building strength people were only at greater risk at night in areas with a weak building strength, implying that it is worthwhile investing in stronger buildings and tougher building regulations. The third test case showed that stronger magnitude earthquakes cause more fatalities during the night than weaker earthquakes, which is also intuitively correct since stronger earthquakes are more likely to cause more buildings to collapse than weaker earthquakes which cause damage to buildings and only a few totally collapse.

In the fourth test case the importance of building strength was once again highlighted along with the higher risk of becoming a fatality or casualty due to earthquakes occurring during the night in areas with intermediate and weak building strength.

An additional test case wes identified, which investigated whether more earthquakes occur during the night or early morning hours than during the day and whether there is a correlation between building strength and the number of fatalities and injuries. The test showed that there are significantly more strong earthquakes occurring between 0 and 7 a.m. compared with the rest of the day, especially between 4 and 5 a.m., but this is only for strong earthquakes not for weak earthquakes or earthquakes overall.

There are several other factors that could be investigated regarding possible correlations between earthquakes and human casualties and damage to increase the accuracy of earthquake vulnerability models. This could, for example, be earthquake depth and additional natural hazards such as the tsunamis and landslides.

List of References

6Cs Congestion Management (2008) Traffic Congestion Data Survey Results, http://www.ecotownforleicestershire.coop/assets/pdf/6Cs%20Traffic%20Congestion%20Survey%20Results.pdf or http://www.melton.gov.uk/pdf/6cs_congestion_management_study_summary_report.pdf

Adams, M. N., Field, M., Gelenbe, E., Hand, D. J., Jennings, N. R., Leslie, D. S., Nicholson, D., Ramchurn, S. D., Roberts, S. J., Rogers, A. (2008) The ALADDIN project: Intelligent Agents for Disaster Management: http://www.aladdinproject.org/publications/RISE08.pdf

AIAA (2007) PLANETARY DEFENSE CONFERENCE WHITE PAPER: SUMMARY AND RECOMMENDATIONS http://impact.arc.nasa.gov/news_detail.cfm?ID=173

Alabama (1996) ALABAMA HURRICANE EVACUATION STUDY TECHNICAL DATA REPORT: BEHAVIORAL ANALYSIS

alcula (2015) Statistics Calculator: http://www.alcula.com/calculators/statistics/correlation-coefficient/

Allen T. I., Wald D. J., Earle P. S., Marano K. D., Hotovec A. J., Lin K., Hearne M. G. (2009) An Atlas of ShakeMaps and population exposure catalog for earthquake loss modelling, Bill Earthquake Eng 7:701-718 DOI 10.1007/s10518-009-9120-y

Armitage, A. (1962) William Herschel. Thomas Nelson and Sons Ltd

ASCE (2010) Minimum design loads for buildings and other structures, American Society of Civil Engineers: Structural Engineering Institute, http://www.ce.udel.edu/courses/CIEG407/ASCE003c04_p09-14.pdf

Atkinson, H. et al. (2000) Report of the Task Force on potentially hazardous Near Earth Objects: http://spacecentre.co.uk/__spaw/uploads/files/neo_report.pdf

AZT1 http://ec.europa.eu/environment/impel/pdf/lessons_learnt_en.pdf

AZT2 http://www.orbin.nl/papers/AIChE2008.pdf

AZT3 http://www.aristatek.com/newsletter/0709September/TechSpeak.pdf

Bailey, N. J., Swinerd, G. G., Crowther, R. C. (2007) A Tool for Assessing the Consequences for Populations and Infrastructure resulting from an Asteroid Impact. 2007 Planetary Defense Conference: Protecting Earth from Asteroids

Bailey, N. (2009) NEOIMPACTOR – A TOOL FOR ASSESSING EARTH'S VULNERABILITY TO THE NEO IMPACT HAZARD. PhD thesis, University of Southampton

Balk, D. L. et al. (2005) Determining Global Population Distribution: Methods, Applications and Data. Advances in Parasitology, Volume 62

Baker, E. J. (1991) Hurricane Evacuation Behavior, International Journal of Mass Emergencies and Disasters, August 1991, Vol. 9, No. 2, pp. 287-310

Baker, E. J. (1995a) Alabama Hurricane Evacuation Study Technical Data Report, Behavioral analysis, http://chps.sam.usace.army.mil/USHESdata/Behave_Start_Frame.htm

Baker E. J. (1995b) Public Response to Hurricane Probability Forecasts, Professional Geographer, 47 (2) 1995, pages 137-147

Baker E. J. (1997) Hurricanes Bertha and Fran in North and South Carolina: Evacuation Behavior and Attitudes Towards Mitigation, http://www.csc.noaa.gov/hes/docs/general_info/Location%20Specific/HURRICANES%20BERTHA%20AND%20FRAN%20IN%20NORTH%20AND%20SOUTH%20CAROLINA%20EVACUATION%20BEHAVIOR%20AND%20ATTITUDES%20TOWARD%20MITIGATION.pdf

Baker et al. (2006) Hurricane Evacuation Behavioral Survey and Analysis for the Marryland Western Shore, http://www.nab.usace.army.mil/HES/Draft_HES-B&A.pdf

Bali http://en.wikipedia.org/wiki/2002_Bali_bombings

Bateman et al. (2002) Gender and evacuation: A closer look at why women are more likely to evacuate for hurricanes, Natural Hazards Review, August 2002, pp. 107-117

Batty, M. (1994) Fractal Cities, ISBN 0-12-455570-5

Batty, M. (2005) Cities and Complexity, ISBN 0-262-02583-3

BBC (2010) Cholera death toll jumps in Haiti, http://www.bbc.co.uk/news/world-latin-america-11616535 accessed October 2010

BBC EarthNews (2010) Toads can 'predict earthquakes' and seismic activity, http://news.bbc.co.uk/earth/hi/earth_news/newsid_8593000/8593396.stm

Beirut http://en.wikinews.org/wiki/Large_explosion_in_Beirut_kills_many_including_former_prime_minister

Ben-Menahem, A. (1975) SOURCE PARAMETERS OF THE SIBERIAN EXPLOSION OF JUNE 30, 1908, FROM ANALYSIS AND SYNTHESIS OF SEISMIC SIGNALS AT FOUR STATIONS. Phys. Earth Planet. I nter., 11, 1-35.

Bernardi, F., Boattini, A., Abramo, G.. D., Di Paola, A., Masi, G., Valsecchi, G. B. (2002) The Campo Imperatore Near Earth Objects Survey (CINEOS), Proceedings of Asteroids, Comets, Meteors - ACM 2002. International Conference, 29 July - 2 August 2002, Berlin, Germany. Ed. Barbara Warmbein. ESA SP-500. Noordwijk, Netherlands: ESA Publications Division, ISBN 92-9092-810-7, 2002, p. 801 - 804

Blaikie, P., Cannon, T., Davis, I., Wisner, B. (1994) At Risk natural hazards, peoples vulnerability and disasters: ISBN 0-415-08476-8, Routledge

Blair, B. R. (2003) Decision Model for Potential Asteroid Impacts. Research Paper EB560, Decision Analysis, Division of Economics and Business, Colorado School of Mines.

Bond A., Hempsell M. (2008) A Sumerian Observation of the Köfels' Impact Event; Alcuin Academics, ISBN 1904623646

Bootke, W. F., Melosh, H. J. (1996) Binary Asteroids and the Formation of Doublet Craters. Icarus 124, 372-391

Boslough, M. B. E., Crawford, D. A. (2008) Low-altitude airbursts and the impact threat: International Journal of Impact Engineering, 35, 1441-1448

Boulougouris, E., K., Papanikolaou, A. (2002) Modelling and Simulation of the Evacuation Process of Passenger Ships: http://www.naval.ntua.gr/~sdl/Publications/Proceedings/IMAM2002_Proceed57.pdf

Bourque, L. B., Shoaf, K. I., Nguyen, L. H. (1997) Survey Research, International Journal of Mass Emergencies and Disasters, Vol. 15, No. 1, pp. 71-101

Bowell, E., Koehn, B., Skiff, B. (2011) The Lowell Observatory Near-Earth-Object Search (LONEOS): Ten years of asteroid and comet discovery, Astronomical Review, http://astroreview.com/issue/2012/article/the-lowell-observatory-near-earth-object-search-loneos-ten-years-of-asteroid-and-comet-discovery

British Library (2013) The Rice of Cities, http://www.bl.uk/learning/histcitizen/georgians/cities/riseofcities.html

Brown, P. et al. (2002) The Flux of small near-Earth objects colliding with the Earth. Nat. Vol. 420

Brunn, S. D. (1983) Cities of the world, ISBN 0-06-381225-8

Bryant, E. (2005) Natural Hazards, second edition, Cambridge University Press.

Butcher, L. (2013) Road: Speed Limits, House of Commons Library, http://www.google.dk/url?sa=t&rct=j&q=urban%20rural%20speed%20limits%20pft&source=web&cd=3&cad=rja&ved=0CDEQFjAC&url=http%3A%2F%2Fwww.parliament.uk%2Fbriefing-papers%2FSN00468.pdf&ei=sQGzUZ22CYyAPfirgdAI&usg=AFQjCNHfpkleE3U0mlevOaJmKxnaodNihA&bvm=bv.47534661,d.d2k

California http://www.monocounty.ca.gov/online_services/documents/cocode/level2/T15_C15.04.html

Canada http://www.nrc-cnrc.gc.ca/obj/irc/doc/pubs/tn/tn395.pdf

Cardona, O. D. (1997) Management of the volcanic crises of Galeras volcano: Social, economic and institutional aspects: Journal of volcanology and geothermal research: Volume 77 pp. 313--324, 1996, Elsevier

Carry, B. (2012) Density of asteroids: http://arxiv.org/pdf/1203.4336.pdf

Cascadia Region Earthquake Workgroup (2009) Cascadia Shallow Earthquakes 2009. http://www.crew.org/PDFs/CREWshallowFinalSmall.pdf

Cashell, B. W., Labonte, M. (2005) The Macroeconomic Effects of Hurricane Katrina: CRS Report for Congress, Order Code RS22260, September 13, 2005, http://fpc.state.gov/documents/organization/53572.pdf

Cellino, A., Somma, R., Tommasi, L., Paolinetti, R., Muinonen, K., Virtanen, J., Tedesco, E. F., Delbo, M. (2006) NERO: General concept of a Near-Earth object Radiometric Observatory, Advances in Space Research, Vol. 37, Issue 1, 2006, pp. 153-160

Chaisson, E., McMillan, S. (2002) Astronomy Today, Prentice Hall, Fourth Edition, ISBN 0-13-091542-4

Chapman, C. R. (2004) The Hazard of near-Earth asteroid impacts on earth. Earth and Planetary Science Letters 222, 1-15, Elsevier

Chapman, C. R., Durda, D. D., Schweickart, R. L. (2006) Mitigation: Interfaces between NASA, Risk Managers, and the Public; White Paper to NASA Workshop on “Near-Earth Object Detection, Characterisation, and Threat Mitigation”; June 2006: http://www.b612foundation.org/papers/wpChap.pdf

Chapman, C. R. (2008) Meteoroids, Meteors, and the Near-Earth Object Impact Hazard, Earth Moon Planet (2008) 102:417–424, DOI 10.1007/s11038-007-9219-6

Chang, C. M., Lee, L., Connor, k. m., Davidson, J. R. T., Lai, T. (2008) Modification effects of coping on post-traumatic morbidity among earthquake rescuers: Psychiatry Research: Volume 158, pp. 164—171

Chatterjee, S., Guven, N. (2002) The Shiva geophysical structure: another possible KT boundary impact crater on the western shelf of India. Abstract, 8th International Symposium on Mesozoic Terrestrial Ecosystems, Cape Town, South Africa

Chen, W., Meaker, J. W., Zhan, B. (2006) Agent-Based Modelling and Analysis of Hurricane Evacuation Procedures for the Florida Keys: Natural Hazards, 38: 321--338, Springer

Cheng, A. et al. () Binary and Multiple Systems: http://www.lpi.usra.edu/decadal/sbag/topical_wp/AndrewFChengFINAL.pdf

Chesley, S. R. et al. (2002) Quantifying the Risk Posed by Potential Earth Impacts. Icarus 159, 423-432

Chodas, P. W. (2011) Keyholes as Providers of Deflection Leverage, 2011 IAA Planetary Defence Conference

Chung, M. C., Farmer, S., Werrett, J., Easthope, Y., Chung, C. (2001) Traumatic stress and ways of coping of community residents exposed to a train disaster: Australian and New Zealand Journal of Psychiatry: Volume 35:4, pp. 528--534

City and County of Swansea (2009) The road to city status, http://www.swansea.gov.uk/index.cfm?articleid=30071

Coburn, A. W., Spence, R. J. S., Pomonis, A. (1994) Vulnerability and Risk Assessment: United Nations Disaster Management Training Programme

Coburn, A. W., Spence, R. J. S., Pomonis, A. (1994b) Disaster mitigation: United Nations Development Programme, Disaster Management Training Programme 1994

Coch, N. K. (1995) GEOHAZARDS NATURAL and HUMAN, ISBN: 0-02-322992-6

Collins, G. S., Melosh, H. J., Marcus R. A. (2005) Earth Impact Effects Program: A Web-based computer program for calculating the regional environmental consequences of a meteoroid impact on Earth: Meteoritics & Planetary Science 40, Nr 6, 817-840

Connors, M., Wiegert, P., Veillet, C. (2011) Eart's Trojan asteroid, Nature 475, 481-483, doi: 10.1038/nature10233

Cornell (2008) Arecibo Radar Discovers Triple Near-Earth Asteroid. Cornell Press release: http://www.naic.edu/~pradar/asteroids/2001SN263/

Courtland, R. (2009) Meteorite hunters 'strike gold' in Sudan, http://www.newscientist.com/article/dn16843-meteorite-hunters-strike-gold-in-sudan.html?full=true

Crawford, D.A., Mader C. (1998) Modeling asteroid impact and tsunami. *Science of Tsunami Hazards* **16**, 21-30.

Cross, J. A. (2001) Megacities and small towns: different perspectives on hazard vulnerability: Environmental Hazards: Volume 3 pp. 63—80

Cutter, S. L., Boruff, B. J., Shirley, W. L. (2003) Social Vulnerability to Environmental Hazards: Social Science Quarterly, Volume 84, Number 2, June 2003

D'Arriago, P., Barucci, M. A., Lagerkvist, C-I (2002) The Ishtar Mission, Proceedings of Asteroids, Comets, Meteors

Dachwald, B., Kahle, R. (2006) Solar Sailing Kinetic Energy Impactor (KEI) Mission Design Tradeoffs for Impacting and Deflecting Asteroid 99942 Apophis, AIAA/AAS Astrodynamics Specialist Conference and Exhibit 21 - 24 August 2006, Keystone, Colorado

Danish Statistics (2011) Varedeclaration: Byopgørelsen pr. 1. januar, http://www.dst.dk/Statistik/dokumentation/Varedeklarationer/emnegruppe/emne.aspx?sysrid=766#vd0 accessed in june 2011

Dash et al. (2007) Evacuation Decision-making and Behavioral Responses, Natural Hazards Review, August 2002, pp. 69-77

David, D., Mellman, T. A., Mendoza, L. M., Kulick-Bell, R., Ironson, G., Schneiderman, N. (1996) Psychiatric Morbidity Following Hurricane Andrew: Journal of Traumatic Stress: Volume 9, No. 3

Dearborn, D. S., Patenaude, S., Managan, R. A. (2007) The Use of Nuclear Explosives To Disrupt or Divert Asteroids, 2007 Planetary Defence Conference

Delbo, M., Tanga, P., Mignard, F. (2008) On the detection of the Yarkovsky effect on near-Earth asteroids by means of Gaia, Planetary and Space Science, Volume 56, Issue 14, p. 1823-1827

Department for Transport (2005) FORGE The Road Capacity & Costs Model, Research Report http://www.rudi.net/files/FORGE.pdf

Dicks, D. R. (1970) Early Greek Astronomy to Aristotle, Thames and Hudson, ISBN 0 500 40013 x

Dilley, M., Boudreau, T. E. (2001) Coming to terms with vulnerability: a critique of the food security definition. Food Policy 26 (2001) 229–247

Dilley, M., Chen, R. S., Deichmann, U., Lerner-Lam, A. L., Arnold, M., Agwe, J., Buys, P., Kjekstad, O., Lyon, B., Yetman, G. (2005) Natural Disaster Hotsports: A Global Risk Analysis Synthesis Report

Directgov (2011) The Highway Code: Control of the vehicle (117-126), http://www.direct.gov.uk/en/TravelAndTransport/Highwaycode/DG_070304 and http://www.direct.gov.uk/prod_consum_dg/groups/dg_digitalassets/@dg/@en/@motor/documents/digitalasset/dg_188029.pdf

Directgov b (2011) Managing motorway congestion, http://www.direct.gov.uk/en/TravelAndTransport/Usingmotorwaysandroads/Keepingtrafficmoving/DG_184978

Docklands()http://books.google.com/books?id=g-L1O4YszQgC&pg=PA7&lpg=PA7&dq=1996+docklands+bombing+tnt&source=bl&ots=tMiOxsGSOV&sig=bcRintyzDirjHEB92eRvnFNgs-A&hl=en&ei=iwMVS8POKMKk4Qay_pHPBg&sa=X&oi=book_result&ct=result&resnum=5&ved=0CBYQ6AEwBA#

Dotto, E.; Barucci, M. A.; Yoshikawa, M.; Koschny, D.; Boehnhardt, H.; Brucato, J. R.; Coradini, M.; Franchi, I. A.; Green, S. F.; Josset, J. L.; Kawaguchi, J.; Michel, P.; Muinonen, K.; Oberst, J.; Yano, H. and Binzel, R. P. (2008). Marco Polo: near Earth object sample return mission. Memorie della Societ`a Astronomica Italiana - Supplementi, 12(Supple), pp. 102–109.

Dow et al. (2002) Emerging Hurricane Evacuation Issues: Hurricane Floyd and South Carolina, NATURAL HAZARDS REVIEW / FEBRUARY 2002, DOI: 10.1061/~ASCE!1527-6988~2002!3:1~12!

Doxiadis, C. (1968) ECUMENOPOLIS: Tomorrow's City; BRITANNICA Book of the year 1968, Encyclopaedia Britannica, Inc, http://www.doxiadis.org/files/pdf/ecumenopolis%20tommorow's%20city.pdf

Drabek, T. E.: Understanding Disaster Warning Responses (1999) The Social Science Journal, Volume 36, Number 3, pages 515-523: Elsevier Science Inc.

EM-DAT (2009) http://www.emdat.be/database first accessed in 2009

Emergency Planning Consultants, San Diego, California (2004) City of Whittier Natural Hazards Mitigation Plan, http://www.cityofwhittier.org/pdfs/City_of_Whittier_Natural_Hazards_Mitigation_Plan.pdf

Enschede1 http://www.stop-fireworks.org/accidents_enschede.htm

Enschede2 () http://books.google.com/books?id=3LTJ4miALEsC&pg=PA1679&lpg=PA1679&dq =S.E.+Fireworks+explosion+tnt+blastwave&source=bl&ots=DCMvUJOsJv&sig=Iueg_gdFm4xQa2JLblaj3XKCCRo&hl=en&ei=O-ZySomAIuagjAfkt-CnBg&sa=X&oi=book_result&ct=result& resnum=1#v=onepage&q=&f=false

Enschede3 http://www.docstoc.com/docs/2369202/CHAF-Workpackage-4-Report-Literature-review-of-fireworks

Evans, J. B., Shelly, F. C., Stokes, G. H. (2003) Detection and Discovery of Near-Earth Asteroids by the LINEAR Program, Lincoln Laboratory Journal, Vol. 14, No. 2, pp. 199-220

Federal Emergency Management Agency (1995) ALABAMA HURRICANE ECACUATION STUDY TECHNICAL DATA REPORT

FEMA (2004) Using Hazus-MH for Risk Assessment, http://www.fema.gov/pdf/plan/prevent/hazus/fema433.pdf.

Fischhoff, B., Slovic, P., Lichtenstein, S. (1978) How Safe is Safe Enough A Psychometric Study of Attitudes Towards Technological Risks and Benefits: Policy Sciences 9, pp 127-152

Flixborough1 http://www.urv.es/catedres/enresa/en_historic_catastrofics.html

Flixborough2 http://www3.interscience.wiley.com/cgi-bin/fulltext/119410280/PDFSTART

Florida (1996) Northwest Florida Hurricane Evacuation Study Technical Data Report

Galea, S., Brewin, C. R., Gruber, M., Jones, R. T., King, D. W., King, L. A., McNally, R. J., Ursano, R. J., Petukhova, M., Kessler, R. C. (2007) Exposure to Hurricane-Related Stressors and Mental Illness After Hurricane Katrina: ARCH GEN PSYCHIATRY/VOL 64 (NO. 12), DEC 2007, page 1427-1434

Garretson, P. A. (2008) AF/A8XC Natural Impact Hazard (Asteroid Strike) Interagency Deliberate Planning Exercise After Action Report December 2008: http://www.nss.org/resources/library/planetarydefense/2008-NaturalImpactAfterActionReport.pdf

Germany () http://www.nat-hazards-earth-syst-sci.net/8/1/2008/nhess-8-1-2008.pdf

Gibraltar () http://www.gibraltarlaws.gov.gi/articles/2007s095.pdf

Gillick, T. J. (2005) Assessment and Mitigation of Risks to Physical Security, Information Security, and Operational Security: http://www.facilitiesnet.com/security/article/Taking-Security-To-the-Next-Level--2566#

Gisler, G., Weaver, R. (2009) Near-Field Effects of Asteroid Impact in Deep Water: First IAA Planetary Defense Conference

Gisler, G. Weaver, R., Gittings, M. (2010) Calculations of Asteroid Impacts into Deep and Shallow Water: Pure Appl. Geophys. 168, page 1187-1198, DOI 10.1007/s00024-010-0225-7

Gisler, G. (2011) Calculation of the Impact of a Small Asteroid on a Continental Shelf: Second IAA Planetary Defense Conference

Glasstone, S., Dolan, P. J. (1977) The Effects of Nuclear Weapons, Third edition. Available in digital form on http://www.princeton.edu/sgs/publications/articles/effects/effects-1.pdf or http://www.fourmilab.ch/etexts/www/effects/

GlobalSecurity.org (2012) Map of the Galveston and Houston area. http://www.globalsecurity.org/military/facility/html/houston-cat4.htm

Goldblatt, R. B., Weinisch, K. (2005) Evacuation Planning, Human Factors, and Traffic Engineering, TR NEWS, May-June 2005 Number 238

Gwynne, S., Galea, E. R., Owen, M., Lawrence, P. J., Filippidis, L. (1999) A Review of the Methodologies Used in Evacuation Modelling: Fire and Materials, 23, 383-388

Hallenbeck, M. et al. (1997) VEHICLE VOLUME DISTRIBUTIONS BY CLASSIFICATION, Chaparral Systems Corporation and Washington State Transportation Center, http://depts.washington.edu/trac/bulkdisk/pdf/VVD_CLASS.pdf

Harris, A. W. (2009) Estimating the NEO Population and Impact Risk: Past, Present and Future: The Asteroid-Comet Hazard Conference Proceedings, 2009

Harris County Office of Homeland Security & Emergency Management () Hurricane Rita Evacuation of a Major Urban Area, https://www.gov.uk/government/uploads/system/.../hurricane_rita.ppt

Harrison, E. (2007) Suffering a Slow Recovery: Scientific American: December 2007 Special Editions: http://www.scientificamerican.com/article.cfm?id=katrina-suffering-a-slow-recovery

Hartevelt, J. (2011) Crown to buy worst-hit Christchurch homes http://www.stuff.co.nz/the-press/news/christchurch-earthquake-2011/5179960/Crown-to-buy-worst-hit-Christchurch-homes accessed June 1022

Hartmann, W. K.: The Impact that Wiped Out the Dinosaurs, http://www.psi.edu/projects/ktimpact/ktimpact.html

Harwit, M. (2004) The Herschel mission, Advances in Space Research, volume 34, Issue 3, Pages 568-572

Hazard Management Group, Inc. (1988) Hurricane Evacuation, Behavioral Assumptions for Connecticut.

HAZUS, NVHUG Loss-Estimation Modeling of Earthquake Scenarios for Each County in Nevada Using HAZUS-MH,http://www.nbmg.unr.edu/hugs.pdf

HMA (Head Mann Associates Ltd) (2010) MINERALS WORKING & SITE RESTORATION POTLOCKS HOUSE FARM, WILLINGTON, DERBYSHIRE, Report Ref: R/374/1

http://www.derbyshire.gov.uk/applications/ESplanningapps/Planning-Applications/CM9-0610-43/9.922.3/01-Application-Documents/3%20-%20Technical%20Appendicies%20Document/Appendix%208%20-%20Transport%20Assessment/1%20-%20Report/Transport%20Assessment.pdf

Helbing, D., Farkás, I. J., Molnár, P., Vicsek, T. (2002): Simulation of Pedestrian Crowds in Normal and Evacuation Situations: . Pages 21-58 in: M. Schreckenberg and S. D. Sharma (eds.) Pedestrian and Evacuation Dynamics (Springer, Berlin) or http://www.tu-dresden.de/vkiwv/vwista/publications/evacuation.pdf

Hemel1 http://www3.interscience.wiley.com/journal/119410280/abstract?CRETRY=1&SRETRY=0

Hemel2 http://www.fireworld.com/pdf/BuncefieldFire.pdf

Highways Agency (2006) A453 Widening M1 Junction 24 to A52 Nottingham Report of Transport Surveys, Report Reference: A021959-REP-T-SA-014 Revision: 2, http://www.persona.uk.com/a453widening/Core_docs/DD-32.pdf

Hildebrand, A. R. et al. (2008) THE NEAR EARTH OBJECT SURVEILLANCE SATELLITE (NEOSSat) MISSION WILL CONDUCT AN EFFICIENT SPACE-BASED ASTEROID SURVEY AT LOW SOLAR ELONGATIONS, Asteroids, Comets, Meteors

Hills, J.G., Nemtchinov I.V., Popov S.P., Teterev A.V. (1994) Tsunami generated by small asteroid impacts.: Hazards due to Comets and Asteroids, (Univ. Arizona Press, Tucson), 779-790.

Hills, J. G., Goda, M. P. (2001) The Asteroid Tsunami Project at Los Alamos: Science of Tsunami Hazards, Volume 19, Number 1, pp 55--66

Hobeika, A. G., Kim, C. (1998) Comparison of Traffic Assignments in Evacuation Modeling: IEEE Transactions on engineering management, Vol. 45, No. 2, May 1998

Holling, C., S. (1973) Resilience and stability of ecological systems: Annual Review of Ecology and Systematics, Volumne 4, pp. 1—23.

Hogan, D. (2001) Predicting quakes is an uncertain science, http://www.oregongeology.com/sub/earthquakes/eqprediction.htm

Hoult, I. (2009) Personal communication, Hampshire County Council Emergency Planning Unit, 3 March 2009

Hugill, M. (1988) Advanced Statistics. Unwin Hyman Ltd.

Hyland, D. C., Ge, S., Kim, H., Medina, L., Munoz, R., Marqulieux, R., Young, B., Bai, X., Satak, N. (2011) Multi-tiered Implementation for Near-Earth Asteroid Mitigation, 2011 IAA Planetary Defense Conference.

Ikast-Brande Kommune (2009) Kommuneplan 2009, http://www.kommuneplan.ikast-brande.dk/site.aspx?MenuID=612&Langref=175&Area=&topID=&ArticleID=11112&expandID=3914&moduleID= accessed in june 2011

Impact Craters (2008), http://www.crystalinks.com/craters.html, viewed in 2008

Impact Earth: http://www.purdue.edu/impactearth/

Jaggard, V. (2007) “Killer Asteroid” Debate Pits Gravity Tractors Against Bombs, Projectiles: National Geographic, March 8 : http://news.nationalgeographic.com/news/2007/03/070308-asteroids.html

India (2009) http://www.scribd.com/doc/27116198/Is-875-Part-2, vieved in 2009

Jaiswal, K., Wald, D. J. (2008) Creating a Global Building Inventory for Earthquake Loss Assessment and Risk Management. http://pubs.usgs.gov/of/2008/1160/downloads/OF08-1160.pdf

Jaiswal, K., Wald, D., Porter, K. (2010) A Global Building Inventory for Earthquake Loss Estimation and Risk Management: Earthquake Spectra, Volume 26, No. 3, pages 731–748, http://earthquake.usgs.gov/research/pager/prodandref/Jaiswal_Wald_Porter_(2010)_PAGER_Building_Inventory_Spectra.pdf

Jedicke, R., Denneau, L., Granvik, M., Wainscoat, R. (2009) Asteroid Detection with the Pan-STARRS Moving Object Processing System, Proceedings of the Advanced Maui Optical and Space Surveillance Technologies Conference, September 1-4, 2009, http://www.amostech.com/TechnicalPapers/2009/Astronomy/Denneau.pdf

Johnson, C. W. (2005) The Glasgow-hospital evacuation simulator: Using Computer Simulations to Support A Risk-Based Approach For Hospital Evacuation: http://www.dcs.gla.ac.uk/~johnson/papers/G-HES.PDF

Joost …(todo)

Jorgensen, T. D. (2011) Private conversation with Thomas Jorgensen, Aviva insurance, June 2011.

JPL Small Body Database: http://ssd.jpl.nasa.gov/sbdb_query.cgi

Kang et al. (2007) Hurricane Evacuation Expectations and Behaviour in hurricane Lili, Journal of Applied Social Psychology, 37, 4, pp. 887–903

Kaplinger, B., Wie, B., Dearborn, D. (2011) Nuclear Fragmentation/Dispersion Modeling and Simulation of Hazardous Near Earth Objects, 2011 Planetary Defence Conference

Keller, G., Adatte, T, Berner, Z., Harting, M, Baum, G., Prauss, M., Tantawy, A., Stueben, D. (2007) Chicxulub impact predates K-T boundary New evidence from Brazos, Texas: Earth and Planetary Science Letters 225

Kirchner, A., Klüpfel, H., Nishinari, K., Schadschneider, A., Schreckenberg, M. (2003) Simulation of competitive egress behavior: Comparison with aircraft evacuation data: Elsevier science, http://citeseerx.ist.psu.edu/viewdoc/summary?doi=10.1.1.15.8525

Kleiman, L. A. (1979) Project Icarus: an MIT Student Project in Systems Engineering, Cambridge, Massachusetts : MIT Press

Kuligowski, E. (2005) Review of 28 Egress Models: http://www.fire.nist.gov/bfrlpubs/fire05/PDF/f05008.pdf

Kumpulainen, S. (2006) Vulnerability concepts in hazard and risk assessment: Geological Survey of Finland, Special Paper 42, 65—74

Leipold, M., von Richter, A., Hahn, G., Harris, A., Kuhrt, E., Michaelis, H., Mottola, S. (2002) Earthguard-I: a NEO detection space mission, Proceedings of Asteroids, Comets, Meteors - ACM 2002. International Conference, 29 July - 2 August 2002, Berlin, Germany. Ed. Barbara Warmbein. ESA SP-500. Noordwijk, Netherlands: ESA Publications Division, ISBN 92-9092-810-7, 2002, p. 107 - 110

Lahart et al. (2013) The Design Manual for Urban Roads & Streets (DMURS), http://www.environ.ie/en/Publications/DevelopmentandHousing/Planning/FileDownLoad,32668,en.pdf

Levasseur-Regourd, A., Hadamcik, E., Lasue, J. (2006) Interior structure and surface properties of NEOs: What is known and what should be understood to mitigate potential impacts. Advances in Space Research 37, 161–168

Lichtenstein, S., Slovic, P., Fischhoff, B., Layman, M., and Combs, B. (1978) Judged Frequency of Lethal Events: Journal of Experimental Psychology: Human Learning and Memory, Vol. 4, No. 6

LINEAR (2008) http://www.ll.mit.edu/mission/space/linear/ viewed in 2008

Lindell, M. K., Prater, C. S., Peacock, W. G.. (2005) Organizational Communication and Decision-making in Hurricate Emergencies: Hazard Reduction & Recovery Center, Texas A&M University

Lomnitz, C. (1970) CASUALTIES AND BEHAVIOR OF POPULATIONS DURING EARTHQUAKES, Bulletin of the Seismological Society of America, Vol. 60, No. 4, pp. 1309-1313

Mann, P. H. (1965) An approach to Urban Sociology, Routledge & Kegan Paul Limited, ISBN 0 7100 68964

Marano, K. D. et al. (2010) Global earthquake casualties due to secondary effects: a quantitative analysis for improving rapid loss analysis. Nat. Hazards, 52, 319-328

Marcus, R., Melosh, H. J., Collins, G.. Earth Impact Effects Program. http://impact.ese.ic.ac.uk/ImpactEffects/

Margot, J. L. et al. (2002) Binary Asteroids in the Near-Earth Object Population. Science 296, 1445; DOI: 10.1126/science.1072094

Margot, J. L., Brown M. E. (2003) A Low-Density M-type Asteroid in the Main Belt. SCIENCE VOL 300 20 JUNE 2003

Martinot, V., Morbidelli, A. (2006) The EUNEOS mission: A European NEO space-based observatory, Acta Astronautica, Selected Proceedings of the Fifth IAA International Conference on Low Cost Planetary Missions, Volume 59, Issues 8-11, Pages 679-688

Marusek, J., A. (2007) Impact Disaster Preparedness Planning: American Institute of Aeronautics and Astronautics, 2007 Planetary Defence Conference.

McCall G. J. H., Howarth R. J., Bowden A. J. (2006) The History of meteoritics and key meteorite collections : fireballs, falls and finds. ISBN: 1862391947, Geological Society of London

McInnes, C. R. (2004) Deflection of Near-Earth asteroids by kinetic energy impacts from retrograde orbits: Planetary and Space Science, 52, 587--590

McGraw-Hill (1955) Series in Sociology, Urban Sociology

McMillan, R. S. (2009) SPACEWATCH SUPPORT OF DEEP WIDE-FIELD NEO SURVEYS, NRC Committee to Review Near-Earth Object Surveys and Hazard Mitigation Strategies, http://spacewatch.lpl.arizona.edu/Spacewatch_NRC_NEOs.pdf

Milani, A., Chesley, S. R. (2000) Virtual Impactors: Search and Destroy. Icarus 145, 12--24. Academic Press

Milani, A., Valsecchi, G., Paolicchi, P., Lognonne, P., Benz, W., Foerstner, R., Bello, M., Gonzalez, J. A. (2003) Near Earth Object Space Mission Preparation: Don Quijote Mission Executive Summary, European Space Agency, Issue 2.0

Mitchell, J. K. (1999) Megacities and natural disasters: a comparative analysis. GeoJournal, 49: 137-142

Morbidelli, A., Bottke Jr., W. F., Froeschle, Ch., Michel, P. (2002) Observatoire de la Cote d'Azur: http://www.oca.eu/morby/papers/AstIII_NEO.pdf

Morley, A. (2005) Casualty rate prediction for Near Earth Object Impact, Individual project

Morley, A. (2009) NEOSim: A Near Earth Object impact simulator

Morris, A. E. J. (1994) History of urban form – Before the industrial revolution, Third edition, ISBN 0-582-30154-8

Morrison, D, Harris, A. W., Sommer, G., Chapman, C. R., Carusi, A. (2003) Dealing with the Impact Hazard, Chapter for Asteroids III book edited by Bottke, W., Cellino, A., Paolicchi, P., Binzel, R. P., University of Arizona Press, Tucson (2003)

Murakami, Y., Minami, K., Kawasoe, T., Ishida, T. (2002) Multi-Agent Simulation for Crisis Management: Proceedings of the IEEE Workshop on Knowledge Media Networking

Napier, B. (1997) Cometary Catastrophes, Cosmic Dust and Ecological Disasters in Historical Times: The Astronomical Framework: Second SIS (Society for Interdisciplinary Studies) Cambridge Conference, Natural Catastrophes During Bronze Age Civilisations: Archaeological, geological, astronomical and cultural perspectives

Napier, B., Asher, D. (2009) The Tunguska impact event and beyond: A&G, Vol. 50

NASA (2005a) Impact Risk Assessment: An Introduction: http://neo.jpl.nasa.gov/risk/doc/sentry.html

NASA (2005b) Palermo scale: http://neo.jpl.nasa.gov/risk/doc/palermo.html

NASA (1992) Spaceguard Survey: NASA Ames Space Science Devision: http://impact.arc.nasa.gov/downloads/spacesurvey.pdf

NASA (2005c) Torino Impact Scale: http://impact.arc.nasa.gov/torino.cfm

NASA (2007) Near-Earth Object Survey and Deflection Analysis of Alternatives: http://www.nasa.gov/pdf/171331main_NEO_report_march07.pdf

NASA (2013) Additional Details on the Large Fireball Event over Russia on Feb. 15, 2013: http://neo.jpl.nasa.gov/news/fireball_130301.html

National Hurricane Center (2005) Rita Graphics Arcvhive. http://www.nhc.noaa.gov/archive/2005/RITA_graphics.shtml

NEAT (2008) http://neo.jpl.nasa.gov/programs/neat.html viewed in 2008

Nelson, C. E., Crumley, C., Fritzsche, B. and Adcock, B. (1989) Lower Southeast Florida Hurricane Evacuation Study," University of South Florida Department of Psychology.

NEODyS: http://unicorn.eis.uva.es/neodys/index.php?pc=0

NHC (2013) http://www.nhc.noaa.gov/modelsummary.shtml accessed 2013

NOAA (2009) http://www.noaa.gov/ocean.html accessed January 2009

Norlund, C. C. F. (2009) Evacuation Simulation Modelling in the event of a Near Earth Object impact: Nine month report

Norlund et al. (2011) "NEOMiSS: A Near Earth Object decision support tool" at the 2011 IAA Planetary Defense Conference, Bucharest 2011

Norway http://www.sintef.no/uploadpages/266000/Prediction%20of%20local%20snow%20loads%20on%20roofs.pdf

OECDs glossary: http://stats.oecd.org/glossary/detail.asp?ID=2886

Oklahoma1 http://www.fema.gov/rebuild/mat/mat_fema277.shtm

Oklahoma2 http://en.wikipedia.org/wiki/Oklahoma_City_bombing

Oxford Dictionaries (2010) http://oxforddictionaries.com/definition/english/exposure

PASSC, The Planetary and Space Science Centre, 2011. Earth Impact Database. http://www.passc.net/EarthImpactDatabase/index.html

Perry et al. (1988) Minority Citizens in Disasters, American Sociological Association, Contemporary Sociology, Vol. 17, No. 5 (Sep., 1988), pp. 589-590

Pierazzo, E., Garcia, R. R., Kinnison, D. E., Marsh, D. R., Lee-Taylor, J., Crutzen, P. J. (2010) Ozone Perturbation from medium-size asteroid impacts in the ocean, Earth and Planetary Science Letters 299, 263-272, ELSEVIER

Pomonis, A. et al. (1999) Risk assessment of residential buildings for an eruption of Furnas Volcano, São Miguel, the Azores. J. Volcanol, 92, 107–131

Porter, K. A., D. Wald, T. Allen, and K. Jaiswal (2007) An empirical relationship between fatalities and instrumental MMI. 1st International Workshop on Disaster Casualties, Kyoto University

Porter, K. A., Jaiswal, K. S., Wald, D. J., Greene, M., Comartin, C. (2008) WHE-PAGER PROJECT: A NEW INITIATINE IN ESTIMATING GLOBAL BUILDING INVENTORY AND ITS SEISMIC VULNERABILITY: The 14th World Conference on Earthquake Engineering

Post et al. (1990) HURRICANE HUGO ASSESSMENT

Post et al. (1993) Hurricane Andrew Assessment, http://www.csc.noaa.gov/hes/docs/postStorm/H_ANDREW_ASSESSMENT_REVIEW_HES_UTILIZATION_INFO_DISSEMINATION.pdf

Post et al. (1999) HURRICANE BONNIE ASSESSMENT

Post et al. (1999b) Hurricane Georges Assessment

Post et al. (2001) Hurricane Evacuation Transportation Analysis, http://www.csc.noaa.gov/hes/docs/hes/HURRICANE_EVACUATION_TRANSPORTATION_ANALYSIS_HURRICANE_GEORGES.pdf

Post et al. (2003) Hurricane Lili post storm assessment, http://www.csc.noaa.gov/hes/docs/postStorm/Lili_%20final.pdf

Post et al. (2005) Hurricane Isabel Assessment

Puerto Rico http://www.google.co.uk/url?sa=t&rct=j&q=building%20regulation%20puerto%20rico%20snow%20load&source=web&cd=1&sqi=2&ved=0CE0QFjAA&url=https%3A%2F%2Fwww.sip.pr.gov%2Fweb%2Fguest%2Fservlet%2FFileServlet%3FfileAlfresco%3Dee3b748c-88e4-4052-8f89-846ab7b43a62%26fileName%3DPR-Building_Code.pdf%26fileDescripcion%3DPR-Building_Code.pdf&ei=XT3jT9CeHcSh8QOlp8XVDg&usg=AFQjCNGjo1k9jbxkXHp3QxUF4JhfkEss-Q

Ramirez M., Peek-Asa C. (2005) Epidemiology of Traumatic Injuries from Earthquakes, Epidemiologic Reviews Vol. 27, No. 1, pp. 47-55

Reinhard, R. (1986) The Giotto encounter with comet Halley, Nature Vol.321

The Task Force (2000) Report of the Task Force on Potential hazardous Near Earth Objects, http://www.nearearthobjects.co.uk/report/pdf/full_report.pdf or http://www.nss.org/resources/library/planetarydefense/2000-ReportOfTheTaskForceOnPotentiallyHazardousNearEarthObjects-UK.pdf

Reverso dictionary: http://dictionary.reverso.net/english-definitions/likelihood

Rincon, P. (2010) Clues to Antarctica space blast, http://news.bbc.co.uk/1/hi/sci/tech/8547534.stm
Rivers, D. (2006) PAKISTAN EARTHQUAKE VICTIMS STRUGGLE THROUGH WINTER: Online NewsHour: http://www.pbs.org/newshour/bb/asia/jan-june06/pakistan_1-19.html accessed in 2009

Rodriguez, T. et al. (2010) A natural-disaster management DSS for Humanitarian Non-Governmental Organisations. Knowl.-Based Systems 23

Rogers, G. (2007) Comparison of the Efficiency of Various Asteroid Hazard Mitigation Techniques: Planetary Defense Conference, White papers: http://www.aero.org/conferences/planetarydefense/documents/ISP%20White%20paper%20(Rogers).pdf

Romania http://www.teknikengel.gov.tr/docs/ROU_12_text_EN.pdf

Rose, A. (2007) Economic resilience to natural and man-made disasters: Multidisciplinary origins and contextual dimensions: Environmental Hazards: Volume 7 pp. 383—398

Roughan & O'Donovan AECOM Alliance, Goodbody Economic Consultants (2011) National Roads Traffic Management Study, http://www.nra.ie/RepositoryforPublicationsInfo/file,17943,en.pdf

Ryongchon1 http://www.democraticunderground.com/discuss/duboard.php?az=view_all&address=102x559875

Ryongchon2 http://www.munichre.com/publications/302-04321_en.pdf

Ryongchon3 http://www.atwonline.org/scripts/2003/0429.html

Ryongchon4 http://www.statemaster.com/encyclopedia/Ryongchon

Saudi Arabia http://www.scribd.com/doc/37462362/Saudi-Building-Code-Loads-and-Forces

Scawthorn C., Yamada Y., Iemura H. (1978) World large destructive earthquakes since 1900. Proc. 33rd JSCE Annual Meeting, Sendai, Japan, September 1978, pp. 318-319

Schuiling, R. D., Cathcart, R. B., Badescu, V., Isvoranu, D., Pelinovsky, E. (2007) Asteroid impact in the Black Sea. Death by drowning or asphyxiation?: Nart Hazards , 40: 327—338

Schweickart, R., Chapman, C., Durda, D., Hut, P. (2007) Threat Mitigation: The Gravity Tractor, White paper 042 http://www.aero.org/conferences/planetarydefense/documents/wpGT%20(Schweickart).pdf

Schweickart, R., Chapman, C., Durda, D., Hut, P., Bottke, B., Nesvorny, D. (2007b) Threat Characterisation: Trajectory Dynamics, White paper 039)

Schweickart, R. (2008) Asteroid Threats: A Call for Global Response

Schweickart, R. (2008b) Decision Program on Asteroid Threat Mitigation. Presented at the International Astronautical Congress, October 2008. http://www.space-explorers.org/committees/NEO/docs/IAC08_paper.pdf

Science Daily (2009) Lessons From Hurricane Rita Not Practiced During Hurricane Ike. http://www.sciencedaily.com/releases/2009/03/090313110752.htm

SEDAC (2010) http://sedac.ciesin.columbia.edu/gpw/ first accessed in 2008

Seddon, G.. (1970) Meteor Crater: AQ Geological Debate, Geol. Soc. Aust. Jour. 17:1-12

Seest1 http://www.kolding.dk/brand/0032151.asp?sid=32151

Seest2 http://www.springerlink.com/content/a3g420r0622x351l/fulltext.pdf

Seest3 http://wapedia.mobi/en/List_of_the_largest_artificial_non-nuclear_explosions

Shen, T-S. (2005) ESM: a building evacuation simulation model: Building and Environment 40, 671—680

Siebeneck, L. K., Cova, T. J. (2008) An Assessment of the Return-Entry Process for Hurricane Rita 2005. International Journal of Mass Emergencies and Disasters, August 2008, Vol. 26, No. 2, pp. 91-111

Silvertown http://en.wikipedia.org/wiki/Silvertown_explosion

Soika, K (2006) Evacuation Planning in Texas: Before and After Hurricane Rita. Interim News Number 79-2

Solis et al. (2009) DETERMINANTS OF HOUSEHOLD HURRICANE EVACUATION CHOICE IN FLORIDA, Selected Paper prepared for presentation at the Southern Agricultural Economics Association Annual Meeting, Atlanta, Georgia, January 31-February, 2009, http://ageconsearch.umn.edu/bitstream/45338/2/DS.MT.DL.SAEA.2008.pdf

Spence, R. J. S. et al. (2005) Residential building and occupant vulnerability to tephra fall. Nat. Hazards Earth Syst Sci, 5, 477–494

Spence, R. J. S. et al. (2005b) Modelling expected physical impacts and human casualties from explosive volcanic eruptions. Nat. Hazards Earth Syst. Sci., 5, 1003–1015

Springer (2008) The Biographical Encyclopedia of Astronomers, http://www.springerreference.com/docs/navigation.do?m=The+Biographical+Encyclopedia+of+Astronomers+(Physics+and+Astronomy)-book59

Starr, C. (1969) Social Benefit versus Technological Risk: Science, Volume 165, No. 3899 (Sep. 19. 1969), pp. 1232—1238: American Association for the Advancement of Science.

St Davids City Council website, accessed in June 2011, http://www.stdavids.gov.uk/

Steele, D. (1998) Crater chain points to impact of fragmented comet. The University of Chicago Chronicle, March 19, 1998, Vol. 17, No. 12

Stiles, L. (2009) Catalina Sky Survey Spawns Catalina Real-Time Transient Survey, UA News, The university of Arizona, August 21, 2009, http://uanews.org/story/catalina-sky-survey-spawns-catalina-real-time-transient-survey

Strasser, U. (2008) Snow loads in changing climate: new risks? Nat. Hazards Earth Syst. Sci., 8, 1–8

Sublette, C. (1997) Section 5.0 Effects of Nuclear Explosions.
http://nuclearweaponarchive.org/Nwfaq/Nfaq5.html

Svoboda, E. (2007) "Gravity Tractor" Super Telescopes Enlisted to Battle Killer Asteroids: National Geographic: February 17: http://news.nationalgeographic.com/news/2007/02/070217-asteroid-impact.html

Tancredi, G.., Ishitsuka, J., Schultz, P., Harris, S., Brown, P., ReVelle, D. (2009) The Carancas Event: A Recent Hypervelosity Impact Crater in the Altiplano: First IAA Planetary Defence Conference

Taton, R., Wilson, C. (1989) The General History of Astronomy, Volume 2, Planetary astronomy from the Renaissance to the rise of astrophysics. Part A: Tycho Brahe to Newton. Cambridge University press, ISBN 0 521 24254 1

Taylor, D. A. (1980) Roof Snow Loads in Canada. Canadian Journal of Civil Engineering. Vol. 7, No. 1, pp. 1-18

Texas1 http://www.sciencedirect.com/science?_ob=ArticleURL&_udi=B6TGF-4RMFP3M-H&_user=126770&_rdoc=1&_fmt=&_orig=search&_sort=d&_docanchor=&view=c&_searchStrId=972043281&_rerun

Texas2 http://www.aiche-chicago.org/symposium06/2006_AIChE_Refinery_Symposium_TxCtyReport.pdf

TFL/222 (2005) Thames Gateway Bridge Inquiry Note Assessment of Commercial Vehicle Benefits, http://www.persona.uk.com/thamesgateway/TFL_docs/Gen_docs/TFL_200-249/TFL-222.pdf

The Southeast Louisiana Hurricane Taskforce (2005) Citizen Hurricane Evacuation Behaviour in Southeastern Louisiana: A Twelve Parish Survey

theguardian (2013) Meteorite explosion over Russia injures hundreds:
http://www.guardian.co.uk/science/2013/feb/15/meteorite-explosion-shakes-russian

The Infrastructure Security Partnership (2006) Regional Disaster Resilience: A Guide for Developing an Action Plan: American Society of Civil Engineers: ISBN 0-7844-0880-7: June 2006

The Philippines () http://www.riskfrontiers.com/newsletters/rfnews1_2.pdf

Thomas, J. M. (2006) Near-Earth Object Resource, Museum Astronomical Resource Society and the NASA/JPL Solar System Ambassador Program, http://www.marsastro.org/presentations/MARS_NEO-Resource.pdf

Thorpe, N. (2009) Kosovo's poisoned generation: http://news.bbc.co.uk/1/hi/world/europe/ 7827031.stm Accessed in 2009

Times online, May 16 (2008) Shops track customers via mobile phone,
http://technology.timesonline.co.uk/tol/news/tech_and_web/article3945496.ece

Toon, O. B.,Turco, R. P., Covey, C. (1997) Environmental Perturbations Caused by the Impact of Asteroids and Comets. Reviews of Geophysics, vol. 35, 1, pp. 41--78. American Geophysical Union

Trinidad http://www.scribd.com/Andiholic/d/20748625-Trinidad-Tobago-Small-Building-Code-Draft

Tüysüz (2006) Earthquake Geology: Seismic Waves.
http://www.eies.itu.edu.tr/dersnotlari/notlar/Y%C3%BCksek_lisans/Earthquake_Geology/Seismic%20waves.pdf

UNDP (2004) Reducing Disaster Risk A challenge for development: www.undp.org/bcpr

UN-Habitat (2007) Mitigating the Impacts of Disasters: Policy Directions, http://www.unhabitat.org/downloads/docs/GRHS.2007.Abridged.Vol.3.pdf

UN News Centre (2008) Half of global population will live in cities by end of this year, predicts UN, http://www.un.org/apps/news/story.asp?NewsID=25762

United Nations (2011) World Urbanization Prospects The 2011 Revision, http://esa.un.org/unup/pdf/FINAL-FINAL_REPORT%20WUP2011_Annextables_01Aug2012_Final.pdf

United Kingdom http://www.scribd.com/doc/41428848/BS-6399-3-1988-Loading-for-Buildings-Part-3-Code-of-Practice-for-Imposed-Roof-Loads

US Army Corps of Engineers, Federal Emergence Management Agency (1994). Connecticut Hurricane Evacuation Study Technical Data Report. http://www.ct.gov/dep/lib/dep/long_island_sound/coastal_hazards/ace1994tdr.pdf

US Army Corps of Engineers, Federal Emergence Management Agency (1997). Southern Massachusetts Hurricane Evacuation Study Technical Data Report. http://www.iwr.usace.army.mil/nhp/HES/MA/Current1997HES/Report/matechnicaldatareport.pdf

USGS (2010) http://earthquake.usgs.gov/ first accessed 2009

USGS (2011) FAQs - Earthquake Myths, http://earthquake.usgs.gov/learn/faq/?categoryID=6&faqID=13

USGS (2013) M6.2 Taiwan Earthquake of 02 June 2013, http://earthquake.usgs.gov/earthquakes/eqarchives/poster/2013/20130602.pdf

Valsecchi, G. B., Milani, A., Gronchi, G. F., Chesley, S. R. (2003) Resonant returns to close approaches: Analytical theory, A&A Volume 408, Number 3, September IV 2003

Van De Hulst, H. C. (1994) Jan Hendrik Oort (1900-1992), Quarterly Journal of the Royal Astronomical Society, 35, 237-242

Vočadlo, L. (2002) THE STRUCTURE OF THE EARTH FROM SEISMIC WAVES. Detailed Lecture Notes Lecture 7, University College London, Department of Earth Sciences: http://bowfell.geol.ucl.ac.uk/~lidunka/GlobalGeophysics/Revised%20Course/Detailed%20Lecture%20Notes/LECTURE7.PDF

Wagner R. M., Joines N. P., Smith G. S. (1994) Risk factors for casualty in earthquakes: The application of epidemiologic principles to structural engineering **, Structural Safety 13, 177-200

Ward, S., Asphaug, E. (2000) Asteroid Impact Tsunami: A Probabilistic Hazard Assessment, Icarus 145, 64-78

Ward, S. V. (2007) City Status in the British Isles, 1830-2002, by John Beckett, English Historical Review CXXII (495): 271-272. doi: 10.1093/her/cel453, link: http://ehr.oxfordjournals.org/content/CXXII/495/271.full

Weaver, R. P., Plesko, C. S., Dearholt, W. R. (2011) Los Alamos RAGE Hydrocode Simulations of Effective Mitigation of Porous Objects, 2011 Planetary Defence Conference

Wells, N., Walker, R., Green, S., Ball, A. (2006) SIMONE: Interplanetary microsatellites for NEO rendezvous missions, Acta Astronautica, Volume 59, Issue 8-11, Pages 700-709

Whipple, F. L., Green, D. W. E. (1986) The Mystery of Comets, Smithsonian Institution Press, Second printing, ISBN 0-87474-968-9

Whitehead et al. (2000) Heading for Higher Ground: Factors Affecting Real and Hypothetical Hurricane Evacuation Behavior, http://www.cs.rice.edu/~devika/evac/papers/Heading%20for%20higher%20ground.pdf

Wilcock, W. (2013) 5. Seismology, http://www.google.co.uk/url?sa=t&rct=j&q=seismic%20waves%20s-wave%20velocity%204-6%20km%2Fs&source=web&cd=1&cad=rja&ved=0CC0QFjAA&url=http%3A%2F%2Fwww.ocean.washington.edu%2Fcourses%2Foc410%2F2011%2Flectures%2Fclass05_seismology.ppt&ei=lru9Ud7IBo6sPPDUgeAC&usg=AFQjCNE0qc4AiuMrwuVrxTcaiz-62NsRYA

Writers, S. (2009) Surprise Recovery Of Meteorites Following Asteroid Impact: http://www.spacedaily.com/reports/Surprise_Recovery_Of_Meteorites_Following_Asteroid_Impact_999.html

Yeomans, D. K. et al. (2000) Radio Science Results During the NEAR-Shoemaker Spacecraft Rendezvous with Eros, Science, Volume 289, Issue 5487, pp. 2085-2088

Bibliography

Conference papers:

"Evacuation Simulation Modelling in the event of a Near Earth Object impact" presented at The First International Conference on Evacuation Modelling and Management in 2009 (ICEM09)

"NEOMiSS: A Near Earth Object decision support tool" presented at the 2011 IAA Planetary Defence Conference, Bucharest 2011

"NEOMiSS: A global human vulnerability estimator and evacuation simulator" presented at the 9th Remote Sensing For Disasters workshop, Stanford 2011

Journal papers:

"Modelling HumanVulnerability to a Near Earth Object Impact: a Multi-Hazard Approach"

"A Statistical Analysis of Time of Day's Influence on Human Vulnerability during Earthquakes"